PROCESS DEVELOPMENT FOR THE SIMULTANEOUS MICROBIAL PRODUCTION OF *n*-BUTANOL AND 1,3-PROPANEDIOL

Vom Promotionsausschuss der
Technischen Universität Hamburg-Harburg

zur Erlangung des akademischen Grades

Doktor-Ingenieurin (Dr.-Ing.)

genehmigte Dissertation

von

Christin Prescher (geb. Groeger)

aus

Schwedt/Oder

2018

Erster Gutachter: **Prof. Dr. An-Ping Zeng**

Zweite Gutachterin: **Prof. Dr.-Ing. Irina Smirnova**

Mündliche Prüfung: **23.02.2018**

Abstract

The increasing demand of fuels and chemicals, whilst fossil resources diminish, arouses the interest in new biotechnological processes using renewable resources. *Clostridium pasteurianum* is a newly established chassis for the production of two important bulk chemicals: *n*-butanol (BuOH) and 1,3-propanediol (1,3-PDO). The bacterium is able to use glycerol as well as glucose as carbon sources, which can be received from renewable biomass. Although it is known that the selectivity of either BuOH or 1,3-PDO and the loss of carbon atoms in side products is mainly influenced by the cultivation conditions, it is not sufficiently clarified how the mechanism works and how it can be influenced. Furthermore, its growth and product formation rate are ultimately limited by the accumulation of inhibiting products, especially by BuOH itself. Therefore quantitative physiological analysis, proteomic and bioengineering approaches were used to overcome these drawbacks and to further optimize the simultaneous production of both target products.

The reduction degree of the utilized substrate was found to have a significant effect on the product profile. Glycerol and glucose as well as mixtures of both have been analyzed. Increasing the glucose content supported growth and acids formation, whilst 1,3-PDO formation decreased. For the simultaneous production of both, BuOH and 1,3-PDO in high product titers, a mixture of glucose and glycerol was used. The usage of raw substrates and cultivation under unsterile conditions showed no limitation of process performance in lab and pilot scales studies. At pilot scale the simultaneous production of 13 g/L BuOH and 18 g/L 1,3-PDO was achieved. Product formation by *C. pasteurianum* was also influenced by the iron content in the growth medium. Whereas BuOH and 1,3-PDO are both produced under iron excess condition, iron limitation strongly limits the formation of BuOH and hydrogen. Proteomic analysis revealed an up-regulation of pyruvate:ferredoxin oxidoreductase, hydrogenases, as well as electron transfer flavoproteins under iron excess conditions, which are all involved in the conversion of ferredoxins. Redox balance studies showed the involvement of an additional H_2 formation route in *C. pasteurianum* that is coupled to the ferredoxin-dependent conversion of crotonyl-CoA to butyryl-CoA, which significantly affects product selectivity. Manipulation of redox conditions was also tested in electrobioreactors. In the applied range of +500 mV till -500 mV no significant effect on the growth and product pattern was observed. On the other hand, addition of the redox active dye Brilliant Blue R250 (BB) showed a positive effect on growth and target products formation, while fewer acids were produced. The optimized supplementation of BB resulted in a substrate yield of 0.44 $g_{BuOH+1,3\text{-}PDO}/g_{glycerol,}$ which is the highest yield achieved in this work. For further improvement of process performance, and to overcome the inhibitory effects of BuOH, *in situ* gas stripping was implemented in the fermentation process. At first, the type of the stripping gas and the effect of different flowrates on the microbial physiology and product formation were examined. Subsequently the influences of gas flow rate and stirrer speed were analyzed regarding their effects on the volumetric mass transfer coefficient of BuOH, BuOH selectivity and the general fermentation performance. Finally an optimized bioprocess for the simultaneous production of BuOH and 1,3-PDO was established, suitable for the prospective application in biorefineries. The best results could be achieved in a fed-batch cultivation on pure glycerol and with gas stripping by fermentation gases, which resulted in the simultaneous production of 39 g/L BuOH and 53 g/L 1,3-PDO.

Identifier

DOI: https://doi.org/10.15480/882.1666

Handle: http://tubdok.tub.tuhh.de/handle/11420/1669

Other: urn:nbn:de:gbv:830-88221152

Jegliches hat seine Zeit,
Steine sammeln - Steine verstreun´.
Bäume pflanzen - Bäume abhaun´,
Leben und Sterben und Frieden und Streit.

(Wenn ein Mensch lebt, Phudys, 1973)

Acknowledgements

First and foremost I would like to thank my academic advisor, Prof. Dr. An-Ping Zeng, for accepting me in his group and giving me the opportunity to work in this project. I dearly appreciate all contributions in form of ideas, discussions, revisions, and understanding in difficult times, to finally complete this thesis.

Additionally I would like to thank Prof. Dr.-Ing. Irina Smirnova for her effort as reviewer of this thesis.

I am especially grateful for the support of Dr. Wael Sabra throughout the whole time. Thank you for every fruitful discussion, explanations and encouraging words.

Moreover, I would like to thank Dr. Wei Wang for the help and collaborative work on the proteomic analysis and beyond.

I also like to thank Dr.-Ing. Dirk Holtmann for the chance to work in his research group "Biochemical Engineering" at DECHEMA e.V. and the kind help of Thomas Krieg.

This work was developed within the European project "EuroBioRef" (European Multilevel Integrated Biorefinery Design for Sustainable Biomass Processing) and financially supported by the European Union Seventh Framework Program (FP7/2007-2013) under grant agreement no. 241718. I like to thank the European Union and all supporting partners from the "EuroBioRef" project.

Most of all would like to thank Simon Prescher for his endless love and moral support throughout the whole time of my work and beyond. I dearly thank Theresa Prescher for the eternal source of smiles and happiness. I thank my family and friends for every lovely word and wordless help.

Many results described in this thesis were accomplished with the kind help and support of all my Bachelor students, Master students, Project workers and HiWis.

And last but not least thanks to all colleagues, that became friends, for the great time in the Institute!

Alberto Robazza
Anna Gorte
Anke Trautwein-Schult
Anibal Mora
Birgit Stacks
Enrico Hans
Jan Bomnüter
Johannes Kern
Merve Öner
Olaf Schmidt
Raoul Schuler
Sugima Rappert
Trinath Pathapati
Uwe Jandt
Vignesh Samapath

Table of content

Abbreviation list

1,3-PDO	1,3-propanediol
3-HPA	3-hydroxypropionaldehyde
A	area
ABE	acetone–butanol–ethanol
adhE	aldehyde/alcohol dehydrogenase
ADP	adenosine diphosphate
ATP	adenosine triphosphate
BB	Brilliant Blue R250
BES / BER	bioelectrochemical systems / reactors
BH	biomass hydrolysate
BM	biomass
BuOH	*n*-butanol
c	concentration
c_{CL}	heat capacity of cooling liquid [J/(kgK)]
CDW	cell dry weight [g/L]
CoA	coenzyme A
d_m	diameter [m]
DS	downstream processing
EtOH	ethanol
F1,6B	fructose-1,6-biphosphate
Fe+, Fe-	iron excess or iron limited condition
$Fd_{red / ox}$	ferredoxin reduced / oxidized
FG	fermentation gases
Glu	glucose
Gly	glycerol
GMO	genetically modified organism
GS	gas stripping
H_2	molecular hydrogen
H_{ij}^{cp}	Henry´s coefficients of component i in component j [mol/m^{3}Pa]
h_i	specific enthalpy of a component i
HPLC	high performance liquid chromatography
IBC	intermediate bulk container
k	thermal transmittance coefficient
k_{Hij}^{px}	Henry´s coefficient of component i in component j [Pa]
$K_S a$	volumetric mass transfer coefficient for stripped compounds [h^{-1}]
$\dot{m}_i$	mass flow of component i [kg/s]
MEC	microbial electrolysis cell
Med	mediator
MFC	microbial fuel cell
MO	microorganism
mol%	molar percent
MV	methyl viologen
N_2	nitrogen
NAD^+	oxidized nicotinamide adenine dinucleotide
NADH	reduced nicotinamide adenine dinucleotide
$NADP^+$	oxidized nicotinamide adenine dinucleotide phosphate
NADPH	reduced nicotinamide adenine dinucleotide phosphate

NR	Neutral Red
OD	optical density [-]
PFOR	pyruvate-ferredoxin oxidoreductase
PFL	pyruvate formate lyase
p_i	partial pressure of compound i
$\dot{Q}$	heat flow [W]
RCM	Reinforced Clostridial Media
RP	redox potential
RID	refractive index
r_P	product formation rate [g/(Lh)]
r_s	stripping rate [g/(Lh)]
r_{SU}	substrate consumption rate [g/(Lh)]
rpm	rotation per minutes [1/min]
RT	room temperature [K]
SHE	standard hydrogen electrode
T	temperature [K]
t	time [s]
UV	ultra violet
w	weight fraction [-]
w-%	weight percent [-]
w/v	weight per volume [g/L]
V	Volume [m³]
$Y_{i/j}$	yield of i over j [g/g]

Indices

P	product
S	substrate
X	biomass
i	variable compound

Greek Symbols

α	selectivity [-]
γ_i	activity coefficient [-]
Δ	difference
κ	degree of reduction [-]
μ	growth rate [1/h]
ϕ_i	fugacity coefficient [-]

1 Introduction and objectives

The future depletion of crude naphtha and therefore fluctuating cost for petrochemical derived products arouses the necessity for new independent processes. One solution for material economy represents biorefineries, where a variety of renewable biomass delivers the carbon backbone for fuels and chemicals, produced in biotechnological conversion reactions. Known biorefineries processes produce multiple products, take advantage of the various components in biomass and therefore maximizing the value derived from the biomass feedstock. Biodiesel and bioethanol are chemicals with a successful integration into society as alternatives of petrol-derived transport fuels.

The alcohol *n*-butanol (BuOH) is considered as a new high potential candidate for biomass-derived fuels. It attracted more and more attentions as it can be easily utilized in existing technologies and exhibits outstanding properties compared to bio-ethanol, like higher energy content, higher mixing ratio with diesel and less corrosiveness (Dürre, 2007), (García et al., 2011), (Branduardi et al., 2014). Another example for biotechnological produced chemicals with high value and an increasing global market is 1,3-propanediol (1,3-PDO), a versatile monomeric precursor for polyesters, polyether and polyurethanes. For example, its derivate polytrimethylene terephthalate (PTT) can be processed into fibres, suitable for the production of biodegradable apparel or carpets (Lee et al., 2015).

So far both chemicals are still also produced petro-chemically, but besides prospective limited resources, these processes require high temperature, high pressure, and expensive catalysts from (semi-) precious metals. The microbial cell factories most extensively studied for the production of these chemicals belong to the *Clostridium sp.* For example *C. butyricum* and *C. acetobutylicum* were used for the production of either 1,3-PDO or butanol, sometimes at commercial scale in the ABE (acetone-butanol-ethanol) process. Due to the current low process performance and the high substrate costs, the production cannot outperform the chemical synthesis process and reduce the chances of broad established biorefinery process for these products.

The bacterium *Clostridium pasteurianum* is a natural microbial chassis for the production of both chemicals, BuOH and 1,3-PDO, in one process due to unique features compared to other industrial *Clostridium* strains. C*. pasteurianum* can convert a wide range of substrates and shows robust growth in simple media, even under moderate and unsterile process conditions (Kaeding et al., 2015). Therefore, it has received considerable interests for the simultaneous production of both chemicals from renewable, non-food sources like raw glycerol, a side product from biodiesel production or glucose containing biomass hydrolysates from agricultural and forestry waste (Kao et al., 2013), (Groeger et al., 2016), (Jensen et al., 2012b), (Lee et al., 2015), (Sabra et al., 2016).

For the simultaneous production of both chemicals several aspects have to be further optimized. One example is to understand the product selectivity of either 1,3-PDO or BuOH, and their dependence on varying cultivation conditions. Additionally, and for the further increase of product yield, several fermentative side products should be minimized. The side products of *C. pasteurianum* include ethanol and organic acids, which not only represent loss of carbon atoms but also hamper downstream

processing, due to a final multi-component mixture present in the fermentation broth. However, similar to the older ABE process, the major hurdle in such bioprocess is the growth limitation caused by BuOH toxicity, which leads to low product titres and reduced productivities. Altogether, the low BuOH concentration at the end of fermentation result in cost intensive separation techniques and thus a reduced economic feasibility of a possible biorefinery process to compete with petrochemical production. Different approaches were used to overcome this hurdle: One solution represents further genetic engineering of strains with increased BuOH tolerance or the metabolic engineering of new pathways in resistant hosts (Branduardi et al., 2014). Another approach is based on process engineering, where BuOH is removed *in situ* from the fermentation broth to reduce inhibition and simultaneously separates the product. So far several downstream processing techniques for the recovery were investigated by different groups, for example liquid-liquid extraction (Groot et al., 1990), salting out extraction (Sun et al., 2013), adsorption (Nielsen and Prather, 2009), (Barski et al., 2012), or pervaporation processes with incorporated ionic liquids (Heitmann et al., 2012). Despite the efforts, most of them are hardly industrially applicable or suitable for *in situ* processes, due to membrane fouling, toxicity of solvents and removal/binding of important broth components. These impairments can be avoided by gas stripping as an *in situ* removal technique (Ezeji et al., 2003). The influences of gas stripping, especially the type of gases, on the growth and metabolism of the production strains have been seldom systematically studied.

Objectives

The objective of this work is the development of a basic biorefinery process for the simultaneous production of *n*-butanol and 1,3-propanediol with enhanced process performance, using *C. pasteurianum* growing on regenerative carbon sources. Hence, the specific objectives were as follows:

- Investigation of the effect of raw substrates on process performance and product selectivity. At first different substrates with different reduction degree, namely glycerol and glucose, were analyzed individually in mono as well as co-substrate fermentation. Besides the lab scale experiments with substrate mixtures and raw substrates (raw glycerol and biomass hydrolysates) further cultivations were also conducted in semi-pilot scale and pilot scale.

- Performance of an in-depth study to explain the effect of iron availability on product selectivity and the underlying mechanisms of pathway regulation. Therefore stoichiometric, kinetic and proteomic analyses were performed.

- Examination of the possibility to enhance the productivity by deriving additional reducing power from chemical mediators and/or from electrical current in electro-bioreactors. The effect of different redox active compounds on the growth and product formation of *C. pasteurianum* were analyzed and the utilization of the most effective dye was further optimized. Additionally the performance of *C. pasteurianum* cultivated in electro-bioreactors with different potential and with/without mediator was investigated.

- Definition of different parameters for an efficient *in situ* BuOH removal by gas stripping in growing *C. pasteurianum* cultures. In particular, the influence of gas type and gas flow rate on the product formation of *C. pasteurianum,* grown on varying substrates was analyzed. The study includes also the characterization and optimization of the BuOH mass transfer coefficient (K_Sa) and the BuOH selectivity under different process conditions.

In conclusion, an optimized bioprocess for the simultaneous production of both chemicals was established that ensures high product titers of 1,3-PDO together with the formation and separation of increased amounts of *n*-butanol.

2 Theoretical and technical background [1]

2.1 Biorefineries

The fundamental task for future industry is the change of petroleum-based processes into sustainable processes from local and renewable resources to overcome increasing public demands of energy and material supply. Renewable energy can be received from different sources like solar power, water or wind, but material economy mainly depends on the carbon inherent in biomass (Kamm and Kamm, 2004). According to this, biorefineries use a variety of biomasses for the carbon backbone generation, to refine a variety of chemicals and fuels. The main goal is to produce high-value low-volume (HVLV) chemicals for profit and low-value high-volume (LVHV) biofuels for public issues, but also for itself to work autonomic (Melero et al., 2012). Biodiesel and bioethanol are perfect examples for a successfully integration in society as alternatives of petrol-derived transport fuels (Serrano-Ruiz et al., 2012). Analogous to conventional refineries, biorefineries consist of unit operations. One main part is the up-stream, including the pre-treatment of the biomass to unlock the desired substrate components. This is followed by a thermic, catalytic or fermentative conversion of substrates into the desired products. In the downstream processing the products are separated and purified, according to their final application. However, since a lot of different biomass types exist, every biorefinery is unique and works with different units.

Plant biomass typically consists of 75 % carbohydrates, 20 % lignin and 5 % compounds like lipids and proteins, which contain further molecular building blocks, suitable for biorefinery processing (Fig. 2-1) (Kamm and Kamm, 2004). Separation of plant biomass generally provides three main process streams: carbohydrates, in the form of starch, cellulose, hemicellulose and monomeric sugars; lignin, a strong network containing aromatics; and lipids (hydrocarbons), in the form of plant triglycerides. On the contrary algae biomass contains no lignin, 10 % carbohydrates and up to 75 % lipids, which offers great potential for oleo-chemicals (Serrano-Ruiz et al., 2012). Proteins might be part of the biomass feedstock, like in protein rich grains or algae, but the percentage is very low. Protein rich residues are usually used at the very end of the process line and mostly converted via fermentation into biogas or will be directly used as animal feed.

The cost of biomass (BM) depends on regional supply, but in general it increases in the following order: cellulosic BM < starch/sugar BM < triglyceride-based BM. The cost of conversion technology is vice versa, since existing technologies from petro-chemistry can be adapted easily to oleo-containing BM (Huber and Corma, 2007). Currently the aim is to replace intermediates of petrochemical routes by bio-based ones and feed them into existing technologies. This reduces economical risks and development time of new biorefinery processes. Nevertheless it should be kept in mind that today (bio) refineries aim to degrade big molecules into monomers to build up new intermediates. At the same time this means a waste of energy already stored in the high molecular complexes. Instead of just replacing crude oil with biomass, new integrated conversion processes of complex molecules are needed to save energy and to

[1] Parts of this chapter are based on Groeger et al. (2015) and Sabra et al. (2015).

ensure an optimal and sustainable usage of natural resources (Preisig and Wittgens, 2012). The biological conversion of complex molecules like starch, glucose, glycerol or lignin by enzymes or bacteria represents such alternative conversion.

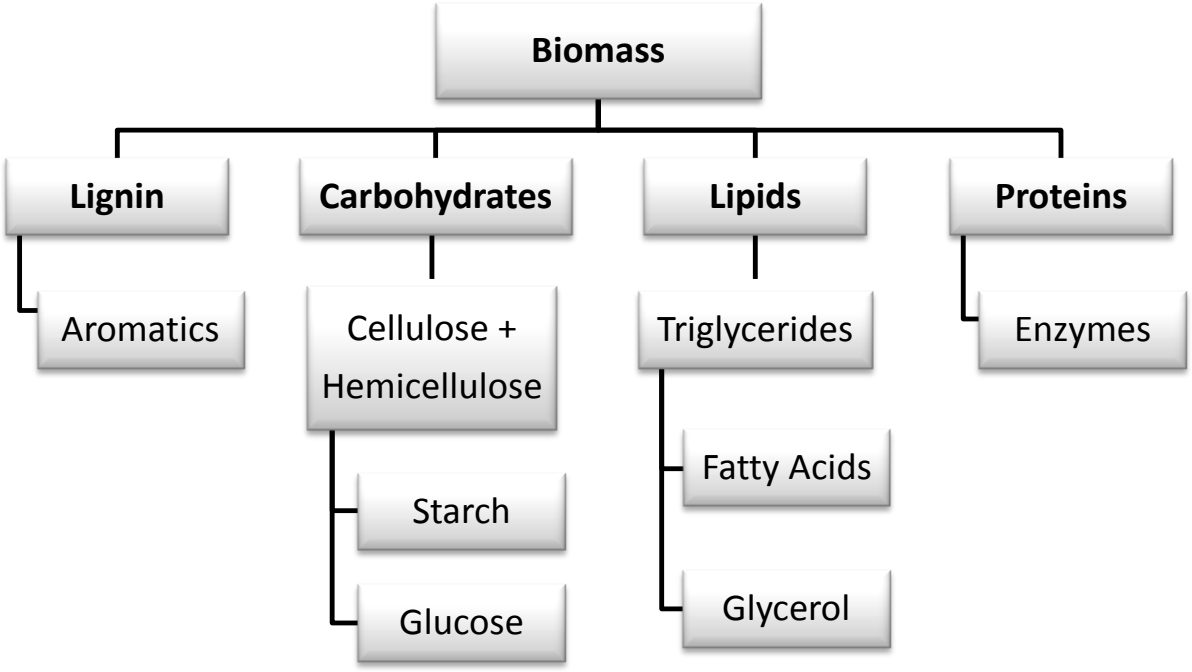

Fig. 2-1: Different basic precursors in biomass suitable for the conversion in biorefineries. The fractions vary according to the type of biomass. (Figure partly from Groeger et al., 2015).

2.1.1 Lipids and glycerol

Many plants contain lipids, but the highest potential as renewable carbon source regarding content and agricultural application possess sunflower, safflower, soybean, cottonseed, rapeseed, canola, corn and peanuts (Huber and Corma, 2007). To avoid the competition with food crops, low quality waste oils (e.g. from restaurants or animals) as well as oil from non-edible plants like *Jatropha* and *Camelina* or algal oil are to be preferred for biorefinery processes (Serrano-Ruiz et al., 2012). Plant lipids contain free fatty acids, triglycerides, but also terpenes, terpenoids, alkaloids, and waxes. Triglycerides are the main component of oleaginous feedstock, which consists of glycerol (1,2,3-propanetriol) esterified with long alkyl-chain fatty acids. The fatty acids (FA) have got a length between C8 and C20, whilst C16, C18 and C20 are most common. It is worth mentioning that FA molecules exhibit one of the highest H/C atomic ratios in biomass, combined with low oxygen content, which make them an attractive precursor for fuels and LVHV chemicals (Melero et al., 2012).

A main part of plant triglycerides are converted to biodiesel in a homogenous transesterification reaction. Under mild temperatures (50 - 80°C), with methanol as reactant and a basic catalyst, a mixture of fatty methyl esters (FAME) is formed, which is used as biodiesel. The residual glycerol appears as a 10 % side product and is subsequently separated from the biodiesel by decantation (Serrano-Ruiz et al., 2012). After distillative purification with grades above 99.5 % it can be used as a HVLV in pharmaceutical or cosmetic industries, as long as the market price is high enough (Lee et al., 2015). On the other hand, glycerol holds the potential of being an extremely versatile building block within biorefinery processes and it also represents a suitable substrate for microorganism like C*lostridium sp.*

or *Klebsiella sp.* The usage of crude glycerol for fermentation arouses increasing interest, if its global market price drops and it can be considered as a LVHV side product in biodiesel production. Crude glycerol is not further purified after decantation, thus it is cheaper. However, besides 40-50 % glycerol it contains impurities such as methanol, fatty acids, soaps, salts, water and heavy metals (Chatzifragkou and Papanikolaou, 2012). Thus, a pre-treatment to remove the inhibitory compounds might be mandatory (Drożdżyńska et al., 2011). Among several pretreatments analyzed, like acidification (Asad-ur-Rehman et al., 2008), carbonation or electrodialysis, the combination of activated carbon and simple storage for 10 month was the most effective and cheapest solution (Jensen et al., 2012a). The term raw glycerol or crude glycerol is sometimes used for different stages of the purification, but no clear definition exists.

Until 1999 glycerol was mainly produced from petrochemicals, but already 2009 biodiesel companies became the main supplier (Ciriminna et al., 2014). At the moment the EU is the largest producer of biofuels, with up to 70 % biodiesel and 28 % bioethanol (Abdelradi and Serra, 2015). But developments in the biodiesel market have a huge impact on the availability and use of glycerol. Since the biodiesel production strongly increased in the end of the last century, glycerol became a low cost and available substrate for biotechnological conversion. At the same time the glycerol prices for refined glycerol (99.5 % purity) decreased from 4000 €/t in 1995 to 450 €/t in 2010 in the EU and US market. Crude glycerol (~80 % purity) was even considered as waste stream with no value, which made it an attractive building block for the biorefinery (Ciriminna et al., 2014). Nowadays the European biodiesel production stagnates due to decreasing prices for petroleum (Fig. 2-2), even though at a high level between $8*10^6$ - $10*10^6$ t/y between 2010 and 2013 [2]. This led to glycerol prices around 450 €/t for pharmaceutical grade and 200 €/t for crude glycerol in early 2015 [3].

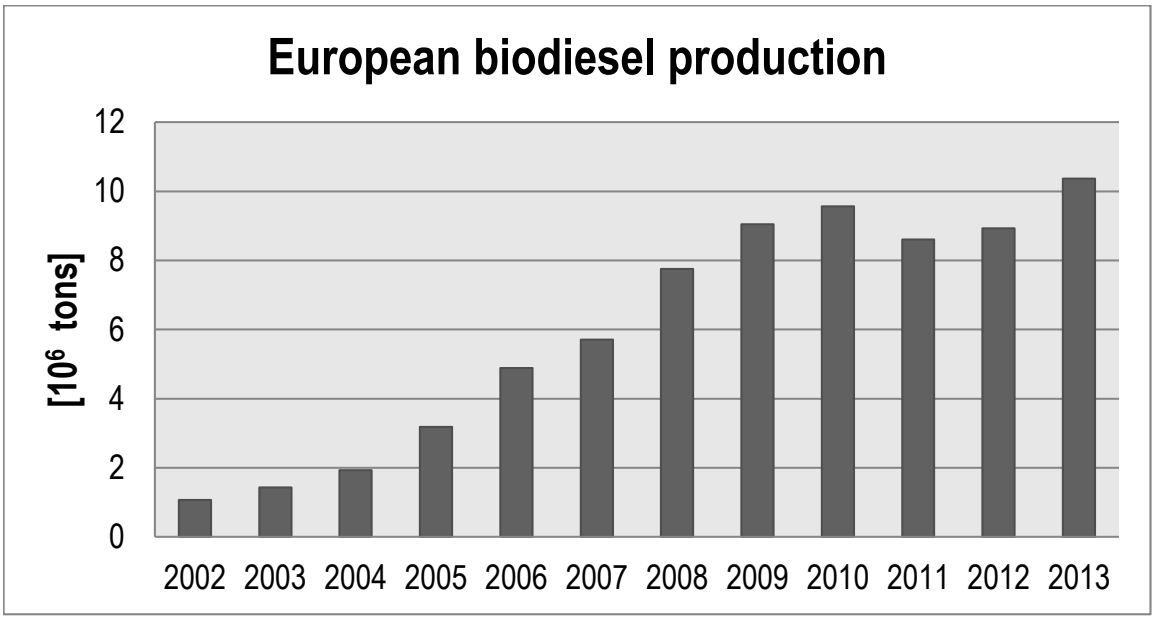

Fig. 2-2: Annual European production of bio-based glycerol. (Data from [2]).

[2] http://www.ebb-eu.org/stats.php, 08.09.2017

[3] https://mediathek.fnr.de/grafiken/daten-und-fakten/preise-und-kosten/preise-glycerin-interaktiv.html, 08.09.2017

2.1.2 Glucose

Carbohydrates in form of cellulose and hemicellulose represent the main components of plants. They arouse high interest due to their beneficial applications in various agro-industrial processes, including efficient conversion of cellulosic biomass to fuels and chemicals via fermentation (Saha, 2003). Cellulose is an unbranched homopolymer of D-glucose monomers, linked by β-1,4-glycosidic bonds. Hemicelluloses are heterogeneous polymers consisting of pentoses (D-xylose, D-arabinose), hexoses (D-mannose, D-glucose, D-galactose) and sugar acids. Xylans and glucomannans are the common compounds of hardwood or softwood, respectively (Kumar et al., 2008). Several cracking methods are well studied to break the macromolecules into its basic structures of hexoses and pentoses. These degradation products can be produced from agricultural waste streams and thus represent a cheap, non-food carbon source for biotechnological processes. Glucose is a key intermediate for the energetically profitable bio-formation of various chemicals, like bio-ethanol, bio-butanol, acetone, lactic or itaconic acid as well as amino acids, e.g. glutamine, lysine, tryptophan (Kamm and Kamm, 2004).

Degradation processes

The first pretreatment step of lignocellulosic biomass disintegration into hemicellulose and cellulose prior enzymatic hydrolysis has to be considered carefully and with regards of costs and further applications. Thermo-mechanical methods like milling, grinding, shearing or extruding are among the first steps. Further degradation techniques are based on chemical or thermal treatment, e.g. fractionation with acids (H_2SO_4, HCl), alkalis (NaOH, H_2O_2, NH_3), organic solvents (MeOH, EtOH, phenols), CO_2 or ammonia fiber explosion, but also pyrolysis, steam explosion or hot water treatment (Saha, 2003), (Kumar et al., 2009). These pretreatments mostly require high temperatures from 100°C-270°C to provide water soluble sugars, but conversion rates up to 100 % can be reached (Kumar et al., 2009). However, resulting phenolic compounds, like furan derivatives and aliphatic acids, are possible inhibitors for microorganisms. Hence, ion-exchange resins, charcoal, ligninolytic enzymes, or removal of non-volatile compounds by extraction, alkali or sulfite treatment are suitable methods developed for the detoxification of hydrolysates (Saha, 2003).

Another possibility is the enzymatic degradation, which sometimes might require a prior mechanical or thermal disruption. Cellulose hydrolyzing enzymes can be divided in three groups: endoglucanases, cellobiohydrolases (exoglucanases), and β-glucosidases (Kumar et al., 2008). The first splits internal bonds of the polymer randomly, whereas the second one attacks only the ends and release cellobiose, which are two linked glucose molecules. These are subsequently cleaved to glucose by the β-glucosidases (Kumar et al., 2008). Hemicellulose has to be degraded by several enzymes with different specifities. E.g. xylan is cleaved by endo-1,4-β-xylanase, β-xylosidase, α-glucuronidase, α-L-arabinofuranosidase and acetylxylan esterase (Saha, 2003). The cellulytic enzymes are mostly gained from fungi like *Trichoderma viride, Fusarium oxysporium, Penicillium echinulatum, Aspergillus niger* and *A. fumigates* or bacteria like *Rhodospirillum rubrum, Clostridium stercorarium, Bacillus polymyxa,* and *Pyrococcus furiosus* (Kumar et al., 2008). One major hurdle is the crystalline structure of cellulose, which is more resistant to microbial and enzymatic degradation compared to the amorphous structure. The hydrolysis process of lignocellulosic biomass runs at ambient temperatures around 50°C-70°C as well as pH 4-5. The resulting mixtures of sugars are mostly a viscous liquid with low pH, which need to be diluted and adjusted prior usage as fermentation substrate.

Large scale production

In 2012 several companies were running biorefinery processes from lignocellulosic biomass. Borregard Industries Ltd. possess a demonstration plant using spruce pulp with a capacity of 15.8 kt/a. The company Inbicon (Dong Energy) uses wheat straw as substrate with a capacity of 4.3 kt/a. In Germany also wheat straw is used by the Süd-Chemie AG for a refinery with a capacity of 1 kt/a. Commercial plants with capacities 60-75 kt/a are Beta Renewables (Chemtex) in Italy, Abengoa Bioenergy and POET-DSM Advanced Biofuels in the USA (Waldron, 2014). In 2014, Biochemtex and Beta Renewables announced the construction of a new plant with Energochemica SE, which is a cellulose-based refinery with a capacity 55 kT/a, for the combined production of ethanol, power, and steam [4].

2.2 The products *n*-butanol and 1,3-PDO

2.2.1 *n*-Butanol

The chemical *n*-butanol (1-butanol) is a 4-carbon primary alcohol, which appears as clear liquid with an ethanol-like odor. It is completely soluble in organic solvents, but shows a miscibility gap in water above concentration of 7.7 w-%, which results in the formation of a biphasic mixture (Weast, 1980). Further physical and chemical properties are summarized in Table 7-1 in Appendix.

The solvent butanol is known as an important intermediate for bulk chemicals as well as diluents for several applications (Dürre, 2007). Nowadays nearly 50 % of produced BuOH is converted into acrylates and 25 % into glycol ethers. It can be also used directly as a solvent or plasticizer for many applications in chemical and pharmaceutical industry (Harvey and Meylemans, 2011). Recently BuOH raises increasing interests as an advanced biofuel that can contribute to the worldwide growing demand. Several advantages outperform ethanol as bio-fuel. Butanol possesses a 30 % higher energy content, it is less hygroscopic, has higher mixing ratio with gasoline or diesel, and can be converted into aviation fuel. Besides that it is less corrosive and shows a lower vapor pressure, which makes it a safer fuel for many applications. On the other hand it is very similar to conventional fuels, thus it can be used in existing facilities and engines without mechanical alterations (Dürre, 2007), (García et al., 2011), (Branduardi et al., 2014), (Becerra et al., 2015).

Chemical Production

Nowadays the chemical industry uses two main processes for the production of *n*-butanol, which are based on the conversion of petroleum (Fig. 2-3), (Lee et al., 2008).

Hydroformylation (oxo synthesis): The most important petrochemical process uses carbon monoxide and hydrogen that dock to the double bounding of propene by means of copper, rhodium or ruthenium catalysts. The resulting butyraldehyde is transformed via catalytic hydrogenation into butanol. This homogenous catalyzed reaction is performed at high temperature (150-200°C) and high pressure (50-300 bar) (Chauvel et al., 1989), (Hahn et al., 2013).

[4] http://www.biofuelsdigest.com/bdigest/2015/01/15/beta-renewables-biofuels-digests-2015-5-minute-guide/, 08.09.2017.

Reppe Synthesis: The Reppe process equals the hydroformylation, except that the molecular hydrogen is substituted with water vapor. Therefore, additional carbon dioxide is produced, but the process conditions are more economical with 100°C and 5-20 bar (Chauvel et al., 1989). However, this process has never been so successful, due to expensive technologies. In both processes, hydroformylation and Reppe synthesis, the by-product 2-methylpropanol (MP) is formed (Fig. 2-3). Improvement of catalyst like modified Rh-catalysts can shift the formation rates from 75:25 (BuOH:MP) to 95:5. (Chauvel et al., 1989), (Hahn et al., 2013).

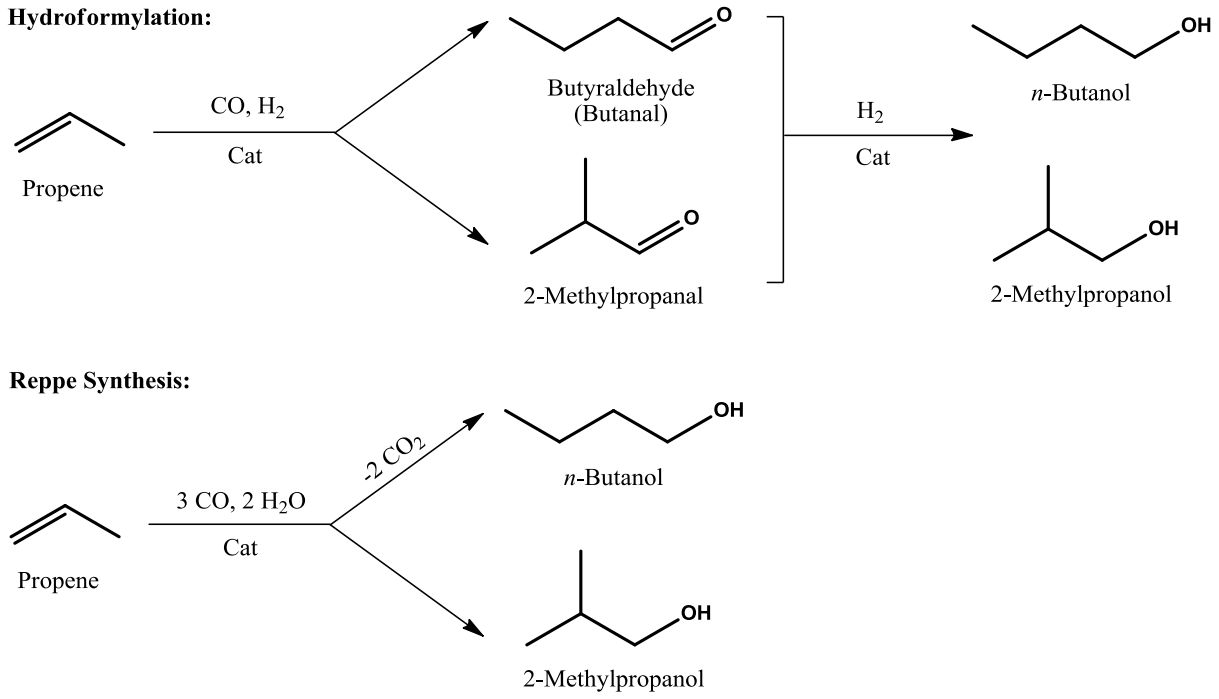

Fig. 2-3: Hydroformylation and Reppe Synthesis for the chemical production of *n*-butanol.

Biological Production

The future depletion of fossil resources together with increasing impacts on ecology forces industry to new processes from renewable resources. The fermentative production of butanol and other solvents are well known processes from the beginning of the 20th century. For example, the production of the solvent mixture acetone, butanol, and ethanol (ABE) with *Clostridium acetobutylicum* is one of the oldest biotechnological large scale processes (Jones and Woods, 1986). The production was developed by Chaim Weizmann in the 1910´s to overcome the increasing demands of acetone during the First World War (Chauvel et al., 1989). The classical ABE fermentation was performed as ~50 h batch fermentation, using corn or molasses as substrate. Butanol was produced with a maximum of 14 g/L and a yield of 0.26-0.33 g/g substrate. The solvents were subsequently recovered by distillation.

Some *Clostridium* sp. are well known producers of BuOH and to overcome the first hurdle by avoiding food crops as carbon source. Different substrates were analyzed for efficient conversion processes. For example, several studies report the successful growth of solventogenic *Clostridium* on hexose and pentose hydrolysates from wood and agricultural waste stream, like rice straw (Gottumukkala et al., 2013), wheat straw (Qureshi et al., 2007), (Valdez-Vazquez et al., 2015), maple beech and birch wood

pulp (Lu et al., 2013), or cassava bagasse (Lu et al., 2012). Even though in conflict with comestible goods, ABE solvents can also be produced by the fermentation of sago starch (Madihah et al., 2001) or potato starch (Grobben et al., 1993). Untreated waste streams from food production, like cheese whey (Becerra et al., 2015) or apple pomace (Voget et al., 1985), can be fermented by these bacteria. *Clostridium sp.* are mostly known for sugar fermentation, but they are also able to convert glycerol, a side product from biodiesel production (Biebl, 2001), (Clomburg and Gonzalez, 2013). The advantage of this carbon source is the natural high reduction degree of glycerol. Another interesting approach is the usage of algal biomass as substrate producer. The algae *Dunaliella* fixes carbon dioxide and converts it into glycerol. With some additional glycerol (4 %), *C. pasteurianum* was able to grow on the algal biomass and produce butanol together with 1,3-PDO (Nakas et al., 1983).

The general pathway of *Clostridium sp.* to form BuOH is given in Fig. 2-4 A. At first glucose is transformed into pyruvate via glycolysis under the formation of ATP and NADH. Pyruvate is subsequently degraded to acetyl-CoA, the main intermediate to form biomass, organic acids, like acetic butyric or lactic acid, as well as the solvents EtOH, BuOH or acetone. The fermentation profile of many solventogenic *Clostridium sp.* is divided into two phases: acidogenesis, in which acids and cell biomass are produced, followed by solventogenic phase, in which solvents are formed. *Clostridium sp.* can also convert glycerol as a main carbon source. In this case no such generic phase separation was observed (Sabra et al., 2014). A collection of BuOH titers and productivities performed by different *Clostridium sp.* can be found in Table 2-1. Another natural producer of butanol, besides other alcohols, is the yeast *Saccharomyces cerevisiae (*Fig. 2-4 B). In the Ehrlich pathway amino acids are transformed into keto acids and further decarboxylated into aldehydes. Butyraldehyde is reduced to *iso*-butanol, which differs from *n*-butanol in its isomeric structure. However, the production rate is very low, due to conversion of growth important amino acid, which impedes industrial application (Hazelwood et al., 2008), (Becerra et al., 2015).

Until today there are three major hurdles of biological BuOH producing process to compete successfully with the chemical production (Lee et al., 2008): (I) high costs of substrates (II) relatively low final product concentrations, and resulting from this (III) high product recovery costs. The high costs of substrate could be overcome by the usage of agricultural waste streams for the production of sugar containing hydrolysates or the utilization of biodiesel derived glycerol. The second hurdle of butanol fermentation, the low product titer, results from the fact that butanol is toxic to the bacteria itself. It was observed that already concentrations above 5 g/L lead to growth cessation. One possibility is the genetically enhancement of solvent tolerance, which was successfully studied by Jia et al. with *C. acetobutylicum* (Adams et al., 1989) or the inclusion of new pathways for BuOH production in different hosts (Becerra et al., 2015), (Branduardi et al., 2014). Another option based on process engineering is the *in situ* separation on BuOH within fermentation. This has the advantage that no genetically modified organisms (GMO) are needed and that the product is already separated on line. This saves process time and facilitates the product recovery. For *in situ* removal of BuOH several techniques have been studied. This part together with the downstream will be further described in Chapter 2.4.2.

Due to the increasing demand of chemicals and fuels, and even though the process needs to be optimized, several companies started producing bio-butanol. In 2008, the global market comprises 2.8 million tons BuOH (ca. $5 billion value) with highest demands in Asia, USA and Europe (Green, 2011). The market research institute “Research and Markets” (USA) released the study “Global Bio-based Butanol Market 2015-2019” (ID 3365757) in July 2015. For the period of 2014-2019 they forecast

an annual growth of 9.3 % of the bio-butanol market. The major driver is the application as sustainable bio-fuel, but the high price of the feedstock is a major challenge. The worldwide most active companies in bio-based butanol production are: Butalco GmbH (Switzerland), Butamax™ Advanced Biofuels LLC (joint venture of BP and DuPont), (Cobalt Technologies – just shut down), Gevo® (USA), Green Biologics Ltd. (UK), Laxmi Organic Industries Ltd. (India), Novozymes® (Denmark), Syntec Biofuel Inc. (Canada), ZeoChem® (Switzerland), Butyl Fuel LLC (USA, part of Green Biologics Ltd.), Cathay Industrial Biotech Ltd. (China), Eastman™ (acquired TetraVitae Biosciences Inc.), and METabolic Explorer S.A. (France). Within the spectra of companies, the process types vary: For example, Butamax™ is based on engineered yeast using corn as substrate for iso-butanol production. On the other hand Gevo® uses genetically engineered *E. coli* to produce up to 50 g/L iso-butanol from corn sugar and beets, since 2013 in a 1000 m³ scale (Elvers and Wagemann, 2014).

Table 2-1: Comparison of BuOH production by different species, substrates and fermentation modes.

Organism	**Substrate**	**Fermentation mode**	**BuOH [g/L]**	**Yield [g/g]**	**Productivity [g/(Lh)]**	**References**
C. pasteurianum	Crude glycerol pretreated	GS, fed batch	25	-	0.68	(Jensen et al., 2012a)
C. pasteurianum	Glycerol	Batch	17	-	-	(Biebl, 2001)
S. cerevisiae (GMO)	Glucose	Batch	1.6 (iso-BuOH)	0.016	-	(Matsuda et al., 2013)
C. pasteurianum (GMO)	Glycerol + 5 g/L yeast	Batch	17.8	0.30	0.43	(Malaviya et al., 2012)
C. acetobutylicum	Glucose	Fixed bed, GS fed batch, 326 h	113	0.24	0.35	(Xue et al., 2012)
C. beijerinckii	Glucose	GS, fed batch, 201 h	152	0.30	0.75	(Ezeji et al., 2004)
C. acetobutylicum	Glucose, Mannose, Arabinose, Xylose (5:1:2:4)	Batch	14.6	0.25	-	(Liao et al., 2016)
C. beijerinckii	Glucose, malt extract +50g/L beef extract	Batch	19.4	0.27	-	(Isar and Rangaswamy, 2012)

GMO = genetically modified organism.

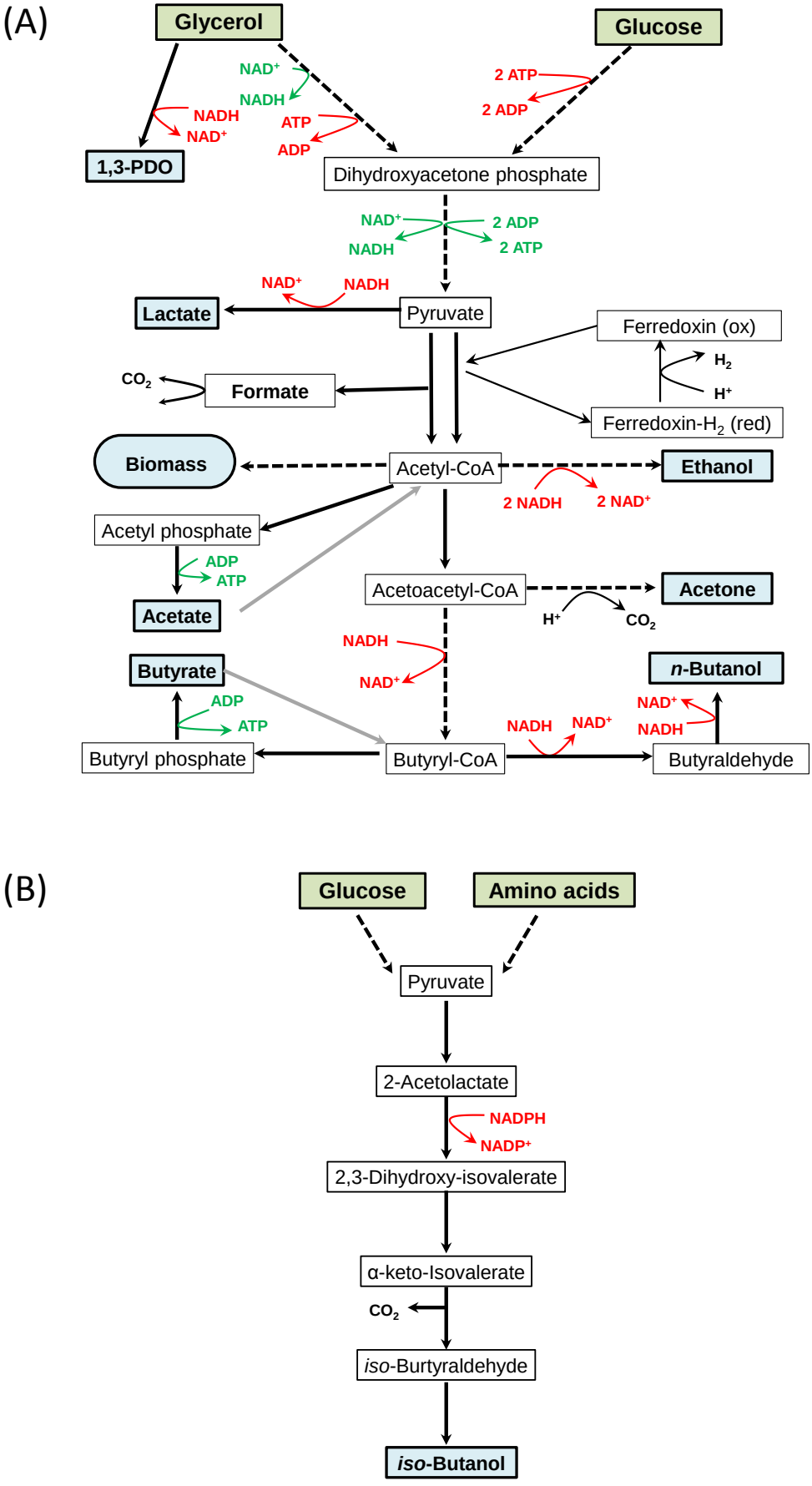

Fig. 2-4: A) General pathway of glycerol or glucose degradation in *Clostridium sp.* B) *iso*-Butanol formation from glucose and amino acids by *Saccharomyces cerevisiae*.

2.2.2 1,3-Propanediol

1,3-Propanediol (also propylene glycol) is a clear colorless organic compound with the molecular formula of $C_3H_8O_2$. It is very hygroscopic and mixes easily with water. Due to the two hydroxyl-groups this diol possess a broad application range. It can be used directly as solvent for adhesive, laminate, resin, detergents and cosmetics (Saxena et al., 2009). Additionally it is a valuable intermediate for many synthesis reactions, in particular as a monomer for polymerization reactions to produce polyesters, polyether and polyurethanes. Especially the production of the polymer polytrimethylene terephthalate (PTT) from 1,3-PDO represents an increasing market. This polymer exhibits suitable mechanical properties, thermal stability and is biologically degradable, which makes it a valuable fiber for applications in textile industry, for carpets and furniture. The global market of 1,3-PDO increases steadily and studies revealed a demand of 60 kT/a in 2012, with a prediction to further 150 kT/a in 2019 (Lee et al., 2015).

Chemical Production

With growing importance of chemicals for industrial applications, the synthetic production of 1,3-PDO, among other diols, was developed based on cheap available petroleum as carbon source. In 1990 two important processes for chemical synthesis have been established by the companies of DuPont / Degussa and Shell (Fig. 2-5), which are still used nowadays.

DuPont / Degussa Process: This two stage process uses water and acrolein as precursors, which react at 50-70°C, mediated by acid catalysts. Within this hydration reaction 3-hydroxypropionaldehyde (3-HPA) is produced. The next stage is a high pressure hydrogenation to form 1,3-PDO, supported by nickel or ruthenium catalysts (Kraus, 2008).
Shell Process: In the hydro formylation process, ethylene oxide reacts with carbon monoxide by means of an organometallic catalyst to 3-HPA. In the next step the hydroxy aldehyde is reduced to 1,3-propanediol. This is enabled by a copper chromite catalyst combined with synthesis gas as the hydrogen source (Kraus, 2008).

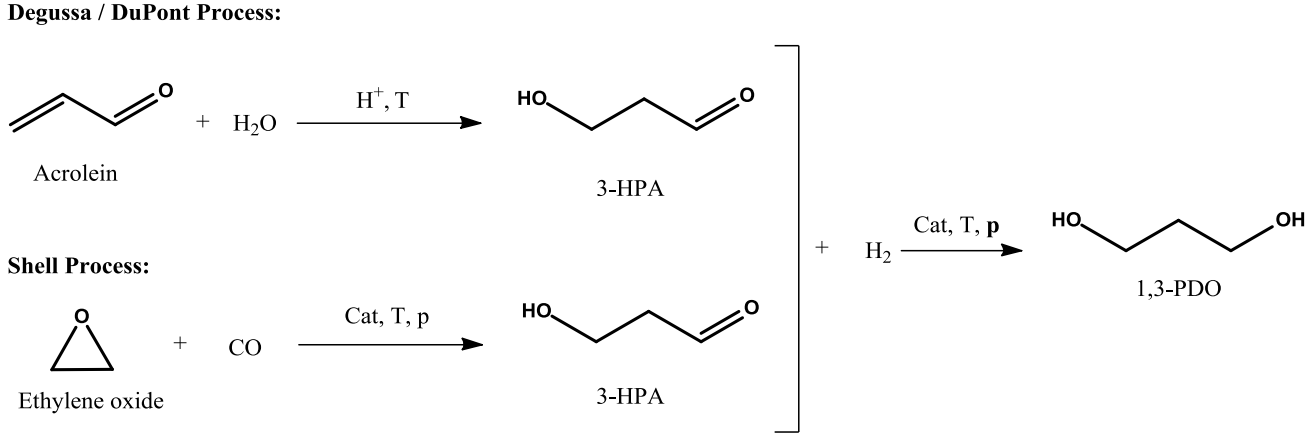

Fig. 2-5: Du Pont / Degussa and Shell process for the chemical synthesis of 1,3-propanediol (Figure according to Kraus, 2008).

Biological productions

Instead of a chemical process to produce 1,3-PDO, fermentative production from abundant raw materials are possible and gain increasing interest. Already in 1881 August Freund, an Austrian chemist, discovered 1,3-PDO as a product of glycerol conversion by a mixed bacterial culture, most likely containing *C. pasteurianum* (Biebl et al., 1999). The diol is a naturally metabolite from anaerobic glycerol fermentations and produced by several bacteria like *Klebsiella*, *Clostridia, Citrobacter, Enterobacter* and *Lactobacillus*. A detailed overview of organisms, substrate and achieved titers can be found in Sabra et al. (2015). The detailed pathway from glycerol in *C. pasteurianum* DSMZ 525 is given in Fig. 4-14.

Among the most-studied organisms are *Klebsiella pneumoniae* and *Clostridium butyricum*. Both show a relatively high substrate tolerance and achieve high yields. Hartlep et al. reported that *K. pneumoniae* produced up to 84 g/L 1,3-PDO and *C. butyricum* up to 86 g/L (Hartlep and Zeng, 2002). Another study analyzed a fed batch fermentation of *C. butyricum* and achieved up to 65 g/L with a yield and productivity of 0.57 g/g and 1.2 g/(Lh), respectively (Saint-Amans et al., 1994). High results also have been reported by Dietz et al. (Dietz and Zeng, 2014) for a *Clostridium* mixed culture, with a 1,3-PDO titer of 70 g/L and a productivity of 2.6 g/(Lh). *Clostridium* species are suitable to ferment raw substrates, which makes this process economically competitive with petro chemical routes. Different studies successfully produced 1,3-PDO in unsterile processes from raw glycerol using either mixed culture (Dietz and Zeng, 2014) or pure culture of *C. butyricum* (Chatzifragkou et al., 2011) and *C. pasteurianum* isolate K1 (Kaeding et al., 2015).

For further improvement of diol production, fermentations with electron transferring mediators or artificial electron supply in bio-electrochemical system (BES) are recently investigated. Zhou et al. analyzed the effect on a mixed population of *Citrobacter, Pectinatus* and *Clostridia*. It could be shown that an electrode potential of -0.9 mV increased the 1,3-PDO yield to 0.5 mol/mol glycerol, compared to 0.25 mol/mol under non polarized conditions (Zhou et al., 2013). Hence, the providing of external reducing equivalents led to increased formation of reduced product, which represents an interesting development. Additionally Choi et al. (Choi et al., 2014) applied a BES on glycerol fermentation by *C. pasteurianum*. However, the electron flow from the cathode was relatively low and the effect on 1,3-PDO production was not significant. In fact, the combination of biotechnology and electrochemical processes for biorefinery applications are still poorly understood and need further investigation (Herrmann et al., 2008).

Another interesting approach of an alternative substrate is the conversion of CO_2 to glycerol and subsequently to 1,3-PDO. Using a co-cultivation of an engineered cyanobacteria and *K. pneumoniae* the final 1,3-PDO titer did not exceed 5 g/L (Wang et al., 2015). Even though the only natural pathway to produce 1,3-PDO comes from glycerol, co-substrate fermentations with other carbon sources are possible. For example, bacteria of the genera *Lactobacillaceae* can ferment an additional substrate for growth and generation of the reducing equivalents. In their study with *L. diolivorans* Pflügl et al. achieved 42 g/L 1,3-PDO from sole glycerol as substrate, but a further increase to 74 g/L by glucose addition and 85 g/L by vitamin B12 and glucose addition (Pflügl et al., 2012). Many of the studied strains were found to produce high amounts 1,3-PDO in the range of 60-70 g/L. However, only addition of growth supporting compounds, like yeast or vitamins led to an increased productivity. Thus, the transfer

of these processes into large scale productions is partially hampered by several problems: I) The high titer results from complex media with expensive components. This not only leads to increased additional costs, but also further difficulties in DS processing. II) Most of the high performance strains are pathogenic, e.g. *Klebsiella*, which represents a large economic impact on equipment and process costs due to safety precautions.

Despite these problems, a few companies established first large scale biorefineries for 1,3-PDO production. So far the biggest producer is DuPont, where an engineered *Escherichia coli* strain converts sugar from starch containing grains into 1,3-PDO. In 2015 DuPont reports the usage of bio-based 1,3-PDO for the production of polyurethane-based leather and other fabrics. The most recent products are Zemea® propanediol for cosmetic, pharmaceutical and nutritional applications as well as Susterra® propanediol as monomer building block for chemical industry [5]. In 2013 also the Chinese company Glory Biomaterial reported the large scale production of bio-based 1,3-PDO for PTT production [6].

2.2.3 Metabolic pathway of *C. pasteurianum* DSMZ 525

C. pasteurianum DSMZ 525 (former ATCC 6013) is a non-pathogenic, spore-forming, Gram positive bacterium, which was isolated in 1891 by Sergei Winogradsky and named in honor of Louis Pasteur (Winogradsky, 1894). The rod-shaped bacterium is the first discovered wild-type organism that has the ability to fix nitrogen from the air. This obligate anaerobe ferments glycerol and/or glucose into the main produces butanol, ethanol, 1,3-PDO as well as acetic, butyric, lactic, and formic acid, though 1,3-PDO can only be produced from glycerol. Besides the liquid products, the fermentation gases hydrogen and carbon dioxide are formed. In contrast to *C. acetobutylicum, C. pasteurianum* does not produce acetone and did not show distinguishable production phases like acidogenesis and solventogenesis when grown on glycerol (Biebl, 2001), (Sabra et al., 2014). Fig. 4-14 shows the main metabolic pathways from both substrates with according enzymes, which will be explained in detail below. The stoichiometric conversion equations are given in Table 7-6 in the Appendix.

Glycerol as substrate

Glycerol shows a strong reductive character and it can be very well metabolized by microorganisms that do not need external electron acceptors, but can provide internal electron sinks in form of further reduced products. Nevertheless some MO are able to convert glycerol with the usage of O_2 as electron sink. The degree of reduction can be expressed by the value κ. The microbial biomass of *C. pasteurianum* contains in average the following composition of main elements, $C_4H_7O_2N$ (Biebl, 2001), and shows a κ of 4.0, which is lower than the value for glycerol (κ = 4.67). Thus, biomass growth forms excess reducing equivalents, which are free for the formation of further reduced products, like 1,3-PDO (κ = 5.33) or EtOH (κ = 6) (Biebl et al., 1999). The main aspect for a balanced substrate degradation and product formation is the balance of the internal reducing equivalent couples, NAD^+/NADH and NADP+/NADPH. It determines the biomass production as well as product formation from different carbon sources. In *C. pasteurianum*, glycerol is fermented by a dismutation process, which combines simultaneous oxidation and reduction to maintain the internal redox balance. The oxidative pathway

[5] http://www.duponttateandlyle.com, 08.09.2017.
[6] http://www.glorybiomaterial.com, 08.09.2017.

channels glycerol into glycolysis, where different by-products are formed under the release of energy rich NADH. The reductive pathway consumes the released NADH for the formation of 1,3-PDO. Here, at first glycerol is converted into 3-hydroxypropionaldehyde (3-HPA) by the coenzyme B12 dependent enzyme glycerol dehydratase, which is subsequently reduced to 1,3-PDO via 1,3-PDO dehydrogenase under the consumption of NADH. In the oxidative pathway glycerol is metabolized to dihydroxyacetone (DHA) by glycerol dehydrogenase under the release of NADH. In the next step DHA is phosphorylated into DHA-phosphate (DHAP), catalyzed by dihydroxyacetone kinase under the consumption of ATP. DHAP is then converted with triosephosphate isomerase into glyceraldehyde-3-phosphate (G3P). G3P is subsequently metabolized by glycolytic reactions into pyruvate. Biomass production is also an oxidative pathway and consumes NADH and ATP. From 1 mol glycerol 2 mol NADH and 1 mol ATP are formed in pyruvate formation.

Glucose as substrate

In the initial steps, glucose is catabolized to pyruvate via glycolysis (Embden–Meyerhof–Parnas pathway)[7] together with the net release of 2 mol ATP and 2 mol NADH per mol of glucose. At the start glucose is converted into glucose-6-phosphate by glucokinase and then into fructofuranose-6-phosphate by glucose-6-phosphate isomerase. In the next step fructose-1,6-bisphosphate (F1,6B) is formed with the assistance of 6-phosphofructokinase. F1,6B is subsequently transformed into D-glyceraldehyde-3-phosphate and dihydroxyacetone phosphate by fructose-1,6-bisphosphate aldolase. Those intermediates are also received from glycerol degradation, and from there on both pathways are equal.

One side product in the metabolic pathway, lactic acid, is a direct degradation product from pyruvate by means of lactate dehydrogenase and the consumption of 1 mol NADH. In *C. pasteurianum*, pyruvate is converted to acetyl-CoA in two different ways. One is the formation of formate and acetyl-CoA by means of different pyruvate formate lyases (PFL). Formate is later degraded in H_2 and CO_2 by a formate dehydrogenase. The second possible way from pyruvate to acetyl-CoA is via the ferredoxin complex. In both cases the coenzyme Coenzyme A is needed. The ferredoxin complex works in two steps: At first pyruvate, CoA and an oxidized ferredoxin complex is reduced to acetyl-CoA, 2 protons, carbon dioxide and a reduced ferredoxin complex via pyruvate:ferredoxin oxidoreductases (PFOR). This is followed by a recovery of reduced-ferredoxin to oxidized-ferredoxin and the formation of molecular hydrogen from protons via hydrogenases (see Eq. (4-4) in Chapter 4.2.1).

The resulting acetyl-CoA is a key intermediate, which is transformed into several products: I) It is a precursor for biomass formation. II) By means of acetaldehyde dehydrogenase, alcohol dehydrogenase and the consumption of 2 mol NADH, ethanol is formed. III) With phospho transacetylase it is converted to acetyl phosphate and subsequently into acetate via acetate kinase. In the last step ATP is generated, an important energy carrier. IV) Further, it is converted to acetoacetyl-CoA by acetyl-CoA acetyltransferase, and then into 3-hydroxybutyryl-CoA by the consumption of NADH. This product is dehydrated to crotonyl-CoA, by a dehydratase. Crotonyl-CoA is further metabolized into butyryl-CoA, which can be performed in two different steps. The most common way is the conversion by butyryl-CoA

[7] The pathway and enzymes presented are received from the BioCyc database collection for *C. pasteurianum* DSMZ 525 (https://biocyc.org/organism-summary?object=CPAS1262449, 08.09.2017).

dehydrogenase. A new suggested pathway step (Buckel and Thauer, 2013) that involves an oxidized ferredoxin dependent butyryl-CoA dehydrogenase / electron transfer flavoprotein complex (BCdH-ETF) will be explained in detail in Chapter 4.2. The resulting butyryl-CoA can be converted into butyrate under the regeneration of ATP. Butyrate can be transformed back into butyryl-CoA, which supports the formation of more BuOH. In another step butyryl-CoA is used for the production butyraldehyde and finally *n*-butanol, connected with the consumption of 2 mol NADH. The ATP, which is generated by the formation of acetic and butyric acid, are mainly utilized for biomass production. Therefore an increased acid production is mostly connected with a higher biomass formation rate.

2.3 Mediators and bioelectrochemical systems

The overall electron transfer in a fermentation process is based on intracellular processes as well as interactions with the surrounding media and it can be expressed by the reduction-oxidation potential (redox potential, RP). The extracellular redox potential can be measured online whereas information about intracellular potential are mainly obtained from the stoichiometric pathway like the ratio of $NADH/NAD^+$ or $NAD(P)H/NAD(P)^+$. The extracellular RP is influenced by media components like oxygen or cysteine but also bacterial excretions like hydrogen or fermentation products. However, the redox balance is a flexible system, which works in both directions: the bacteria determine the internal and external redox balance by product formation and a changed external RP can cause an internal metabolic response. Especially the latter effect can be used to influence or even determine a certain product pattern in biotechnological processes. There are different approaches to influence the external RP of the bacterial environment, e.g. with chemical supplements or artificial electron carriers (mediators) or with electrical current via electrodes.

A redox reaction, either extra- or intracellular, requires an electron donor and an electron acceptor. The tendency of a compound to gain or receive electrons is expressed by the redox potential (E^0 [mV]). This potential is measured against a standard hydrogen electrode (SHE), usually at pH 7, and can be determined for every redox couple. A higher value represents a higher affinity for electrons. Table 2-2 gives an overview of some biotechnological important redox reaction in *Clostridium* cultivations.

Table 2-2: Redox potentials of several biotechnological systems and mediators.

System	E^0 [mV]	Reference
$2H^+ + 2e^- \rightarrow H_2$	-414	(Thauer et al., 1977)
pyruvate + CoA-SH $\rightarrow$ CO_2 + Acetyl-CoA + $H^+ + 2\ e^-$	-500	(Thauer et al., 1977)
formate $\rightarrow$ CO_2	-420	(Thauer et al., 1977)
$Fd_{ox} + e^- \rightarrow Fd_{red}$	-400 ….-500	(Buckel and Thauer, 2013)
$NAD^+ + 2\ e^- + H^+ \rightarrow$ NADH	-320	(Bennett et al., 2009)
$NADP^+ + 2\ e^- + H^+ \rightarrow$ NADPH	-320	(Bennett et al., 2009)
methyl viologen	-446	(Rosenbaum et al., 2011)
Neutral Red	-325	(Rosenbaum et al., 2011)

2.3.1 Mediators

Mediators are soluble chemical compounds able to shuttle electrons. Some work independent from a BES, others can be recharged on electrodes. Depending on their origin, different types of mediators are distinguished: a) endogenous mediators produced by the MO itself, b) naturally available compounds in the environment, e.g. humic acid in soil, or c) exogenous mediators that are synthetic organic molecules added to a fermentation system (Marsili E., Zhang X., 2010). In natural electron transferring enzymes the redox active center is mostly located in the central area, which requires a high overpotential to surmount the distance to the electrode. This result in a reduced electron transfer rate or requires higher potentials as usually necessary for this reaction. Artificial electron shuttles can overcome this drawback, because of their reduced molecular weight and/or higher reactivity. Thus, processes can be realized that even might not be possible without this catalytic acting redox shuttle either as donor or acceptor. Ideally, mediators lower the required overpotential of the BES and can be adapted to the required potential of catalyzed processes. Depending on the organism it might be necessary that they are lipophilic to transfer the electrons inside the cells or organelles for electron transfer (Marsili E., Zhang X., 2010). Others might act on the cell surface directly. If mediators are used in combination with a BES, they should be rechargeable multiple times with a high stability. Consequently, only low concentrations would be necessary in a fermentation process, presupposed they are well mixed and do not bind permanently in the biomass. The most widely studied mediators are methyl viologen (Peguin et al., 1994), Neutral Red (Hongo, 1958) and thionin (Choi et al., 2003). However, the chemicals might interfere with other metabolic processes, are harmful or toxic for the environment or reveal higher additional costs (Rabaey and Rozendal, 2010).On account of this recent researches focus on cheap and non-toxic mediators, like organic dyes or endogenous produced compounds (Nørskov and Mellor, 1996).

Methyl viologen (MV)

One widely studied mediator with high impact on fermentation processes is methyl viologen (1,1-dimethyl-4,4-bipyridinium dichloride, Table 2-3). It shows a redox potential, which is in the range of natural flavodoxins or ferredoxin in *Clostridium*. Therefore, MV is able to substitute the natural electron transfer proteins. Peguin et al. (Peguin et al., 1994) analyzed the influence of MV as sole mediator without a BES on glucose fermentation by *C. acetobutylicum*. The addition of MV as an electron donor redirects the metabolism to NAD(P)H formation resulting in the most reduced product butanol at the expense of acetone, butyric and acetic acids. Hydrogen evolution was reduced as well and redirected to the formation of NADPH. However, addition of MV led to a lower growth rate and longer lag phase. Combined with a BES, Kim et al. (Kim and Kim, 1988) showed with *in vitro* experiments the successful electron transfer from an electrode via MV to the regeneration of a $NAD^+/NAD(P)^+$:ferredoxin oxidoreductase complex of *C. acetobutylicum*, as shown in Fig. 2-6. A subsequent analysis of the system *in vivo* resulted in 26 % higher butanol formation on the expense of acetone. Even though MV improves the process performance of BuOH production, it is a harmful and highly toxic compound, which hampers broad application in large scale processes. Due to this, less harmful dyes from food coloring were tested *in vitro* by Nørskov and Mellor (Nørskov and Mellor, 1996). They found dyes like curcumin, patent blue and azure A, to show the same or even better electron transfer properties as MV on oxido-reductase and nitro-reductase. But so far, the mechanisms and binding sites are still unclear.

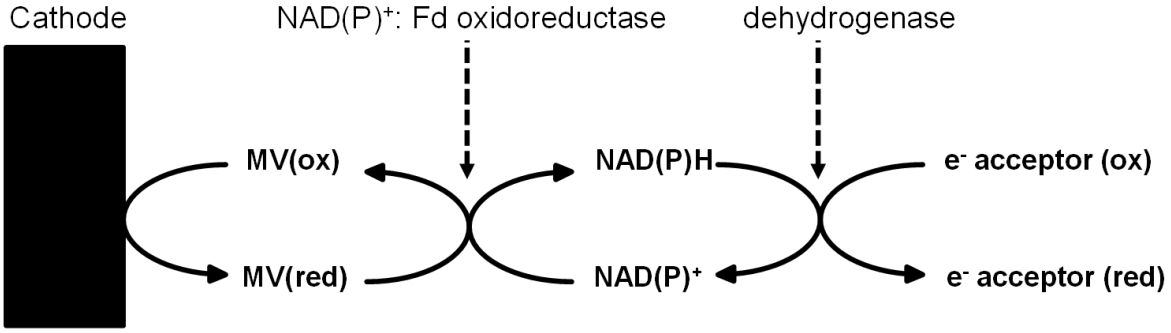

Fig. 2-6: Electron transfer from an electrode through MV and NAD(P)H to reduced products. (Figure according to Kim and Kim, 1988).

Neutral Red

One of the first approaches to use mediators was performed in 1958 by Hongo (Hongo, 1958), who discovered an influence of the dye Neutral Red (3-amino-7-dimethylamino-2-methyl-phenazine hydrochloride, Table 2-3) on the solvent production. The electron carrier Neutral Red (NR) used in concentrations of 0.1 % decreased the redox potential of the broth and hence increased the NADH/NAD^+ ratio in *Corynebacterium crenatum*, which led to an enhanced yield of succinic acid (Chen et al., 2012). Girbal et al. (Girbal et al., 1995) discovered that the addition NR increased the yield of alcohols and butyrate and decreased hydrogen formation in fermentation of glucose by *C. acetobutylicum*. The authors found a reduced activity of hydrogenase at the presence of NR, but no influence on pyruvate:Fd oxidoreductase, NADH:Fd reductase or hydrogen uptake. But the simultaneous utilization of Fd and NR increased Fd:NAD reductase activity, which led to an increased Fd_{ox} and NADH pool. This increased NADH-dependent aldehyde and alcohol dehydrogenase activities, leading to an enhanced formation of reduced alcohols. Moreover, using a BES, Park and Zeikus (Park and Zeikus, 1999) showed that cell-wall bounded NR can be directly reduced in contact to a cathode and is consequently used to recover intracellular NAD^+ to NADH.

Brilliant Blue R250 (BB)

Brilliant Blue R250 ($C_{45}H_{44}N_3NaO_7S_2$) is a blue Coomassie® dye with slight reddish shades (indicated by R), which is used for the colorization of proteins in molecular biological analysis, like gel electrophoresis (Westermeier, 2016). On the contrary Brilliant Blue G250 ($C_{47}H_{48}N_3NaO_7S_2$), which possesses two additional methyl groups at internal aromatic rings, shows a slight greenish tint. The different colors within each dye result from different charged states of the molecule. In general, in BB R250 the nitrogen atoms are positively and the sulfonic groups negative charged (Table 2-3). The formation of a protein-dye complex stabilizes the anionic form that results in the blue color. At neutral conditions, i.e. pH 7, it appears blue with an absorption maximum between 590 nm (free dye) or 620 nm (bound to proteins). However, it is known that BB binds in different quantities to several proteins. Tal et al. (Tal et al., 1985) found that the complex is formed due to the electrostatic connection between the negative sulfonic groups and basic amino acids. The quantitative amount of BB molecules per protein is therefore mainly defined by their content of basic amino acids, like lysine, histidine, and arginine. For

example, it was found that cytochrome C, lysozyme or RNAase are very susceptible for BB-R250 binding, compared to pepsin or trypsin (Tal et al., 1985). For BB G-250 it is also known that hydrophobic interactions connect the neutralized dye molecule to the amino acids tryptophan and phenylalanine (Georgiou et al., 2008).
To the author´s best knowledge Brilliant Blue R250 is not used as a redox active compound or mediator in any microbial fermentation system yet.

Table 2-3: Chemical structures of methyl viologen, Neutral Red and Brilliant Blue R250.

Chemical	Chemical structure
Neutral Red	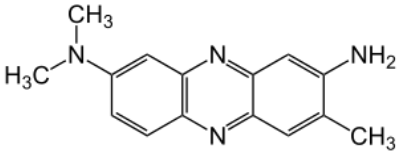
Methyl viologen	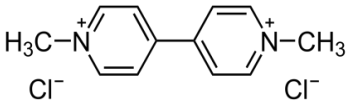
Brilliant Blue R250	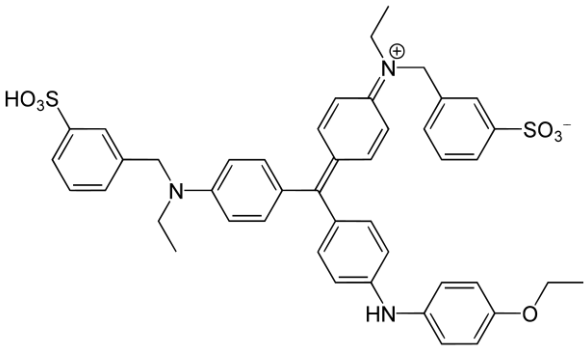

2.3.2 Bioelectrochemical systems

The RP of a fermentation system can be influenced by using direct electron input in form of bioelectrical reactors (BERs). They are equipped with an artificial electron source in form of electrical current, electrodes in an electrolytic liquid and a separating membrane (Rabaey and Rozendal, 2010) (See Fig. 2-7 A). The interaction of electron transport can occur in both directions: the microorganisms deliver electrons to the anode (microbial fuel cell, MFC) or receive them from the cathode (microbial electrolysis cell, MEC) (Rabaey and Rozendal, 2010). The interactions of microorganism and electrodes are crucial for the efficiency of the system, but they strongly depend on the organism itself, as well as electrode material and size. According to Lovley (Lovley, 2012) several interactions between electrodes and microorganisms are possible (Fig. 2-7 B): a) Short range electron transfer by redox-active proteins on the outer cell surface of bacteria (e.g. cytochromes) b) Electron transfer by electron shuttles (mediators) c) Long-range electron transport through conductive pili, maybe also in combination with biofilms (Lovley, 2012).

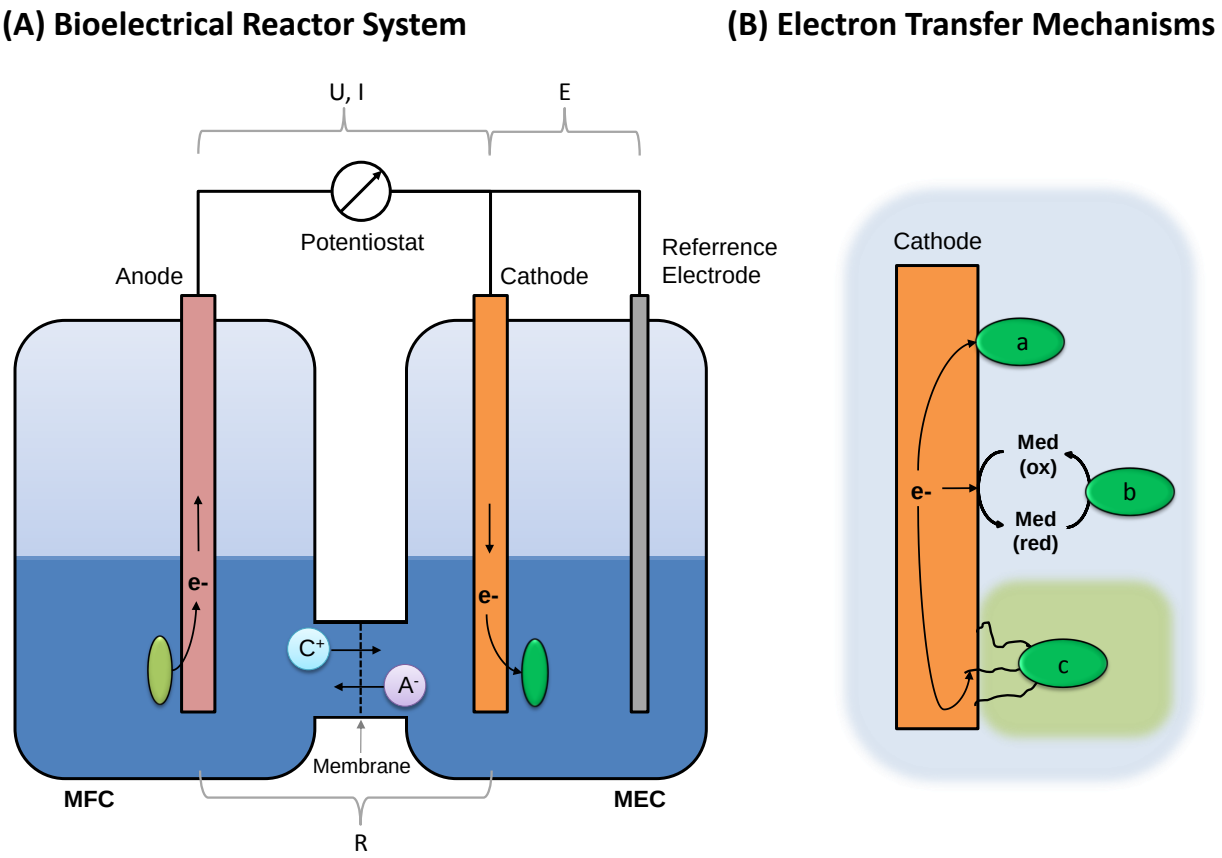

Fig. 2-7: A) Scheme of a bioelectrical reactor system with electron uptake at the anode (microbial fuel cell, MFC) and/or electron disposal at the cathode (microbial electrolysis cell, MEC). U = potential between electrodes [V], I = measured current [A], E = controlled potential between anode and cathode [V], R = resistance of the system [Ω]. C+ = cations, A- = anions, e- = electrons. B) Possible electron transfer mechanisms between cathode and microorganisms: a) direct b) via electron shuttles (mediators) c) through pili and/or conductive biofilms.

In a BES the potentiostat applies a constant potential U for the desired reactions and the controlled potential E between cathode and reference electrode should be kept constant. The resistance of the system varies, depending on membrane conditions, ion concentration (i.e. status of MO and media composition), but also physical distance of the electrodes. Accordingly, the flowing current varies over time, due to biochemical and electrochemical reactions in the system. In a simplified system the current is described as the potential divided by the resistance (Eq. (2-1)).

$$I = \frac{U}{R} \qquad (2\text{-}1)$$

I = current [A]
U = potential [V]
R = resistance [Ω]

2.4 Downstream processing of *n*-butanol [8]

2.4.1 General considerations

The development of a sustainable and economic biorefinery processes not only comprises the efficient bioconversion of the substrate by microorganism or enzymes, but also well-chosen and economical feasible downstream processing (DS) techniques. Conventionally the downstream process is an end of pipe process after (bio) conversion, consisting of basic units like filtration, distillation, adsorption etc. However, bioprocesses are even more unique and require individual solutions. Microorganisms are not only a set of simple determined chemical reactions, but small cell factories itself with complex metabolic pathways. They produce the desired solvent and additional metabolic side products that are necessary for their own growth, maintenance and function. This might represent a waste of carbon atoms and also leads to difficulties in the subsequent separation of the desired product. Prior usage, the final product has to be separated from water, by-products and other fermentation residues.

In an ideal process, the main costs of the process are based in the substrate. But other large economic factors represent the investment cost for fermenter and DS equipment as well as operation costs for the product recovery (Oudshoorn et al., 2009). These process steps are the most influencing factors and can contribute up 50-70 % of the total production costs of the final product, mainly due to low product concentration and high energy demands for recovery (Xiu and Zeng, 2008). Thus, the determination of a reasonable downstream process is of major economic interest.

Sometimes the fermentation products of the bacteria inhibit the organism itself. As already mentioned, BuOH represents such a self-inhibiting product in *Clostridium* cultivation. Using genetic and metabolic engineering, the tolerance against butanol can be enhanced (Branduardi et al., 2014). This creates GMO, which requires additional safety precautions (and investment costs) and does not overcome the drawback of a versatile fermentation broth. Therefore, process engineering solutions can be applied to combine both, the *in situ* removal of BuOH, and simultaneous separation of the product. Several groups analyzed *in situ* recovery of BuOH using liquid-liquid extraction (Roffler et al., 1987), (Groot et al., 1990), salting out techniques (Sun et al., 2013), adsorption (Nielsen and Prather, 2009), (Barski et al., 2012), or pervaporation with novel membranes materials (Qureshi et al., 2005), (Borisov et al., 2014), (Heitmann et al., 2012), (Chen et al., 2013). Even though high recovery rates and selectivities can be achieved, these techniques expose problems like membrane fouling, toxic supplements or removal of other broth components. These drawbacks can be partially overcome by gas stripping (Ezeji et al., 2003). In the following sections several downstream techniques for BuOH are explained in more detail.

[8] Parts of this chapter are based on Groeger et al. (2015).

2.4.2 Examples for recovery methods of BuOH from fermentation broth

2.4.2.1 Extraction

The solvent BuOH exhibits excellent solubility in organic solvents, which make it an attractive candidate for extractions processes. The selectivities achieved by using organic solvents are very high with values of 440 for soy oil or even 4100 for octane (Groot et al., 1990). Many screenings for extractants are performed for alcohols, alkanes, esters, different plant oils as well as surfactants, ionic liquids, and supercritical carbon dioxide (Groot et al., 1990), (Dhamole et al., 2012), (Ishizaki et al., 1999), (Roffler et al., 1987), (Santangelo et al., 2011), (Laitinen and Kaunisto, 1999), (Dooley et al., 1997). The most common extractants that fulfill many criteria are dodecanol and oley alcohol. Evans and Wang (Evans and Wang, 1988) used a mixture of both for *in situ* from recovery of BuOH in a fermentation of *C. acetobutylicum* and accomplished a 72 % higher BuOH titer. Nevertheless, problems connected to liquid-liquid extraction are for example fouling of the extractant or the formation of emulsions, due to direct contact with other broth components or fermentation products. This can be partly avoided by membrane extraction (perstraction), where a membrane excludes solid broth components. For this technique the membrane must ensure high and selective permeation rates. Another drawback is the backflow of the extractant into the fermentation broth, causing loss of extractant and, in case of toxicity, inhibition of bacterial growth. Furthermore, large membrane areas and high viscous extractants are difficult to operate in large scale processes (Groot et al., 1990). Another possibility represent salting-out processes or the combination of extractants and salts. By the addition of salts in high concentrations (>25 %), water soluble constituents are supplanted from the aqueous phase, due to the increased ionic strength, and the excluded liquids form a new organic phase with the extractant. Simultaneously other by-products, proteins or cells are separated by precipitating as a solid phase. Sun et al. (Sun et al., 2013) successfully used acetone and K_2HPO_4 to extract 98 % of the BuOH in ABE fermentation, but it was applied as an end of pipe process. Additionally it has to be considered that the process economic also depends on an efficient recovery of BuOH from the extractant or salt/extractant mixture, which is mainly realized with additional decantation, distillative separation or stripping processes (Groot et al., 1990).

2.4.2.2 Pervaporation

In a pervaporation process the product diffuse selectively through a membrane, whilst water and undesired components are excluded. The product molecules absorb into the membrane, permeate through it and evaporate, due to the vacuum applied. Thus, the driving forces are the permeability and the differences in partial pressure of the broth components. In a second step, the vapor phase is condensed by removing the vacuum. Because of the relatively high volatility of BuOH, this method is quite attractive as an *in situ* downstream process for the production of bio-butanol. Higher concentration of BuOH in the feed solution increases the flux through a membrane, whereas increased membrane thickness decrease the flux (Oudshoorn et al., 2009). The utilized membranes can be divided into two groups: hydrophobic membranes, e.g. for product recovery from fermentation broth or hydrophilic membranes, for instance for the dehydration of high concentrated alcohols (Huang et al., 2008), (Vane, 2005). Hydrophilic membranes can be made of polyvinyl alcohol, polyacrylic acid or polyacrylo nitrile.

The most common hydrophobic membrane consists of polydimethylsiloxane. Depending on the type of membranes, selectivities values between 3 till 209 can be achieved (Oudshoorn et al., 2009). In terms of sustainability also biopolymers, like cellulose (Dubey et al., 2002), chitosan (Uragami and Takigawa, 1990) or sodium alginate (Kanti et al., 2004) are of increasing interest, especially for the dehydration of aqueous alcohol mixtures. A new approach is reported by Heitmann et al. (Heitmann et al., 2012), who used membranes with incorporated ionic liquids. Application in synthetic media exhibits enhanced selectivities for BuOH, but insufficient permeability fluxes, due to high membrane thickness. This lead to a final butanol concentration of 55 w-% in the condensate, which require an additional distillation step. Considering the energy requirements, values around 14 MJ/kg BuOH were reported by Qureshi et al. (Qureshi et al., 2005) for the pervaporative separation of BuOH from cultivations of *C. beijerinckii* and *C. acetobutylicum*. The main bottleneck of this technique is the fact that membranes are quite susceptible for fouling and in large scale processes immense membrane areas would be necessary.

2.4.2.3 Gas stripping

Volatile compounds like ethanol or butanol are very suitable for the removal by gas stripping in a fermentation process. In this technique the cultivation broth is sparged with an inert gas that collects and carries the volatile compounds from the aqueous phase due to vapor pressure equilibria. The gas loaded with solvent and water is led over a cooling or flash unit where the product condenses. The depleted gas is either removed or led back through the system.

Gas stripping shows several advantages as *in situ* process over other DS techniques. It is not susceptible for fouling or clogging, like membrane-based methods (Ezeji et al., 2003). It is relatively selective to solvents, thus no other nutrients are removed or trapped by the gas. One advantage is the fact that the cells are not adsorbed or harmed directly, especially when their own produced gases are used. However, the sparging influences the redox-potential and partial pressure of hydrogen, which might interfere with the bacterial metabolism. And even though butanol is removed, other side-products like acids accumulate and can also cause inhibition. Besides this, the energy requirements for cooling and gas recycling, as well as the addition of antifoam have a significant effect on operation costs of this method.

Gas stripping is not a classical downstream method. It was mainly used for the removal of volatile compounds in waste water treatment (Truong and Blackburn, 1984). However, many researchers implemented gas stripping for BuOH removal into ABE fermentations and it clearly enhanced the growth, the final product titer and the yield, compared to fermentation without GS (Jensen et al., 2012a), (Xue et al., 2012), (Ezeji et al., 2004), (Vrije et al., 2013). In an ABE fermentation of immobilized *C. acetobutylicum* Xue et al. (Xue et al., 2013) analyzed a two stage stripping process with effluent fermentation gases to remove BuOH from the broth, which increased the final BuOH yield and productivity to 0.25 g/g and 0.4 g/(Lh), respectively, compared to 0.20 and 0.3 g/(Lh) without gas stripping. Indeed, different gases have been analyzed for the stripping, mainly N_2 (Vrije et al., 2013) or own fermentation gases (Ezeji et al., 2004). Liao et al. used synthetic media to analyze influencing parameters on the gas stripping process. He showed that the highest BuOH removal rates can be achieved with N_2, followed by O_2 and CO_2 (Liao et al., 2014). For gas stripping in general the achieved selectivities are lower, compared to other downstream processing techniques, due to high amounts of

water that are stripped and condensed as well and the reported values range from 4 – 22 (Oudshoorn et al., 2009). Another drawback represents the high energy requirements for the cooling or condensing unit. Due to the low concentration of BuOH in the feed solution energy requirements of 14 - 22 MJ/kg BuOH (Qureshi et al., 2005), (Xue et al., 2012) are reported. An optimization in form of a two stage stripping process is suggested by Xue et al. (Xue et al., 2013). There the aqueous phase of the condensates is stripped again with effluent gases to gain a larger quantity of the high concentrated organic phase, which should reduce the energy requirements down to 5 MJ/kg BuOH.

Mathematical descriptions and thermodynamic correlations for the gas stripping process

A high removal rate of BuOH depends on a high mass transfer rate between the liquid and gas phases of the stripping gas system. This can be characterized by using the volumetric mass transfer coefficient $K_S a$ of the target compound. (Note: The mass transfer coefficient "$K_S a$" is different from the coefficient "$K_L a$". The latter one is mainly used to describe the oxygen transfer rate in fermentation processes, i.e. the transfer of a gas into the liquid. In a gas stripping process, the notation $K_S a$ is used to describe the transfer of a liquid into a gas phase. Present literature for gas stripping of volatile compounds (mainly BuOH or EtOH) from waste water or fermentation broths, uses the notation "$K_S a$" or the notation $K_a^{St} a$ to describe the volumetric mass transfer coefficient of the target compound and clearly distinguish it from the oxygen transfer coefficient $K_L a$ (Vrije et al., 2013), (Liao et al., 2014), (Ezeji et al., 2005), (Truong and Blackburn, 1984)). Based on the two-film theory Truong and Blackburn (Truong and Blackburn, 1984) modeled the volumetric mass transfer coefficient, also called stripping rate constant, $K_s a$ for a static system without product formation according to equation (2-2). It is influenced by temperature T [K], but also liquid volume V [m³], interfacial area A [m²], universal gas constant R [J/(molK)], the coefficients for gas and liquid mass transfer k_g and k_l [m/s] and the Henry´s coefficient k_{Hij}^{px} [Pa*m³/mol]. The second model for the determination of the $K_s a$ (Eq. (2-3)) also considers the gas flow rate Q [L/s] over the liquid volume, the power function constants b and m and the dimensionless Henry´s coefficient H´ (Truong and Blackburn, 1984). The gas stripping of solvents from an aqueous solution can be described with a first order kinetic as shown in Eq. (2-4). In this equation r_S [g/(Lh)] is the stripping rate of a substance from a liquid over time t [h], c_i [g/L] the substance concentration in the liquid and c_i^* [g/L] the liquid concentration in equilibrium with the gas phase (Truong and Blackburn, 1984).

$$K_S a = \frac{A}{V} \times \left[\frac{1}{k_l} + \frac{RT}{k_{Hij}^{px} k_g} \right]^{-1} \tag{2-2}$$

$$K_S a = b \frac{Q}{V} (H')^m \tag{2-3}$$

$$r_S = \frac{\partial c_i}{\partial t} = K_S a \times (c_i - c_i^*) \tag{2-4}$$

The Henry coefficient describes the thermodynamic behavior of a component mixture (see also paragraph below) and thus it can be used for a first evaluation of the suitability for a stripping gas / solvent combination. However, two mechanisms and two different expression forms of the Henry coefficients should be distinguished. 1) The dissolution of the stripping gas into the liquid: Dissolved gas is known to lower the effective butanol concentration (activity) and therefore decreases the stripping efficiency (Liao et al., 2014). The ability for dissolution into the aqueous fermentation broth can be expressed with the Henry coefficient H_{ij}^{cp} [mol/m^{3}Pa], describing the solubility. Here a higher value represents a better solubility of the gas in the liquid. 2). The evaporation of butanol into a certain gas phase: The evaporation ability can be expressed with the Henry coefficient k_{Hij}^{px} [Pa]. A higher coefficient represents a higher tendency of BuOH to evaporate. Table 2-4 shows the different Henry coefficients describing the volatility of BuOH and EtOH as well as for the dissolution of N_2, H_2 and CO_2 into water.

Table 2-4: Henry´s coefficients describing the solubility (H_{ij}^{cp}) and volatility (k_{Hij}^{px}) for BuOH, EtOH, N_2, H_2 and CO_2 at ambient temperature and pressure.

	H_{ij}^{cp} [mol/m^{3}Pa]		**Reference**
N_2	$6.4*10^{-6}$	Solubility into water	(Sander, 2015)
CO_2	$3.4*10^{-4}$	Solubility into water	(Sander, 2015)
H_2	$7.7*10^{-6}$	Solubility into water	(Massoudi and King Jr, 1973)
	k_{Hij}^{px} [Pa]		
BuOH	$2.14*10^{8}$	Volatility into N_2	(Massoudi and King Jr, 1973)
BuOH	$3.80*10^{8}$	Volatility into H_2	(Katayama and Nitta, 1976)
BuOH	$1.36*10^{7}$	Volatility into CO_2	(Massoudi and King Jr, 1973)
EtOH	$2.84*10^{8}$	Volatility into N_2	(Katayama and Nitta, 1976)
EtOH	$4.96*10^{8}$	Volatility into H_2	(Katayama and Nitta, 1976)
EtOH	$4.44*10^{7}$	Volatility into CO_2	(Luehring and Schumpe, 1989)

A successful gas stripping process is also determined by the efficient distribution of BuOH in the gas phase, and the subsequent efficient cooling in the condenser to separate the liquid BuOH from the gas phase. This behavior can be expressed by thermodynamic correlations for vapor/liquid equilibria and the heat transfer.

In an ideal system consisting of a liquid and a vapor phase, the Raoult´s law states that the partial pressure of a compound i equals the molar fraction of the compound i in the liquid multiplied by its saturated vapor pressure (Eq. (2-5)). For real non-ideal behavior of a liquid, the Raoult´s law is extended by adding the activity coefficient (Eq. (2-6)), which is determined as the ratio of real partial pressure to the ideal partial pressure. The Dalton´s law expresses the partial pressure of the component i as a function of the total pressure of the system and the molar fraction of the component i in the vapor phase (Eq. (2-7). The non-ideal behavior of a real vapor phase is considered by including the correction coefficient fugacity, which is determined experimentally or by modeling (Eq. (2-8)). The Henry´s law for solutions describes the solubility behavior of a gas in a liquid (Eq. (2-9)). It states that the partial pressure of a compound i equals its molar fraction in the liquid times the Henry´s coefficient. (All equations described by Sattler (2012)).

Raoult´s law: (ideal) $$p_i = x_i \times p_i^0 \quad (2\text{-}5)$$

(non-ideal) $$p_i = \gamma_i \times x_i \times p_i^0 \quad (2\text{-}6)$$

Dalton´s law: (ideal) $$p_i = y_i \times p_{total} \quad (2\text{-}7)$$

(non-ideal) $$p_i = \phi_i \times y_i \times p_{total} \quad (2\text{-}8)$$

Henry´s law: $$p_i = k_{Hij}^{px} \times x_i \quad (2\text{-}9)$$

p_i = partial pressure of compound i [Pa]
p_{total} = total pressure of a mixture [Pa]
p_i^0 = saturation vapor pressure of compound i [Pa]
x_i = molar fraction of component i in liquid phase [mol/mol]
y_i = molar fraction of component i in vapor phase [mol/mol]
γ_i = activity coefficient [-]
ϕ_i = fugacity coefficient [-]
k_{Hij}^{px} = Henry´s coefficient of component i in component j [Pa]

In gas stripping processes the volatile solvent from the broth, i.e. BuOH, can be recovered from the gas by condensation. That means the vapor is cooled below the dew point and transferred into a liquid state. In surface condensers the vapor is cooled down on a surface, which is in contact with a cooling liquid. The heat transfer in a heat exchanger is basically determined by the heat exchange area A, the inlet and outlet temperatures as well as the mass flow of the fluids. The heat flow that has to be dissipated can be calculated in different ways: The heat flow through a wall is in general dependent on the material dependent thermal transmittance coefficient k, the temperature difference ΔT, and the heat exchange area (Eq. (2-10)). The heat flow for surface condensers can also be described with either Eq. (2-11), considering the vapor site, and Eq. (2-12), considering the cooling liquid site (Grote and Feldhusen, 2011). The resulting calculation for the required surface of the cooling area is described in Eq. (2-12). In a heat exchanger, the logarithmic mean temperature difference is the average difference between the smallest and highest temperature differences at each end of the exchanger (Eq. (2-13) (Grote and Feldhusen, 2011)).

Dissipated heat flow $$\dot{Q} = k \times A \times \Delta T \quad (2\text{-}10)$$

$$\dot{Q} = \dot{n}_v (h_V - h_C) = \dot{n}_{CL}\, c_{CL} (T_{CLout} - T_{CLin}) \quad (2\text{-}11)$$

Surface of cooling area $$A = \frac{\sum \dot{Q}_i}{k \times \Delta T_m} \quad (2\text{-}12)$$

Logarithmic mean temperature difference

$$\Delta T_m = \frac{\Delta T_{hi} - \Delta T_{sm}}{\ln(\frac{\Delta T_{hi}}{\Delta T_{sm}})} \quad (2\text{-}13)$$

$\dot{Q}$	=	heat flow [W]
$\dot{n}_V$, $\dot{n}_{CL}$	=	molar flow of vapor or cooling liquid [kg/s]
h_V, h_C	=	specific enthalpy of vapor or condensate [J/kg]
c_{CL}	=	heat capacity of cooling liquid [J/(kgK)]
T_{CLin}, T_{CLout}	=	inlet and outlet temperature of cooling liquid [K]
ΔT_m	=	mean temperature difference [K] for co- and countercurrent flow
ΔT_{hi}, ΔT_{sm}	=	highest and smallest temperature difference in the system
A	=	heat transfer area
k	=	thermal transmittance coefficient [W/(m²K)]

The mixture of butanol and water

After the gas stripping process, the condensates appear as mixture of butanol, water, small amounts of ethanol and maybe other broth components. Even though it is a multicomponent mixture, the thermodynamic properties of a binary water-butanol mixture are crucial to find adequate separation methods. At ambient pressure and temperature this binary mixture forms an azeotrope at 55.5 w-% BuOH. At BuOH concentrations higher as 7.7 w-% in water, a mixing gap occurs, which exhibits as a biphasic system. The lower aqueous phase contains around 7.7 w-% BuOH, whereas the upper organic phase contains up to 79.9 w-% BuOH (Weast, 1980). This heterogeneous azeotropic mixture has its temperature minimum at 92.7°C, which is below the boiling points of the two pure components.

Distillative separation of BuOH and water

Taking advantage of the phase separation, a combination of two distillation columns and a phase separator allows the efficient purification of BuOH from binary aqueous mixture. The process suggested by Matsumura et al. (Matsumura et al., 1988) is shown Fig. 2-8 and further improved by Fischer and Gmehling (Fischer and Gmehling, 1994) or Mariano et al. (Mariano et al., 2011). The two liquid phases are at first separated in a gravity decanter at 92.7°C. The organic phase is lead into the top of the BuOH column, and a mass fraction of 0.999 BuOH is reached at the bottom at 118°C. The vapor phase is led to a condenser and back into the decanter, where it is mixed with fresh feed. The lower watery phase is transferred to the aqueous column, which works at 100°C and releases nearly pure water at the bottom. There the BuOH rich vapor is led through a condenser back into the decanter. Using heat integrations between the columns, condenser and decanter, an energy requirement of ca. 4 MJ/kg BUOH is needed for feed solution containing 40 w-% BuOH (~366 g/L) (Matsumura et al., 1988). However, in fermentations only BuOH concentrations around 20 g/L or less are reached. BuOH shows a combustion heat of 36 MJ/kg, thus a downstream process necessarily has to be below this value to become

feasible. Conventional distillation of an aqueous 5 g/L BuOH solution requires 79 MJ/kg BuOH, due to the high boiling points of both components (Matsumura et al., 1988). Already an increase to ~40 g/L reduces the energy input to ~12 MJ/kg BuOH (Vane, 2008). A recovery method of pre-concentrated BuOH is required for the application of distillation in a biorefinery process.

Alternatively a combination of distillation and other DS methods are possible. Matsumura et al. used an *in situ* pervaporation process with membranes containing oley alcohol. The resulting condensates are purified via distillation, achieving 99 w-% BuOH with a total energy demand of 7.4 MJ/kg (Matsumura et al., 1988). Kraemer et al. (Kraemer et al., 2011) suggested a combined extraction-distillation method for BuOH removal from an ABE fermentation broth. Therefore BuOH is extracted with 1,3,5-trimethylbenzene and subsequently recovered via distillation. *In silico* modelling results in a reduced energy demand of 4.8 MJ/kg butanol. If BuOH is an intermediate for further chemical applications, reactive distillation can be used to improve process economics. For example, water, BuOH and acetic acid form butyl acetate, which is catalyzed by ionic exchange resins that are directly located in the column. BuOH and water are recycled at the column head, whereas butyl acetate is removed at the bottom and can be further proceeded (Steinigeweg and Gmehling, 2002).

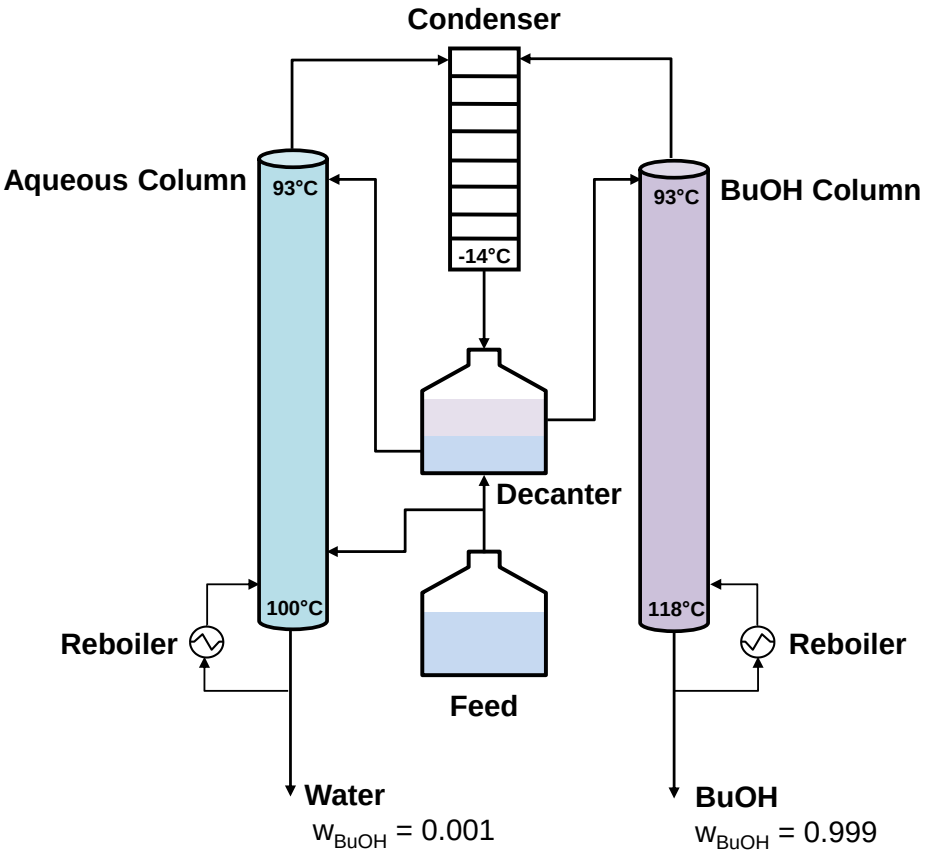

Fig. 2-8: Possible separation method of aqueous butanol mixtures. (Figure according to Matsumura et al. (1988).

3 Methods

3.1 Microorganisms

The Gram-positive, rod shaped anaerobic bacteria *Clostridium pasteurianum* DSMZ 525 was received from the Leibniz-Institut DSMZ-Deutsche Sammlung von Mikroorganismen und Zellkulturen GmbH, Braunschweig, Germany. The strain was maintained as cryo cultures in 20 % (v/v) glycerol at -80˚C.

3.2 Media compositions

3.2.1 Reinforced Clostridial Media

For pre-cultures of *C. pasteurianum,* Reinforced Clostridial Media (RCM) was produced. Table 3-1 gives the concentrations of the components, dissolved in 1 L MiliQ® water. The mixture was boiled at 90°C for 30 min and subsequently cooled to RT under nitrogen sparging. At ambient temperature cysteine HCl was added. The RCM was filled in anaerobic bottles (100 mL) under nitrogen sparging. Resazurin (7-hydroxy-10-oxidophenoxazin-10-ium-3-one) acts as indicator for anaerobiosis by changing the media from colorless to pink. The bottles were autoclaved and stored at RT until usage.

Table 3-1: Reinforced Clostridial Media.

Chemicals	Concentration [g/L]
Cysteine HCl	0.5
Glucose	5.0
Meat extract	10.0
$NaC_2H_3O_2$	3.0
NaCl	5.0
Peptone	10.0
Starch	1.0
Yeast extract	3.0

3.2.2 Cultivation medium for *C. pasteurianum* DSMZ 525

Pre-culture media

For the second pre-culture of *C. pasteurianum* modified media after Biebl (Biebl, 2001) was used. Here cysteine HCl was added to further reduction of the redox potential of the fermentation media. The pre-culture media was prepared in anaerobic bottles in the same steps like RCM media. The composition is given in Table 3-2. Calcium carbonate acts as pH buffer, because the pH was not regulated in pre-cultures.

Table 3-2: Pre-culture media for *C. pasteurianum* DSMZ 525.

Chemicals	Concentration [g/L]
$CaCl*2H_2O$	0.02
$CaCO_3$	2.0
Cysteine HCl	0.5
$FeSO_4*7H_2O$	0.005
Glycerol	25.0
K_2HPO_4	0.5
KH_2PO_4	0.5
$MgSO_4*7H_2O$	0.2
$(NH_4)_2SO_4$	3.0
Resazurin solution	1 mL
Trace element solution S7	2 mL
Yeast extract	1.0

Trace element 7 solution

Trace element solution was prepared with the following components in 1 L MiliQ® water (Table 3-3).

Table 3-3: Trace element solution.

Chemicals	Concentration [mg/L]
$CoCl_2*6H_2O$	200
$CuCl_2*2H_2O$	20
H_3BO_3	60
HCl (95 %)	0.9 mL
$MnCl_2*4H_2O$	100
$Na_2MoO_4*2H_2O$	40
$NiCl_2*6H_2O$	20
ZnCl	70

Cultivation media

For cultivation in the reactor the following standard media composition was used (Table 3-4). In experiments with co-substrate of glycerol and glucose, different concentrations of both carbon sources were used as given below (Table 3-5).

Table 3-4: Composition of cultivation media for *C. pasteurianum* DSMZ 525.

Chemicals	Concentration [g/L]
$CaCl*2H_2O$	0.02
Cysteine HCl	0.5
$FeSO_4*7H_2O$	0.005
Glycerol	80.0
K_2HPO_4	0.5
KH_2PO_4	0.5
$MgSO_4*7H_2O$	0.2
$(NH_4)_2SO_4$	5.0
Resazurin solution	0.2 mL
Trace element solution S7	2 mL
Yeast extract	1.0

Table 3-5: Start concentrations of glucose and glycerol in the media in different mono- and co-substrate fermentations. Pre-cultures contained only glycerol.

Denotation Glucose content	Glucose [g/L]	Glycerol [g/L]
0 %	0	80
20 %	20	80
50 %	50	50
80 %	80	20
100 %	80	0

Several experiments in co-substrate fermentations were performed with biomass hydrolysates instead of pure glucose. The biomass hydrolysates were produced from spruce wood by Borregaard AS (Sarpsborg, Norway) and showed the following composition (Table 3-6), as provided by the company. The hydrolysates were diluted to achieve 50 g/L glucose and autoclaved separately, prior to the addition into the media.

Table 3-6: Composition of biomass hydrolysates received from Borregaard AS.

	Sugar	[g/L]	Sugar	[g/L]
Hydrolysate 1	Glucose	460	Mannose	24
(2 L scale)	Xylose	32	Galactose	1.9
BALI DP-1827	Glucose	183	Mannose	3.9
(2000 L scale)	Xylose	5.6		

Iron concentrations

In each fermentation $FeSO_4*7H_2O$ was added as a source of metabolic important iron. The iron in the molecule has a mass fraction of Fe = 20.1 %. Therefore 5 mg/L $FeSO_4*7H_2O$ contain 1 mg Fe^{2+}/L. At standard conditions 5 mg/L $FeSO_4*7H_2O$ were added in the reactor medium. For iron excess conditions (Fe+) 10 mg/L $FeSO_4*7\ H_2O$ (2 Fe^{2+}/L) were added, whereas at iron limitation (Fe-) no additional iron was supplemented into the media. Iron originally present on the pre-culture volume added (0.07 Fe^{2+}/L) and those present in the yeast extract (up to 0.05 Fe^{2+}/L) were the sole iron concentration in the Fe-cultivations.

3.3 Cultivation

3.3.1 Pre-culture preparation

C. pasteurianum DSMZ 525 was kept as cryo culture at -80°C in 20 % (v/v) glycerol and thawed at RT prior usage. For the preparation of pre-culture, one cryo (2 mL) was suspended in 50 mL RCM (section 3.2.1) in anaerobic bottles. After 24 h at 37°C, 2 mL of this culture was transferred into a 100 mL pre-culture media (section 3.2.2). The sterile filtered $FeSO_4$ was added immediately and the culture incubated at 37°C for further 24 h.

To achieve the same start OD in the fermentation reactors, the amount of pre-culture used was calculated by equation (3-1).

$$V_{inoc} = \frac{OD_{exp} * V_w}{OD_{pre} - OD_{exp}} \quad (3\text{-}1)$$

V_{inoc} = volume of pre-culture for inoculation of reactor
V_w = working volume of fermentation
OD_{exp} = OD to achieve for experiment (usually 0.4)
OD_{pre} = OD of the pre-culture

3.3.2 Lab scale cultivation

The fermenter for lab scale cultivation was a stirred tank bioreactor (Type VSF, Bioengineering AG, Wald, CH). It had the dimensions of 16 cm height and 10 cm diameter with an average working volume of 1.2 L in batch fermentations. Within gas stripping experiments the working volume varied over fermentation time between 1.2 and 1.4 L, due to liquid addition by feeding substrate and liquid removal by gas stripping. Two baffles were installed on the sides of the bioreactor to enhance mixing. The stirrer comprised a six-blade impeller (0.8 cm x 1 cm) 13 cm above bottom and a propeller (1 cm x 3 cm) 5 cm above the bottom. If not stated otherwise, the stirrer agitation speed was set at 500 rpm.

The cultivation media was prepared according to Table 3-4, directly autoclaved in the bioreactor and cooled down to 35°C under sparging of sterile nitrogen. If glucose or biomass hydrolysates were used as carbon source, they had been autoclaved separately and filled into the reactor, when the temperature was below 40°C. In the next step cysteine HCl and $FeSO_4*7H_2O$ were supplemented, followed by the inoculum (amount according to Eq. (3-1)). To achieve anaerobic conditions the autoclaved medium was sparged with sterile O_2-free N_2 until pre-culture was injected. *C. pasteurianum* was cultivated at 35°C and pH 6. During the fermentation the pH was regulated with 5 M KOH. Fermentations with gas stripping were performed as fed-batch. Feeding solutions with the following concentrations of substrate in MiliQ® water were added: 557 g/L glycerol in mono substrate fermentation; 290 g/L glycerol and 290 g/L glucose in co-substrate fermentation. The feed was added in three batches of 120 g feeding solution. With the first amount of feed all media components from Table 3-4, water, except cysteine HCl and resarzurin, were dissolved in 40 mL MiliQ® and added through sterile filter. Additionally, 0.1 mL of antifoam (Silicon-Antischaumemulsion, Roth) was added, when required.

3.3.3 Fermentation with Brilliant Blue R250 and electro-bioreactors

Brilliant Blue R250

Fermentations with the mediator Brilliant Blue R250 (BB) were either performed in pre-culture flask, lab scale reactors VSF with the set up and procedure as described above (Chapters 3.3.1 and 3.3.2) or DASGIP reactors. The different concentrations tested are listed below in Table 3-7. In the experiments with BB after concentration optimization an amount of 0.06 g/L was adjusted in the cultivation systems. BB was dissolved in water prior addition to the system, the solution showed pH 6.2.

Table 3-7: Concentration of mediator in different cultivation vessels.

Mediator	Concentration [g/L]	Cultivation Vessel
BB	0.02 / 0.04 / 0.06 / 0.08 / 1.00	pre-culture flask
	0.06 (1x)	DASGIP
	0.06 (1x and 2x)	VFS

Some experiments of mediator influence were performed in Dasgip Parallel Bioreactor Systems (DASGIP Bioblock Advanced Stirrer Line SR) consisting of four reactor units (SR0700), each with a working volume of 1000 mL (d_m = 10 cm). The reactors possessed an overhead driven stirrer (two 6 blade stirrer, 1 cm²), which were run at 400 rpm. The redox potential, pH and temperature were measured online with the Dasgip controller system. The pH was regulated with 5 M KOH. Reactor vessels including media were autoclaved separately. Anaerobiosis was maintained by sparging sterile O_2-free N_2 through a sparger needle at the reactor bottom until pre-culture was injected. Pre-culture and fermentation media equals Chapters 3.3.1 and Table 3-4.

Pre-experiments of redox active substances: The following chemicals were added to a cultivation of *C. pasteurianum*, grown under standard conditions in DASGIP reactors. Values in brackets give the final concentration in the reactor: Curcumin (1.3 g/L), Cysteine HCl (4.5 g/L), Na_2S (6 g/L), Brilliant Blue R250 (0.24 g/L).

Electro-bioreactors

The experiments with electro bioreactors were performed in cooperation with Dr. Dirk Holtmann and M.Sc. Thomas Krieg at the research group “Biochemical Engineering”, DECHEMA e.V.

In Fig. 2-7 A (Theory) a picture of the reactor set up (H-cell) is given. Two cell departments (working volume 120 mL) were separated by a Naphion®117 membrane (d_m= 2.6 cm), which was pre-wetted in MiliQ®-water for 24 h. The left cell contained phosphate buffer with pH 6 (23 g/L K_2HPO_4, 118 g/L KH_2PO_4) and the counter electrode. The right cell contained the fermentation media, working electrode and reference electrode (Ag/AgCl, Sensortechnik Meinsberg, Weilheim, D). The reference electrode was placed into the chamber through a Luggin capillary containing 3 M NaCl as an electrolyte near the working electrode. Counter and working electrodes were graphite sticks (d_m = 5 mm, Graphite24, Bad Neuenahr, D), which were covered by liquid over a length of 4 cm. For cultivation in H-cell electro bioreactors, fermentation media according to Table 3-4 was used. After assembly of the compartments including electrodes, the cells were filled with water and autoclaved. Afterwards separately autoclaved cultivation media and phosphate buffer were poured into the according chambers. The pH probes (Mettler Toledo) were arranged in the set and the electrodes were connected with the potentiostat (PCI4, Gamry Instruments). Stirring was realized via magnet stirrer and the headspace was sparged with sterile nitrogen to maintain anaerobic atmosphere. Within fermentation the pH was controlled with 1 M KOH. To avoid foaming 100 µL Antifoam 205 was added. Cultivation temperature of 37°C was maintained with a heater box (Certomat HK, B. Braun International GmbH, D). Within fermentation, samples of 1.5 mL were taken via syringe. If used in the experiment, mediator BB was added at first in the exponential growth phase to reach a concentration of 0.06 g/L in the reactor. Within fermentation time BB was added 2 more times.

3.3.4 Up scaled cultivation

The pre-cultures until 100 mL were prepared in accordance with section 3.3.1., and with the media described in Table 3-2. For the next pre-culture steps the same medium was prepared in 500 mL bottles, which were used as a third pre-culture and inocula for the 30 L reactor. The 30 L reactor acted as pre-culture for the 300 L reactor. For further large scale cultivations in 3 m³ at Biokraftwerke Fürstenwalde GmbH (BKW), the 300 L reactor presented the pre-culture and was transported in a plastic composite IBC (intermediate bulk container, 500 L) vessel to BKW. The IBC had no temperature, no pH control and no stirrer. Effluent gas was released through a water filled bottle.

Cultivations in 30 L scale and 300 L were performed in bioreactors from Bioengineering, including the Bioengineering periphery for the regulation of temperature, pH and stirring. Dimensions of the reactors can be found in the Table 7-2 (Appendix). The 30 L reactor (Type NLF) had a working volume of 20 L, two 6-blade stirrer and four baffles. The 300 L reactor (Type P) had a working volume of 200 L, two 6-blade stirrer and four baffles. The pH was measured with a Bioengineering probe. The whole process, including temperature, pH, stirring, and sterilization processes was controlled with the PCS control software. The piping systems as well as the reactor vessels including media were autoclaved in place with hot steam. Glucose was autoclaved separately in a 300 L media storage vessel (Bioengineering) and added shortly prior inoculation. Fermentations were performed at 35°C and pH 6, regulated with 2.5 M KOH. Stirrer speed did not exceed 125 rpm.

In the company BKW an 8 m³ stainless steel tank was used for pilot scale fermentation with a working volume of 5 m³. For anaerobiosis the vessel was filled with water, which was subsequently released with simultaneous sparging of nitrogen. The media was pasteurized at 80°C through a heating coil inside the vessel, which was also used for temperature control within cultivation. The pH was measured on line in a by-pass system, which was also the feeding point of 5 M KOH for pH regulation. The redox probe was injected in the side of the vessel. Mixing was realized via mechanical turnover of the fermentation broth in 3 min intervals by an internal friborator that sparged headspace gases back through the fermentation broth.

The fermentation media composition for all pilot scales can be found in Table 3-4. The variations of glucose and glycerol concentrations are given in the following Table 3-8.

Table 3-8: Concentrations of glucose and glycerol in different co-substrate fermentations in 200 L and 2000 L scale.

Experiment	Mode	Feed at Time [h]	Glucose	Glycerol
200 L	batch		50 g/L	58 g/L
2000 L BH	fed-batch	0	0	45 g/L (92 kg)
		23, 42	13 kg BH + 17 kg pure	30 kg
		65, 74	13 kg BH + 17 kg pure	60 kg
2000 L rGly	fed-batch	0	0	48 g/L (96 kg) rGly
		17, 27	60 kg pure	60 kg rGly
		43	0	60 kg rGly

BH = biomass hydrolysates, rGLy = raw glycerol.

3.4 Gas stripping

3.4.1 Pre-experimental estimations of gas flow rate and heat transfer area

Required gas flow rates

The calculations are based on the assumption of a binary mixture, consisting of BuOH and water, with the ideal behavior of each component. At first the partial pressure of BuOH and water as well as their molar fractions in the vapor phase were calculated for different possible BuOH concentrations in the range of 5-20 g/L, according to Raoult´s law and Dalton´s law (Eq. (2-5) and (2-7)). The conversion of weight fractions into mole fractions were calculated with Eq. (3-2). Considering a static system, the best results of a gas stripping process can be achieved with the assumption that the amount of stripped BuOH equals the amount of produced BuOH, which was set to be 1 g/(Lh) (Eq. (3-3)). The stripped amount of BuOH equals the molar gas flow times the molar fraction of BuOH in the vapor phase (Eq. (3-4)). To ensure a sufficient removal of BuOH exemplarily security factors of 75 % and 90 % were chosen, to describe the abbreviation of real behavior from the assumed ideal gas behavior and equilibria data concerning the molar fraction of BuOH in the vapor phase (Eq. (3-5)). Further fixed values and assumed data are given in Table 3-11.

$$x_{\mathrm{BuOH}} = \frac{1}{1 + \frac{\widetilde{M}_{BuOH}}{\widetilde{M}_{H2O}} \left(\frac{1 - w_{BuOH}}{w_{BuOH}}\right)} \quad (3\text{-}2)$$

$$\dot{n}_{\mathrm{BuOH\ stripped}} = \dot{n}_{\mathrm{BuOH\ produced}} \quad (3\text{-}3)$$

$$\dot{n}_{\mathrm{BuOH\ stripped}} = \dot{n}_{\mathrm{gas\ total}} \times y_{\mathrm{BuOH}} \quad (3\text{-}4)$$

$$y_{\mathrm{BuOH}} = y_{\mathrm{BuOH\ ideal}} \times 0.75\ (or \times 0.9) \quad (3\text{-}5)$$

x_i = molar fraction of component i in the liquid phase [mol/mol]
y_i = molar fraction of component i in vapor phase [mol/mol]
$\widetilde{M}_i$ = molar weight of component i [g/mol]
w_i = weight fraction of component i [g/g]
$\dot{n}_i$ = molar flow of BuOH [mol/h]

The results of the estimation are summarized in Table 3-9. Additionally the values for 60°C and high BuOH concentrations in the reactors were calculated for the case that gas stripping was used as an end of pipe process at the end of the fermentation. According to these estimations, different compressors with gas flow rates in the range of 1–10 L/min were used (see Table 3-10) to ensure efficient removal of BuOH in the gas stripping experiments described in Chapter 4.4.

Table 3-9: Estimated required gas flow rates for sufficient BuOH removal from the fermentation broth at selected BuOH concentrations and temperatures in the reactor with 1.2 L working volume.

BuOH concentration in reactor	**[g/L]**	**5**	**10**	**20**	**20**
Temperature in reactor	**[°C]**	**35**	**35**	**35**	**60**
Required gas flow rate [vvm]					
(security factor 0.75)	**N_2** [L/min]	5.9	2.9	1.4	0.4
	FG [L/min]	5.5	2.7	1.3	0.4
(security factor 0.90)	**N_2** [L/min]	4.9	2.4	1.2	0.3
	FG [L/min]	4.6	2.3	1.1	0.3

Table 3-10: Utilized compressors and according flowrates for gas stripping experiments.

Compressor	**Flowrate [L/min] → average vvm in experiments**
Miniport	10 → 7 vvm
Mini Laboratory Pump	6 → 4.5 vvm
Mini Vacuum Pump	1 – 2 → 0.8 vvm – 1.5 vvm

Required cooling area in the heat exchanger

For the estimation of the required cooling area in the heat exchanger, the following assumptions were made: The vapor phase with a temperature of 35°C, was considered as a ternary system, consisting of BuOH, water, and nitrogen as the stripping gas. All components exhibit ideal behavior. Further given values and assumed data are shown in Table 3-11. The mean temperature difference was calculated with Eq. (2-13) (see Theory). The heat flow that has to be dissipated from the stripping gas was calculated by the individual values $\dot{Q}_i$ for the condensation of BuOH, H_2O and the cooling of stripping gas (Eq. (3-6) and (3-7)). For the required heat exchanging area Eq. (2-12) (see Theory) was used.

$$\dot{Q}_i = \dot{n}_i \times \Delta h_i \quad (3\text{-}6)$$

$$\dot{Q}_{N2} = \dot{n}_{N2} \times c_{P_{N2}} \times \left(T_{vapor\,in} - T_{vapor\,out}\right) \quad (3\text{-}7)$$

Δh_i = specific enthalpy of condensation i [J/mol]

Under the conditions described above, a required cooling area of 0.021 m² in the heat exchanger was estimated for lab scale cultivation, with an according cooling liquid flow of 0.102 kg/s delivered by the cooling bath. The used condenser was a heat plate exchanger with a cooling surface of 0.340 m², which is ~15 times bigger and therefore considered as sufficient. Even if the BuOH formation rate would increase to 2 g/(Lh), only an area of 0.086 m² would be required.

Table 3-11: Utilized parameters for estimation of required gas flow and area of the heat exchanger.

Parameter	Value	Parameter	Value
V_{broth}	1.2 L	Flow direction	Counter current
$\dot{m}_{BuOH\ produced}$	1 g/(Lh)	$\dot{m}_{cooling\ liquid}$	0.102 kg/s
p_{total}	1 bar	T_{vapor} in /out	35°C / 5°C
p_i^0 (BuOH 35°C)	0.018 bar *	$T_{cooling\ liquid}$ in /out	1°C / 5°C
p_i^0 (H_2O 35°C)	0.056 bar *	Δh_{BuOH}	43290 J/mol *
p_i^0 (BuOH 60°C)	0.0787 bar *	Δh_{H2O}	40680 J/mol *
p_i^0 (H_2O 60°C)	0.1992 bar *	c_{P_H2O}	75 J/(molK) *
k (heat exchanger)	292 W/m²K	c_{P_N2}	30 J/(molK) *

* data received from EuroBioRef project partner TU Dortmund

3.4.2 Reactor set up for gas stripping

For experiments with gas stripping, the standard bioreactor (VSF, Bioengineering) as explained above was used. A scheme of the reactor set up with additional devices for gas stripping is given in Fig. 3-1.

In case of nitrogen sparging, gas stripping with nitrogen was performed in an open system. The reactor was continuously sparged with pure, sterile N_2 from an external source (Linde gases) and regulated by a flow regulator (EL-Flow, Bronkhorst High-Tech, Ruurlo, NL). After condensing butanol, the depleted nitrogen was released as effluent gas. In case of sparging with fermentation gas (containing CO_2 and

H_2) produced by *C. pasteurianum* itself, the gas was taken from the headspace of the reactor and circulated in the closed bioreactor system. In both cases the stripping gas was pumped through the fermentation broth via a gassing needle (outlet needle diameter = 3 mm), which outlet was 3 cm above the reactor bottom in the direction of the stirrer. The gas was collected in the headspace and led through the condenser, a heat plate exchanger (Ewt-B3-12 x 50, Edelstahl-Wärmetauscher, Hannover, Germany) with a copper cooling surface of 0.34 m². The gas was cooled down to 1°C, with the gas and the condensate in co-current flow and the cooling liquid in counter-current flow. The cooling liquid (20 % ethanol in water) was provided by a cooling bath circulation thermostat (ministat 230, Huber, Offenburg, Germany). The resulting condensate was collected in a cooled bottom vessel with a separate outlet for samples. In case of internal stripping the fermentation gas was led back into the fermentation broth. In different experiments the flow rate of gases was varied between 0.7 vvm and 7 vvm, depending on the compressors used. An overview of compressing devices is given in Table 3-10. If necessary, excess gas amounts were collected in a PLASTIGAS®-bag (Linde AG), which was fixed on the reactor head and released in the end of the fermentation, or when the reactor pressure was too low, due to removal of liquids.

The collected condensates consisted mainly of water, butanol and trace amounts of ethanol, which formed a biphasic, azeotropic mixture. It contained up to 70 g/L butanol in the lower phase, and up to 700 g/L butanol the upper phase. For sample analytics both phases were separated manually with a syringe.

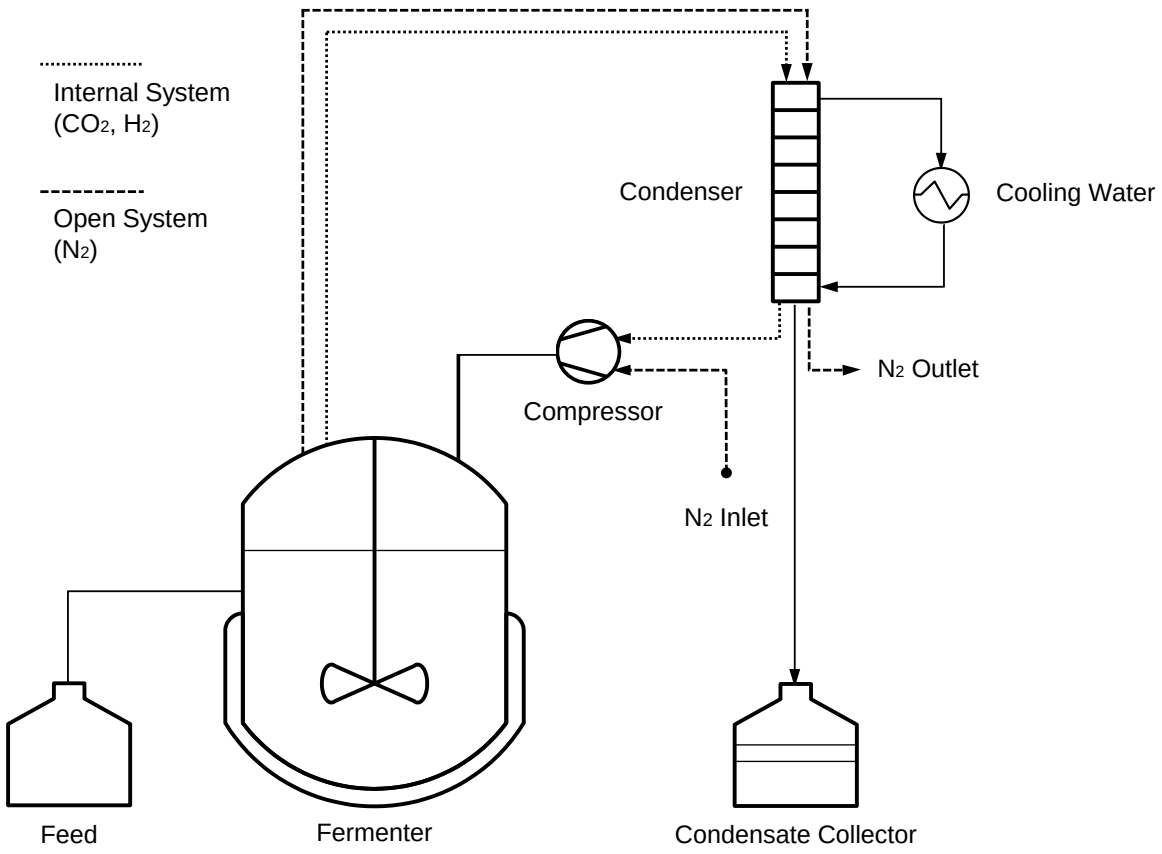

Fig. 3-1: Scheme of the fermenter with gas stripping set up and for sparging either CO_2/H_2 or N_2(Figure from Groeger et al., 2016).

For evaluation of the influence of gas flow rate and stirrer speed on the butanol stripping efficiency and determination of the K_Sa for butanol, 1.2 L synthetic medium (Table 3-12) at a liquid temperature of 35°C was sparged with air (78 % N_2), pure N_2 or a mixture of CO_2 and H_2 (simulated FG: 60 mol% H_2 and 40 mol% CO_2). If not varied, the flow rate was 5.3 vvm and the stirrer speed 550 rpm. The composition of synthetic medium simulates the broth composition in the mid exponential phase of a batch-fermentation with *C. pasteurianum*.

Table 3-12: Composition of synthetic media.

Chemicals	Concentration [g/L]
Glycerol	20
BuOH	10
1,3-PDO	7
EtOH	2
Butyrate	0.5
Acetate	0.5

3.4.3 Mathematical descriptions of the gas stripping process

The stripping rate of a component i in liquid (r_i) for a static system follows a first order kinetic (2-4) as suggested by Truong and Blackburn to (Truong and Blackburn, 1984). The volumetric mass transfer coefficient for the stripped component is expressed by K_Sa [h^{-1}], including the interfacial area *a* [m²] of the boundary layer. The K_Sa values for gas stripping of butanol out of the synthetic medium as described above were calculated by equation (3-8), where c_{B0} and c_{Bt} are the BuOH concentrations [g/L] in the reactor, at time points 0 and t, respectively. During gas stripping applied to a cultivation of *C. pasteurianum*, butanol was produced and stripped out simultaneously. Thus, the concentrations in the culture vary and the equation ((2-4) could not always be applied. For that the butanol stripping rates $r_{B\ cond}$ [g_{BuOH}/(Lh)] were calculated as an average from the total amount of collected BuOH in the condensates c_{BCi} [g/L] over the gas stripping time t_{Si} [h] (3-9). The selectivity α is a dimensionless value to express the preferential recovery of component i from a mixture. It was calculated by equation (3-10) as the ratio of the butanol weight fractions in the condensate (w_c) and the remaining butanol weight fractions in the fermentation broth (w_{fb}), respectively (Ezeji et al., 2004).

$$K_Sa \times t = \ln \frac{c_{B0}}{c_{Bt}} \tag{3-8}$$

$$r_{B\ cond} = \frac{c_{BC1} - c_{BC0}}{t_{S1} - t_{S0}} \tag{3-9}$$

$$\alpha = \frac{w_c/(1 - w_c)}{w_{fb}/(1 - w_{fb})} \tag{3-10}$$

3.5 Sample preparation and analytics

3.5.1 Cell concentration and growth

Within cultivation of *C. pasteurianum* samples were taken every hour in the exponential phase and every 2 h within the stationary phase. The optical density (OD) was determined via spectrophotometry (VWR Spectrophotometer V-1200, Leuven, BE) at 600 nm. In case of fermentation with Brilliant Blue R250 (BB), the OD of BB in the media was determined separately. Short centrifugation (30 s, 5000 rpm) pelleted the cells and the OD of the supernatant, containing the BB, was measured. The resulting OD was subtracted from the OD of the mixture. Correlation of OD and cell dry weight (CDW) for the biomass content with and without BB in the broth showed the same results. A correlation between OD and cell dry weight for the biomass concentration (BM in [g/L]) is shown in Fig. 3-2. For determination of BM the cell suspension was centrifuged at 13.000 rpm for 10 min. The supernatant was discarded and the pellet dried at 80°C for 24 h prior weight measurement. The linear regression is given in formula (3-11).

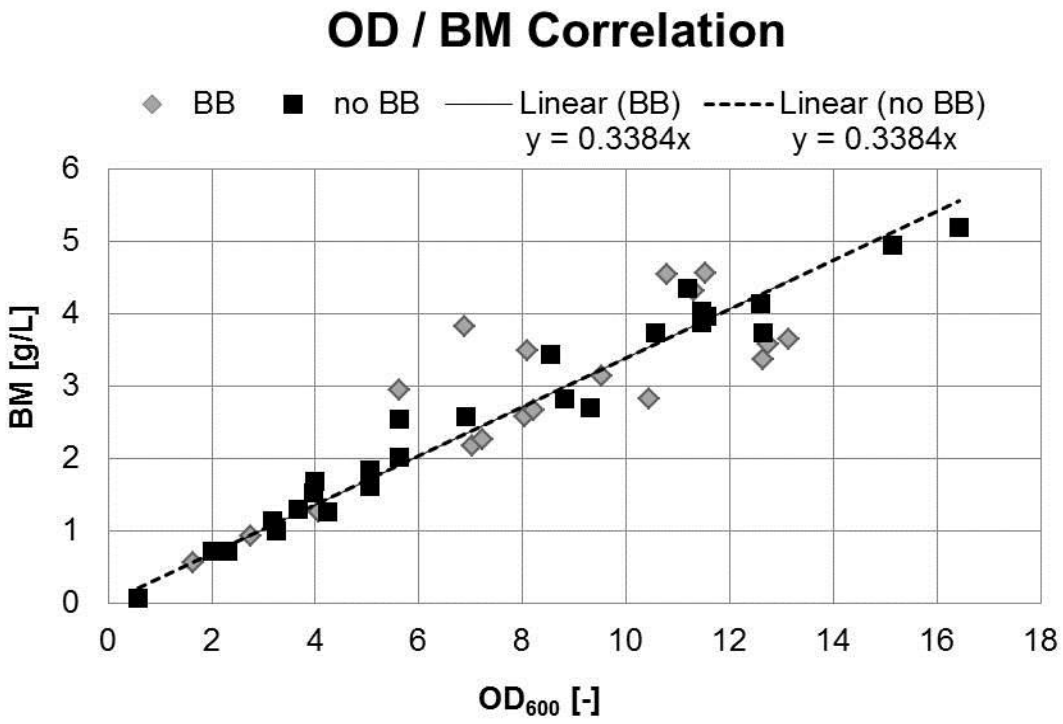

Fig. 3-2: Linear regression of optical density and biomass concentration. Black = without dye. Grey = with Brilliant Blue R250 dye.

$$\mathrm{BM}\ \left[\frac{\mathrm{g}}{\mathrm{L}}\right] = 0.3384\ \times \mathrm{OD}_{600} \tag{3-11}$$

The specific growth rate μ [h^{-1}] was determined from smoothed data of biomass concentration (using the software Origin 8.5.1 G SR1, OriginLab Corporation, Northampton, USA), according to equation (3-12), where x_i is the concentration of cells in [g/L] and t_i the time [h].

$$\mu = \frac{\ln x_2 - \ln x_1}{t_2 - t_1} \tag{3-12}$$

3.5.2 Substrate and product concentration

The substrates (glycerol, glucose) and product concentrations (*n*-butanol, 1,3-propanediol, ethanol, acetic-, butyric-, lactic- and formic acid) were analyzed with high performance liquid chromatography (HPLC), containing refractive index and ultraviolet detectors. Prior analysis the samples were centrifuged (13.000 rpm, 3 min) and filtered (0.22 μm mesh). The HPLC system used is from the company Kontron instruments (details see Table 3-13). The separation was realized with an Aminex HPX-87H column at a working temperature of 60°C. The flow rate was adjusted to 0.6 mL/min with 0.005 M H_2SO_4 as eluent. Solvent compounds as well as glucose and glycerol were detected via refractive index (RID) and organic acids via ultra violet sensors.

Table 3-13: Operation parameters of Kontron HPLC devices.

Devices	Parameter
Kontron HPLC Autosampler 360 (Kontron, Rossdorf, D)	8°C
Kontron HPLC Pumpe 322 (Kontron, Rossdorf, D)	0.6 mL/min
Aminex HPX-87H column (300 x 7.8 mm) (Kontron, Rossdorf, D)	60°C
HPLC 332 detector (Kontron, Rossdorf, D)	λ= 210 nm
Refractive Index detector RID-6A (Shimadzu, Kyoto, J)	

3.5.3 Effluent gas concentration

The composition of the effluent gas from cultivations of *C. pasteurianum* was measured with a mass spectrometer (MS, OmniStar 300, Balzer Instruments/ Pfeiffer Vacuum GmbH). The bacteria were grown in the standard bioreactor (VFS, Bioengineering) under standard conditions, as well as iron excess and iron limitation. The effluent gas was led through a MilliGascounter (Dr.-Ing. Ritter Apparatebau GmbH & Co. KG) for the measurement of the volumetric gas flow. The MS took 0.5 mL/min for a continuous measurement on 8 masses for the concentration analysis of H_2, CO_2, O_2, N_2 and Ar with the following conditions, summarized in Table 3-14.

Table 3-14: Operation parameters of the Omnistar mass spectrometer.

Device	Parameter
Inlet tube	T = 60°C
Ionsource: Thungsten filament	SEM Voltage = 800 V
Pre-and high Vacuum pumps	Min. Pressure: ~8*10^{-7} mbar
Detector: Channeltron	Detected masses: 2, 12, 14, 28, 32, 40, 44
	Measuring time per mass: 1 s

3.5.4 Proteomics

The 2D-gel electrophorese was performed by Jan Bomnüter and Anna Gorte. Analytics in the MS as well as software analytics were performed by Dr. Wei Wang.

Samples for proteomics were taken in the early (OD 2-4) or late exponential growth phase (OD 8-10) within cultivation of *C. pasteurianum* DSMZ 525 and a protease-inhibitor cocktail (complete Mini, Roche) was added immediately. After centrifugation (15 min, 5000 rpm, 4°C) the supernatant was frozen for storage. The pellets were washed two times with tris-buffer and stored at -20°C.

In the following the intracellular proteins were separated by a two-dimensional gel electrophoresis method (2-DE) established in the Institute of Bioprocess and Biosystems Engineering, TU Hamburg-Harburg. The cell pellets were resuspended in a lysis/rehydration buffer (containing 7 M urea, 2 M thiourea, 4 % w/v CHAPS, 100 mM DTT, 0.5 % IPG buffer 3–10, protease inhibitors cocktail). They were disrupted using silica beads in a FastPrep-24 high-speed homogenizer (MP Biomedicals) at a speed of 6.0 m/s for 8 cycles of 60 s, with 5 min intervals for cooling on ice between the cycles. The crude proteins were extracted from the lysate by phenol-precipitation. Therefore, the samples were mixed with phenol and incubated for 10 min at 4°C, followed by washing steps with water and cooled acetone (-20°C). Finally the pellet was freeze dried in a vacuum-centrifuge (30 min, 39°C, 15 mbar; Christ) and the samples are stored at -80°C. Prior further proceedings the pellets were resuspended in lysis buffer and the protein concentration was determined with the 2D quant Kit (GE Healthcare), according to the manufacturer's instruction.

The chromatographic separation of the proteins occurred in two steps: The first dimension isoelectric focusing (IEF) was conducted using 18 cm IPG strips (pH 4–7) in an Ettan IPGPhor 3 IEF system (GE Healthcare) with the following voltage program: 30 V for 6 h, 60 V for 6 h, 200 V for 1 h, 500 V for 1 h, 1000 V for 1 h, gradient to 8000 V within 30 min and 8000 V for 8 h. Subsequently, the focused IPG strips were equilibrated in two steps of 15 min each with 15 mL of equilibration buffer (50 mM Tris-HCl, pH 8.8, 6 M urea, 30 % w/v glycerol, 2 % w/v SDS) supplemented with 1 % w/v DTT in the first and 2.5 % w/v iodoacetamide in the second step. The second dimension SDS-PAGE was performed with the Ettan DALTtwelve vertical system (GE Healthcare) using 12.5 % polyacrylamide gels and the following parameters: 1.5 W/gel for 1 h and 10 W/gel until the bromophenol blue dye front reached the bottom of the gels. Afterwards, the gels were stained with self-made ruthenium II bathophenanthroline disulfonate chelate (RuBPS) fluorescent dye. For the identification of protein spots with statistically

significant changes in their expression levels due to different cultivation conditions, the gels were scanned with the molecular imager VersaDoc MP4000 (Bio-Rad) and analyzed using the Progenesis SameSpots software (v3.3, Nonlinear dynamic, UK).

After that, the proteins spots were determined by nanoLC-ESI-MS/MS analysis using an Ultimate 3000 RSLCnano HPLC system (Thermo Fisher Scientific) coupled to an amaZon ETD ion-trap mass spectrometer (Bruker Daltonics). The proteins were tryptic digested in-gel at 37°C overnight and subsequently purified with C18 peptide cleanup pipette tips (Agilent). Finally the tryptic peptides were dissolved in 0.1 % trifluoroacetic acid and pre-concentrated on an Acclaim PepMap100 C18 (100 µm x 2 cm, 5 µm) column and then separated on an Acclaim PepMap RSLC C18 (75 µm x 15 cm, 2 µm) column. As mobile phase were used: A) 0.1 % formic acid in water and B) 10.1 % formic acid in acetonitrile:water (90:10). The peptides were separated with a 30 min linear gradient from 2 % B to 45 % B delivered at a flow rate of 300 nL/min. The tryptic peptides received from the C18 analytical column were led into the mass spectrometer through a CaptiveSpray nano-ESI source (Bruker Daltonics) operating at positive mode controlled by the trapControl acquisition software (version 4.0). The operation parameters applied are: -1500 V capillary voltage, 3 L/min flow rate, 160°C drying gas temperature. The scan ranges were 300–1500 m/z for MS and 100-2400 m/z for MS/MS. The MS/MS analysis was carried out in data-dependent auto MS/MS mode using a 4 Da window for precursor ion selection and an absolute threshold of 25000 Da. After the acquisition of 2 MS/MS spectra from the same precursor ion the m/z was excluded from the precursor selection for 1 min. The results of nanLC-ESI-MS/MS analysis were transferred into XML files via Compass DataAnalysis software (version 4.1) with the 300 most intense MS/MS spectra per MS/MS analysis were converted and used for protein database search. Subsequently, the XML files were compared with a specific protein database of *C. pasteurianum* DSMZ 525 installed in-house on a licensed Mascot server by the ProteinScape™ software, with the following parameters: allow up to 1 missed cleavage, 0.6 Da tolerance both for peptide and MSMS, 1+, 2+ and 3+ peptide charges, carbamidomethyl (C) as fixed modification, oxidation (M) as variable modification, only accept protein identified by at least 2 peptides with false positive rate <1 %.

3.6 Production rates and mass balances

Product yields and production rates were calculated using the following equations (3-13) until (3-18):

Product yield per substrate [g/g]

$$Y_{P/S} = \frac{\Delta C_P}{\Delta C_S} = \frac{C_{P,t_2} - C_{P,t_1}}{C_{S,t_1} - C_{S,t_2}} \quad (3\text{-}13)$$

Specific product yield [g/g]

$$Y_{P/X} = \frac{\Delta C_P}{\Delta C_X} = \frac{C_{P,t_2} - C_{P,t_1}}{C_{X,t_1} - C_{X,t_2}} \quad (3\text{-}14)$$

Specific substrate consumption [g/g]

$$Y_{S/X} = \frac{\Delta C_S}{\Delta C_X} = \frac{C_{S,t_2} - C_{P,t_1}}{C_{X,t_1} - C_{X,t_2}} \quad (3\text{-}15)$$

Product formation rate [g/(Lh)]

$$r_P = \frac{C_{P,t_2} - C_{P,t_1}}{t_2 - t_1} \quad (3\text{-}16)$$

Substrate consumption rate [g/(Lh)]

$$r_{Su} = \frac{C_{S,t_2} - C_{S,t_1}}{t_2 - t_1} \quad (3\text{-}17)$$

Specific product formation rate [g/(gh)]

$$q_P = Y_{P/X} \times \mu \quad (3\text{-}18)$$

C_P = product concentration [g/L]
C_S = substrate concentration [g/L]
C_X = biomass concentration [g/L]
t_i = time [h]

Except for gas stripping, all concentrations were used in g/L. In the gas stripping experiments, the butanol amounts were measured in the condensate in g and can only be related to the absolute product and biomass amounts in the reactor [also in g]. Besides this, the concentration of other products in the broth varies, due to fed-batch addition of substrate.

ATP formation rate

For the specific ATP formation rate (q ATP [mmol/(gh)]) the following Eq. (3-19) was used, which is based on the stoichiometric equations of glycerol conversion in *C. pasteurianum* (Table 7-6 in Appendix). The specific formation rate of each product (q_P) was calculated according to Eq. (3-18) and Eq. (3-14), with the exception that Eq. (3-14) was calculated with the concentration in [mmol/L] instead of [g/L].

$$\mathrm{q\,ATP} = 2\,\mathrm{q_{acetate}} + 1\,\mathrm{q_{ethanol}} + 3\,\mathrm{q_{butyrate}} + 2\,\mathrm{q_{butanol}} + 1\,\mathrm{q_{lactate}} \quad (3\text{-}19)$$

Carbon balance

The general balance for anaerobic bacterial growth and product formation from a substrate can be expressed by the following macroscopic equation (3-20) suggested by Zeng et al. (Zeng, 1995):

$$\mathrm{a\,CH_mO_l} + \mathrm{b\,NH_3} = \mathrm{y\,CH_pO_nN_q} + \mathrm{z\,CH_rO_sN_t} + \mathrm{c\,H_2O} + \mathrm{d\,CO_2} + \mathrm{e\,H_2} \quad (3\text{-}20)$$

CH_mO_l = substrate
NH_3 = ammonia source
$CH_pO_nN_q$ = biomass
$CH_rO_sN_t$ = products

The main extracellular products of glycerol and/or glucose fermentation by *C. pasteurianum* are butanol, 1,3-PDO, ethanol, acetate, butyrate, lactate and formate. The coefficients for the concentrations of substrate (a) and products (z) are based on the HPLC results according to section 3.5.2. The amount of cell dry weight was calculated with formula (3-11). The biomass composition of *C. pasteurianum* was assumed to be $C_4H_7O_2N$ with a molar mass of 101.10 g/mol (Biebl, 2001). All concentrations were converted to mol amounts via their molar masses (Table 7-1 in Appendix) and the amounts of carbon atoms per molecule were calculated according to their atomic composition. Stoichiometric assumptions are based on the metabolic pathway were made for the formation of CO_2. 1 mol of CO_2 was produced per 1 mol of ethanol and per 1 mol acetate, respectively. Additionally, 2 mol CO_2 were produced per 1 mol butanol and per 1 mol butyrate.

The recovery of carbon atoms (C) is given in percent and can be calculated by the quotient of carbon input and carbon output by the following equation (3-15).

$$\mathrm{C_{recovery}\,[\%]} = \frac{\sum \mathrm{C_{products}} + \sum \mathrm{C_{CO_2\,formed}}}{\sum \mathrm{C_{substrates}}} \quad (3\text{-}21)$$

C [-] = the number of carbon atoms in the products (incl. biomass) and substrates

NADH balance

The balance for the reducing equivalent NADH, Eq. (3-22) is based on the stoichiometric equations (Table 7-6 in Appendix) of glycerol conversion in *C. pasteurianum*. The molar amounts of products were calculated in the same way like for the carbon balance. The indirect consumption of NADH resulting in H_2 formation is explained in Chapter 4.2 and alters the calculation into (3-23). For the balance, this amount ΔH_2 was calculated by the difference of stoichiometrically produced hydrogen amount and measured hydrogen amount in the effluent gas.

$$\mathrm{NADH_{recovery}}\ [\%] = \frac{\mathrm{c_{1,3-PDO}}}{2\ \mathrm{c_{acetate}} + 2\ \mathrm{c_{butyrate}} + \mathrm{c_{lactate}} + 13.2\ \mathrm{a_{BM}}} \qquad (3\text{-}22)$$

$$\mathrm{NADH_{recovery}}\ [\%] = \frac{\mathrm{c_{1,3-PDO}} + \mathrm{c_{\Delta H2}}}{2\ \mathrm{c_{acetate}} + 2\ \mathrm{c_{butyrate}} + \mathrm{c_{lactate}} + 13.2\ \mathrm{a_{BM}}} \qquad (3\text{-}23)$$

c = concentration of products in [mmol/L] and biomass (BM) in [g/L]

4 Results

4.1 Substrate dependent metabolites production by *C. pasteurianum* DSMZ 525 [9]

C. pasteurianum is able to convert not only glycerol as a carbon and energy source, but also glucose. Considering fluctuations in the substrate prices and availabilities, detailed knowledge about the influence of both pure substrates on the process performance of *C. pasteurianum* is mandatory for their application in biorefinery processes. Also co-substrate fermentation with varying fractions can be applied due to economically aspects, like using cheaper available carbon sources, but also to improve or change the product pattern. For example, regarding 1,3-PDO production, several sugars can be used as co-substrates to glycerol, but the other resulting fermentation products should be highly oxidized to provide sufficient intracellular NADH for the formation of the valuable diol (Biebl and Marten, 1995). In this Chapter *C. pasteurianum* was therefore at first grown on sole glycerol under standard conditions. In the following the influence of pure glucose as substrate, as well as co-substrate fermentations with glycerol and glucose in different ratios was analyzed. In view of possible future application as a biorefinery process also the suitability of raw glycerol and glucose containing wood hydrolysates were analyzed, alongside a transfer into of the cultivation into semi-pilot and pilot scale.

4.1.1 Fermentation of pure glycerol

At first *C. pasteurianum* DSMZ 525 was grown on sole glycerol as duplicate under standard growth conditions in a VSF bioreactor as described in the methods Chapter 3.3. The maximum biomass concentration reached in a fermentation time of ~40 h was 5.1 ± 0.1 g/L, with μ_{max} = 0.17 ± 0.0 h^{-1} in the exponential phase. Within this time pure glycerol was consumed in a rate of 3.5 ± 0.1 g/(Lh). In average 10.5 ± 0.4 g/L BuOH as well as 11.6 ± 2.3 g/L 1,3-PDO were produced, plus a total amount of 4.8 ± 1.6 g/L organic acids. Table 4-1 collects the final titers, formation rates and yields. The carbon recovery reached 98 ± 1 %.

Additionally, in one fermentation the effluent gases produced by *C. pasteurianum* DSMZ 525 itself were measured (see also Table 4-1 and Fig. 4-1). Over the whole fermentation time 403 mmol/L CO_2 and 469 mmol/L H_2 were produced, which equals a fermentation gas amount of 4.3 L/g_{BM}. The average composition was ~60 % H_2 and ~40 % of CO_2 over the whole production time. Gas formation decreased to an undetectable amount in the stationary phase, probably because the increased inhibitory effect of butanol. In fact, in anaerobic serum bottles growth inhibition of *C. pasteurianum* was detected at a concentration around 5 g/L. According to the commonly known pathway, described in Chapter 2.2.3, the theoretical ratio of H_2 to CO_2 equals 1, if the interaction of pyruvate:ferredoxin oxidoreductase and hydrogenase are the only source of H_2 formation. However, the higher final ratio of 1.2 mol/mol achieved here indicates, that another metabolic step is active in the evolution of H_2 in *C. pasteurianum* DSMZ 525, for example the conversion of pyruvate to acetyl-CoA or the conversion of crotonyl-CoA to butyryl-CoA, catalyzed by the ferredoxin-dependent butyryl-CoA dehydrogenase / electron transferring flavoprotein complex. The latter one will be further discussed in the following Chapter 4.2.

[9] Parts of this chapter are based on Sabra et al. (2014) and Sabra et al. (2016).

Table 4-1: Final product titer and yields for batch fermentations of pure glycerol by *C. pasteurianum* DSMZ 525.

		BuOH	1,3-PDO	EtOH	Butyrate	Acetate	Lactate	Formate
final titer	[g/L]	10.5	11.6	1.3	2.7	1.3	0.2	0.6
		± 0.4	± 2.3	± 0.2	± 1.4	± 0.1	± 0.0	± 0.1
formation rate	[g/(Lh)]	0.62	0.63	0.05	0.19	0.07	0.03	0.03
		± 0.25	± 0.18	± 0.00	± 0.08	± 0.01	± 0.00	± 0.01
$Y_{P/S}$	[g/g]	0.20	0.19	0.02	0.04	0.01	0.01	0.01
		± 0.02	± 0.03	± 0.01	± 0.02	± 0.01	± 0.00	± 0.01
$Y_{P/X}$	[g/g]	1.79	1.83	0.14	0.53	0.19	0.08	0.09
		± 0.32	± 0.88	± 0.01	± 0.26	± 0.05	± 0.02	± 0.01
		H_2	**CO_2**					
final titer	[mmol/L]	469	403					
formation rate	[mmol/(Lh)]	26	24					
$Y_{P/S}$	[mmol/g]	7.3	6.5					
$Y_{P/X}$	[mmol/g]	84	75					

Note: Formation rates are calculated in exponential phase. For titer and yield the final amounts are given.

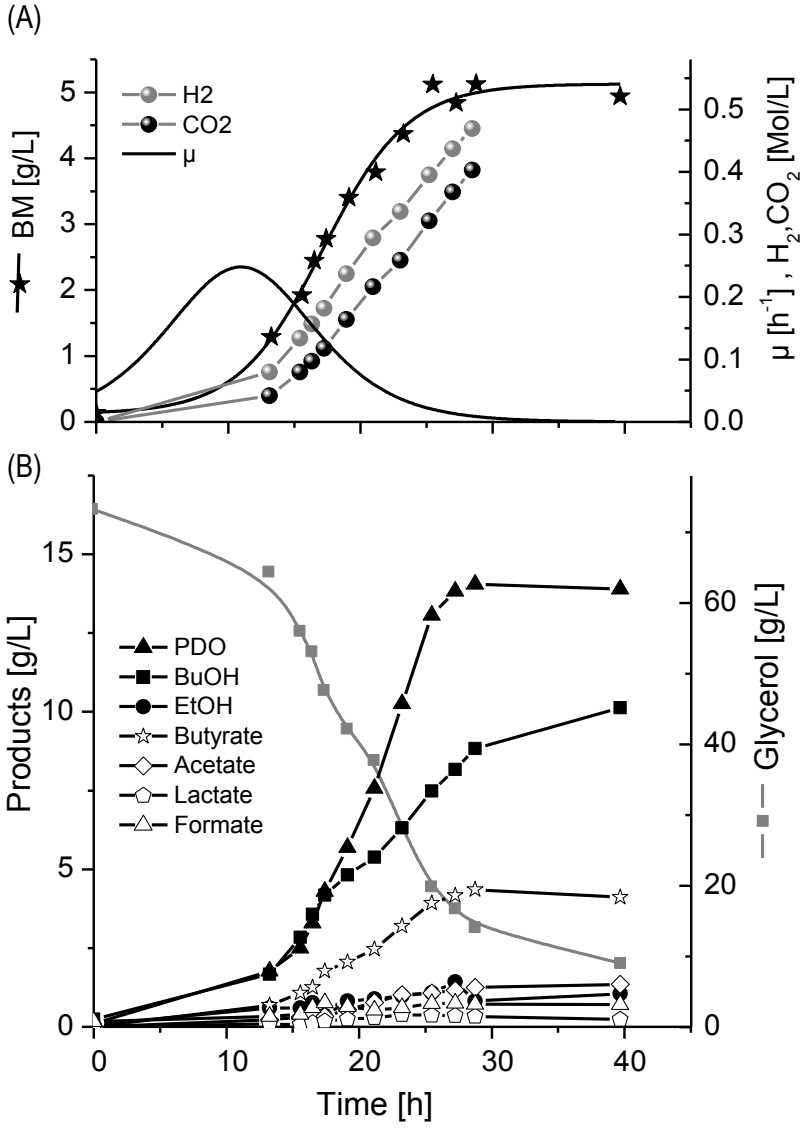

Fig. 4-1: (A) Growth and effluent gas formation, (B) substrate consumption and product formation of *C. pasteurianum* DSMZ 525 during fermentation of pure glycerol.

4.1.2 Co-substrate fermentation with different combination of glycerol and glucose

Glucose from biomass hydrolysates become an alternative, low-cost renewable source of carbon for the bioproduction of chemicals (Xin et al., 2016). Due to the fact that *C. pasteurianum* is able to convert not only glycerol as substrate but also glucose, it appears to be an attractive candidate for the utilization of co-substrates in future biorefinery processes. Therefore, fermentation on sole glucose and co-substrate fermentations with different glucose contents, as well as the suitability of wood hydrolysates were compared. The different amounts of glucose and glycerol in the media of co-substrate fermentations and according denotations can be found in Table 3-5 in Chapter 3.2.2. All results are presented in Fig. 4-2, Fig. 4-3, Fig. 4-4, as well asTable 4-2.

Generally, biomass formation was significantly enhanced with increased glucose content in the medium. The growth rate μ steadily increased from 0.24 h^{-1} at 20 % glucose to 0.29 h^{-1} at 100 % glucose, compared to only 0.19 h^{-1} with pure glycerol as substrate (0 % glucose) (Fig. 4-3 A). Accordingly, the

highest biomass concentration of 13.7 g/L was achieved with pure glucose as substrate (Fig. 4-2, A4). However, with reduced glycerol content in the media, the 1,3-PDO titer decreases, since no natural pathway for the production from glucose exists (Biebl et al., 1999). The 1,3-PDO formation rates were highest on glycerol as sole carbon source (0.63 g/(Lh)) and decreased to 0.39, 0.29, 0.11 and 0 g/(Lh) at 20 %, 50 %, 80 % and 100 % glucose content, respectively. It was also found that the formation of butyric and acetic acid increased strongly with increasing glucose content (Fig. 4-3 B). The formation of either acid from butyryl or acetyl phosphate is connected to the formation of 1 mol ATP. ATP is an important cellular energy carrier, which is among other reactions involved in RNA synthesis, and necessary for biomass formation and maintenance (Schneider and Gourse, 2004). Thus, the increased acid formation and according to this the ATP pool supports the higher growth rates. On pure glucose, acidogenesis and solventogenesis were slightly more separated, compared to glycerol, and co-substrate fermentation (Sabra et al., 2014). Interestingly, the complete consumption of 20 g/L glucose at the 20 % glucose fermentation led to cessation in glycerol consumption and beginning of the stationary growth phase. Whereas in the case of 80 % glucose content, the complete consumption of 20 g/L glycerol did not affect the glucose utilization and the growth rate only slowed down from 0.43 g/(Lh) to 0.23 g/(Lh) (Fig. 4-2, ”1” and “3”). Although *C. pasteurianum* can use either glycerol or glucose separately as a sole carbon and energy source, the observed inhibition of glycerol utilization after the exhaustion of glucose is crucial if an optimization of *n*-butanol production is aimed. This reaction was studied in more detail by Sabra et al. (Sabra et al., 2016). It was shown that the anaplerotic synthesis of oxaloacetate plays a key role in determining the growth behavior of *C. pasteurianum* in co-substrate fermentations. However, in both cases, 20 % and 80 % glucose content, the final BuOH titer was almost equal with 11.4 g/L, which is slightly enhanced in comparison to sole glycerol as substrate. But with 80 % glucose, more acids are formed and less amounts of the second target product 1,3-PDO (Table 4-2). The highest BuOH titer of 21 g/L was achieved with equal amounts of glycerol and glucose in the media. Here, both substrates were consumed almost equally at 2.4 ±0.14 g/(Lh) and no limitation of either substrate were detected. Compared to sole glycerol, the 1,3-PDO formation rate was strongly decreased from 0.63 g/(Lh) to 0.29 g/(Lh). Even though the highest biomass concentration was achieved on pure glucose as substrate, only 7.8 g/L of BuOH were produced, besides a vast amount of acids (Fig. 4-2 “4”, Fig. 4-3).

Andrade and Vasconcelos (Andrade and Vasconcelos, 2003) used a mixture of 50 % glycerol and 50 % glucose in continuous cultures of *C. acetobutylicum,* resulting in 5.4 g/L BuOH and 2.2 g/L total acids. The increase to 66.7 % glucose content enhanced the BuOH titer to 7.6 g/L, but also the amounts of total acids to 7.6 g/L. The maximum BuOH productivity they reached was 0.42 g/(Lh), which is in the range of our results for 50 % glucose, with an overall productivity of 0.43 g/(Lh). Kao et al. (Kao et al., 2013) analyzed the co-fermentation of glucose and glycerol with *C. pasteurianum* CH4. They found the best ratio of glucose to be 25 % (20 g/L glucose + 60 g/L glycerol) resulting in a final butanol titer of 13.3 g/L and an overall formation rate of 0.28 g/(Lh). The authors also observed that increasing glucose content led to lower 1,3-PDO titer. The data are comparable to the presented results for 20 % glucose content, with a final BuOH titer of 11.4 g/L and an overall production rate of 0.23 g/(Lh). However, at the same time only ~4.5 g/L 1,3-PDO are produced by *C. pasteurianum* CH4 (Kao et al., 2013), compared to the 10.3 g/L reported within this work.

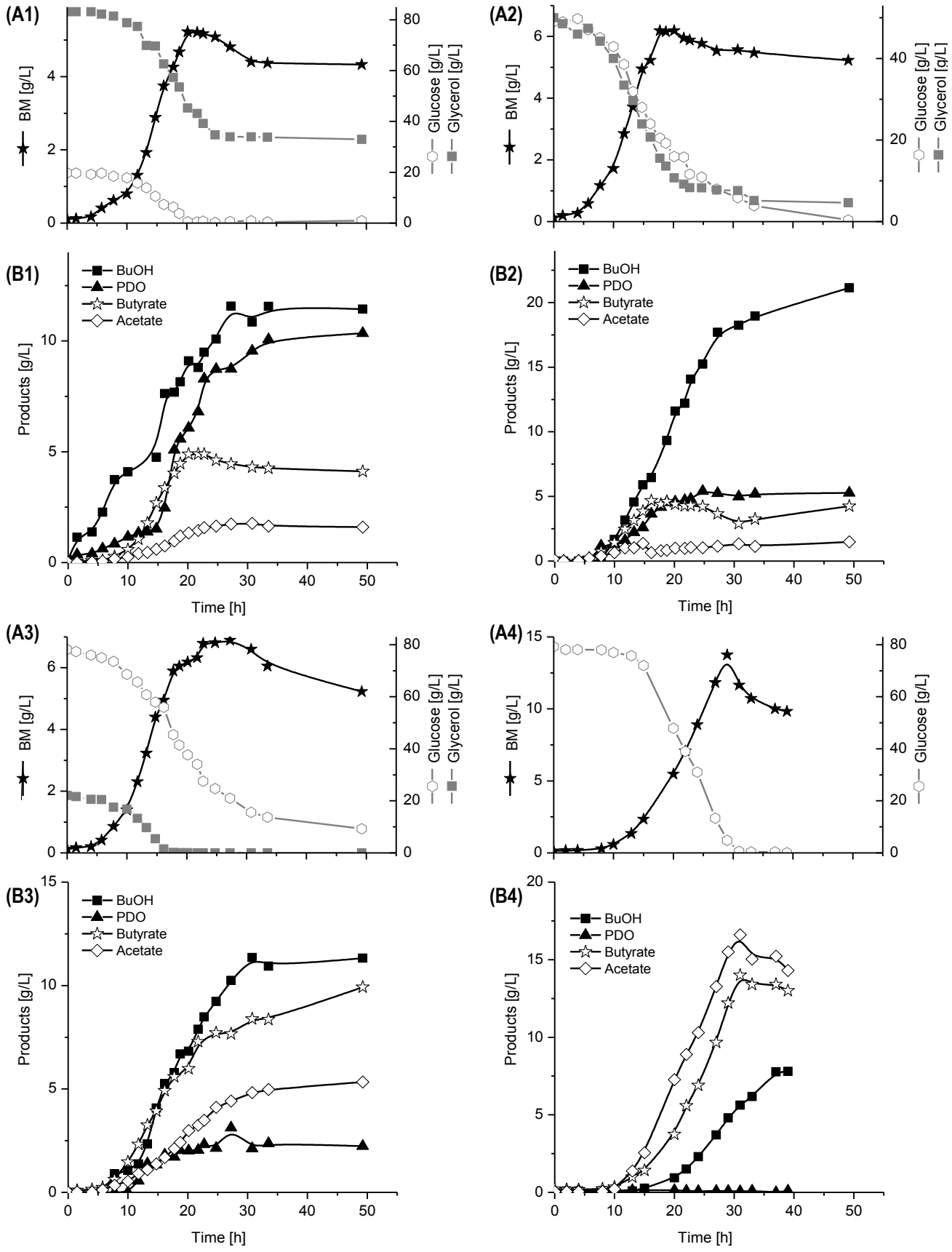

Fig. 4-2: (A) Growth and substrate consumption and (B) product formation of *C. pasteurianum* DSMZ 525 during co-substrate fermentation with different glucose amounts: (1) 20 % (2) 50 % (3) 80 % (4) 100 %. (Figures base partly on Sabra et al., 2014).

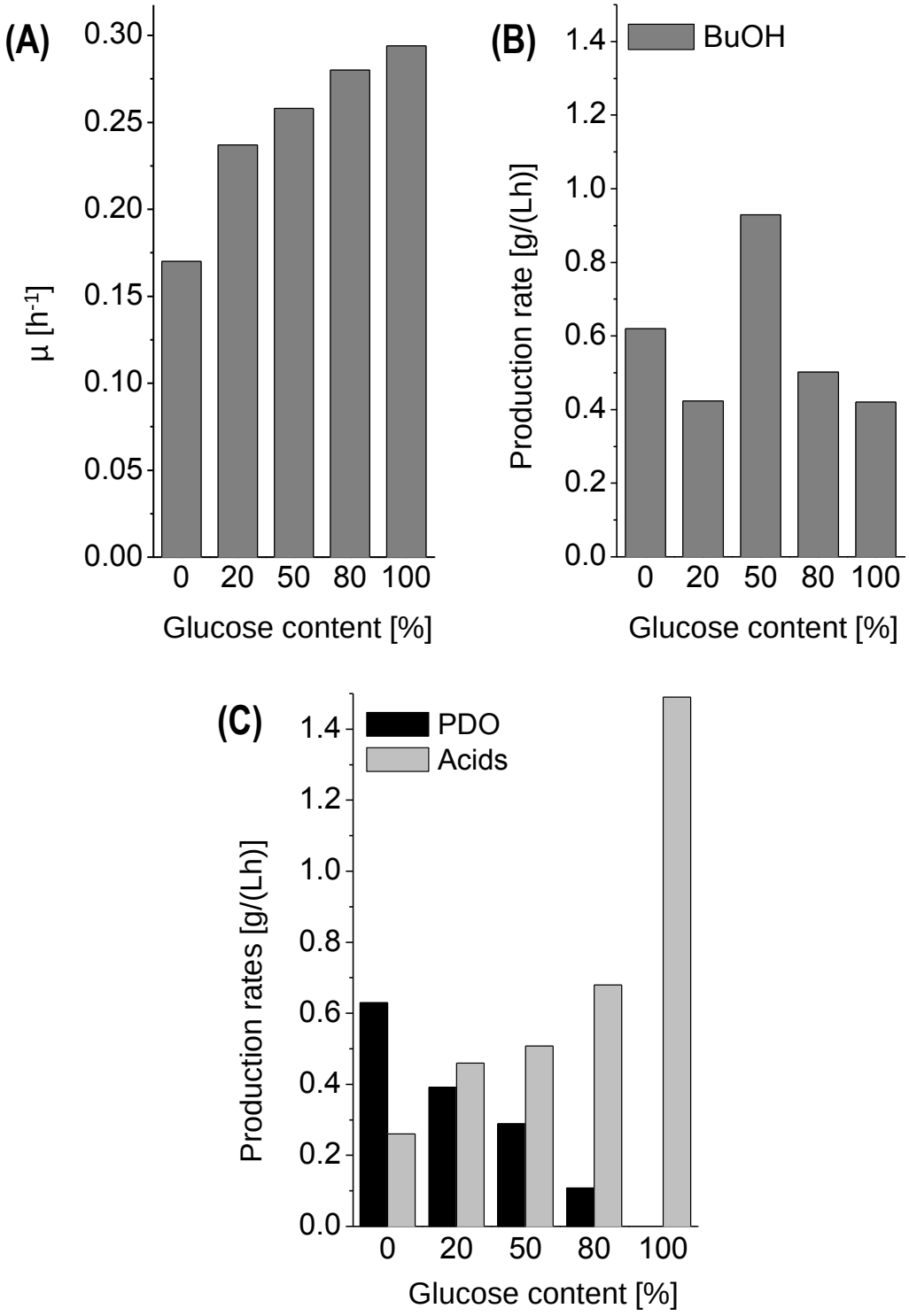

Fig. 4-3: (A) Growth rate μ and (B) BuOH production rate as well as (C) product formation rates for 1,3-PDO and acids of *C. pasteurianum* DSMZ 525 during cultivation of co-substrates with different glucose contents in the substrate mixture.

Co-substrate fermentation with biomass hydrolysate

Considering the application of renewable biomass as carbon sources for biotechnological productions, it is mandatory to analyze the suitability of real biomass hydrolysates, containing glucose and other hexose or pentose sugars, for fermentation by *C. pasteurianum*. Using 50 g/L glycerol and 50 g/L glucose from spruce wood hydrolysate as substrate, resulted in a slightly reduced growth rate of 0.23 h^{-1} compared to pure glucose. Nevertheless, relatively high amounts of 17.4 g/L BuOH with a formation rate of 1.11 g/(Lh) in the exponential phase were achieved. In contrary to pure glucose, only 1.8 g/L of 1,3-PDO was produced (Fig. 4-4, Table 4-2). Interestingly in this case, the glucose consumption rate was with 3.33 g/(Lh) higher than 2.18 g/(Lh) for glycerol, which might explain the reduced 1,3-PDO formation and further increase in acid production. In the same experiment the glucose limitation resulted in a stop of glycerol consumption and is in the time range with the onset of the stationary growth phase. This further limited the 1,3-PDO formation. Similar results were reported by Kao et al. (Kao et al., 2013) using *C. pasteurianum* CH4 for the conversion of raw glycerol and 20 % glucose from bagasse hydrolysate. The authors achieved 11.8 g/L BuOH (0.14 g/(Lh)) and 3.9 g/L 1,3-PDO, which is also below their results of pure glucose.

According to the supplier, the biomass hydrolysate mixture provided (Hydrolysate 1) contained besides glucose also xylose and mannose. *Clostridium* species can convert hexoses, like mannose, via the glycolysis pathway, whereas pentoses, like xylose, are metabolized in the pentose phosphate pathway (Jang et al., 2012). However, the final concentrations of these sugars in the medium are too low compared to glucose, for a significant shift of the product selectivity.

In general it must be noted that even though the biomass hydrolysates used in this work were received from the same company, they exhibit very different compositions and appearances (e.g. color, viscosity), which might depend on the type of biomass and the pretreatment process. Thus, a clear influence of the usage of BH on metabolism of *C. pasteurianum* DSMZ 525 is relative and the results are only meaningful in context of the BH types analyzed here.

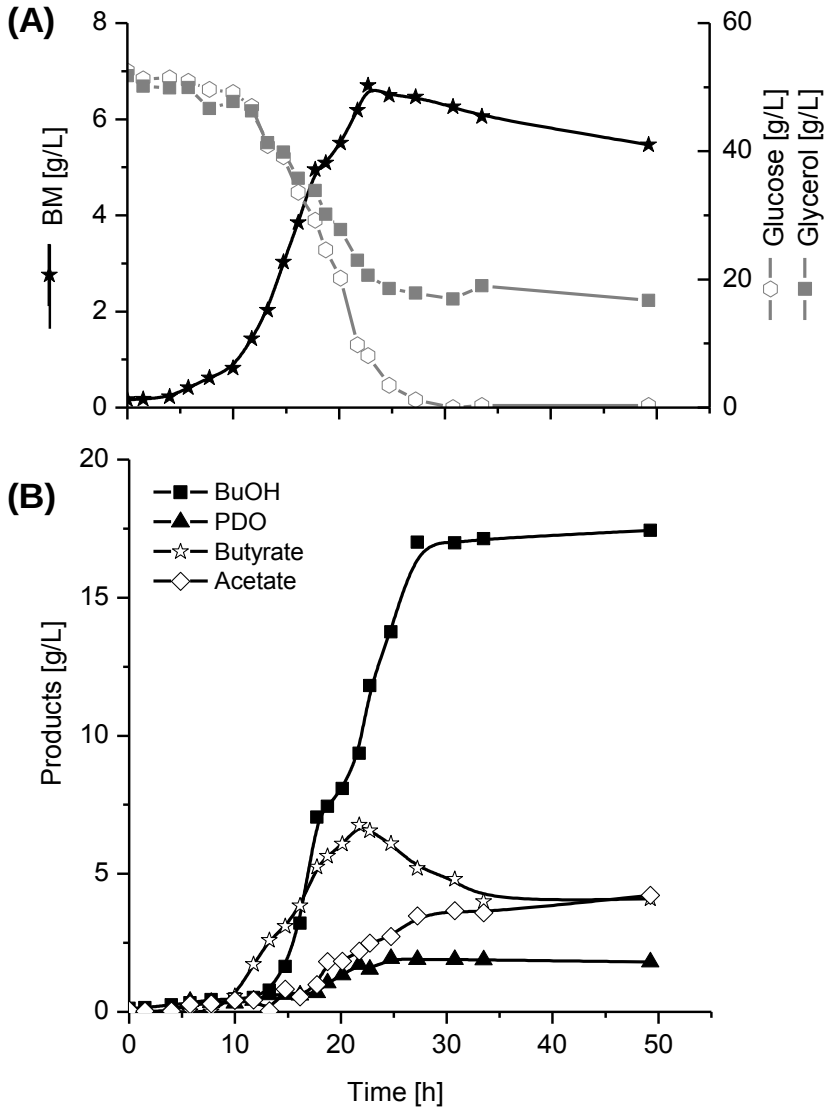

Fig. 4-4: (A) Growth and substrate consumption, and (B) product formation of *C. pasteurianum* DSMZ 525 during cultivation on co-substrate of glycerol and biomass hydrolysates.

Table 4-2: Growth data, final product titer and yields of *C. pasteurianum* DSMZ 525 during cultivation of media with different glucose contents. (Table partly from Sabra et al., 2014).

Glucose content	μ [h^{-1}]	BM max [g/L]	BuOH [g/L]	1,3-PDO [g/L]	Butyrate [g/L]	Acetate [g/L]
20 %	0.237	5.2	11.4	10.3	4.1	1.6
50 %	0.258	6.2	21.1	5.3	4.2	1.5
50 % BH	0.230	6.7	17.4	1.8	4.1	4.2
80 %	0.280	6.9	11.3	2.2	9.9	5.3
100 %	0.294	13.7	7.8	0.1	14.3	13.0

	Consumption rate	Formation rate [g/(Lh)]				$Y_{P/S}$ [g/g $_{C3+C6}$]			
	[g/(Lh)]	BuOH	1,3-PDO	Butyrate	Acetate	BuOH	1,3-PDO	Butyrate	Acetate
20 %	3.27 Gly 1.70 Glu 2.35 Gly**	0.42	0.39	0.37	0.09	0.17	0.15	0.06	0.02
50 %	2.53 Gly 2.25 Glu	0.93	0.29	0.43	0.08	0.22	0.06	0.05	0.02
50 % BH	2.18 Gly 3.33 Glu	1.11	0.13	0.54	0.22	0.20	0.02	0.05	0.05
80 %	1.78 Gly 1.97 Glu 3.04 Glu**	0.50	0.11	0.46	0.22	0.12	0.02	0.11	0.06
100 %	4.59 Glu	0.42	0.00	0.83	0.66	0.10	0.00	0.18	0.16

Note: Growth rate μ and formation rates are calculated for exponential phase. For yield and titer the final amounts are given. Gly = Glycerin, Gly** = after complete glucose consumption, Glu = Glucose, Glu** = after complete glycerol consumption.

4.1.3 Co-substrate fermentation in semi-pilot and pilot scale

The fermentation of co-substrate with glycerol and glucose was transferred into semi-pilot scale with 200 L working volume and into pilot scale with 2000 L working volume. In the pilot scale the ratio of 50 % glucose and 50 % glycerol as substrate mixture was analyzed in a batch fermentation mode. The pilot scale fermentation was performed at the company BKW Biokraftwerke Fürstenwalde GmbH under unsterile conditions. Here glucose in different ratios (20 - 40 %) was added. Additionally the fed-batch addition of glucose started later, in the early exponential phase, when the biomass concentration reached 1.5 - 2.5 g/L, to avoid a contamination by nutrition competitors at unsterile conditions. The amounts of substrates added in this fed-batch fermentation are recorded in Table 3-8, Chapter 3.3.4. All results are collected in Fig. 4-5, Fig. 4-6, Fig. 4-7 and Table 4-3.

Semi-pilot scale

Fig. 4-5 shows the growth and product formation of *C. pasteurianum* in the 200 L scale, growing on co-substrate with 50 % glucose. The growth rate of μ = 0.24 h^{-1} achieved in the semi-pilot scale fermentation is well in the range of the lab scale results with 0.26 h^{-1} at the same glucose concentration. The consumption rates of both substrates are with 1.27 g/(Lh) glycerol and 1.01 g/(Lh) glucose almost in the same range, even though the values are lower in the 200 L scale compared to lab scaled. Also the final BuOH titer was reduced to 14.6 g/L, but the formation of 1,3-PDO increased to 11.4 g/L, compared to 21.1 g/L BuOH and 5.3 g/L 1,3-PDO in the 2 L scale. Accordingly, the yield of both products is increased to 0.36 $g_{BuOH+PDO}/g_{C3+C6}$, compared to 0.28 $g_{BuOH+PDO}/g_{C3+C6}$. This is a benefit for the simultaneous production of both products in larger scale. Interestingly, acetate production was slightly enhanced. The molar butyrate / acetate ratio in the exponential phase decreased from 2.8 in the 2 L scale to 1.2 in the 200 L scale. In the contrary to butyrate formation, no NADH is consumed for the formation of acetate. Thus more NADH is available for the formation of reduced products like 1,3-PDO or ethanol, as observed in this fermentation. Moreover, the data presented show quite clearly the "second" phase of growth, where the 1,3-PDO formation stopped, which is coupled with butyrate re-consumption with the continuous production of BuOH (Fig. 4-5 at ~ 26 h and Fig. 4-4 at ~21 h).

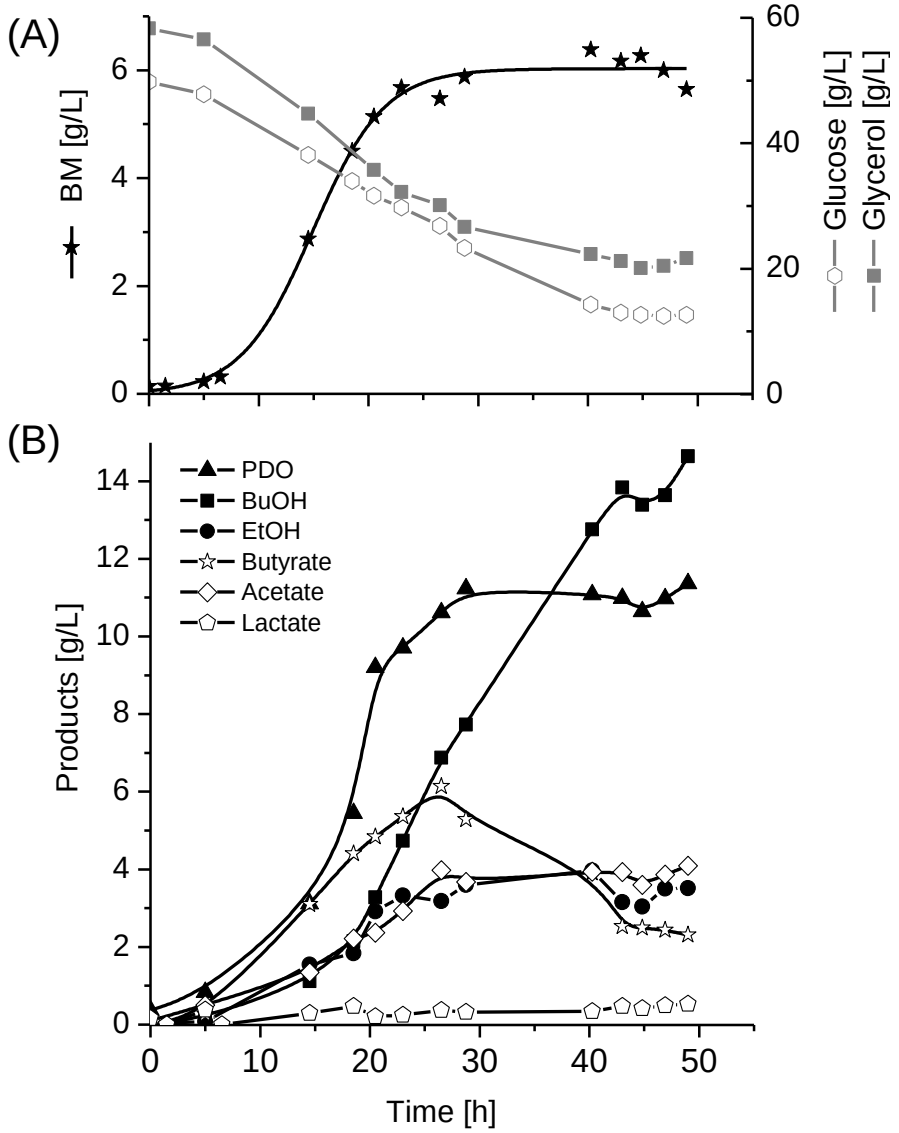

Fig. 4-5: (A) Growth and accumulated substrate consumption, and (B) product formation of *C. pasteurianum* DSMZ 525 during cultivation on co-substrate in 200 L working volume.

Pilot scale

At the company BKW two pilot scale fermentations were performed under uncontrolled and unsterile conditions. Due to the unsterile conditions, and to avoid contamination with lactic acid bacteria, glucose was added when the growth reached more than 1.3 g/L BM on glycerol as sole carbon source. Additionally, the glucose content was reduced to 20 %, to ensure the production of 1,3-PDO in sufficient amounts. In the first experiment (abbreviated BH) pure glycerol, together with a mixture of pure glucose and biomass hydrolysates from Borregard AS (BALI DP-1827) was used. In Fig. 4-6 A the accumulated amounts of consumed glucose and glycerol are shown. In the time period between 50 h and 65 h the glucose graph is constant, which is caused by a limitation due to uncontrolled conditions. Interestingly, in this time period, the glycerol consumption increased from 0.63 g/(Lh) to 1.5 g/(Lh), the butyrate concentration decreased, i.e. it are re-converted into butyryl-CoA, and accordingly the BuOH formation increased from 0.02 g/(Lh) to 0.56 g/(Lh) (Fig. 4-6 B). The final titer of the target products reached in this

experiment were 8.8 g/L BuOH and 22.3 g/L 1,3-PDO. Especially the increase in glycerol consumption is in contrary to previous observations, where a limitation of glucose led to growth cessation and decrease in glycerol consumption (Sabra et al., 2014), (Sabra et al., 2016). In the pilot scale experiments the cells were grown on sole glycerol for the first 23 h, which might have led to an adaption and less sensitivity for glucose limitation. To avoid glucose limitation in the second fermentation (abbreviated rGly), it was added earlier and in higher amounts (40 %) in relation to the raw glycerol, delivered by Novance SAS. In this experiment the consumption rates are closer together with 0.67 g/(Lh) glucose and 0.77 g/(Lh) glycerol (Fig. 4-7 A). Similar to the laboratory scale, less acetic acid was formed, compared to the usage of glucose from BH. The final titers of the main products reached 17.9 g/L 1,3-PDO and 12.6 g/L BuOH (Fig. 4-7 B). In total both fermentation resulted in 64 kg 1,3-PDO and 25 kg BuOH (BH) as well as 45 kg 1,3-PDO and 32 kg BuOH (rGly).

Compared to laboratory fermentations, the biomass formation in pilot scale was slower and growth rates of 0.08 h^{-1} (BH) and 0.11 h^{-1} (rGly) were achieved. This might be explained by the difficult transport conditions in the IBC (intermediate bulk container, 500 L) vessel for more than 4 h, prior inoculation in the 2 m^3 reactor. Within this time, the IBC had no temperature or pH regulation, which might have caused spore formation and subsequently longer lag phase in the large scale reactor. Noteworthy, the final titers of 1,3-PDO achieved in the pilot scale fermentations (18-22 g/L) even exceeds the results achieved on pure glycerol. Even though the same amounts of iron were added each time, this might be the result of iron limitation, which is supported by the fact that a relatively lower BuOH titer and increased lactate formation, compared to the laboratory scale (Table 4-3), was detected. The effect of iron limitation on product formation will be discussed in detail in the following Chapter 4.2. Additionally the redox values of the fermentation broth were lower in the pilot scale, with -554 mV in the BH experiment and -546 mV in the rGly experiment, whereas in the semi-pilot scale values of -517 mV were recorded. This also supports the formation of the reduced products like 1,3-PDO and lactate (Table 4-3, see also Chapter 4.4.3).

The results achieved in the pilot scale fermentation are in general comparable with the lab scale. For example, the yield of both target products were 0.33 $g_{BuOH+PDO}/g_{C3+C6}$ (BH) and 0.33 $g_{BuOH+PDO}/g_{C3+C6}$ (rGly) in pilot scale experiments, compared to 0.32 $g_{BuOH+PDO}/g_{C3+C6}$ at lab scale the fermentation with 20 % glucose amount. Using 50 % glucose in lab scale, the yield was even less with 0.28 $g_{BuOH+PDO}/g_{C3+C6}$ (pure glucose) and 0.22 $g_{BuOH+PDO}/g_{C3+C6}$ (BH). Even though the growth was slower in the pilot scale, also the fermentation time is comparable to the laboratory results, due to the fact that the highest concentrations are almost reached after 65 h (BH) and 45 h (rGly). Thus, the process is transferable into pilot scale without any reduction in performance.

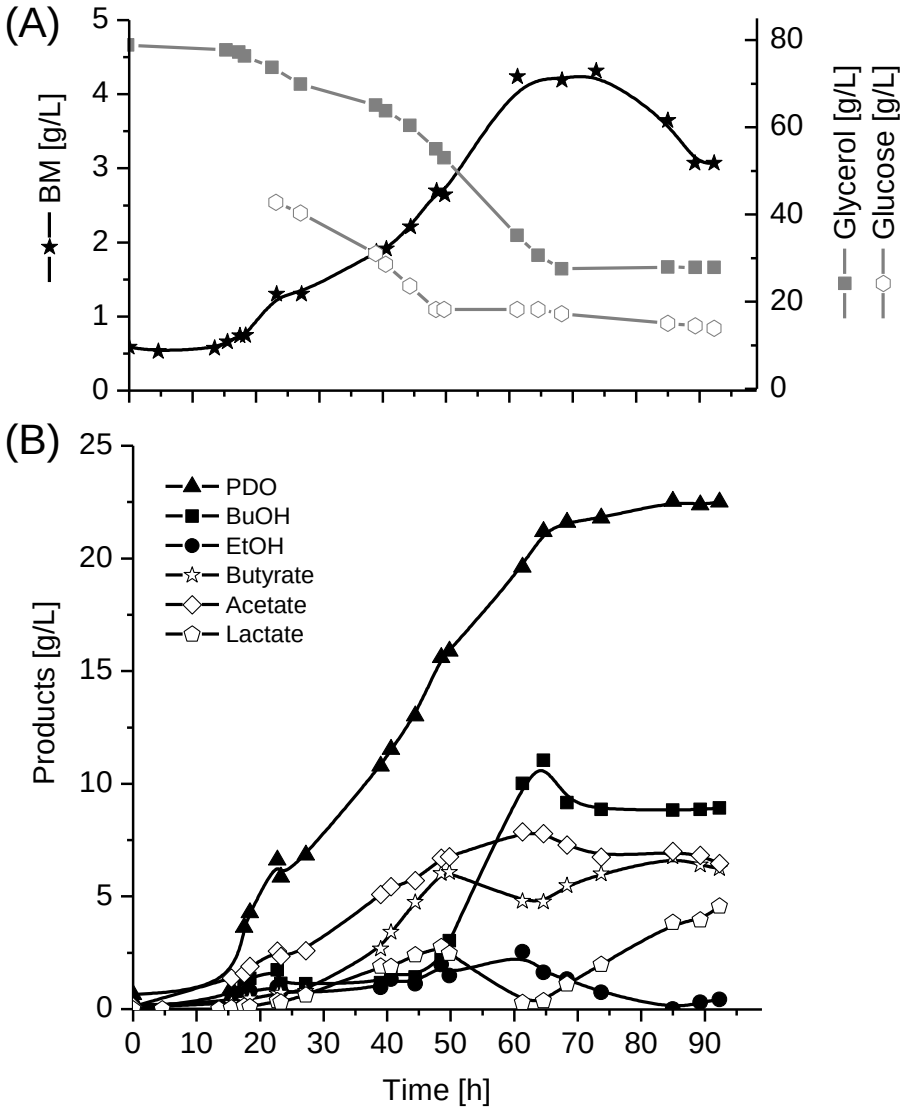

Fig. 4-6: (A) Growth and accumulated substrate consumption, and (B) product formation of *C. pasteurianum* DSMZ 525 during cultivation on co-substrate in 2000 L working volume under unsterile conditions, and with pure glycerol as well as glucose from BH.

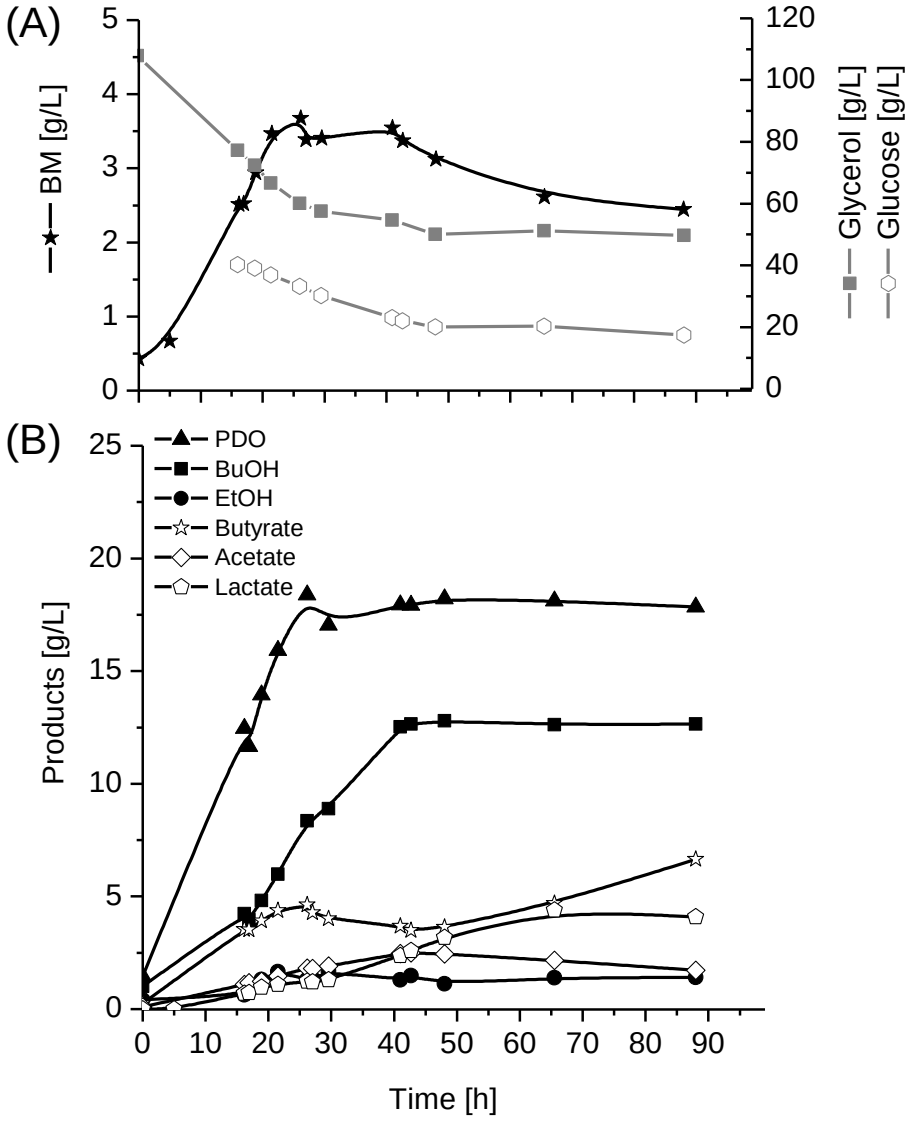

Fig. 4-7: (A) Growth and accumulated substrate consumption, and (B) product formation of *C. pasteurianum* DSMZ 525 during cultivation on co-substrate in 2000 L working volume under unsterile conditions, and with raw glycerol as well as pure glucose as substrate.

Table 4-3: Final product titer, formation rates and substrate yields of *C. pasteurianum* DSMZ 525 during cultivation of co-substrate in 200 L and 2000 L scale.

	Carbon Recovery [%]	μ [h^{-1}]	BM max [g/L]	BuOH [g/L]	1,3-PDO [g/L]	Butyrate [g/L]	Acetate [g/L]	Lactate [g/L]	Formate [g/L]
200 L	99	0.24	6.4	14.6	11.4	2.3	4.1	0.5	1.5
2000 L BH	101	0.08	4.3	8.8	22.3	6.2	6.4	5.6	0.6
2000 L rGly	97	0.11	3.7	12.6	17.9	6.7	1.7	4.4	0.3

	Consumption rate [g/(Lh)]	Formation rate [g/(Lh)]					$Y_{P/S}$ [g/g $_{C3+C6}$]				
		BuOH	1,3-PDO	Butyrate	Acetate	Lactate	BuOH	1,3-PDO	Butyrate	Acetate	Lactate
200 L	1.27 Gly 1.01 Glu	0.34	0.49	0.28	0.16	0.01	0.21	0.15	0.03	0.06	0.01
2000 L BH	1.07 Gly 0.95 Glu	0.16	0.38	0.17	0.15	0.09	0.09	0.24	0.07	0.07	0.06
2000 L rGly	0.77 Gly 0.67 Glu	0.30	0.42	0.18	0.06	0.07	0.11	0.22	0.08	0.02	0.12

Note: Consumption rates are calculated, when both substrates are in media. Formation rates are calculated in exponential phase. For titer and yield the final amounts are given. Gly = Glycerin, Glu = Glucose, BH = biomass hydrolysates, rGLy = raw glycerol.

4.1.4 Conclusion

From co-substrate fermentation of glucose and glycerol by *C. pasteurianum* DSMZ 525 it can be concluded, that glucose addition increased biomass formation, which is in general advantageous for enhanced product titers. Pure glucose as substrate for *C. pasteurianum* resulted in the highest growth rates, but the carbon flow is mainly directed to acids, and 1,3-PDO cannot be produced at all. The mixture of 50 % glucose and 50 % glycerol, led to the highest BuOH titer reported so far and high BuOH production rates. Nevertheless, considering the desired simultaneous formation of both products, 1,3-PDO and BuOH, a relatively lower glucose content around 20 - 40 % is to be preferred, to ensure enhanced formation of reducing equivalents but provide enough glycerol for 1,3-PDO formation. Furthermore, it could be shown that the usage of renewable carbon sources like biomass hydrolysates or raw glycerol is also suitable for large scale fermentations, even under unsterile process conditions. Interestingly, the highest 1,3-PDO titers were achieved in the pilot scale, which might be caused – besides other cultivation conditions - by iron limitation. Therefore the effect of iron availability in the media was studied in detail in the next chapter.

4.2 Influence of iron availability in glycerol fermentation by *C. pasteurianum* DSMZ 525 [10]

The product distribution in fermentations of *C. pasteurianum* DSMZ 525, especially the selectivity between the main products 1,3-PDO or BuOH, is significantly influenced by cultivation conditions and/or media supplements. For instances, several studies analyzed the effect of pH (Gallardo et al., 2017), inoculum conditions (Sarchami et al., 2016a), supplementations of yeast extracts and ammonia (Moon et al., 2011), acetic and butyric acid (Regestein et al., 2015), (Sabra et al., 2014), or phosphate and iron (Dabrock et al., 1992) on product distribution. Among others, iron seems to have significant effects on the selectivity, since its absence leads to a strongly reduced BuOH formation (Gallardo et al., 2017), (Dabrock et al., 1992). In fact, several metabolic pathway steps in *Clostridium* involves enzymes with iron components, e.g. nitrogenases, ferredoxin coupled enzymes, and alcohol dehydrogenases, that play key roles in the maintenance of intracellular redox balance and product formation.

In this section, the variations of production pattern and the pathway regulation for *C. pasteurianum* DSMZ 525 grown on sole glycerol and under varied iron availability have been investigated. To gain more insight into the different pathways involved, proteomic analyses were done with biomass samples taken from the bioreactors at different growth phases and at different iron concentrations. The up and down regulation of different proteins with significant expression changes are discussed then.

4.2.1 Effects of iron availability on the growth and product formation

At first the same pre-culture of *C. pasteurianum* DSMZ 525 was used to inoculate two bioreactors containing the growth medium (according to section 3.2.2 and 3.3.2) and supplemented either with 10 mg/L $FeSO_4 \cdot 7H_2O$ (Fe+, excess iron) or without additional $FeSO_4 \cdot 7H_2O$ (Fe-, limited iron). Whereas Moon et al. (Moon et al., 2011) determined 60 mg/L iron sulfat for an optimized BuOH production via fractional factorial design, preliminary experiments within our institute revealed that 10 mg/L $FeSO_4 \cdot 7H_2O$ are sufficient to achieve similar high productivity rates of 0.9 until 1.1 g/(Lh). The Fig. 4-8 A shows the growth of *C. pasteurianum* under the varying iron conditions. One of the main differences at iron limitation was the relatively shorter lag phase and an early growth cessation. Under these conditions a μ_{max} of 0.23 ± 0.01 $h^{-1,}$ together with a maximum biomass concentration of 3.2 ± 0.01 g/L was achieved. On the contrary, at iron excess a μ_{max} of 0.31 ± 0.01 h^{-1} was observed and 5.1 ± 0.09 g/L biomass were formed (Table 4-4).

The possibility that the growth cessation at Fe- is caused by the inhibitory effect of BuOH can be excluded, because only 3.7 g/L BuOH were produced (Table 4-4), which is lower than the toxic concentration level of > 5 g/L for *C. pasteurianum* (Sabra et al., 2016). It is more likely that the cessation is by accumulated 3-hydroxypropionaldehyde (3-HPA), a highly toxic intermediate in the formation of 1,3-PDO (Abbad-Andaloussi et al., 1996), (Vollenweider and Lacroix, 2004). At Fe+ only 8 mg/L 3-HPA were produced, whereas at Fe- up to 30 mg/L 3-HPA could be detected (Fig. 4-8 B). And, in this time range of relatively high 3-HPA concentrations (23-26 h) the beginning of growth cessation could be

[10] Parts of this chapter are based on Groeger et al. (2017).

observed. Indeed Ávila et al. (Ávila et al., 2014) reported that the growth of vegetative cells of *C. tyrobutyricum* can be completely inhibited when 38 mg/L external 3-HPA were added.

In the proteomic analysis the protein spot of the 3-HPA converting enzyme 1,3-propandiol dehydrogenase (F502_03437) could not be quantified sufficiently, since it appears together with an aldo/keto reductase. However, this spot of two proteins shows an upregulation at Fe+ conditions, compared to Fe-. Thus the accumulation of 3-HPA inside the cells might have strongly contributed to the limited growth under Fe- conditions.

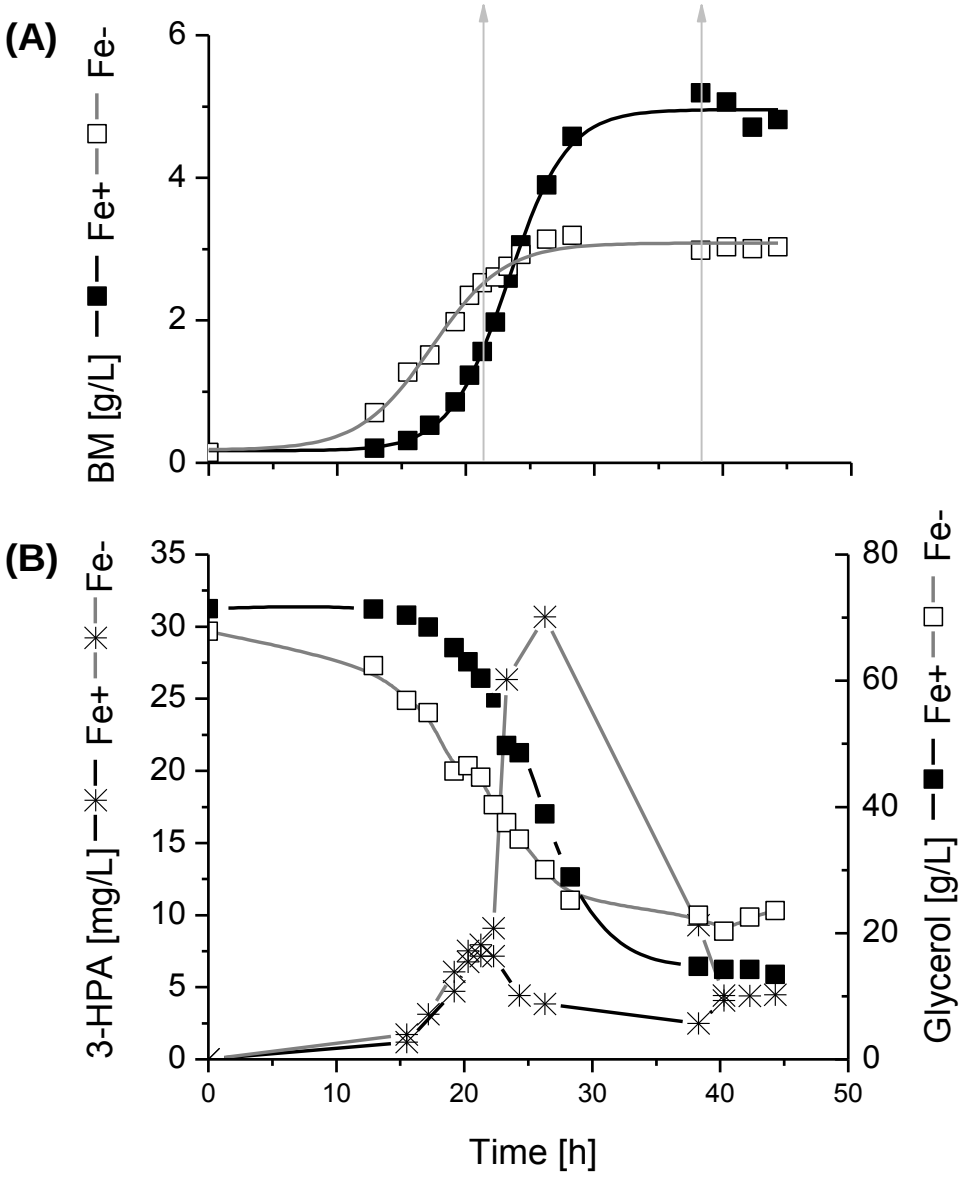

Fig. 4-8: (A) Cell growth behavior and (B) 3-HPA formation and glycerol consumption in cultivation of *C. pasteurianum* DSMZ 525 under iron excess (Fe+) and iron limitation (Fe-) conditions. Arrows indicate time points of sampling for proteomic analysis. (Figure from Groeger et al., 2017).

The Fig. 4-9 as well as Table 4-4 show the formation of fermentation products in *C. pasteurianum* DSMZ 525 grown on glycerol and under the different supplemented iron concentrations. Under Fe+ conditions 12 g/L of BuOH and 11 g/L of 1,3-PDO were produced. On the contrary at Fe- conditions significantly less BuOH (3.7 g/L) was formed, but slightly more 1,3-PDO (14.5 g/L). Due to the lower

biomass formation at Fe- increased the specific yield of 1,3-PDO nearly 4 times from 1.16 ± 0.09 g/g (Fe+) to 4.4 ± 0.52 g/g (Fe-), whereas the specific yield of BuOH decreased from 1.88 ± 0.25 g/g (Fe+) to 0.97 ± 0.13 g/g (Fe-). Alongside with this a remarkable change in the acid formation was observed and especially the lactate titer increase significantly from 0.1 ± 0.0 g/L (Fe+) to 7.5 ± 2.7 g/L (Fe-). The acetate and butyrate yields increased as well under Fe- condition, but to a lesser extent than that of lactate (Table 4-4).

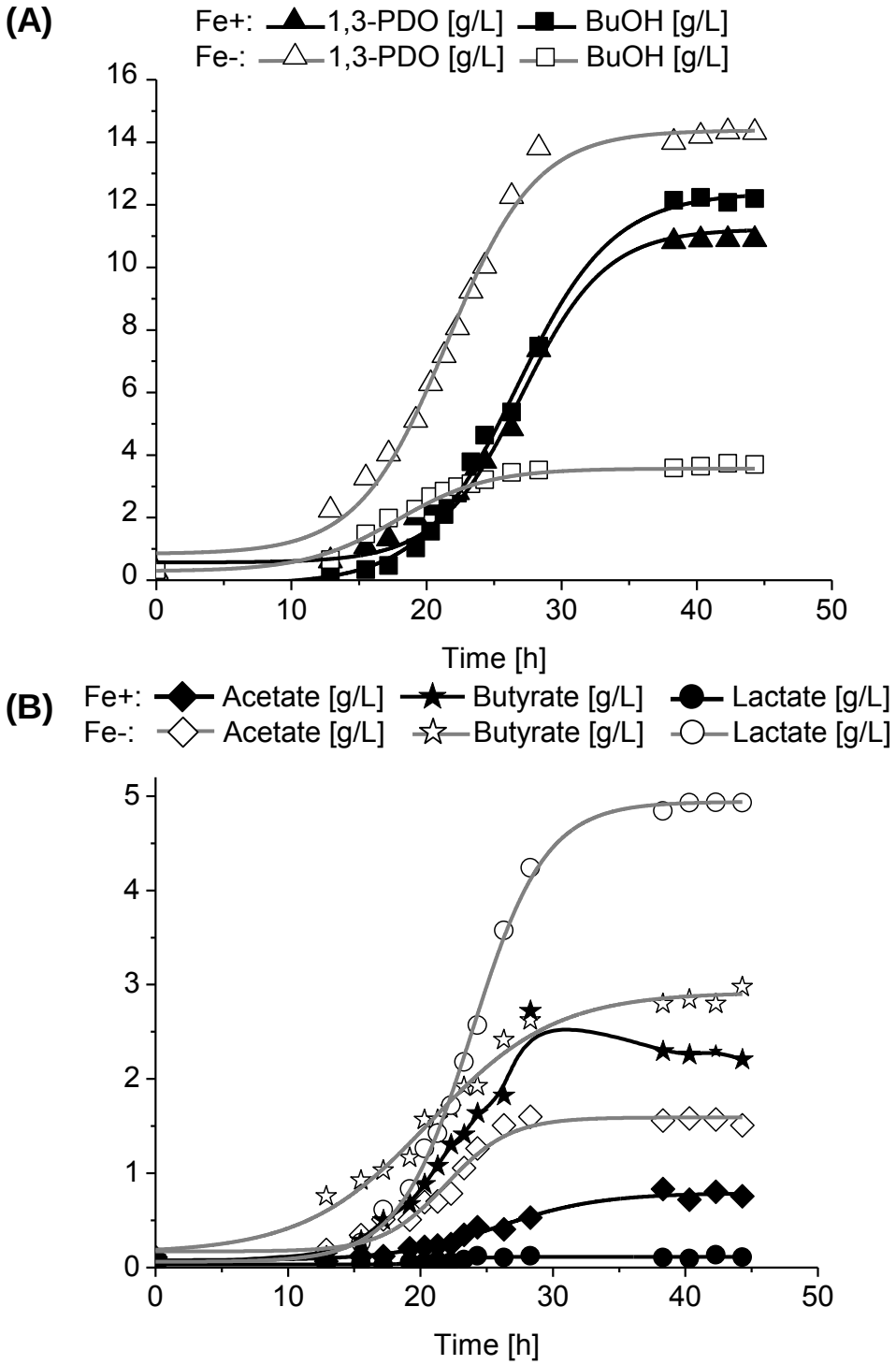

Fig. 4-9: (A) 1,3-PDO and BuOH formation and (B) acid formation in *C. pasteurianum* DSMZ 525 during glycerol fermentation under iron excess (Fe+) and iron limitation (Fe-) conditions. (Figure from Groeger et al., 2017).

Table 4-4: Product formation during the growth of *C. pasteurianum* DSMZ 525 under iron excess (Fe+) and iron limitation (Fe-) conditions. (Table from Groeger et al., 2017).

	Biomass		1,3-PDO		BuOH		EtOH		Acetate		Butyrate		Lactate		Formate	
	Fe+	Fe-	Fe+	Fe-	Fe+	Fe-	Fe+	Fe-	Fe+	Fe-	Fe+	Fe-	Fe+	Fe-	Fe+	Fe-
Final titer [g/L]	5.1 ± 0.09	3.2 ± 0.01	9.4 ± 1.44	16.6 ± 2.26	12.3 ± 0.06	4.4 ± 0.70	1.0 ± 0.12	0.9 ± 0.60	0.8 ± 0.01	1.5 ± 0.02	1.7 ± 0.45	2.8 ± 0.13	0.1 ± 0.00	7.5 ± 2.58	0.5 ± 0.07	1.1 ± 0.11
Formation rate [g/(Lh)]	0.39 ± 0.00	0.16 ± 0.03	0.66 ± 0.17	0.74 ± 0.02	0.53 ± 0.11	0.16 ± 0.04	0.06 ± 0.02	0.03 ± 0.01	0.04 ± 0.01	0.07 ± 0.03	0.14 ± 0.02	0.13 ± 0.01	0.01 ± 0.01	0.28 ± 0.02	0.03 ± 0.01	0.04 ± 0.02
	$Y_{S/X}$		$Y_{P/X}$													
$Y_{i/X}$ **[g/g BM]**	9.6 ± 0.3	13.9 ± 1.2	1.16 ± 0.09	4.40 ± 0.52	1.88 ± 0.25	0.97 ± 0.13	0.15 ± 0.06	0.17 ± 0.13	0.10 ± 0.01	0.39 ± 0.09	0.39 ± 0.08	0.80 ± 0.17	0.02 ± 0.00	1.64 ± 0.37	0.08 ± 0.02	0.25 ± 0.05

Note: Formation rates are calculated for exponential phase. For yield and titer the final amounts are given. Fermentations were performed in duplicates.

4.2.2 Redox regulation and H_2 production

The maintenance of intracellular redox balance is very important for an efficient metabolism of *C. pasteurianum* DSMZ 525, especially when a more reduced substrate like glycerol has to be converted (see Chapter 2.2.3). Indeed, this can be clearly seen in the stoichiometric of the fermentations. The recovery of carbon in the products reached 98 ± 3.9 % for both iron conditions, which is in a sufficient range. On the other hand, the calculated recovery of the reducing equivalents according to Eq. (3-22) reached only 91 % (Fe+) and 94 % (Fe-), indicating a lower consistency according to the assumed pathways.

C. pasteurianum DSMZ 525 contains ferredoxin-dependent hydrogenases, which catalyze the re-oxidation of reduced ferredoxin accompanied with the formation of H_2. Reduced ferredoxins (Fd_{red}) are generally formed in the metabolic conversion of pyruvate into acetyl-CoA, catalyzed by pyruvate:ferredoxin oxidoreductase (PFOR) (see Chapter 2.2.3). Assuming that one mole acetyl-CoA is formed together with one mole H_2, the overall theoretical H_2 production could be calculated according to Eq. (4-1). Here q is the formation rate of each compound [mmol/(gh)].

$$q_{H2} = q_{EtOH} + q_{acetate} + 2\,q_{butyrate} + 2\,q_{BuOH} \quad (4\text{-}1)$$

To verify this equation, the molar amounts of CO_2 and H_2 in the effluent fermentation gas were measured in repeated fermentations to those shown in Fig. 4-8 (results given in Fig. 4-10 A). The analysis revealed that under Fe+ conditions specific yields of 91 (± 1.9) mmol/g H_2 and 82 (± 3.9) mmol/g CO_2 were achieved, whereas under Fe- conditions significantly decreased specific yields of 63 (± 3.3) mmol/g and H_2 and 49 (± 3.1) mmol/g CO_2 were could be detected. Interestingly, it was observed that the theoretical calculated values for H_2 production according to Eq. (4-1) were lower than the real measured ones, particularly under Fe+ conditions (Fig. 4-10 B). Therefore, it must be concluded that the enzymatic step catalyzed by PFOR is not the only source of hydrogen formation. Similar behavior was also described previously by Zeng et al. (Zeng, 1996), (Zeng et al., 1993) for cultures of *C. butyricum* or *Klebsiella pneumoniae*.

One possible H_2 forming step occurs in the following metabolic conversion of crotonyl-CoA into butyryl-CoA, which is in general catalyzed by the NADH dependent trans-2-enoyl-CoA reductase (Ter) enzyme (Eq. (4-2)) (Lan and Liao, 2011).

$$\text{Crotonyl-CoA} + \text{NADH} \xrightarrow{\text{Ter}} \text{NAD}^+ + \text{Butyryl-CoA} \tag{4-2}$$

However, recently Buckel and Thauer (Buckel and Thauer, 2013) proposed a new enzyme complex, which is involved in this pathway step. They suggest that the conversion is catalyzed successively by the ferredoxin-dependent butyryl-CoA dehydrogenase / electron transferring flavoprotein complex (BCdH-ETF) (Eq. (4-3)) and a hydrogenase, which regenerates the Fd_{red} (Eq. (4-4). Altogether this led to an additional route of H_2 formation. Since the measured H_2 production values were significantly higher than the theoretically calculated ones (see Fig. 4-10 B), it is reasonable to assume that in *C. pasteurianum* DSMZ 525, BCdH-ETF together with Ter is actively involved in crotonyl-CoA conversion.

$$\text{Fd}_{\text{ox}} + 2\ \text{NADH} + \text{Crotonyl-CoA} \xrightarrow{\text{BCdH-ETF}} \text{Fd}_{\text{red}} + 2\ \text{NAD}^+ + \text{Butyryl-CoA} \tag{4-3}$$

$$2\ \text{Fd}_{\text{red}} + \text{NADH} + 3\ \text{H}^+ \xrightarrow{\text{H}_2\text{-ase}} 2\ \text{Fd}_{\text{ox}} + \text{NAD}^+ + 2\ \text{H}_2 \tag{4-4}$$

Due to this new suggested pathway step, one mole NADH is additionally required for the formation of one mol butanol or one mol butyrate, and this is accompanied with the formation of one additional mole H_2. Consequently, the calculation of reducing equivalent recovery in Eq. (4-1) should be modified as shown in the following Eq. (4-5), by also taking into account the difference of calculated and measured H_2 values ($c_{\Delta H2}$), representing the additionally consumed NADH.

$$\text{NADH}_{\text{recovery}}\ [\%] = \frac{c_{1,3-\text{PDO}} + c_{\Delta H2}}{2\ c_{\text{acetat}} + 2\ c_{\text{butyrat}} + c_{\text{lactate}} + 13.2\ a_{\text{BTM}}} \tag{4-5}$$

Indeed, using the new equation (4-5), reducing equivalent recoveries of 105 % (Fe+) and 100 % (Fe-) were obtained, which supports the theory of the BCdH-ETF complex. Particularly the results from Fe+ condition are in agreement with the corrected equation (4-5), where more BuOH and H_2 were produced, and the deviation between the calculated and measured H_2 was higher. Moreover, the proteomic results analysis revealed upregulated expressions of an electron transfer flavoprotein subunit alpha (F502_06282) and an electron transfer flavoprotein subunit alpha/beta-like protein (F502_06287) in the late phase of Fe+ conditions, which might be involved in this step and could support this theory (see Table 7-7, Appendix).

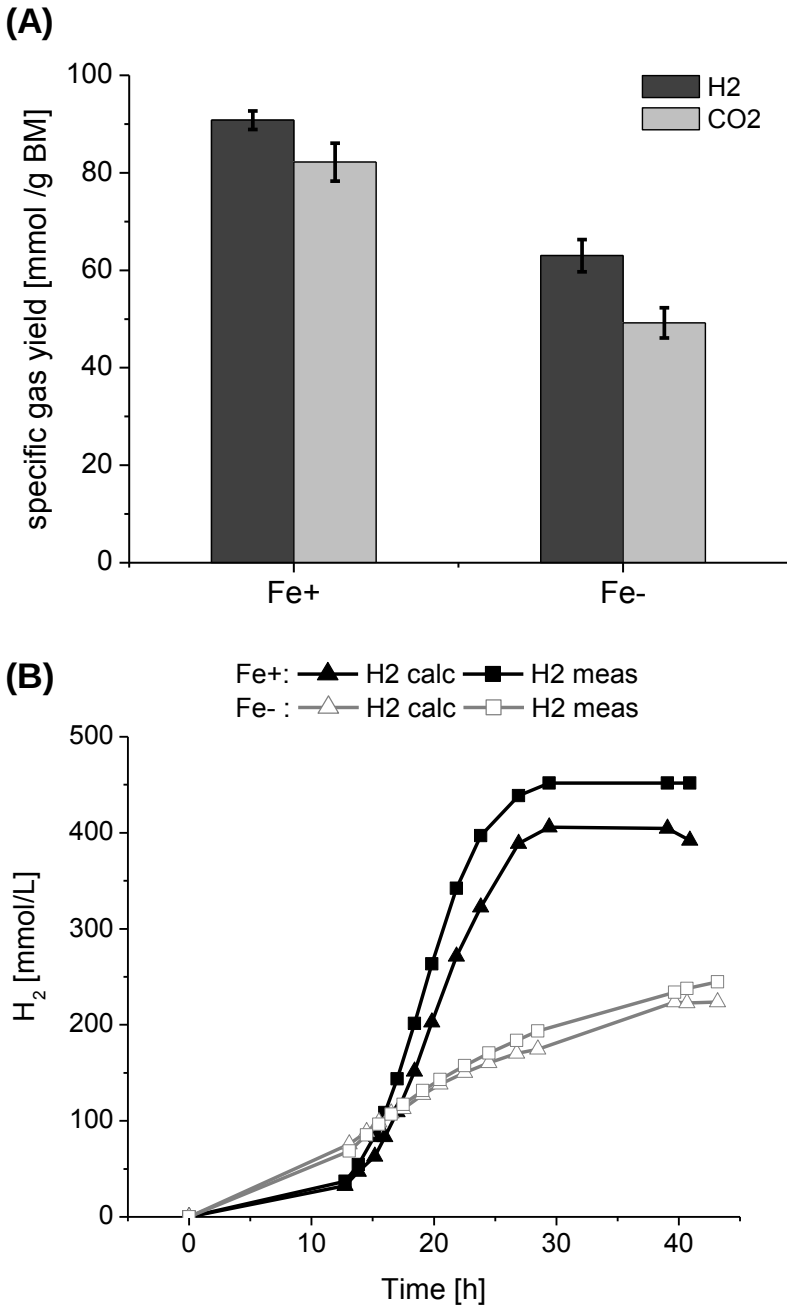

Fig. 4-10: (A) Measured cumulative hydrogen and carbon dioxide production related to biomass and (B) calculated (calc) vs. measured (meas) hydrogen production under iron excess (Fe+) and iron limitation (Fe-) conditions in *C. pasteurianum* DSMZ 525 cultures. (Figure from Groeger et al., 2017).

4.2.3 Comparative proteomic analysis of the iron effect

For proteomic analysis, samples were taken in the exponential growth phase (termed as Fe+ early and Fe- early) and at the stationary growth phase (Fe+ late and Fe- late) (see also Fig. 4-8). According to section 3.5.4 each sample was analyzed in triplicates. Protein spots with statistically significant changes between the mentioned conditions were further identified by LC-MS/MS and the results are summarized in Table 7-7 (Appendix).

Glycerol conversion into 1,3-propanediol

As described previously (Chapter 2.2.3) the conversion of glycerol to 1,3-PDO is performed in two steps: at first glycerol is converted into 3-HPA by means of glycerol dehydratase (GDHt), followed by the formation of 1,3-PDO via 1,3-propanediol dehydrogenase (PDOR) (Fig. 4-13).

The three subunits of GDHt (*pduC* (F502_03402), *pduD* (F502_03407) and *pduE* (F502_03412)) were identified in the proteomic analyses, but they did not appear as single protein spots. However, the large subunit of the glycerol dehydratase reactivating factor (GDHt reactivase, GDHtR) was identified in a single spot and could be quantified (Fig. 4-11). The expression pattern indicates rather a correlation to cell growth phase than to iron availability. For example, the highest expression was detected at Fe+ early, a time point in the mid exponential phase and with the highest growth rate of $\mu = 0.22\ h^{-1}$. In contrary a lower GDHtR level is detected for Fe- early conditions, when the culture already entered the stationary phase, and the growth rates was reduced to $\mu = 0.07\ h^{-1}$. The 3-HPA concentration was almost the same with 7.96 mg/L (Fe+) and 7.15 mg/L (Fe-) at the early sampling point. Under both conditions the GDHtR content in the stationary phases was reduced to barely detectable levels, where 3-HPA was already consumed and the production of 1,3-PDO stagnated (Fig. 4-8). The subsequent active enzyme in this pathway step is PDOR, but as mentioned before, the expression changes under the different iron conditions cannot be quantified sufficiently and thus no correlation to the 1,3-PDO titer can be concluded.

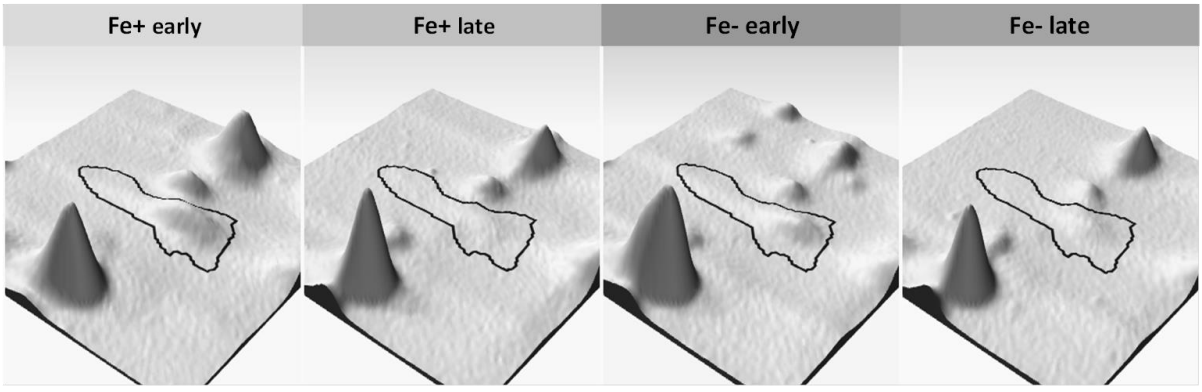

Fig. 4-11: Expression pattern of the large subunit of glycerol dehydratase reactivating factor (GDHtR) under Fe+ and Fe- conditions as well as early and late sampling point. (Figure from Groeger et al., 2017).

The pyruvate acetyl-CoA node

A fundamental metabolic step in all living organisms represents the conversion of pyruvate to acetyl-CoA, which links the glycolysis to the citric acid cycle. In anaerobes, pyruvate can be metabolized through a variety of pathways but it is often oxidized to CO_2 and acetyl-CoA with the parallel reduction of a low-potential redox protein, e.g. ferredoxins or flavodoxins. In many anaerobic bacteria pyruvate:ferredoxin oxidoreductase (PFOR) is responsible for this step. PFORs contain thiamin pyrophosphate for the cleavage of carbon-carbon bonds next to a carbonyl group, as well as iron-sulfur clusters for electron transfer (Moulis et al., 1996, Charon et al., 1999 and references therein). In the genome of *C. pasteurianum* DSMZ 525, three homologue enzymes of PFOR are present: two pyruvate:ferredoxin oxidoreductases (F502_01955 and F502_07648), and one pyruvate:ferredoxin (flavodoxin) oxidoreductase (F502_07643). In the proteomic analysis performed here, two of them could be identified: F502_07648 (termed as PFOR1) and F502_07643 (termed as PFOR2). Both are homologous proteins with nearly identical molecular weights, but the pH value of PFOR1 is more basic than that of PFOR2. As Fig. 4-12 shows, both PFORs appeared as a chain of pI isoform spots on the 2D gels. In general, all isoforms of the two PFORs showed a higher expression at Fe+ compared to Fe-. However, the expression patterns of PFOR1 are similar to each other, with the highest expression at Fe+ late and low values at Fe-. In contrary, the patterns of PFOR2 isoforms differ from each other. While the expression level of spot 87 did barely change between Fe+ early and Fe+ late, the more basic isoforms (spots 70 and 90) showed higher results at Fe+ early, and the more acidic isoforms (spots 75, 76 and 77) were up-regulated at Fe+ late, which was similar to the expression pattern of PFOR1.

As already described in the theory (section 2.2.3), pyruvate can be converted to acetyl-CoA catalyzed by PFORs but also by pyruvate formate-lyase (PFL), which results in formate as a side product. In the genome of *C. pasteurianum* are three genes that encodes enzymes functioning as PFL, namely F502_19556, F502_15690, and F502_15710. In the proteomic data only F502_19556 (formate acetyltransferase) could be identified and appeared in four protein spots (Fig. 4-12). Under Fe+ conditions the expression of PFL was hardly detectable, but under Fe- conditions all four PFL isoforms were significantly up-regulated. The two acidic isoforms (spots 178 and 181) showed a 2.5 and 3.7-fold increase only in the Fe- early sample, whereas the two basic isoforms (spots 174 and 175) were up to 8-fold higher in Fe- early and 6-fold higher in the Fe- late sample. Therefore it could be concluded that under iron limitation *C. pasteurianum* obviously prefers to use the PFL for the conversion of pyruvate to acetyl-CoA. Correspondingly, under Fe- condition the formate yield from glycerol was clearly enhanced to 0.035 ± 0.009 mol/mol (Fe-) compared to 0.015 ± 0.003 mol/mol (Fe+).

Nevertheless, it can be seen that the expression levels of the two PFORs, especially the PFOR2, were clearly higher than that of PFL. Protein synthesis is an energy-demanding process, and bacteria usually do not produce “unnecessary” enzymes, if not required. Previous studies showed that under iron limited conditions many anaerobes synthesize flavodoxins as substitution of ferredoxins for many enzymatic reactions (Buckel and Thauer, 2013). Thus the presence of the two PFORs at Fe- condition might indicate that these enzymes use flavodoxins as the electron acceptor. Indeed, the proteomic results show that the flavodoxin F502_13493 was up-regulated under Fe- conditions, with a 14.3-fold increase at Fe- early, and an 8.0-fold increase in Fe- late, compared to Fe+ conditions. But whether or not the up-regulated expression of this flavodoxin was coupled to the functionality of the PFORs is still unknown.

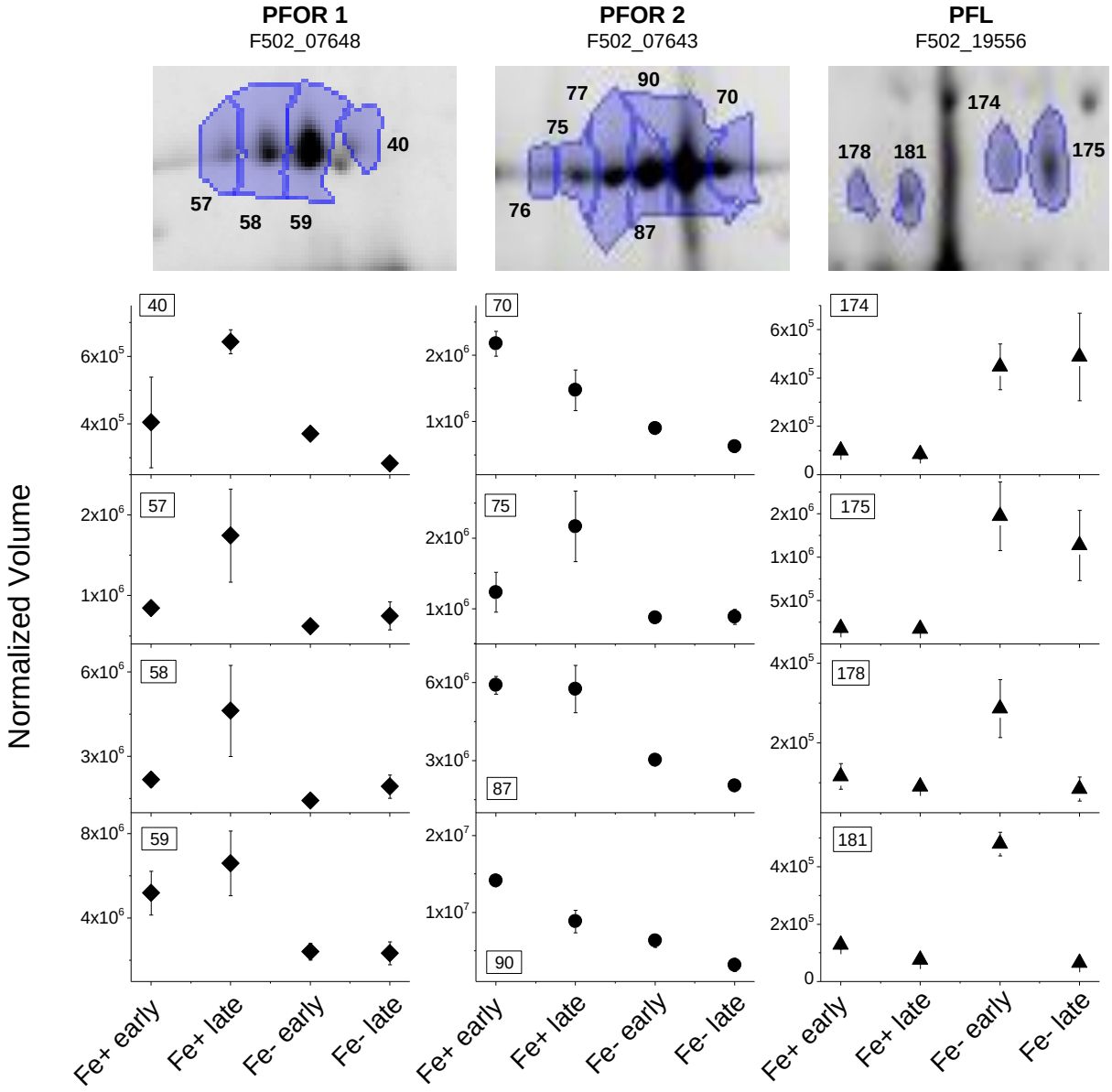

Fig. 4-12: Expression patterns of enzymes catalyzing the conversion of pyruvate to acetyl-CoA under Fe+ and Fe- conditions at exponential growth phase (early) and stationary phase (late). PFOR 1 (F502_07648, pyruvate:ferredoxin oxidoreductase) and PFOR 2 (F502_07643, pyruvate:ferredoxin (flavodoxin) oxidoreductase) are up-regulated at Fe+; PFL (pyruvate formate lyase) is up-regulated at Fe-. (Figure from Groeger et al., 2017).

Regulation of the ferredoxin pool

In the conversion step of pyruvate to acetyl-CoA, oxidized ferredoxin (Fd_{ox}) is used as electron carrier for PFORs, and after the reaction it remains in a reductive state (Fd_{red}). *C. pasteurianum* DSMZ 525 uses different electron acceptors to regenerate Fd_{red} to Fd_{ox}. The fact that the redox potentials of ferredoxins (-400 mV) are in the range of H_2 electrodes (-414 mV at pH 7) reveals that many metabolic reactions with ferredoxins also involves H_2 (Buckel and Thauer, 2013). *Clostridium* species possesses two enzymes classes that have the ability to form H_2 and regenerate Fd_{red}, namely nitrogenases and hydrogenases (Calusinska et al., 2010). However, Hallenbeck and Benemann (Hallenbeck and Benemann, 2002) reported that hydrogenases shows a >1000 times higher turnover rate than

nitrogenases, which makes them more efficient. In *Clostridium sp.* two types of hydrogenases appear, which differ by their metallocenter composition: [NiFe] and [FeFe] hydrogenases (Calusinska et al., 2010).

The proteomic study performed here revealed two [FeFe] hydrogenases: hydrogenase-1 (F502_18287, H_2-ase) and [Fe]-hydrogenase (F502_14390). The [Fe]-hydrogenase could be identified, but it did not appear as a single protein spot and therefore could not be quantified. On the contrary, the H_2-ase shows different expression levels depending on the iron availability. At Fe+ early the expression level was up to 5-fold higher compared to Fe-. In the Fe+ late sample it was down-regulated 2 to 3-fold. This might be caused by the depletion of the iron pool within fermentation time. Nevertheless, it was still higher than under iron limitation. The higher expression of H_2-ase is in accordance with the higher H_2 production under Fe+ conditions (see Fig. 4-10). Consequently it might have contributed to the regeneration of Fd_{red} to Fd_{ox}. Furthermore, the H_2-ase expression is more similar to the basic iso-forms of the ferredoxin-(flavodoxin)-dependent PFOR2 (spots 70 and 90) than the ferredoxin-dependent PFOR1. That means, the highest expression can be found at Fe+ early, followed by Fe+ late and Fe- early, and the lowest at Fe-late. The PFORs-catalyzed pyruvate conversion might be coupled with other unknown Fd_{ox} regenerating reaction(s), catalyzed either by other unidentified hydrogenases (at least 5 genes in the genome of *C. pasteurianum* DSMZ 525 encode hydrogenases) or ferredoxin reductases. Additionally it is known, that PFORs can transfer the electrons from pyruvate conversion directly to protons and thus contribute to H_2 formation (Menon and Ragsdale, 1996).

A different study found that in anaerobes 90 % of ferredoxins are present in their reduced state, which enables them to act as an electron donor (Buckel and Thauer, 2013). In *C. pasteurianum* DSMZ 525 this is generally realized by three ferredoxin-dependent redox reactions: the oxidation of pyruvate to acetyl-CoA and CO_2 (-500 mV), the oxidation of formate to CO_2 (-430 mV, Scherer and Thauer, 1978) and the flavoprotein-based electron bifurcation for the reduction of crotonyl-CoA to butyryl-CoA (Eq. (4-3)). Another possible oxidation of Fd_{red} by NAD^+ has to be excluded due to the absence of the ferredoxin:NAD oxidoreductase activity in this organism (Buckel and Thauer, 2013). Therefore, the hydrogen formation catalyzed by hydrogenase should be a main route of Fd_{ox} formation in *C. pasteurianum* DSMZ 525. Based on this assumption, the hydrogen yield from glycerol between the Fe+ and the Fe- conditions was compared. As shown in Fig. 4-13 A, the H_2 yield decreased significantly from 0.71 $mol/mol_{glycerol}$ (Fe+) to 0.21 $mol/mol_{glycerol}$ (Fe-), which is in agreement with the higher expression of hydrogenase-1 under the Fe+ condition.

The contribution of a BCdH-ETF complex in H_2 production was already proposed above (Buckel and Thauer, 2013). In this reaction step, electron transfer flavoproteins (ETFs) are involved in the reduction of crotonyl-CoA to butyryl-CoA, and coupled to the Fd_{ox} reduction by bifurcating electrons from the reducing equivalent NADH (Fig. 4-13) (Buckel and Thauer, 2013), (Herrmann et al., 2008). The proteomic study revealed the presence of two flavoprotein subunits in *C. pasteurianum*, subunit alpha (F502_06282) and subunit alpha/beta-like protein (F502_06287). Their expressions were 1.5 to 1.7-fold higher under Fe+ late conditions compared to Fe- late. Assuming that they are involved in the BCdH-ETF reaction, this indicates a relative increase in the Fd_{ox} pool, which led to increased H_2 formation in Fe+, due to the Fd_{ox} generation via hydrogenases.

Under the iron limited conditions the hydrogenase-1 as well as the two PFORs were down-regulated, compared to iron excess conditions. Therefore, the relative changes of the expression levels of the two enzymes might be indicative for the overall Fd_{ox} regeneration state in the bacteria. Thus, the protein spot intensities of both enzymes under Fe- and Fe+ conditions and at the two sampling points were

compared. The ratio PFOR / H_2-ase shows a positive correlation to the 1,3-PDO production rate (Fig. 4-13 B). In accordance with this the decrease in the Fd_{ox} fraction at iron limitation (due to reduced H_2-ase presence) will decrease the Fd_{ox} coupled reaction of the BCdH-ETF complex, which is important intermediate step in butyrate and BuOH formation. Under these conditions it is most likely that the intermediate acetyl-CoA will be channeled into the Fd_{ox}-independent acetate formation route rather than the Fd_{ox}-dependent butyrate formation route. This assumption can be supported with the average molar butyrate / acetate ratio, calculated in the exponential phase, which is decreased from 2.7 mol/mol at Fe+ to 1.1 mol/mol at Fe- conditions (Fig. 4-13 C). Consequently, it must be concluded that under iron limitation, Fd_{ox} dependent conversion steps are down regulated and the resulting free reducing power, could be redirected to the production of 1,3-PDO and lactate, instead of BuOH formation. Accordingly, the final 1,3-PDO and lactate titer were much higher under Fe- compared to Fe+ (Table 4-4). Although the enzymes lactate dehydrogenase catalyzing lactate formation and 1,3-propanediol dehydrogenase did not show significant changes in their expression levels (or a least could not be quantified). Both enzymes are not directly involved in the energy metabolism, but they seem to be important for stabilizing the internal redox balance, and their production may be a mechanism to balance perturbations in the NADH/NAD^+ ratio. Nevertheless, it should also be kept in mind that higher or lower protein expression not necessarily corresponds with a higher or lower enzyme activity.

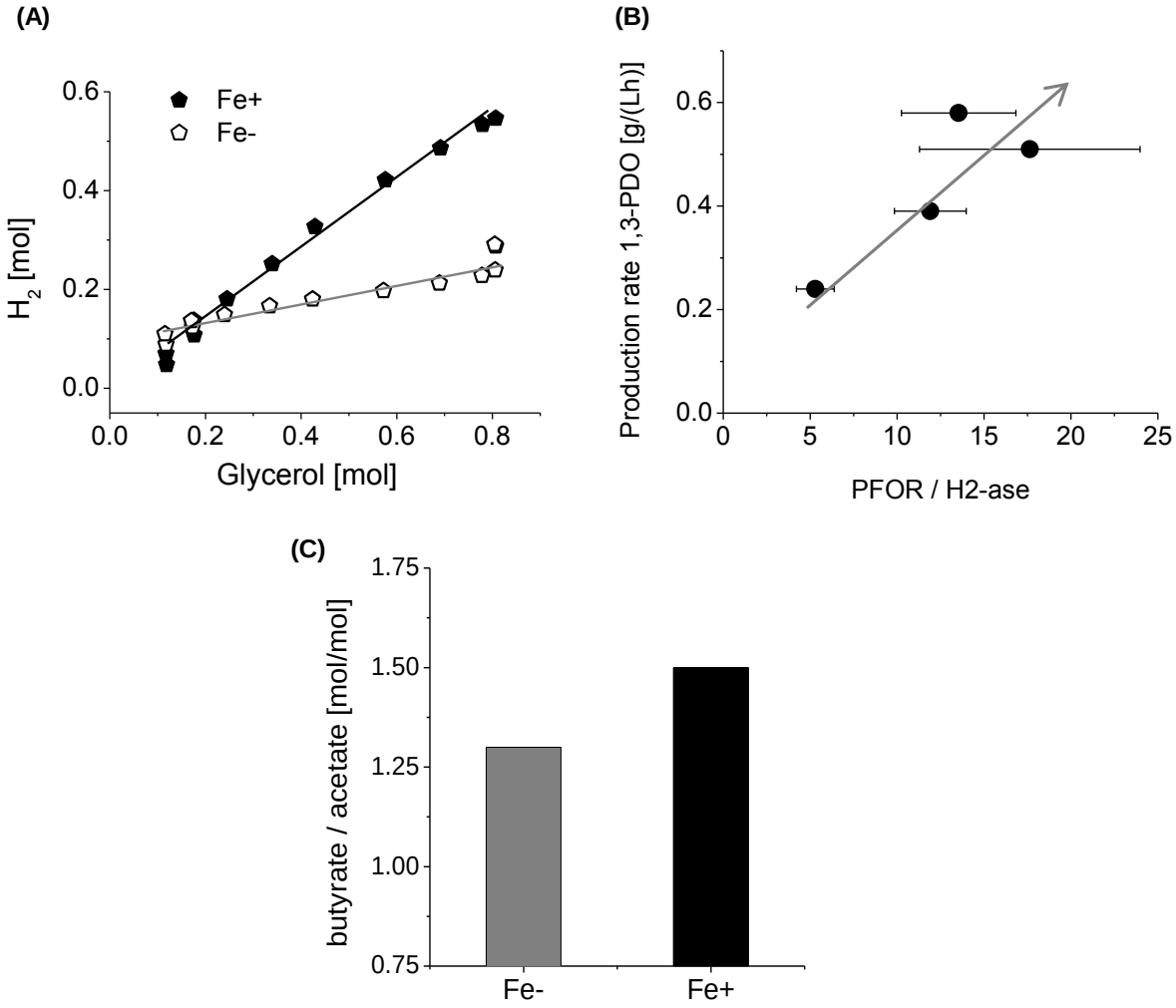

Fig. 4-13: (A) Molar formation of H_2 over consumed glycerol, (B) 1,3-PDO productivity over the ratio PFOR / H_2-ase, and (C) molar ratio of butyrate to acetate under Fe+ and Fe- conditions. (Figure from Groeger et al., 2017).

4.2.4 Conclusion

The iron content in the fermentation media of *C. pasteurianum* DSMZ 525 shows a great impact on the metabolism, the redox balance and consequently the product formation. It could be concluded that for the simultaneous production of both target products, 1,3-PDO and BuOH, a sufficient iron availability is necessary, whereas under iron limited conditions only the 1,3,-PDO formation can be significantly enhanced. The proteomic analysis revealed that under iron excess conditions several enzymes like pyruvate:ferredoxin oxidoreductase (PFOR), hydrogenase and bifunctional acetaldehyde-CoA/alcohol dehydrogenase were up-regulated among others. Hydrogenases play an important role in the regeneration Fd_{red} to Fd_{ox} and thus the maintenance of the internal redox balance. Continuative stoichiometric analysis showed a possible additional H_2 production route coupled to the reaction step of butyryl-CoA formation, which is catalyzed by a Fd_{ox} dependent butyryl-CoA dehydrogenase / electron transfer flavoprotein complex (BCdH-ETF). Therefore, it is suggested that the selectivity of the target products not only depends on the NADH pool, because both are used as electron sink, but also the intracellular Fd_{ox} pool.

However, a further increase in the formation of one or both main products could not be achieved via the influence of iron availability in the media. One major impact that limits the increased productivity is caused by the inhibitory effect of BuOH itself. For this reason one of the following chapters analyses the impact of BuOH recovery within fermentation. Furthermore, it could be shown in that the redox regulation significantly influences the product formation. Therefore the effect of redox active substances and electrodes on fermentations of *C. pasteurianum* DSMZ 525 was investigated in the following chapter.

Next two pages:

Fig. 4-14: Revised main metabolic pathway of glycerol and glucose degradation in *C. pasteurianum*, with involved enzymes and according accession number. Dotted arrows represent intermediate steps pathway steps, which are not shown. Data from BioCyc collection (http://www.biocyc.org/organism-summary?object=CPAS1262449, 08.09.2017). The up-regulated enzymes for cultivations under iron limited (Fe-) and iron excess (Fe+) conditions are highlighted.

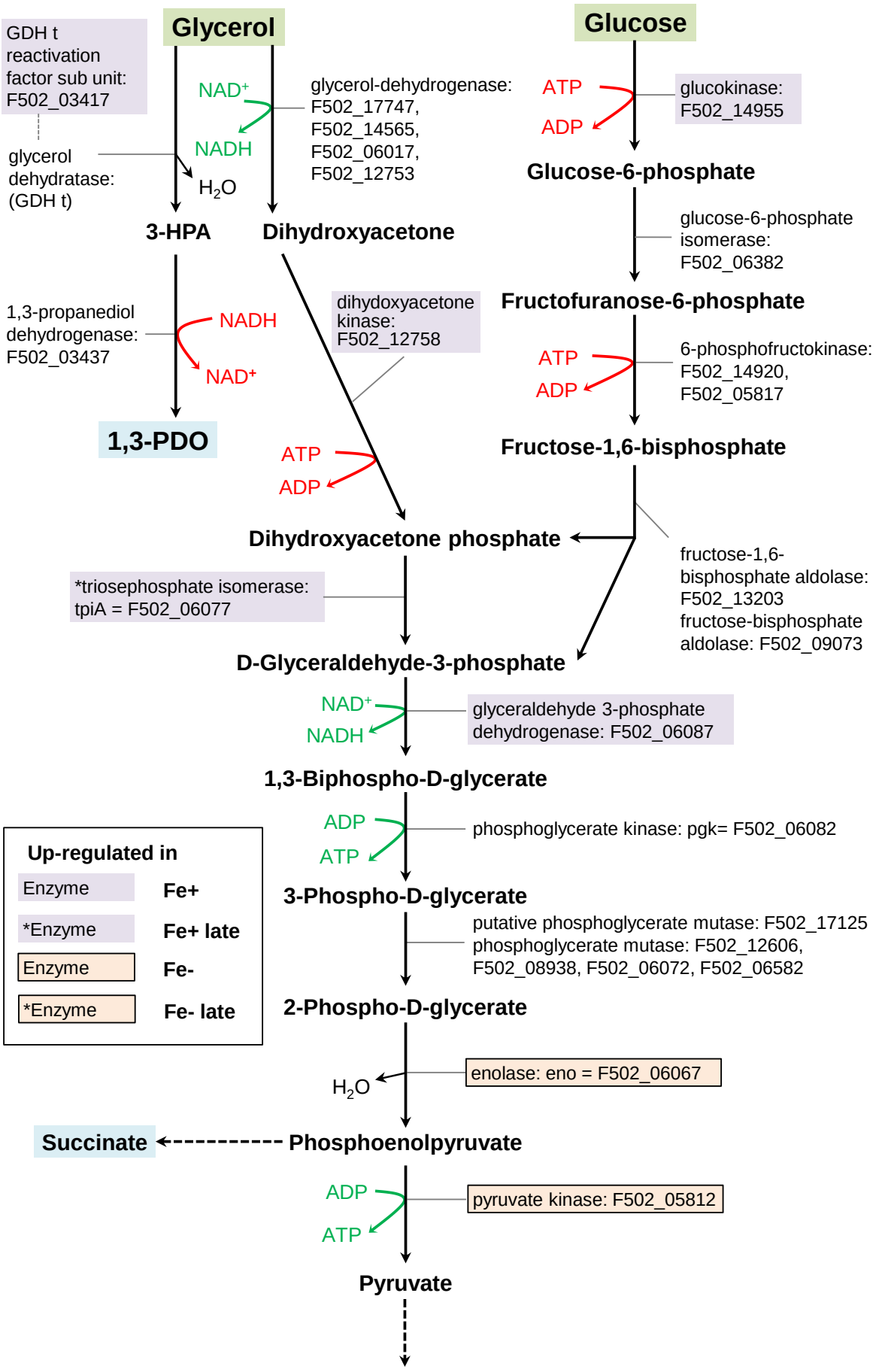
GDH t reactivation factor sub unit: F502_03417
Glycerol
NAD+
NADH
glycerol-dehydrogenase: F502_17747, F502_14565, F502_06017, F502_12753
glycerol dehydratase: (GDH t)
H2O
3-HPA
Dihydroxyacetone
Glucose
ATP
ADP
glucokinase: F502_14955
Glucose-6-phosphate
glucose-6-phosphate isomerase: F502_06382
Fructofuranose-6-phosphate
1,3-propanediol dehydrogenase: F502_03437
NADH
NAD+
1,3-PDO
dihydoxyacetone kinase: F502_12758
ATP
ADP
6-phosphofructokinase: F502_14920, F502_05817
Fructose-1,6-bisphosphate
Dihydroxyacetone phosphate
*triosephosphate isomerase: tpiA = F502_06077
fructose-1,6-bisphosphate aldolase: F502_13203
fructose-bisphosphate aldolase: F502_09073
D-Glyceraldehyde-3-phosphate
NAD+
NADH
glyceraldehyde 3-phosphate dehydrogenase: F502_06087
1,3-Biphospho-D-glycerate
ADP
ATP
phosphoglycerate kinase: pgk= F502_06082
3-Phospho-D-glycerate
putative phosphoglycerate mutase: F502_17125
phosphoglycerate mutase: F502_12606, F502_08938, F502_06072, F502_06582
2-Phospho-D-glycerate
H2O
enolase: eno = F502_06067
Succinate
Phosphoenolpyruvate
ADP
ATP
pyruvate kinase: F502_05812
Pyruvate
Up-regulated in
Enzyme
Fe+
*Enzyme
Fe+ late
Enzyme
Fe-
*Enzyme
Fe- late

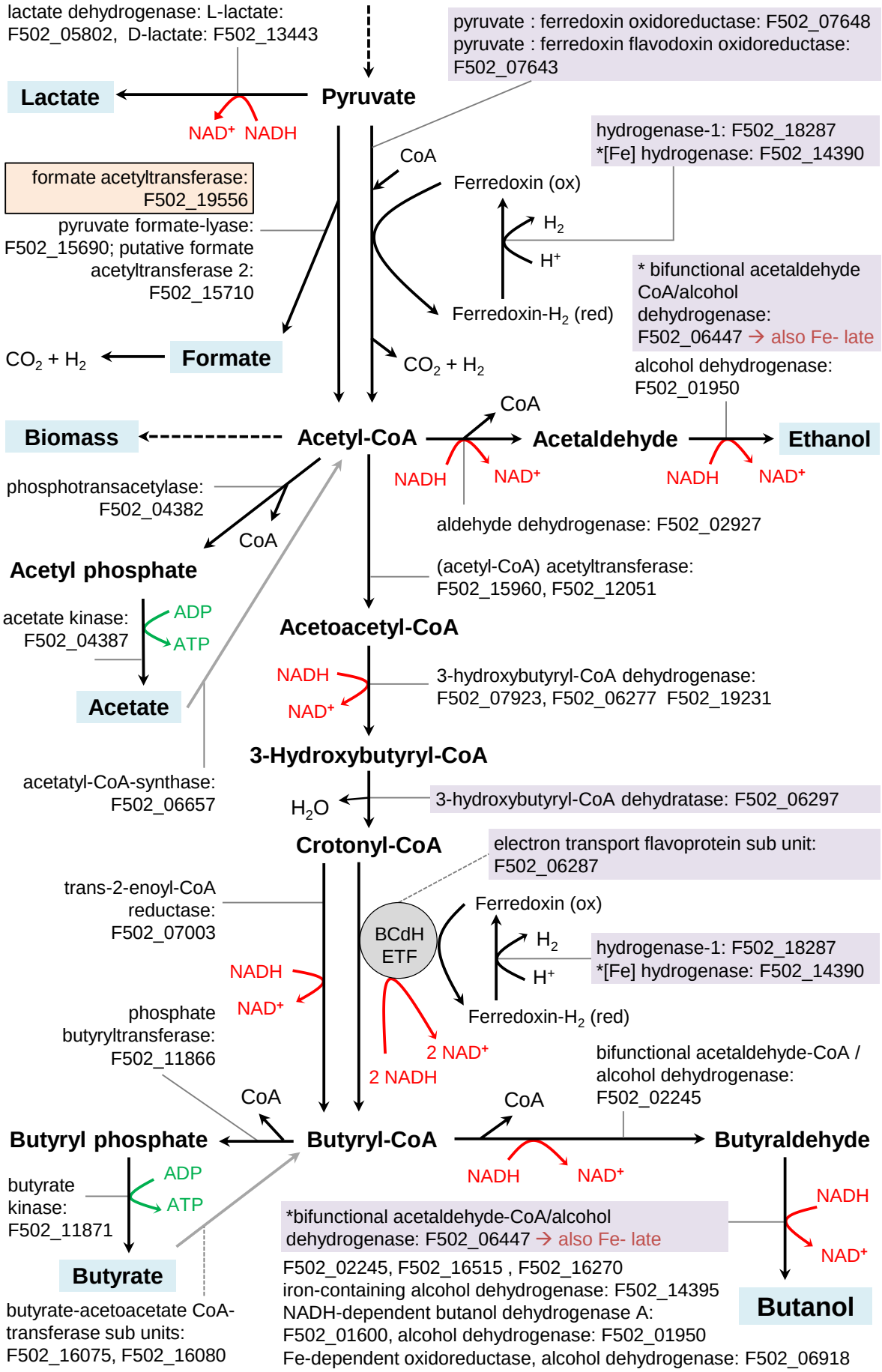
lactate dehydrogenase: L-lactate: F502_05802, D-lactate: F502_13443
Lactate
Pyruvate
NAD+ NADH
pyruvate : ferredoxin oxidoreductase: F502_07648
pyruvate : ferredoxin flavodoxin oxidoreductase: F502_07643
hydrogenase-1: F502_18287
*[Fe] hydrogenase: F502_14390
CoA
Ferredoxin (ox)
H2
H+
Ferredoxin-H2 (red)
formate acetyltransferase: F502_19556
pyruvate formate-lyase: F502_15690; putative formate acetyltransferase 2: F502_15710
CO2 + H2
Formate
CO2 + H2
* bifunctional acetaldehyde CoA/alcohol dehydrogenase: F502_06447 → also Fe- late
alcohol dehydrogenase: F502_01950
Biomass
Acetyl-CoA
CoA
Acetaldehyde
Ethanol
NADH
NAD+
NADH
NAD+
phosphotransacetylase: F502_04382
CoA
aldehyde dehydrogenase: F502_02927
Acetyl phosphate
(acetyl-CoA) acetyltransferase: F502_15960, F502_12051
acetate kinase: F502_04387
ADP
ATP
Acetoacetyl-CoA
NADH
NAD+
3-hydroxybutyryl-CoA dehydrogenase: F502_07923, F502_06277 F502_19231
Acetate
3-Hydroxybutyryl-CoA
acetatyl-CoA-synthase: F502_06657
H2O
3-hydroxybutyryl-CoA dehydratase: F502_06297
Crotonyl-CoA
electron transport flavoprotein sub unit: F502_06287
trans-2-enoyl-CoA reductase: F502_07003
BCdH ETF
Ferredoxin (ox)
H2
H+
hydrogenase-1: F502_18287
*[Fe] hydrogenase: F502_14390
NADH
NAD+
Ferredoxin-H2 (red)
phosphate butyryltransferase: F502_11866
2 NAD+
2 NADH
bifunctional acetaldehyde-CoA / alcohol dehydrogenase: F502_02245
CoA
CoA
Butyryl phosphate
Butyryl-CoA
Butyraldehyde
NADH
NAD+
butyrate kinase: F502_11871
ADP
ATP
*bifunctional acetaldehyde-CoA/alcohol dehydrogenase: F502_06447 → also Fe- late
F502_02245, F502_16515 , F502_16270
iron-containing alcohol dehydrogenase: F502_14395
NADH-dependent butanol dehydrogenase A: F502_01600, alcohol dehydrogenase: F502_01950
Fe-dependent oxidoreductase, alcohol dehydrogenase: F502_06918
NADH
NAD+
Butyrate
Butanol
butyrate-acetoacetate CoA-transferase sub units: F502_16075, F502_16080

4.3 Effects of redox active substances and bioelectrical systems on *C. pasteurianum* DSMZ 525

The results in previous experiments suggested that restoring the redox balance is a key in the metabolic switch from BuOH to 1,3-PDO production under iron limited conditions (see Chapter 4.2). Moreover, sparging with N_2 to strip BuOH out of the fermentation broth increased the redox potential significantly, and *C. pasteurianum* produced more acids (Chapter 4.4). In fact, glycerol shows a higher reduction degree than biomass and products like butanol or the organic acids. For sake of the intra cellular redox balance, the formation of reducing equivalents due to glycerol degradation requires an internal electron acceptor in form of 1,3-PDO or lactate. Hence, it is interesting whether the reduction of the extracellular redox potential (RP) or/and a supply of more electrons would led to the production of more reduced products. The artificially added electrons can be transferred to the bacteria either directly, through bacterial pili or with electron carrying mediators (see Chapter 2.3.1). In this study two different approaches were analyzed; first, the influence of redox active compounds and second the suitability of electro bioreactors for artificial electron supply.

4.3.1 Redox active compounds and their effects on growth and product formation

It has been shown that several chemicals and dyes like methyl viologen and Neutral Red positively influence the product formation in *Clostridium* (Kim and Kim, 1988), (Girbal et al., 1995). Therefore in this study different chemicals and dyes were tested on their ability to influence the external redox potential of the culture of *C. pasteurianum* DSMZ 525 (Table 4-5). Among others (cysteine HCl, Na_2S, curcumin), the dye Brilliant Blue R250 (BB) was found to have the strongest influence on the RP of the culture. The redox potential of the cultivation broth decreased by 130 mV, when the dye was added (Table 4-5). Furthermore, BB did not inhibit the growth, like for example curcumin. In the latter case, growth stopped shortly after addition and the biomass concentration did not exceed 1.5 g/L. With regards to large scale applications, BB is non-toxic, in contrary to the other chemicals tested, such as Na_2S. Due to these positive characteristics it was chosen as a possible mediator with redox decreasing properties for further experiments.

Table 4-5: Effect of several chemicals on the redox potential in fermentations of pure glycerol using *C. pasteurianum* DSMZ 525.

Chemical	Influence on RD	Drawback for fermentation
N_2 sparging	increased RD	not suitable
Curcumin	reduced from -568 mV until -626 mV	immediate growth inhibition
Cysteine HCl	reduced from -473 mV until -502 mV	(already used)
Na_2S	reduced from -560 mV until -588 mV	release H_2S in contact with acids → harmful effluent gases
Brilliant Blue	reduced from -370 mV until -506 mV	additional costs

Fig. 4-15: Increasing concentrations of BB in serum bottles with cultures of *C. pasteurianum* DSMZ 525.

At first the optimal concentration of BB was determined in view of growth and products formation. Triplicate cultivations in serum bottles without BB and with different concentrations of BB were performed and compared after 45 h incubation time (Fig. 4-15).

As shown in Fig. 4-16 A, the concentration of both target products, 1,3-PDO and BuOH, as well as the biomass concentration increases with enhanced concentrations of BB and reaches a maximum at 0.06 g/L of BB. Here it should be noted that the enhanced biomass amount was not caused by the increased OD, due to the dye. Correlations of biomass concentration and OD resulted in the same results, without and with BB (see Chapter 3.5.1). Increasing the dye concentration above 0.06 g/L led to a reduction in solvent concentration as well as biomass. In the case of BB dye addition to the fermentation broth the acid production were lower, compared to control fermentation without dye (Fig. 4-16 B), and the amounts of butyric- acetic- and lactic acid decreased linearly with the increase of BB concentration.

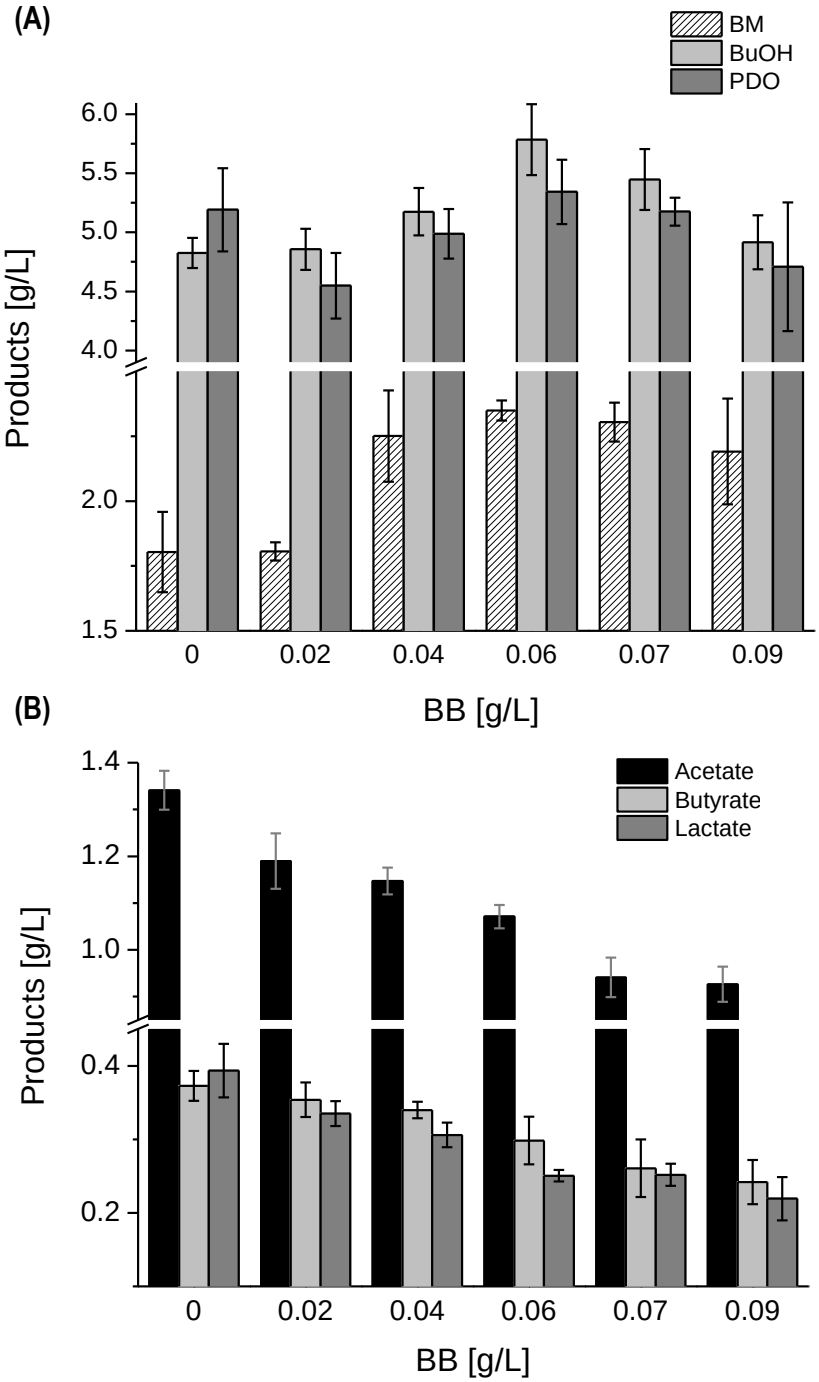

Fig. 4-16: (A) Biomass, BuOH and 1,3-PDO titer, and (B) butyric and acetic acid titer for different concentrations of BB in fermentations of *C. pasteurianum* DSMZ 525 after 45 h fermentation time.

Decreased acids content in response to Brilliant Blue R250 addition: A possible mechanism

Due to the distinctive aromatic character of Brilliant Blue R250 (Fig. 4-17 A), the molecule is mesomerically stabilized and can therefore uptake, delocalize and transfer electrons. Tal et al. (Tal et al., 1985) found that the protein-dye complex is formed due to the electrostatic connection between the negative sulfonic groups of Brilliant Blue and the amine groups of basic amino acids, e.g. arginine, histidine and lysine. The possible constitution of this connection between BB and lysine is shown in Fig. 4-17 A. Assuming uncharged conditions of the amino acid and the sulfonic acid group of BB at neutral conditions, a reactive proton (H^+) originated from BB molecule is formed and stabilized in between the two molecules. A similar molecule constitution has been reported for BB G-250 for neutral molecule conditions (Georgiou et al., 2008). Because of the weak bonding, the proton is easily available for other metabolic reactions, especially if it is bound near to an active center of enzymes. For example, it could support [Fe]-hydrogenase in the recovery of Fd_{red} to Fd_{ox} under the release of molecular hydrogen. [Fe]-hydrogenase from *C. pasteurianum* possess an active center with the [FeFe]-complex, where the terminal Fe atom (termed Fe2) is i) responsible for the reaction of protons in H_2 formation and ii) connected with the molecule surface by a channel for H_2 transfer. The analysis of the molecular structure revealed that a lysine residue is within hydrogen-bonding distance to this part of the active center with Fe2 (Peters, 1999). Thus, lysine might be accessible and susceptible for BB binding, which transfers additional protons into the system. The subsequent increase in the Fd_{ox} pool might also support the increased formation of butanol, as described in the Chapter 4.2. Measuring the effluent gas led to the observation that the addition of BB to the broth induces a short time increased peak of the hydrogen amount in the effluent gas, accompanied by a drop in the redox potential of the broth (Fig. 4-17 B). Also comparing two fermentations, the average RD was slightly reduced to -568 ± 8 mV with BB compared to -529 ± 3 mV without BB. Therefore, like in the gas stripping experiments with circulating fermentation gases (Chapter 4.4), the reduced redox potential might explain the increase in product formation of BuOH and 1,3-PDO to a certain extent. However, the explicit mechanism of the interaction between BB and *C. pasteurianum* DSMZ 525 needs further enquiries.

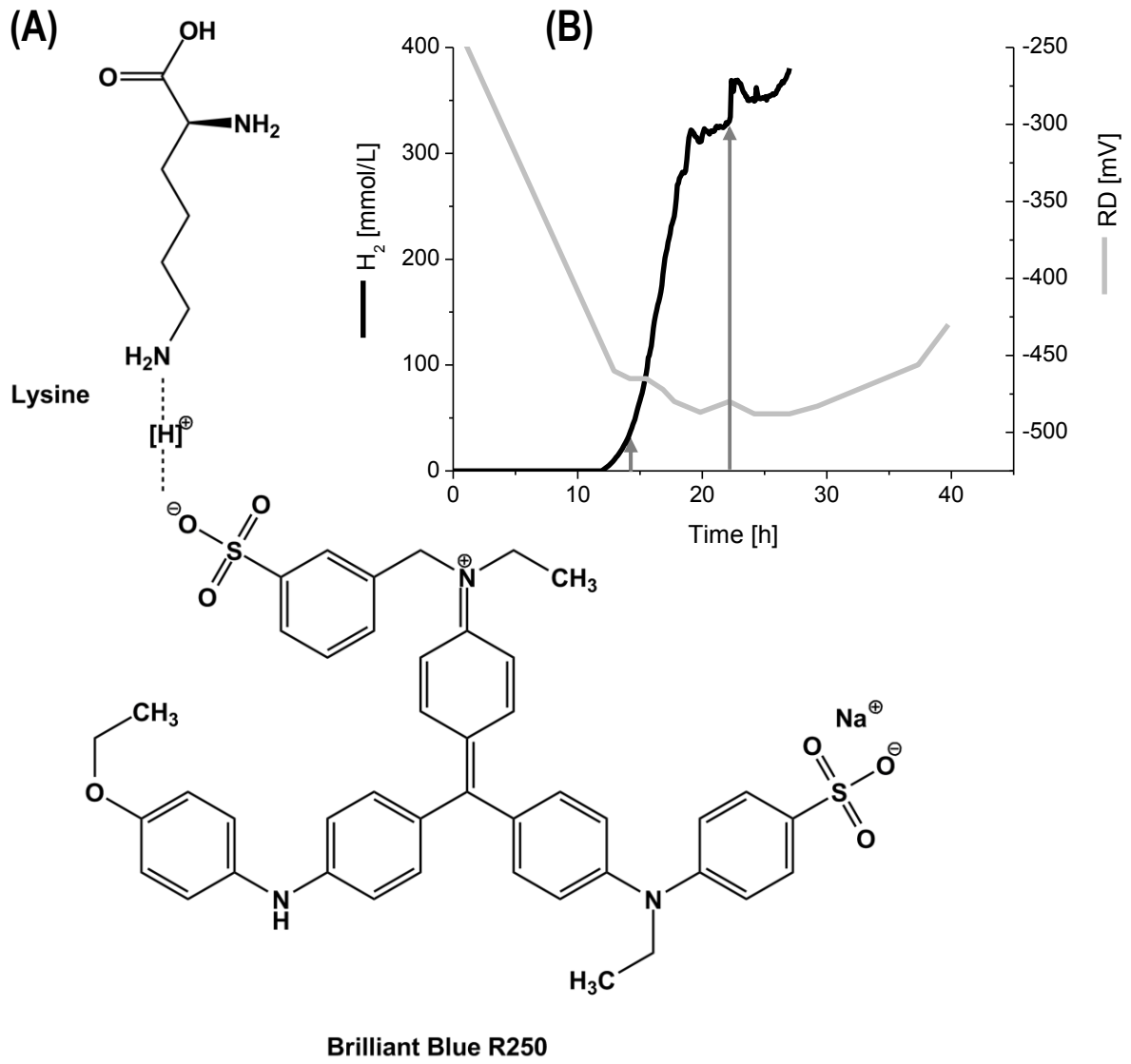

Fig. 4-17: (A) Possible connection between Brilliant Blue R250 and the basic amino acid lysine (B) Increase in H_2 formation by *C. pasteurianum* DSMZ 525 during fermentation of pure glycerol after BB addition (arrows).

Usually, the formation of butyrate and acetate is coupled to the ATP formation, which is necessary for the growth. Since more biomass is produced using BB as supplement, a higher acids production is expected. Nevertheless, the final concentration as well as the acid yield per biomass decreased, when BB is added. Hence, the dye is believed to support primarily the growth by activating or stimulating responsible enzymes, due to additional and easy available protons connected to the BB molecule. For example, an increased H^+ gradient might support the activity of ATP synthase. The resulting enhanced ATP pool could support the growth and less formation of acids would be required. Based on the stoichiometric equations and the different product profiles, the specific ATP formation rate as well as the growth rate μ in the exponential phase for glycerol fermentations by *C. pasteurianum* is shown (Fig. 4-18). The comparison shows results with no addition of BB, one time (1x) and two time (2x) addition of the BB. It can be seen that with increasing BB content in the media, the ATP formation rate decreases, but at the same time, the μ is enhanced. Thus, the formation of acids seems to be not the sole main source of growth supporting ATP formation in cultivations with BB.

It is known that BB is strongly susceptible for binding on RNAase (Tal et al., 1985), which is involved in the cell division. Tal et al. (Tal et al., 1985) reported also that BB showed a high affinity on cytochrome c, which is involved in the energy metabolism. Cytochrome c catalyzes the transformation of aldehydes into alcohols under the consumption of protons, and its enhanced activity might also contribute to the higher butanol and ethanol formations in fermentations with BB. However, if the binding of BB on enzymes like RNAase, or cytochrome c positively affects their function or inhibits them is still unclear.

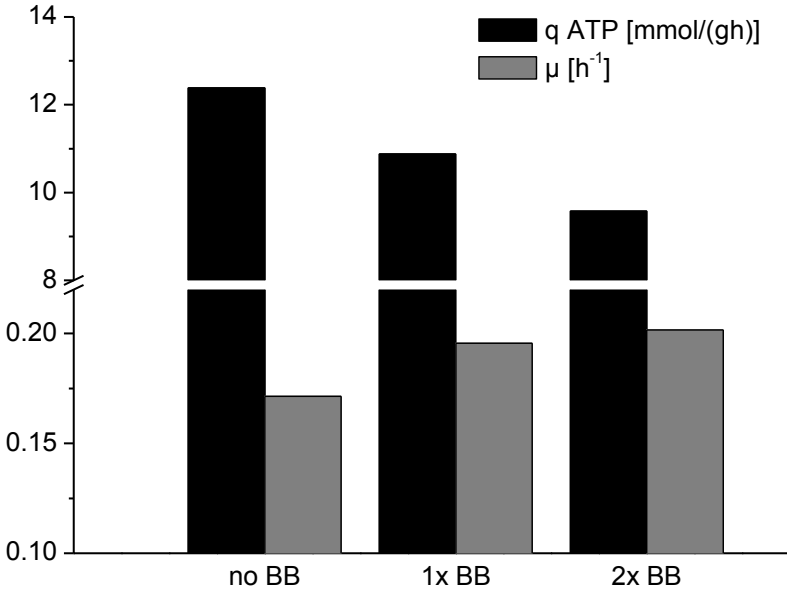

Fig. 4-18: ATP formation rates and growth rates μ in cultivation of *C. pasteurianum* DSMZ 525 with either none, one time (1x) or two times (2x) addition of BB.

Consumption of Brilliant Blue R250 by growing culture of *C. pasteurianum*

It was observed within these experiments, that the dye concentration in the supernatant decreases over time and the cells became more colored, due to the attachment of BB on several proteins. Subsequently, a fed batch culture with a second addition of dye was performed. Fig. 4-19 A shows two fermentations with either one or two time supplementation of 0.06 g/L BB into the culture broth of *C. pasteurianum* DSMZ 525. Dye addition at a concentration of 0.06 g/L was done when the biomass concentration reached 1.3 and 1.7 g/L respectively, which resulted in a biomass formation rate of 0.44 g/(Lh) in both experiments. In control fermentations without BB, biomass was produced at a rate 0.31 g/(Lh) in the exponential growth phase. With one time BB addition, the dye was completely absorbed from the broth after 7.2 h. In this time period the culture enters stationary phase and a maximum biomass concentration of 5 g/L was reached. On the contrary, when BB was added a second time, before it was completely absorbed by the cells, growth continued and the biomass reached a maximum of 5.6 g/L.

The results obtained through the addition of BB were reproduced in different other *C. pasteurianum* DSMZ 525 cultivations and comparisons were done between the following conditions: (I) a control fermentation under standard cultivation conditions; (II) a cultivation with one time addition of BB at

1.6 g/L BM; (III) cultivation with two times additions of BB at 1.8 g/L and 3.8 g/L BM; (IV) experiments without BB addition and with gas stripping by FG at 4.5 vvm; and (V) cultivation with 2x BB addition at 1.6 g/L and 5.4 g/L biomass, and with gas stripping by FG at 4.9 vvm (see also Chapter 4.4.4). It can be seen that the supplementation of BB enhanced the final product titer significantly (Fig. 4-19 B). With GS even more target products were formed, and compared to the standard fermentation without GS, nearly doubled. On the other hand, the amount of carbon channeled into acids reduces slightly. In both cases, with or without GS, the specific product yield per biomass was enhanced for both target products, especially 1,3-PDO, but reduced for butyrate, when BB was added (Table 4-6). Also the substrate yield increased from 0.38 $g_{BuOH+PDO}/g$ in controle fermentation to 0.41 $g_{BuOH+PDO}/g$ and 0.44 $g_{BuOH+PDO}/g$ in cultivations with one or two time addition of BB, respectively.

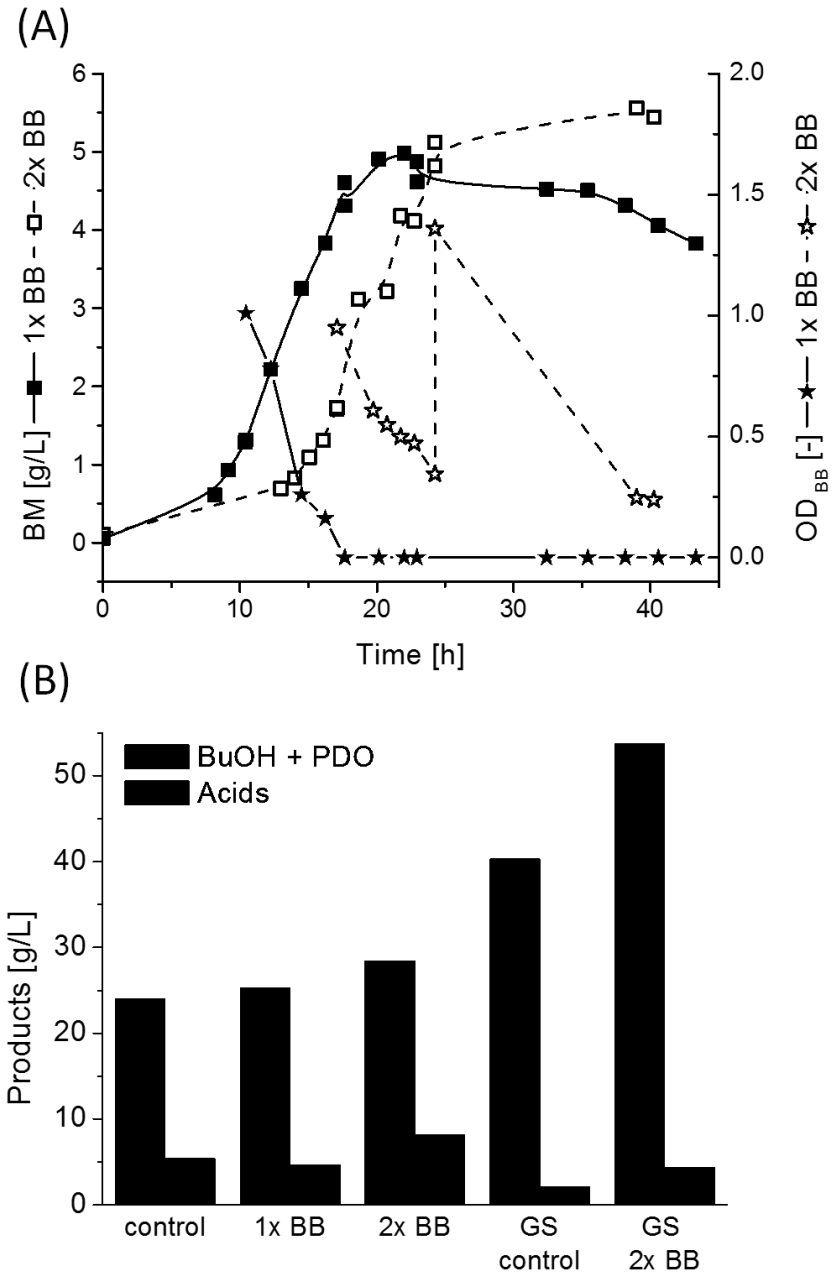

Fig. 4-19: (A) Biomass concentrations and OD of BB in the supernatant of the broth from *C. pasteurianum* DSMZ 525 cultivations with either one time (1x) or two times (2x) addition of BB. (B) Final product concentrations in cultivations with different additions of BB and /or the application of *in situ* gas stripping with FG.

Table 4-6: Carbon recovery and specific product yields in the growth phase in fermentations of pure glycerol using *C. pasteurianum* DSMZ 525 and with BB addition as well as gas stripping (GS).

Experiment parameter	Carbon Recovery [%]	Final titer [g/L]			
		BuOH	1,3-PDO	Butyrate	Acetate
control	100	10.1	13.9	4.1	1.3
1x BB	101	7.2	18.1	2.8	1.9
2x BB	100	8.2	20.3	6.4	1.8
FG 4.6 vvm	95	26.4	13.9	1.1	1.0
FG 4.9 vvm 2x BB	96	32.5	21.3	1.3	3.0
		$Y_{P/X}$ [g/g]			
		BuOH	1,3-PDO	Butyrate	Acetate
control		1.46	3.07	1.07	0.30
1x BB		2.25	5.88	0.92	0.36
2x BB		1.36	3.65	0.89	0.29
FG 4.6 vvm		3.08	2.66	0.44	0.22
FG 4.9 vvm 2x BB		4.26	3.10	-0.07	0.37

Note: For the specific yields the values from the time point BB of addition or start of GS, respectively, until the end of fermentation were compared. The negative value in the butyrate yield represents the high re-consumption of butyrate, i.e. the final titer was lower than the titer at the time point of BB addition.

4.3.2 Cultivation in bioelectrical systems

The experiments with electro bioreactors were performed in cooperation with Dr.-Ing. Dirk Holtmann and M.Sc. Thomas Krieg at the research group “Biochemical Engineering”, DECHEMA e.V.

Recently it was shown that *C. pasteurianum,* living in biofilms, is an electro active organism with the ability to accept electrons from a cathode (Khosravanipour Mostafazadeh et al., 2016), (Choi et al., 2014). The electron supply into the cultivation system is expected to drive the intracellular NADH pool to a more reduced state, with the consequence that more reduced products will be formed (Choi et al., 2014), (Rabaey and Rozendal, 2010). However, the corresponding mechanism of electron uptake is still unclear. In the previous section it was shown that the dye BB exhibits a positive influence on the growth of bacteria and the formation of both target products. These effects were further investigated in bioelectrical system. First it was aimed to investigate whether BB could be recharged on the electrodes of an electro-bioreactor. The cyclic voltammogram (CV) of BB at the concentration of 0.06 g/L in water is given in Fig. 4-20. The CV shows that electrons can be accepted by BB between 0 mV and 140 mV, and will be released at potentials above 200 mV. Thus BB can be used as a rechargeable mediator in bioelectrical system, but only at positive potentials.

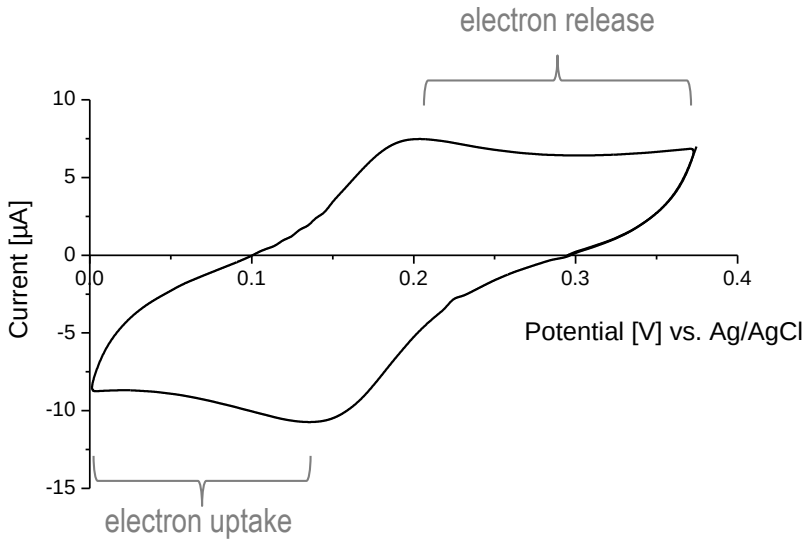

Fig. 4-20: Cyclic voltammogram of 0.06 g/L Brilliant Blue R250 in water.

Hence, cultivations of free cells of *C. pasteurianum* in H-cell electro-bioreactors without BB and with addition of BB were tested. Due to the fact that the CV showed a recharge at positive potential, a potential of +500 mV was applied and compared to uncontrolled potential (open circuit potential, OCP, which is equivalent to the standard batch fermentation) as well as the negative potentials of -500 mV and -300 mV. The negative applied potentials are in the range of the preferred redox potentials for the main reactions in *Clostridium* (see Table 2-2, Theory). All results are collected in Fig. 4-21. The carbon recovery of all experiments reached an average of 98 ± 4.8 %. In general, and similar to the fermentations without applied potential shown above, it was confirmed that BB enhances the growth and the production of BuOH and 1,3-PDO, whilst reducing acid formation (Fig. 4-21). However, the influence of the applied potential is not fully understood yet. Despite the fact that BB enhanced the growth compared to fermentations without BB, the biomass production was not significantly affected by the applied potential, except a slightly higher BM value for the cultivation at -300 mV and BB addition. Considering product formation, the highest product titers of BuOH and 1,3-PDO as well as acids are reached at OCP. Also the positive potential of +500 mV led to higher product titers and specific yields compared to negative potential. With BB as mediator the highest substrate yield of 0.36 $g_{BuOH+1,3\text{-}PDO}$ / $g_{glycerol}$ was achieved at +500 mV, compared to 0.31 ± 0.01 $g_{BuOH+1,3\text{-}PDO}$ / $g_{glycerol}$ at OCP and negative potentials. This might indicate a recharge of the mediator BB with electrons that supports the formation of the target products. Nevertheless, it has to be noted that at any time point of the fermentations and irrespective of the applied potential (or OCP) up to 40 % of the glycerol and up to 25 % of solvents and acids could be found in the buffer cell of the reactor without fermentation broth, but no BB could be detected, if it was used. The movement of molecules might have contributed to the unclear results.

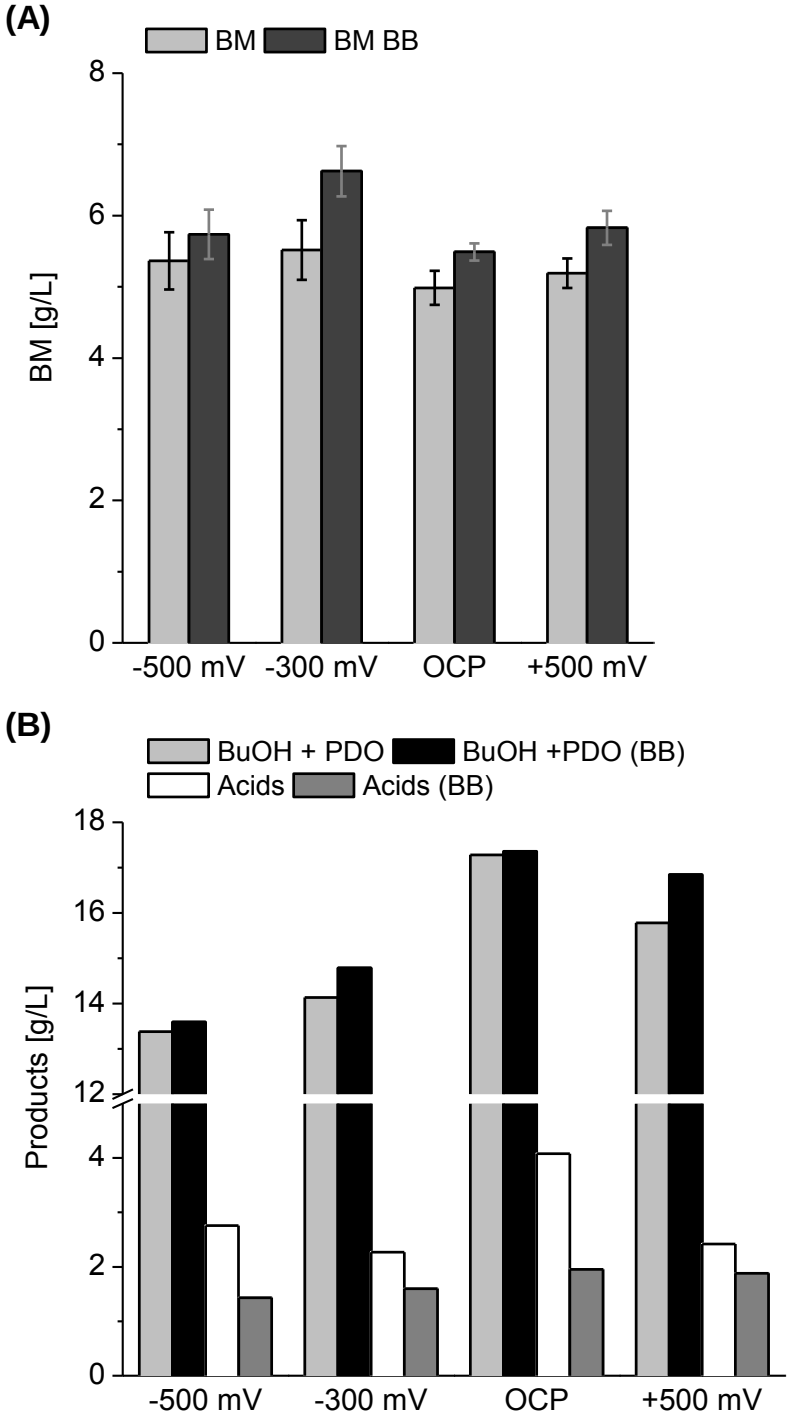

Fig. 4-21: (A) Average biomass concentration in the stationary phase and (B) final product titer after 41 h in fermentations of *C. pasteurianum* DSMZ 525 with and without BB and at different potentials applied in the BES.

Obviously, for the given system the applied potential of -500 mV was not enough to transfer sufficient additional electrons into the system. Rabaey et al. (Rabaey and Rozendal, 2010) reported about the ohmic losses in bio-electrical systems, due to the ionic transfers in the electrolyte and material resistance in the electrode itself, which mostly requires an over potential. Therefore, the applied potential for the fermenter should be lower than -500 mV to achieve a reduced redox state in the fermentation broth and to ensure a sufficient electron supply. For example Khosravanipour Mostafazadeh et al. (Khosravanipour Mostafazadeh et al., 2016) used a higher applied voltage of 1.3 V

in electro-bioreactors for the fermentation of *C. pasteurianum* on sole glucose. They achieved an increased BuOH formation of 13.3 g/L, compared to 10.2 g/L without current. In the experiments shown here and using glycerol as substrate, the applied potential of -500 mV leads to a BuOH titer of 9 g/L, compared to 9.4 g/L at OCP. However, as shown in the Chapter 4.1 the fermentation of mixed substrates with 50 % glucose and 50 % glycerol resulted in 21 g/L BuOH, even without a bioelectrical system.

4.3.3 Conclusion

The experiments show that the addition of Brilliant Blue R250 enhances the growth of *C. pasteurianum* and the formation of both main products BuOH and 1,3-PDO, whilst reducing acid formation. The most efficient concentration was 0.06 g/L BB, but it will be consumed in the process and must be re-added within fermentation time, preferable in the growth phase. The fermentations in a bioelectrical system resulted in no significant effect for the applied potentials of -500 mV and -300 mV, in comparison to control fermentations without artificially added electrons. Nevertheless it could be shown that BB is rechargeable at an applied potential of +500 mV, which led to the highest product yield within this set of experiments.

4.4 Influence of gas stripping on product formation by *C. pasteurianum* DSM 525 [11]

Growth and simultaneous product formation of butanol and 1,3-PDO by *C. pasteurianum* can be improved to a certain extent by optimizing fermentation conditions or media components. However, the final product titer will always be limited by the fact that the target product butanol is inhibiting the growth and productivity already in low concentrations around 5 g/L. Consequential, for further increase of process performance and to reach concentrations competitive with conventional processes, the produced BuOH has to be removed from the fermentation broth as an *in situ* process. Preferably the separation technique should be highly selective, concentrate the product, exhibit a simple set up and does not interfere negatively with the metabolism of the bacteria. Within this field, different downstream processing techniques have been analyzed by several groups, like liquid-liquid extraction, salting out, adsorption or pervaporation (see Chapter 2.4 and Groeger et al., 2015). But despite their effectiveness most of them exhibit problems related to toxicity of the solvents, removal of other important media components, expensive recovery or membrane fouling, which hampers their application in large scale. These drawbacks can be partially avoided by using gas stripping as an *in situ* removal technique for butanol (Ezeji et al., 2003), (Jensen et al., 2012a). However, the impact of gas stripping, especially the gas type, has been barely analyzed in context with the bacterial metabolism. Therefore, in this Chapter the influence of *in situ* gas stripping with different gases on the performance of *C. pasteurianum* growing on different substrates has been investigated. This included also process engineering aspects, such as influence on butanol mass transfer and selectivity under different process conditions. The reactor system for the gas stripping and equations used are given in Chapter 3.4.

4.4.1 Effect of *in situ* gas stripping on glycerol fermentation

Besides technical set up conditions, gas stripping efficiencies applied in fermentations are known to be dependent on biological parameters, like the growth phase, the concentration of butanol in the fermentation broth due to productivity, but also the type of the stripping gas and their effect on bacteria. Hence, at first the effect of growth and product formation on *C. pasteurianum* grown on glycerol was analyzed and the efficiency of butanol removal was investigated with different gas types and gas flow rates. Therefor either external N_2 or effluent fermentation gas (FG, composed of CO_2 and H_2) are used as stripping gas. Considering the high costs of external, pure N_2, a low flow rate of 0.7 vvm was first used to strip BuOH in an open system and compared to stripping with FG circulated at the same flow rate (Fig. 4-22, Fig. 4-23, Table 4-7 on page 109).

Applying N_2 as stripping gas, *C. pasteurianum* grew at a maximum specific growth rate of 0.23 h^{-1}, which is clearly enhanced compared to the μ_{max} of 0.17 h^{-1} reached in the standard fermentation without stripping. However, the BM concentration was slightly enhanced from ~5.1 g/L without GS to 5.5 g/L. In this fermentation a total amount of 18.9 g/L BuOH and 49.6 g/L 1,3-PDO were produced. 10 g/L BuOH remained in the broth and the concentration of butanol in the reactor did not exceed 6 g/L until 47 h. An average stripping rate of 0.21 $g_{BuOH}/(Lh)$ could be achieved, calculated from the BuOH amounts in the

[11] Parts of this chapter had been published in Groeger et al. (2016).

condensates (Eq. (3-9), Chapter 3.4.3). On the other hand, the use of FG for stripping with the same flow rate of 0.7 vvm resulted in only 10.9 g/L 1,3-PDO and 12.5 g/L BuOH. The stripping rate was lower (0.07 g_{BuOH}/(Lh)) and BuOH accumulated in the reactor up to 11.5 g/L after 36 h. This obviously inhibited the growth and further product formation at an early stage, when the BuOH concentration exceeded the inhibiting level. Indeed, the biomass concentration did not exceed 5 g/L (Fig. 4-23). Interestingly, the production of acids decreased significantly with FG. With N_2 as stripping gas, the total acids produced were 12.5 g/L compared to 2.4 g/L when FG was utilized (Table 4-7).

Despite the use of the same flow rate, the stripping efficiencies vary significantly between the two gases. Beside the economic aspects and beneficial behavior towards bacterial metabolism, two physical properties should be considered for the suitability of a stripping gas: I) The dissolution of the stripping gas into the liquid, i.e. fermentation broth, because dissolved gas is known to lower the butanol activity and decreases the stripping efficiency. II) The evaporation of butanol into a certain gas type.
The ability for dissolution into the aqueous fermentation broth can be described with the Henry coefficient H_{ij}^{cp} [mol/(m³Pa)] for a binary mixture of gas and water [12]. The coefficients were reported to be 6.4*10^{-6} mol/(m³Pa) for N_2 and 3.4*10^{-4} mol/(m³Pa) for CO_2, showing a clear preference for CO_2 to go into the water phase (Sander, 2015). The reported H_{ij}^{cp} for H_2 was 7.7*10^{-6} mol/(m³Pa), which is slightly higher than that of N_2 (Massoudi and King Jr, 1973). The evaporation ability can be described by the Henry coefficient k_{Hij}^{px} [Pa]. Massoudi and King (1973) reported a higher volatility for butanol into N_2 gas (k_{Hij}^{px} = 2.14*10^8 Pa) than into CO_2 gas (k_{Hij}^{px} = 1.36*10^7 Pa). Comparing the gases used in the experiments described above, the highest value was recorded for H_2 with k_{Hij}^{px} = 3.80*10^8 Pa (Katayama and Nitta, 1976). As indicated by these Henry coefficients, the FG as a mixture of CO_2 and H_2 might not reach the same stripping efficiency as pure N_2 when the H_2 concentration is too low, which might be the case in the early growth phase.

For making the process economically viable by avoiding N_2 stripping, the following experiments were done using bacterial produced fermentation gases as stripping gas. To further enhance the BuOH stripping efficiencies, an increase of the volumetric mass transfer coefficient K_Sa can be achieved by increasing the (circulation) flow rate. Hence, the stripping performance of FG was tested with increased flow rates of 1.5, 4.5 and 7 vvm.

[12] The given Henry coefficients are values for a binary mixture and at ambient temperature and pressure.

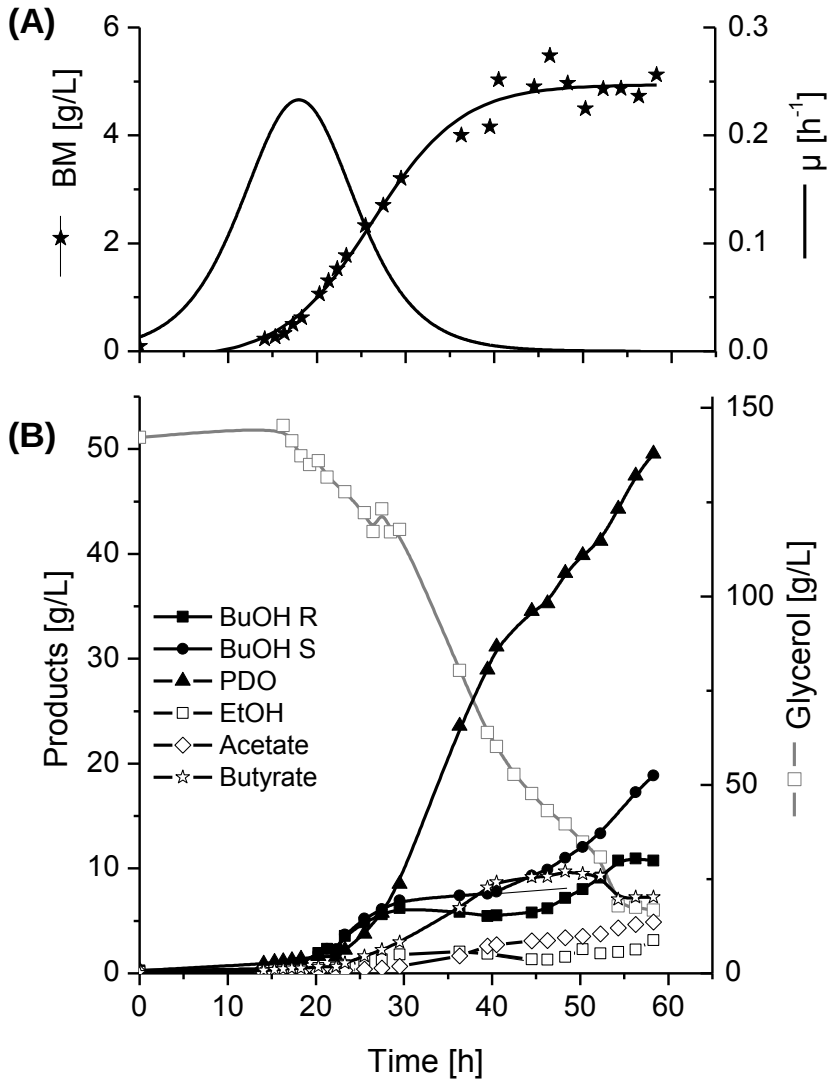

Fig. 4-22: Gas stripping with 0.7 vvm of N_2 (started at 20 h), and its effect on (A) growth as well as (B) substrate consumption and product formation of *C. pasteurianum* DSMZ 525 during growth on pure glycerol. For glycerol cumulated consumed concentrations are shown. BuOH R and BuOH S refer to butanol concentrations in the bioreactor and the accumulated amounts from reactor and condensates, respectively. (Figure from Groeger et al., 2016).

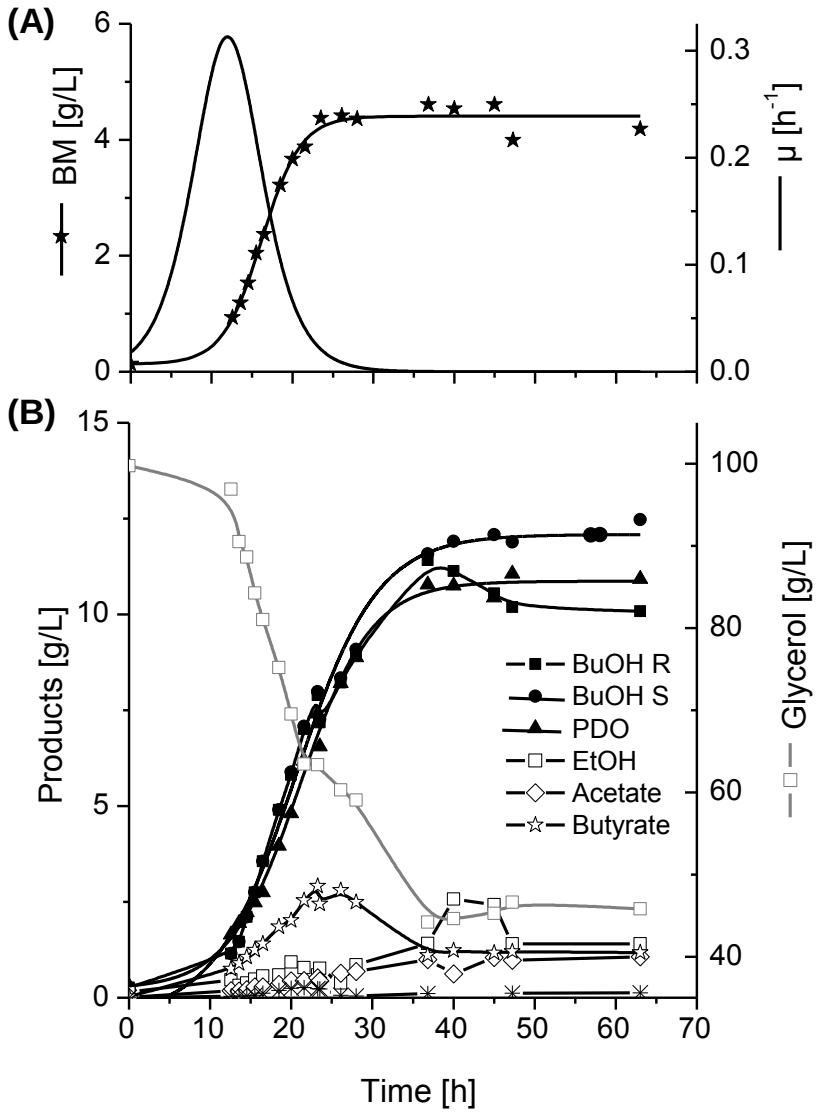

Fig. 4-23: Gas stripping 0.7 vvm of circulated fermentation gases (started at 15 h), and its effect on (A) growth as well as (B) substrate consumption and product formation of *C. pasteurianum* DSMZ 525 during growth on pure glycerol. For glycerol cumulated consumed concentrations are shown. BuOH R and BuOH S refer to butanol concentrations in the bioreactor and the accumulated amounts from reactor and condensates, respectively. (Figure from Groeger et al., 2016).

In general, raising the flow rate of FG from 0.7 to 7 vvm significantly increased the BuOH stripping rate and consequently the maximum biomass concentration in the reactor (Fig. 4-24). At lower flow rates of 0.7 and 1.5 vvm, the stripping rate was only slightly enhanced to 0.07 and 0.14 g_{BuOH}/(Lh) respectively, which could not prevent growth inhibition. In both cases gas stripping was started in the exponential growth phase (OD of 6) with a BuOH concentration in the fermentation broth of ~2.5 g/L. Nevertheless, only 0.2 g/L butanol was stripped in the first 20 h of gas stripping and a constant increase in stripped amount was only achieved, when the BuOH concentration in the reactor was above 8 g/L. A significant increase in the stripping rates to 0.38 and 0.59 g_{BuOH}/(Lh) was reached by increasing the flow rates to 4.5 vvm and 7 vvm, respectively. Accordingly, the average BuOH concentrations in the reactors

decreased with increasing flow rate (Fig. 4-24). Nevertheless, only at a flow rate of 7 vvm, the BuOH concentration in the broth could be kept below 7.5 g/L over the whole fermentation time. This led to an enhanced growth (OD = 20 and up to 7.9 g/L BM), together with a higher product formation of 53.7 g/L 1,3-PDO and a total amount of 39.2 g/L BuOH (Fig. 4-25).

The gas flow rate and the type of stripping gas also affected the substrate consumption by *C. pasteurianum*. Stripping with 0.7 vvm of N_2 led to a glycerol consumption rate of 3.8 g/(Lh) in the growth phase compared to 2.4 g/(Lh) using circulated FG with the same flow rate. On the other hand, increasing the flow rate of FG increased the glycerol consumption rate steadily from 2.8 g/(Lh) at 1.5 vvm, to 3.5 and 3.6 g/(Lh) at 4.5 and 7 vvm (Fig. 4-24). In fact, the decrease of butanol in the fermentation broth as a result of the higher stripping efficiencies explains the higher substrate consumption rate at higher flow rates and reflects the enhanced biomass and product formation.

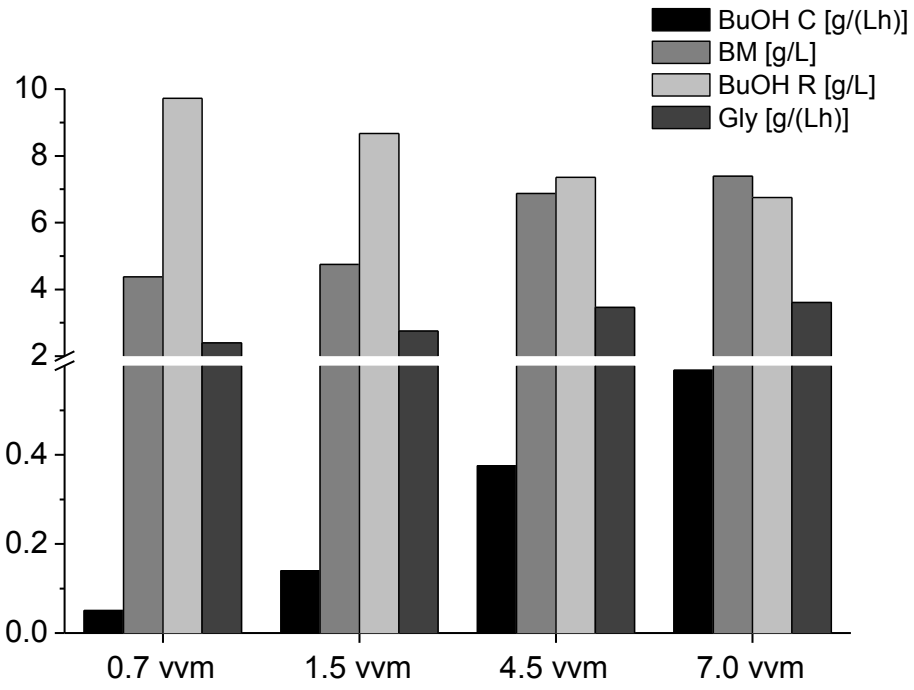

Fig. 4-24: Stripping rate of butanol (BuOH C), average butanol concentration in the reactor during stripping (BuOH R), glycerol consumption rate in the growth phase (Gly), and the maximum biomass concentration of *C. pasteurianum* DSMZ 525 in the reactor (BM) in glycerol fermentation with different FG flow rates. (Figure from Groeger et al., 2016)

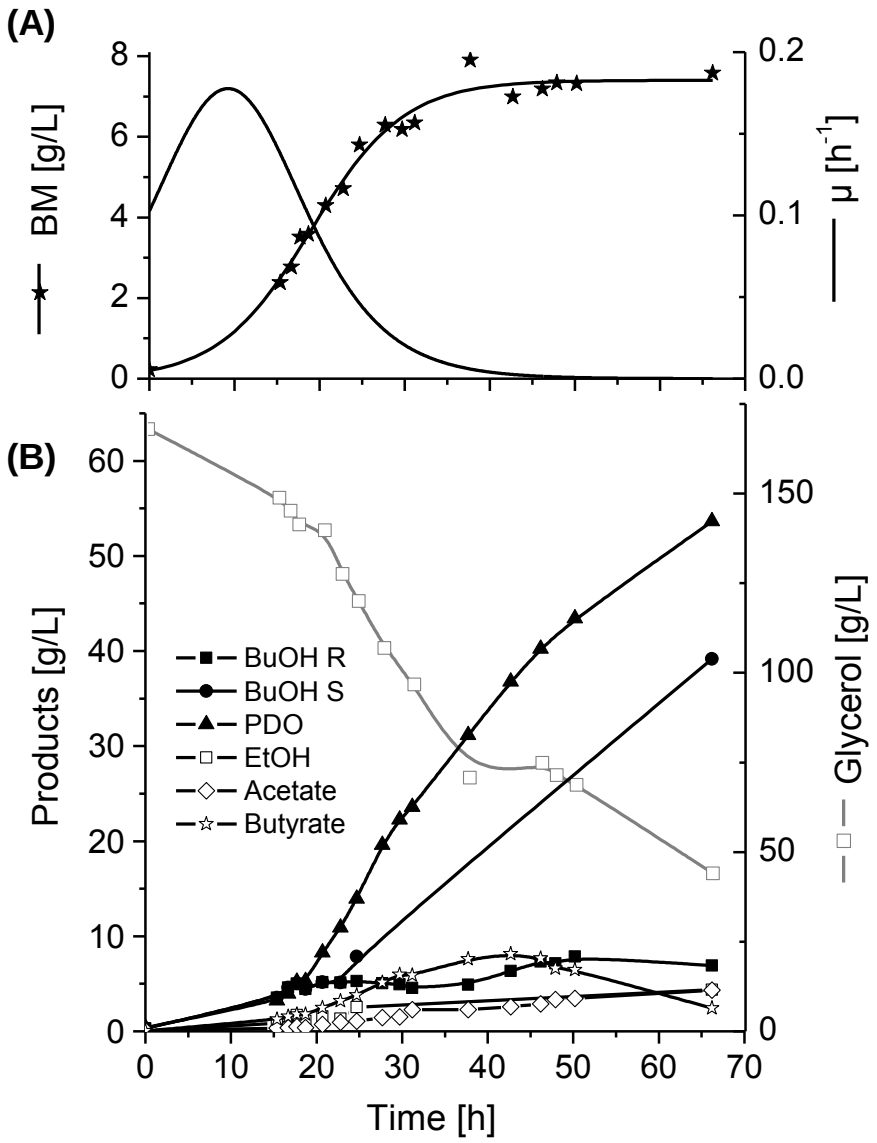

Fig. 4-25: (A) Growth and (B) product formation of *C. pasteurianum* DSMZ 525 during fermentation of pure glycerol. Gas stripping with fermentation gas started at 17 h with 7 vvm. For glycerol cumulated consumed concentrations are shown. BuOH R and BuOH S refer to butanol concentrations in the bioreactor and the accumulated amounts from reactor and condensates, respectively. (Figure from Groeger et al., 2016).

Note: The effect of gas stripping was further analyzed with a slightly different strain, *C. pasteurianum* isolate K1. This bacteria was cultivated on pure glycerol and the same Biebl media and sparged with own effluent fermentation gases at 4.5 vvm. However, the influence of gas stripping on product formation was not significantly changed. Results are collected in Chapter 7.7.1. on page 139 in the Appendix.

4.4.2 Effect of *in situ* gas stripping on co-substrate fermentation

In Chapter 4.1 co-substrate fermentation with glycerol and glucose was described to enhance the growth and butanol titer of *C. pasteurianum* DSMZ 525 up to 21 g/L, even without GS (see also (Sabra et al., 2014)). To examine the influence of *in situ* removal of BuOH in co-substrate fermentation, *C. pasteurianum* was grown on a mixture of glucose and glycerol (ratio 1:1) in fed batch culture and sparged with either N_2 or FG according to the optimal flow rates determined on mono-substrate fermentation using glycerol. Using N_2 as stripping gas, the BuOH concentration in the broth was below 5 g/L and 6.8 g/L were produced in total, which resulted in a low stripping rate of 0.03 g_{BuOH}/(Lh) (Fig. 4-26). The final 1,3-PDO titer accumulated in the broth was reduced to 14.9 g/L. In fact, most of the carbon source was channeled to acids production, and more than 25.1 g/L acids were produced (15.9 g/L butyrate, 6.2 g/L acetate, and 3.0 g/L lactate). Acid formation was strongly enhanced in co-substrate fermentation compared to sole glycerol fermentation, where only 12.5 g/L of total acids were achieved (Table 4-7 on page 109). The simultaneous production of the two main products was slightly enhanced to 12.2 g/L BuOH and 24.1 g/L 1,3-PDO when 7 vvm FG were sparged (Fig. 4-27). The stripping rate achieved was 0.15 g_{BuOH}/(Lh) with 5.3 g/L remaining in the reactor. Again a relatively high amount of acids were formed with 8.4 g/L butyrate, 6.6 g/L acetate, and 5.0 g/L lactate. Interestingly, lactic acid production started when the culture enters stationary phase and it was never detected in batch culture without gas stripping (Sabra et al., 2014). Similar results were obtained from a blend of glycerol and biomass hydrolysates, together with FG stripping at 6.3 vvm. Here 27.8 g/L acids were the major products obtained, with up to 17.8 g/L butyrate, but very low alcohol and diol content.

In comparison to glycerol, glucose significantly supported biomass production of *C. pasteurianum* DSMZ 525 in batch fermentations, as shown before. As can be seen in Fig. 4-26, Fig. 4-27 and Table 4-7 the carbon was mainly directed to acid production when additionally GS was applied. The maximum biomass concentration achieved was 5.2 g/L and 4.8 g/L on co-substrate with N_2 and FG sparging, respectively, compared to 6.2 g/L without sparging. To lower the acid production, lower concentrations of glucose were also used in an experiment with GS of FG at 7 vvm. Growth as well as acid production ceased directly after the consumption of glucose (Sabra et al., 2016). Compared to the co-substrate fermentation without GS, where almost equal consumptions rate of both substrates were recorded (Chapter 4.1), the implementation of GS influenced the consumption of both substrates at the different growth phases (Fig. 4-26, Fig. 4-27). Using N_2 as the stripping gas, 1.98 g/(Lh) glycerol was consumed in the exponential growth phase compared to 1.37 g/(Lh) of glucose. In the stationary phase the uptake rate of both substrates were almost the same with 0.67 g/(Lh) glycerol and 0.70 g/(Lh) glucose. In total 61 g/L glycerol and 54 g/L glucose were metabolized. The fed batch addition of substrate had no influence on the consumption rate (Fig. 4-26, Fig. 4-27 arrows). An even more preferential consumption of the reduced substrate glycerol can be seen in the experiment with FG sparging. In the growth phase 2.12 g/(Lh) glycerol were consumed compared to 0.91 g/(Lh) of glucose and in the stationary phase, the rates decreased to 0.26 and 0.50 g/(Lh), respectively. In total 56 g/L glycerol and only 39 g/L glucose are converted. But even though more substrate was metabolized with N_2 sparging, fewer solvents were formed but more acids. The product yield on consumed substrates with N_2 sparging recorded 0.03 g/g for BuOH, 0.19 g/g for 1,3-PDO and 0.22 g/g for acids, whereas 0.03 g/g for BuOH, 0.33 g/g for 1,3-PDO and 0.18 g/g for acids if FG gases were used for sparging. Considering the results of yield and final titers it must be concluded that co-substrate fermentation is not suitable in combination with GS.

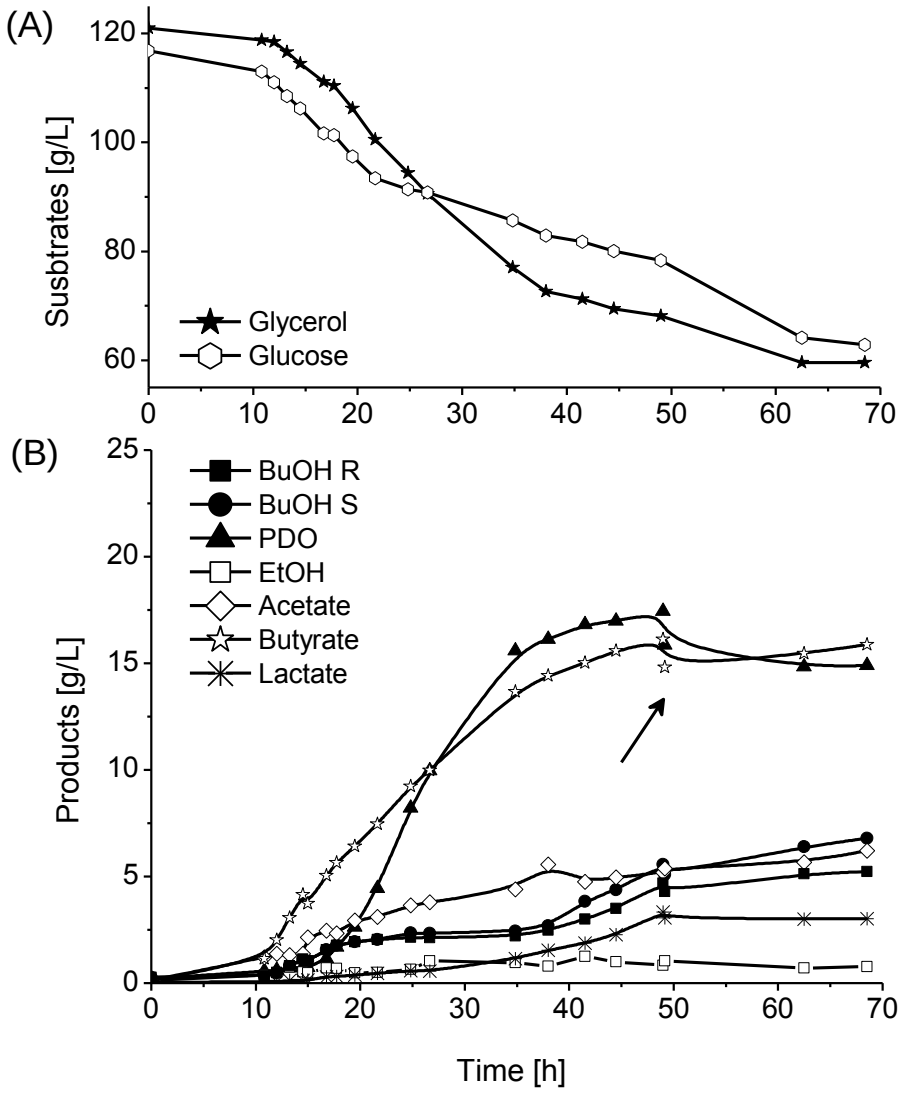

Fig. 4-26: (A) Substrate consumption and (B) product formation of *C. pasteurianum* DSMZ 525 in fermentation of co-substrate (glycerol and glucose at the weight ratio 1:1) and gas stripping with 0.7 vvm N_2. The cumulated consumed concentrations of substrates are shown. BuOH R and BuOH S refer to butanol concentrations in the bioreactor and the accumulated amounts from reactor and condensates, respectively. The arrow indicates the last fed-batch addition of substrate and subsequent dilution. (Figure from Groeger et al., 2016)

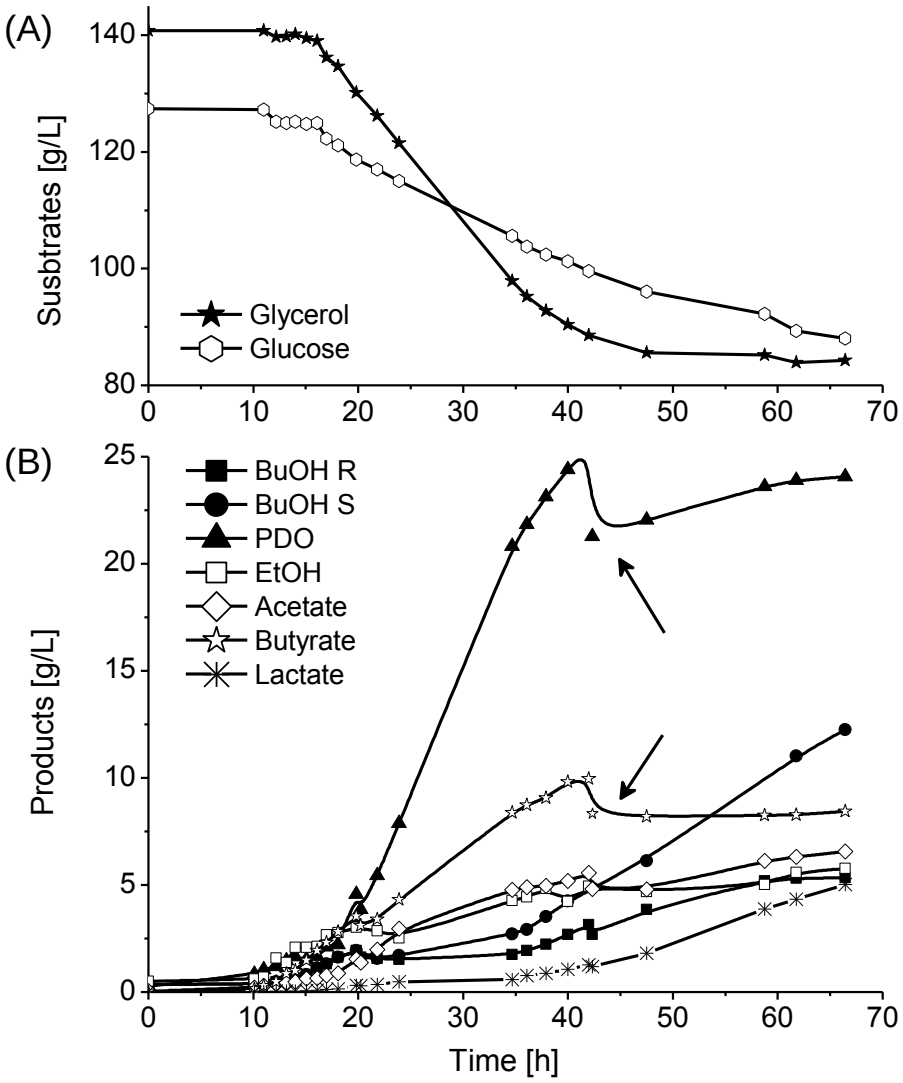

Fig. 4-27: (A) Substrate consumption and (B) product formation of *C. pasteurianum* DSMZ 525 in fermentation of co-substrate (glycerol and glucose at the weight ratio 1:1) and gas stripping with 7 vvm FG. The cumulated consumed concentrations of substrates are shown. BuOH R and BuOH S refer to butanol concentrations in the bioreactor and the accumulated amounts from reactor and condensates, respectively. The arrow indicates the last fed-batch addition of substrate and subsequent dilution. (Figure from Groeger et al., 2016)

4.4.3 Influence of *in situ* gas stripping on external redox potential and the bacterial metabolism

The redox potential of the fermentation media has great impact on microbial physiology and metabolism and can be used to channel the carbons of the substrate into the direction of desired products. It can be influenced not only by the addition of redox-active substances (see Chapter 4.3), but also by sparging of different redox-active gases (O_2, H_2, CO) (Liu et al., 2013a). Pham et al. (Pham et al., 2008) varied the redox potential of the *Saccharomyces cerevisiae* culture by sparging O_2, H_2, and He. H_2 sparging led to a strongly reduced RP in the culture, and more efficient ethanol production compared to the other gases and gassing free cultivation. *C. pasteurianum* re-oxidizes the excess reducing equivalents from glycolysis through the synthesis of alcohols, acids or H_2 to maintain the intracellular redox balance. For

this reason, the reduction degree of the substrate and the redox potential (RP) of the fermentation broth can significantly influence their metabolism. Interestingly, *Clostridium* can maintain the RP of the culture more efficiently, even when growing on a reduced substrate like glycerol.

In the fermentations studied using glycerol as sole carbon source, the RP value was around -500 mV to -450 mV before the start of GS. Using N_2 in co-substrate fermentations the RP increased rapidly to about -280 mV compared to values around -490 mV in the control fermentation without stripping (Fig. 4-28 A). On the contrary, sparging of FG only slightly increased the RP to -450 mV and it decreased further back to -490 mV within fermentation time. Furthermore, independent of the carbon source used, sparging the culture with N_2 in an open system definitely reduce the H_2 partial pressure in the cultivation system. The altered metabolism of *C. pasteurianum* upon gas stripping as reported above may be explained to a certain extent by the change of RP as well.

Stripping off H_2 in mixed cultures from seed sludge was previously reported to improve the H_2 and butyrate productions and alleviate its inhibition in H_2-producing enzymes (Kim et al., 2006). Consequently, two metabolic phenomena were observed in *C. pasteurianum* culture stripped with N_2: I) In co-substrate fermentation, a preferential consumption of the more reduced substrate glycerol is detected, but to a lower extent compared to FG sparging. The molar ratio of consumed glycerol to glucose is decreased to 2.2 at N_2 gassing, but 2.8 for FG gassing (see also Fig. 4-26 and Fig. 4-27). II) A significant increase in the acid production, which was even higher at increased RP levels of -290 mV (N_2) and -436 mV (FG) in co-substrate fermentation. Normally, in *Clostridium* species, the production of acetate and butyrate is associated with energy production in form of ATP, but also H_2 evolution (Petitdemange et al., 1976). Presumably the reduced partial pressure of H_2 can stimulate further H_2 production for the reduction of the environmental RP. According to the pathway in Fig. 4-14 on page 75, the H_2 production is coupled to the formation of acetate and butyrate, but not to lactate. The response to the increased RP under nitrogen sparging is reflected in the strongly enhanced specific production rates of acetate and butyrate, whereas the rate for lactate decreases (Fig. 4-28 B). On the other hand, the stripping with FG had no such significant effect on RP in the culture broth compared to N_2 sparging. Increasing the FG flow rate reduced the average RP from -502 ± 45 mV at 0.7 vvm, to -532 ± 15 mV at 1.5 vvm, -548 ± 6 mV at 4.5 vvm and to -555 ± 12 mV at 7 vvm. Circulating the FG in the system increased the H_2 partial pressure and more reduced metabolites were generated to provide an electron sink. Also Yerushalmi et al. (Yerushalmi et al., 1985) report the increase the formation of more BuOH and EtOH in culture of *C. acetobutylicum,* when the H_2 partial pressure was enhanced. This effect can also be seen in the increased specific production rates of 1,3-PDO and ethanol (on the slight expense of BuOH) for sparging FG at higher flow rates (Fig. 4-28 C). The lower BuOH peak results from the slower biomass growth. Excluding the time aspect, the yield per biomass was enhanced for BuOH at FG sparging, compared to nitrogen sparging. With respect to acids formation, the same trend of enhanced production of butyrate and acetate with N_2 stripping, compared to FG can be found. E.g. butyrate productions were kept minimum at 0.04 g/(gh) ± 0.02, compared to 0.13 g/(gh) with N_2 stripping and reduced H_2 partial pressure. However, the final amounts of lactate were too low, to determine a production rate.

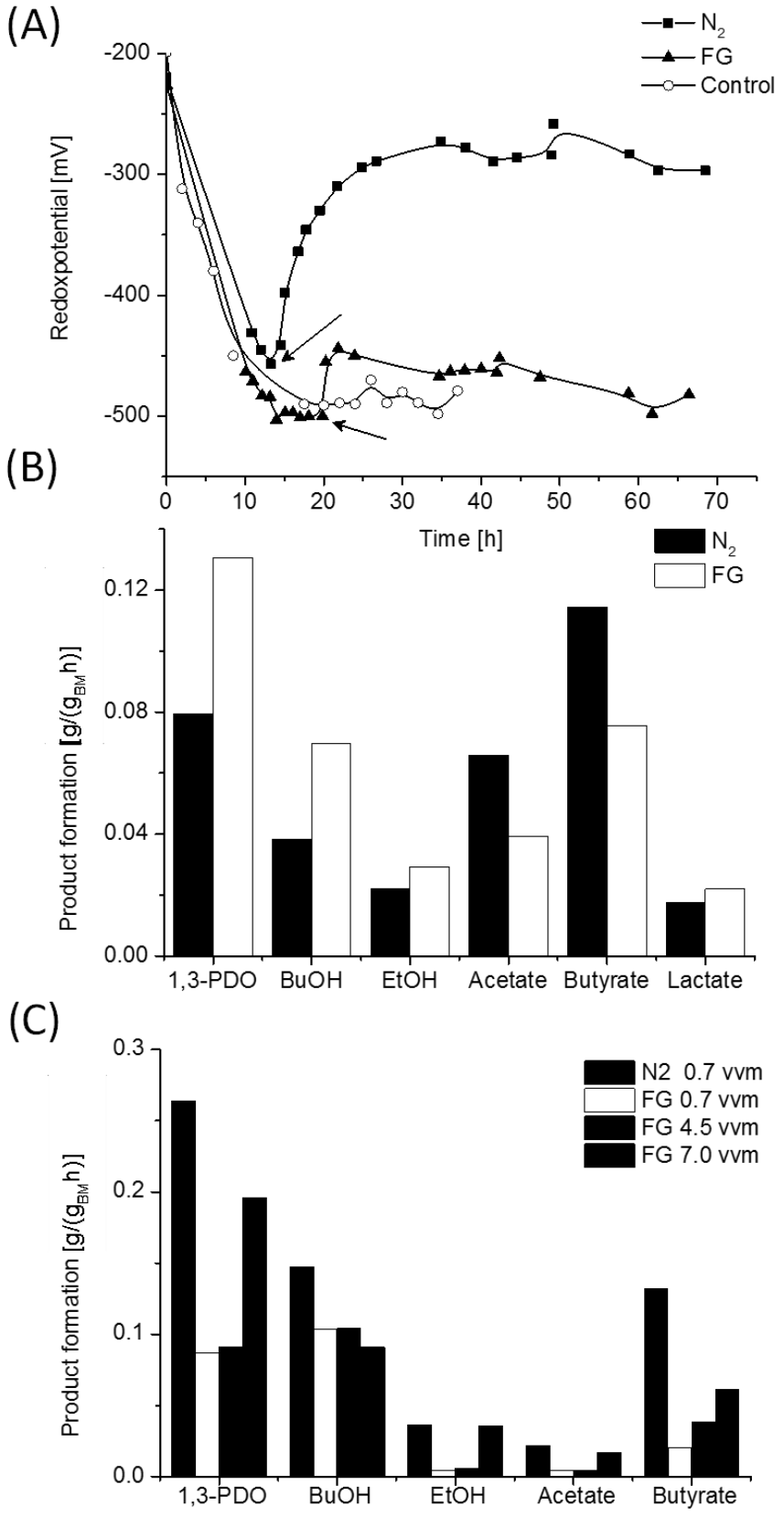

Fig. 4-28: (A) Redox potentials of fermentation broth for sparging with FG (CO_2 and H_2) or N_2, and for a control fermentation without gas stripping. Arrows indicate start of stripping. (B) Specific product formation rates of *C. pasteurianum* DSMZ 525 during growth on co-substrate and gas stripping with either N_2 (0.7 vvm) or FG (7 vvm). (C) Specific product formation rates during growth on glycerol and gas stripping with either N_2 (0.7 vvm) or FG with different circulating flow rates. (Figures from Groeger et al., 2016).

4.4.4 Gas stripping in cultivations with Brilliant Blue R 250 addition

As previously described (Chapter 4.3), the addition of Brilliant Blue R250 enhances the growth and the product formation. Therefore, an experiment with two times addition of BB and gas stripping with FG at 4.9 vvm was performed and compared with the fermentation without BB and a similar flow rate of 4.5 vvm.

The supplementation of the dye BB decreased the average RP of the fermentation broth to -558 mV, whereas without BB only -548 mV could be achieved. This demonstrates that the RP can be reduced with this dye in addition to gas stripping with FG. As shown in Fig. 4-29 the average biomass concentration in the stationary growth phase increased from 6.9 g/L (OD = 20.4) in the fermentation without BB, up to 7.8 g/L (OD = 23.1) in the experiment with BB. The final product concentration was enhanced from 26.4 g/L BuOH and 14.0 g/L 1,3-PDO (without BB) up to 32.5 g/L BuOH and 21.3 g/L 1,3-PDO (with BB). Accordingly, the BuOH stripping rates achieved were 0.38 g_{BuOH}/(Lh) and 0.54 g_{BuOH}/(Lh), without and with BB, respectively. The stripping rate is among the highest achieved in this work and only outperformed by 0.59 g_{BuOH}/(Lh), when the FG are sparged with 7 vvm. At the same time, and as discussed previously, the direction of carbon into acids was decreased, which can be clearly seen in the specific yields of acids per biomass (see Fig. 4-19, Chapter 4.3 and Table 4-7). In conclusion, the positive influence of the dye BB on enhanced growth and product formation can be further improved by the combination with *in situ* gas stripping.

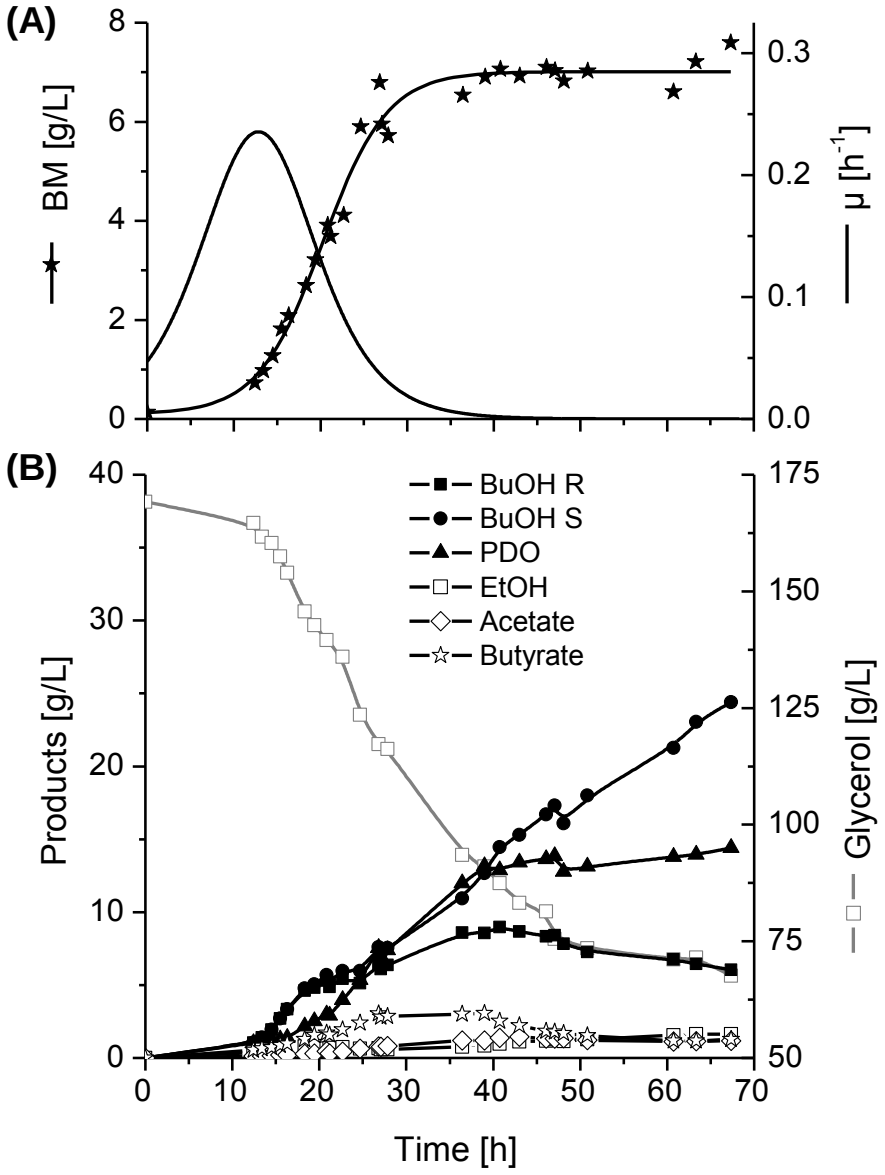

Fig. 4-29: (A) Growth as well as (B) substrate consumption and product formation in fermentations of *C. pasteurianum* without BB and gas stripping with 4.5 vvm FG. For glycerol cumulated consumed concentrations are shown. BuOH R and BuOH S refer to butanol concentrations in the bioreactor and the accumulated amounts from reactor and condensates, respectively.

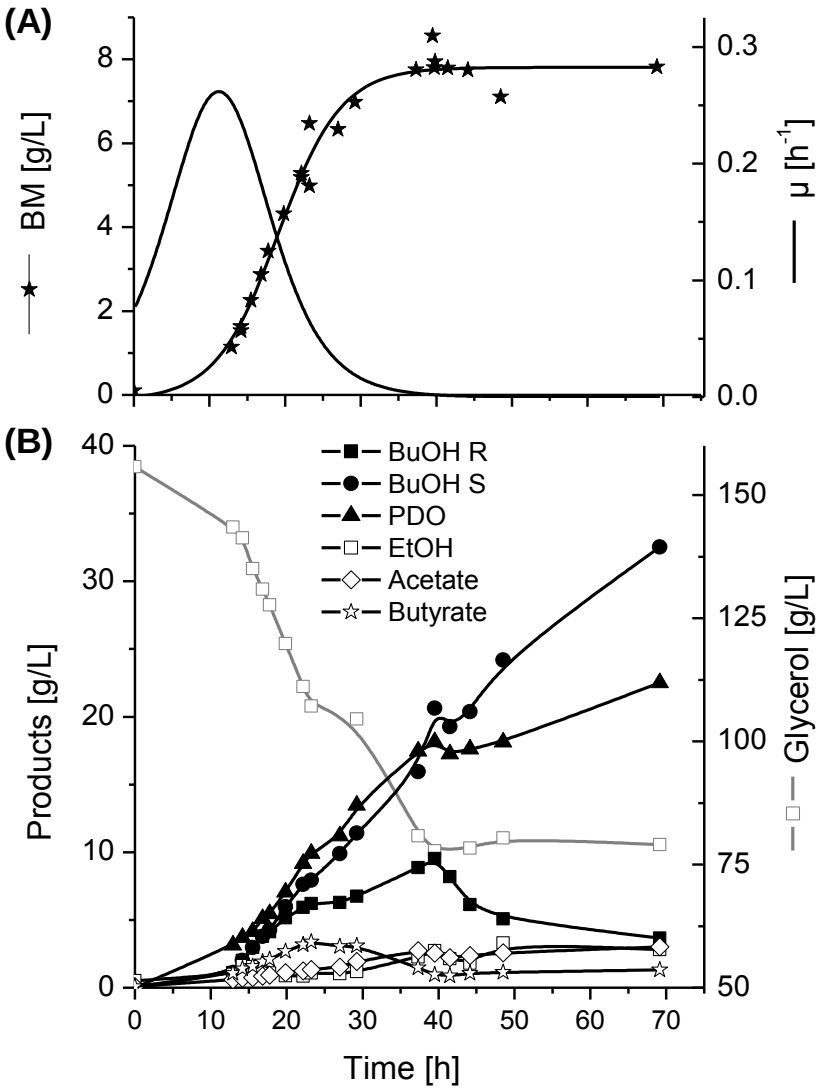

Fig. 4-30: (A) Growth as well as (B) substrate consumption and product formation in fermentations of *C. pasteurianum* with BB addition (at 22 h and 40 h) and gas stripping with 4.9 vvm FG. For glycerol cumulated consumed concentrations are shown. BuOH R and BuOH S refer to butanol concentrations in the bioreactor and the accumulated amounts from reactor and condensates, respectively.

4.4.5 Influences of stripping parameters on butanol stripping efficiency and selectivity

The condensates from gas stripping mainly contained water, BuOH and small amounts of EtOH. The resulting amount of each component is not only determined by the metabolic response of the organism, but also by the process setup and conditions of the gas stripping. This influences not only the mass transfer of BuOH, but also the selectivity of BuOH compared to other broth components.

Butanol mass transfer

An efficient gas stripping process depends on a high mass transfer rate of butanol between the liquid and gas phases, which can be characterized with the volumetric mass transfer coefficient K_Sa. According to the relation suggested by Truong and Blackburn (Eq. (2-2), Theory) the K_Sa in a stripping process is influenced by the volume of stripping gas, but also by the type of gas, temperature, and pressure (Truong and Blackburn, 1984). When *in situ* gas stripping is applied instead of end of pipe separation the temperature and pressure of fermentation cannot be varied due to the optimal growth conditions of *C. pasteurianum*. Another parameter not mentioned in this relation is the stirring speed that determines the gas bubble size and distribution. Therefore, the change of K_Sa at different stirrer speeds were studied on synthetic media, sparged with pure nitrogen at 1.6 vvm ([13]). The equation for the calculation of the K_Sa is given in Chapter 3.4.3 (Eq. (3-8)). As shown in Fig. 4-31 A, the highest K_Sa value was achieved at a relatively low stirring speed of 300 rpm and also a relatively high mass transfer rate was obtained even without stirring.

The results are supported by the study of Liao et al. (Liao et al., 2014) who described similar effects for butanol stripping from synthetic media. They reached the highest K_Sa at 0 rpm, the lowest values at 50 rpm and a further increase until 300 rpm. This effect can be explained by considering the velocity of the gas bubble in relation to the surrounding aqueous medium, which is called u_b [m/s]. Regarding the two-film theory for mass transfer, the boundary layer between the gas and liquid phases is thinner at higher bubble velocity, resulting in less resistance for phase transition of butanol. In the regimes of no stirring, u_b reaches its highest values at a given constant flow rate, which may facilitate the mass transfer. Stirring between 50 rpm and 300 rpm increases the K_Sa due to enhanced Reynolds number with accordingly higher turbulence, thinner boundary layer and thus better diffusion into the gas phase. However, no results for higher stirring rates than 300 rpm were reported in the study of Liao et al. (Liao et al., 2014). As shown within this work, a higher stirring rate resulted in a further decrease of the BuOH mass transfer. This leads to the assumption of increased influence by u_b, rather than the effect of turbulent flow. Increased stirring produces higher shear forces and consequently a reduction in bubbles size. On the one hand, this increases the interfacial area, but on the other hand, smaller bubbles exhibit smaller u_b, because they are more easily forced into the same direction as the liquid. This effect is known to further decrease the mass transfer (Yang et al., 2007). Therefore it can be concluded that higher stirring speeds should be avoided in an efficient gas stripping process. Considering large scale processes, fermentation without stirring positively affects the production and investment costs of a gas stripping process.

Additionally, synthetic medium was sparged with air at varying flow rates at a constant stirring rate of 550 rpm (see Groeger et al., 2016). Increasing flow rate significantly enhances the butanol mass transfer, due to the fact that quantitatively more gas can transport more BuOH from the reactor (see Eq. (2-3), Chapter 2.4.3). For example the raise from 2 vvm to 4 vvm increased the K_Sa from 0.027 h^{-1} to 0.048 h^{-1}, respectively. These values are in agreement with previous data reported by Ezeji et al. (Ezeji

[13] Determination of K_Sa values was performed in cooperation with M.Sc. Alberto Robazza in terms of his master thesis.

et al., 2005), who analyzed GS with N_2 in a synthetic model solution and achieved an increase of K_Sa from 0.024 h^{-1} to 0.059 h^{-1} by enhancing the flow rate from 2.6 vvm to 4.8 vvm. The results of the BuOH stripping rates for real glycerol fermentations with different flow rates of FG and stirrer speeds are given in Fig. 4-31 B. The maximum achieved concentrations in the reactor were between 9 g/L and 11 g/L BuOH in all fermentations. As expected, increasing the gas flow rates increased the amounts of stripped BuOH. Thus an efficient stripping process can be achieved with medium high flow rates of FG, but without or low stirring. In this sense, a bubble column bioreactor is believed be more suitable for BuOH stripping in a simultaneous production of both, BuOH and 1,3-PDO with gas stripping.

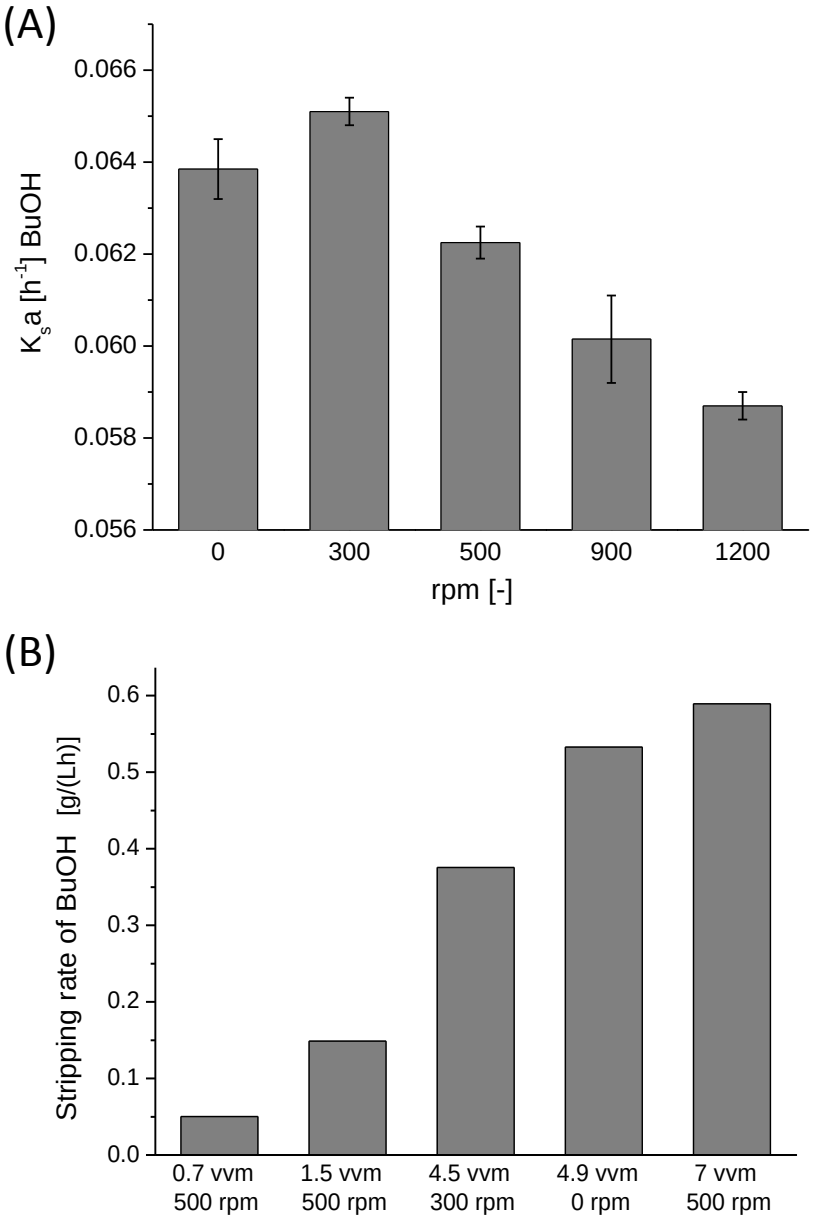

Fig. 4-31: (A) Volumetric mass transfer coefficient for BuOH (K_Sa values [h^{-1}]) from the bioreactor containing a synthetic medium sparged with 1.6 vvm pure N_2 at different stirrer speeds. (B) Stripping rate of BuOH [g/(Lh)] from glycerol fermentations at different flow rates and stirrer speeds. (Figure B partly from Groeger et al., 2016).

Butanol selectivity

Within the experiments using synthetic media it was observed that higher gas flow rates also resulted in higher average water fractions in the condensates. Sparging with FG at different flow rates increased the water fraction from 0.81 at 0.7 vvm, to 0.85 at 1.5 vvm and 4.5 vvm and to 0.92 at 7 vvm FG (Fig. 4-32 A). Comparable results were also reported by Xue et al. (Xue et al., 2014), who used GS on ABE production with immobilized *C. acetobutylicum.* But together with the water content also the BuOH content in the condensates is influenced. This can be expressed by the selectivity value α, which is a dimensionless value, showing the preferential recovery of BuOH over other fermentation broth components (Eq. (3-10), Chapter 3.4). Oudshoorn et al. (Oudshoorn et al., 2009) reported about BuOH selectivities between 4 and 22 that could be achieved in different gas stripping processes. In the current work, increasing the flow rate from 0.7 vvm to 1.5 vvm and 4.5 vvm enhanced the selectivity from 17.6 to 19.5 and 22.7, respectively (Fig. 4-33 A). Ezeji et al. (Ezeji et al., 2004) achieved in an ABE fed-batch fermentation with gas stripping by FG at 6 vvm, BuOH selectivities of 10-22, which are in the range of the obtained results in this study. However, in this paper a further increase to 7 vvm FG resulted in a reduced selectivity of 9.9 (Fig. 4-33 A). A similar effect was reported by Xue et al. (Xue et al., 2014), who found the highest BuOH selectivities from a model solution to be 18.8 at 3.2 vvm, followed by a decrease to 13.2 at 12.8 vvm. This might be explained by the fact that an increased flow rate enhances superficial velocities as well as u_b and subsequently more water was stripped out as well. The Henry´s coefficients k_{Hij}^{px} for water evaporating into the gas phases of N_2, CO_2, and H_2, are a magnitude higher than that of butanol (see Table 2-4, Theory), thus the mass transfer occurs faster. But even though the water content is enhanced, the higher flow rates were necessary in a fermentation process to keep the butanol amount at a non-inhibiting level and hence support further growth and productivity. On the other hand, increased water contents required a relatively higher energy input for the final purification. For large scale processes, the optimized flow rate with high BuOH yields but low water content must be determined. The water content in the condensates could be further decreased by lowering the temperature in the condenser. Experiments with synthetic media, sparged with air at 5 vvm, and varying cooling temperature in the condenser showed a decrease of the water weight fraction from 0.96 at 10°C, to 0.94 at 5°C and 0.88 at 0°C respectively. However, a lower condenser temperature required also a higher energy input and a reduction in cooling temperature is only feasible if this input is below the higher energy demand for water distillation.

One major aspect analyzed in this work is the influence of gas type utilized for the gas stripping. But the usage of either FG or N_2 not only interacts with the bacteria metabolism, it also determines the stripping efficiency. Comparing both gases at 0.7 vvm, the BuOH weight fraction in the condensates reached 0.18 and a selectivity α = 17.6 for FG gases, but only 0.1 and α =11.3 for N_2. The same was observed for the co-substrate fermentations: 0.06 and α = 13.2 with FG as well as 0.02 and α = 6.3 with N_2, even though the flow rate was strongly enhanced at FG sparging. This indicates that not only the flow rates determine the BuOH fraction, but also the gas type used for stripping. Previous gas analysis of *C. pasteurianum,* under standard conditions grown on glycerol, showed that the FG was composed of up to ~60 mol% H_2 and ~40 mol% CO_2 (see Chapter 4.1). The combined Henry´s coefficient for this composition of FG results in k_{Hij}^{px} [FG-BuOH] = $2.3*10^8$ Pa, which is higher than that for pure nitrogen

with k_{Hij}^{px} [N_2-BuOH] = 2.1*10^8 Pa. Sparging a synthetic fermentation broth with different gases resulted in higher K_Sa values for synthetic FG (with 60 mol% H_2 and 40 mol% CO_2), compared to N_2 (Fig. 4-32 B). Similar results were found for the Henry coefficients of EtOH: k_{Hij}^{px} [FG-EtOH] = 3.2*10^8 Pa and k_{Hij}^{px} [N_2-EtOH] = 2.8*10^8 Pa. The values are slightly higher than for BuOH and indeed this results in higher K_Sa values for EtOH compared to BuOH (Fig. 4-32 B), but also higher K_Sa values and higher weight fractions of EtOH achieved with (synthetic) FG, compared to N_2. For example, the weight fractions achieved in the condensates with FG sparging reached 0.008, compared to 0.005 at N_2 sparging, both at the same flow rate of 0.7 vvm. However, the condensates from real fermentations and independent of the flow rate showed a relatively low EtOH fractions (Fig. 4-32 A), which can be explained by the anyway low EtOH concentration in the broth (Table 4-7). The Henry coefficient for water, which are k_{Hij}^{px} [FG-H_2O] = 4.4*10^9 Pa and k_{Hij}^{px} [N_2-H_2O] = 8.9*10^9 Pa, indicates that FG with such high H_2 content not only outperforms N_2 in economic aspects, but also offers the advantages of higher selectivity for BuOH and lower one for H_2O. Indeed, comparing the condensates of both fermentations at 0.7 vvm stripping, the water content is higher for N_2 sparging, compared to FG (Fig. 4-32 A).

Xue et al. (Xue et al., 2012) reported that for an efficient GS with high BuOH amounts in the condensates a minimum BuOH concentration of 8 g/L in the fermentation broth of *C. acetobutylicum* was necessary. As observed in the performed studies herein, the stripping rate as a function of butanol concentration in the broth was dependent on the flow rates. Fig. 4-33 B shows the FG stripping at 4.5 vvm. At first a constant stripping rate of 0.11 g/(Lh) was reached, which suddenly changed to 0.51 g/(Lh). At this time point also the BuOH weight fraction in the condensates increases and two phases were formed. At this time the critical BuOH titer in the broth was 8.6 g/L, abbreviated as $BuOH_{crit}$. The dependency of $BuOH_{crit}$ on the flow rate is shown in Fig. 4-33 A, it decreased with increasing flow rate. For an optimized GS process $BuOH_{crit}$ for a given flow rate should be determined in advance and sparging should not start before this value is reached, but preferable below or around 5 g/L to avoid inhibition of the bacteria.

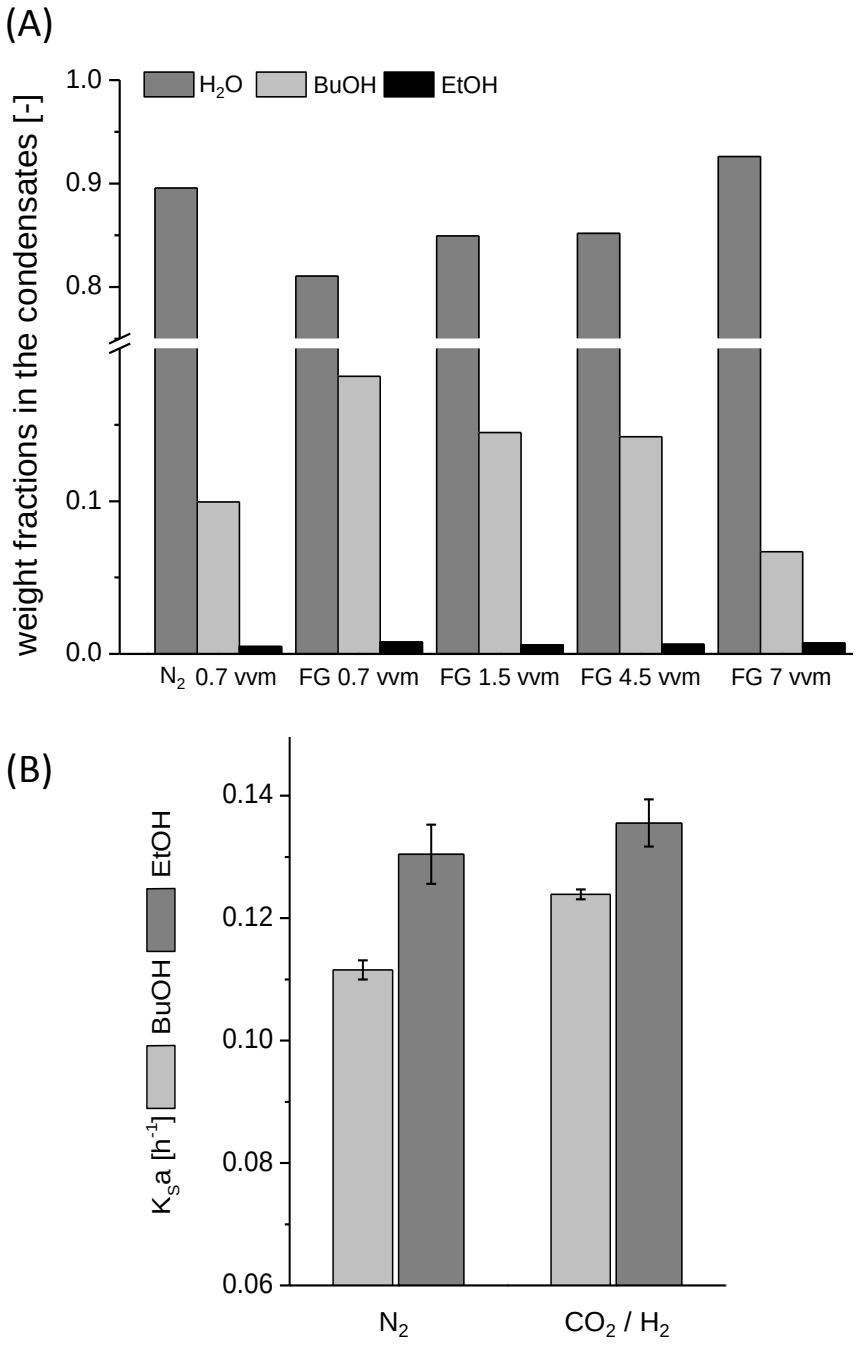

Fig. 4-32: (A) Weight fractions of water, BuOH and EtOH in the condensates of fermentations sparged with N_2 or FG at different flow rates. (B) K_Sa values [h^{-1}] for BuOH and EtOH from synthetic medium and for sparging with N_2 or CO_2/H_2 (synthetic FG) at 2.9 vvm and 300 rpm.

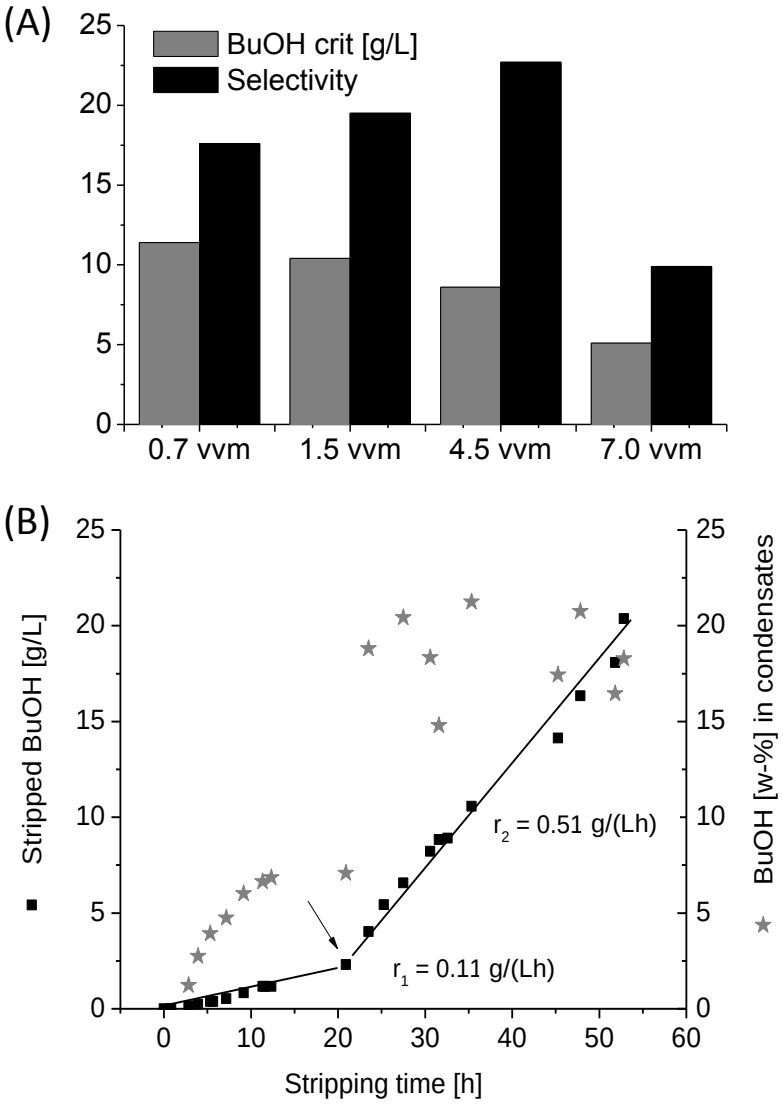

Fig. 4-33: (A) Critical BuOH concentration in reactor ($BuOH_{crit}$), and selectivities of BuOH in the condensates for glycerol fermentation of *C. pasteurianum* DSMZ 525 with different FG flow rates. (B) Accumulated stripped BuOH amounts and BuOH mass fraction in the condensates for FG stripping at 4.5 vvm. The arrow indicates the time point, when the stripping rate changes. (Figures from Groeger et al., 2016).

4.4.6 Comparison to other studies

Several studies showed that the removal of BuOH by gas stripping clearly enhanced the growth, the final BuOH titer and yield in comparison to fermentations without stripping (Jensen et al., 2012a), (Xue et al., 2012), (Ezeji et al., 2004), (Vrije et al., 2013). Xue et al. (Xue et al., 2012) analyzed the effect of circulating FG at 5 vvm on ABE fermentation by an immobilized *C. acetobutylicum* mutant strain with glucose as substrate. They reported a BuOH productivity of 0.35 g/(Lh) with a yield of 0.36 g_{ABE} / $g_{glucose}$ (Xue et al., 2012). Similarly, using *C. beijerinckii* culture stripped with FG at 6 vvm, Ezeji et al. (Ezeji et al., 2004) recorded a BuOH productivity of 0.75 g/(Lh) with a yield of 0.3 g_{BuOH} / $g_{glucose}$. However, not

only BUOH formation is influenced by GS, because *C. pasteurianum* produces also 1,3-PDO. In fact, the value obtained from the immobilized cultures of *C. acetobutylicum* by Xue et al. (Xue et al., 2012) was comparable to the results reported here, but with free, non-immobilized culture at 4.5 vvm (BuOH productivity of 0.38 g/(Lh) and product yield of 0.34 $g_{BuOH+PDO}$ / $g_{glycerol}$). Increasing the flow rate to 7 vvm even further increased the BuOH productivity to 0.59 g/(Lh) and enhanced the yield of both products to 0.43 $g_{BuOH+PDO}$ / $g_{glycerol}$. Groot et al. (Groot et al., 1989) used a strip column with 10 L/min N_2 over 0.3 L/h broth of *C. saccharoperbutylacetonicum* DSMZ 2152, which produces the solvents isopropanol, BuOH and EtOH (IBE) from glucose. Even though a high flow rate is applied, the batch fermentation resulted in a low BuOH productivity of 0.11 - 0.18 g/(Lh), with a yield of 0.34 g_{IBE} /$g_{glucose}$.

Table 4-7: Carbon recovery and final product concentrations in fermentations of pure glycerol or of co-substrate (Co) using *C. pasteurianum* DSMZ 525 with gas stripping at different flow rates. (Table partly from Groeger et al., 2016).

Experiment	Carbon Recovery [%]	BuOH [g/L]	1,3-PDO [g/L]	EtOH [g/L]	Butyrate [g/L]	Acetate [g/L]	Lactate [g/L]
N_2 0.7 vvm	99	18.9	49.6	3.2	7.3	4.9	0.3
FG 0.7 vvm	95	12.5	10.9	1.4	1.2	1.1	0.1
FG 1.5 vvm	96	12.6	13.2	1.3	1.2	1.3	0.3
FG 4.5 vvm	95	26.4	14.0	1.6	1.1	1.0	0.2
FG 4.9 vvm 2xBB	96	32.5	21.3	6.3	1.3	3.0	0.5
FG 7.0 vvm	99	39.2	53.7	4.5	2.4	4.3	0.5
N_2 0.7 vvm (Co)	97	6.8	14.9	1.1	15.9	6.2	3.0
FG 7.0 vvm (Co)	96	12.2	24.1	5.8	8.4	6.6	5.0
FG 6.3 vvm (CoBH)	N*	5.6	1.0	2.0	17.8	10	0.4

N* cannot be calculated due to unknown biomass amounts, because of the high turbidity of biomass hydrolysates (BH)

4.4.7 Conclusion

The simultaneous production of both, 1,3-PDO and BuOH in one single process represents an advantage for the use of *C. pasteurianum* DMS 525. The concentration of both products obtained using gas stripping with FG is among the highest reported for this strain, with 53.7 g/L 1,3-PDO and 39.2 g/L BuOH. Considering large scale processes, the usage of FG instead of N_2 represents a reduction in investment cost; however, high flow rates are necessary to keep the BuOH concentration in the broth below an inhibiting level. The final titer and yield of both target products could be further improved by the supplementation of the Brilliant Blue in combination with gas stripping by FG. Additionally it could be shown that low stirrer speeds or even no stirring increases the BuOH mass transfer and that FG with high H_2 content show a higher selectivity in BuOH, a reduced water fraction in the condensates and positive influence on the redox conditions, compared to nitrogen.

5 Summary and outlook

Biofuels and biochemicals produced from renewable resources represent an attractive alternative to fossil-based products. The anaerobic bacterium *C. pasteurianum* can produce two important bulk chemicals, *n*-butanol and 1,3-propanediol from glycerol as well as from glucose, which makes it an interesting candidate for biorefinery processes. Within this work different process parameters that influence the metabolism of *C. pasteurianum* were investigated to enhance the simultaneous production of both target products.

At first the effect of glycerol and glucose on growth and product formation was analyzed. Using glucose as the sole carbon source, this bacterium exhibit two typical phases, acidogenesis followed by solventogenesis. Despite the favored acid and biomass production, the low final BuOH titer and the absence of a natural 1,3-PDO synthesis pathway from glucose exclude this substrate as sole carbon source for a simultaneous production process. In comparison, using the more reduced substrate glycerol as sole substrate and despite of the lower biomass formation (maximum biomass of 5.1 g/L with glycerol, compared to 13.7 g/L with glucose), *C. pasteurianum* tends to produce less acids and higher quantities of both BuOH and 1,3-PDO. The suitability of glucose as co-substrate to glycerol was analyzed to find the best combination of both carbon sources for the two biomass formations and productivity of solvents. It was found that increased glucose amounts in the media strongly enhanced the growth as well as the formation of acids. Due to the fact that no natural pathway exists for the formation of 1,3-PDO from glucose, its final titer decreased with increasing glucose content. On the contrary, the highest BuOH titer of 21 g/L could be achieved with a weight ratio of 50 % glucose and 50 % glycerol in the media. Similar results were reproduced using biomass hydrolysates from spruce as glucose source. Lower glucose contents (20 % - 40 %) favor the simultaneous production of both target products. Because of that the co–substrate fermentation was further analyzed in a pilot facility with 2 m³ working volume and under uncontrolled and unsterile conditions. There it was shown that using 20 % glucose and 80 % raw glycerol resulted in 18 g/L 1,3-PDO and 13 g/L BuOH. These results even exceed the values of a standard fermentation with pure glycerol in lab scale, but at the expense of a slower productivity (Fig. 5-1 A). In general, with co-substrate fermentation, more acids are produced and thus the substrate yields of both products were significantly lower, compared to the usage of sole glycerol as a substrate (Fig. 5-1 B).

As shown above, with glycerol as the only carbon source, the two main products of *C. pasteurianum* were BuOH and 1,3-PDO. But the relative formation of either product is known to be influenced significantly by the availability of iron in the medium. Several iron containing enzymes play key roles in the maintenance of intracellular redox balance and a limited functionality of them, e.g. due to iron limitation, has to be reflected by a metabolic shift. It was found that 1,3-PDO is most effectively produced under iron limited condition (Fe-), whereas 1,3-PDO and BuOH were both produced under iron rich condition (Fe+), accompanied with an enhanced hydrogen formation. Proteomic analysis revealed an up-regulated expression at Fe+ for of pyruvate:ferredoxin oxidoreductase (PFOR), hydrogenase, electron transfer flavoproteins and bifunctional acetaldehyde-CoA/alcohol dehydrogenase, among others. These proteins were found to be central in the *C. pasteurianum* metabolism and affect the redox status of the cell significantly. For example, in the conversion step from pyruvate to acetyl-CoA, two PFORs were up-regulated at Fe+, whereas a pyruvate formate lyase (PFL) was up-regulated under Fe- conditions, which is also reflected in an enhanced formate production rate.

Furthermore, analyzing the redox balance of different fermentations, it was found that molecular hydrogen biosynthesis, coupled to the reaction step from pyruvate to acetyl-CoA (catalyzed by PFORs), is not the only source for its synthesis. A recently reported H_2 formation route (Buckel and Thauer, 2013), which is coupled to the pathway step of crotonyl-CoA conversion to butyryl-CoA, also contributes to the totally produced H_2 amount. This reaction is catalyzed by the oxidized ferredoxin (Fd_{ox}) dependent butyryl-CoA dehydrogenase / electron transfer flavoprotein complex (BCdH-ETF). Proteomic analysis showed the up-regulation of two electron transfer flavoprotein subunits, which are involved in this step. The importance of hydrogenase in the regeneration of Fd_{ox} from Fd_{red} for maintenance of the internal redox balance was confirmed by its strong up-regulation under Fe+ condition. On the contrary, under Fe- condition, Fd_{ox} regeneration and Fd_{ox} dependent conversion steps by PFORs were reduced and the resulting free reducing power, usually needed for butanol formation, could be redirected to the production of 1,3-PDO and lactate. This is also reflected in the highest substrate yield for 1,3-PDO, namely 0.33 g/g, compared to all other conditions tested (Fig. 5-1 B). Due to limited growth at Fe-, the final amount of both products, as well the productivity, are significantly reduced (Fig. 5-1 A).

Since the intracellular redox balance is correlated to the external redox conditions of the media, the effect of redox manipulation was also studied. The addition of redox active mediators and/or the cultivation in electro-bioreactors equipped with electrodes have been investigated. It was shown that the supplementation of the cheap, non-toxic dye Brilliant Blue R250 (BB) enhanced the growth of *C. pasteurianum.* Beside growth, the optimized concentration of 0.06 g/L BB, led to increased titers of both target products, BuOH and 1,3-PDO. At the same time the redirection of carbon atoms into organic acids decreased significantly with BB addition. The highest product yield of 0.44 $g_{BuOH+PDO}$/g was achieved with the two times addition of BB compared to 0.38 g/g in the control experiment without BB addition in batch fermentation (Fig. 5-1 B). The molecular effect of BB on the metabolism still needs further examination to be clarified. The regeneration of BB as mediator was also tested in electro-bioreactors and it could be shown that BB was recharged at an applied potential of +500 mV, which led to the highest substrate yield of 0.36 $g_{BuOH+PDO}$/g, compared to fermentations with BB and negative potentials as well as with no applied potential. Nevertheless, experiments performed in electro-bioreactors showed no significant influence on growth and product formation for the applied potentials of -500 mV, -300 mV, and +500 mV (all vs. Ag/AgCl), in comparison to fermentations with no applied potential.

In all the experiments above, growth inhibition by BuOH was the main bottleneck for further process optimization. To overcome such a drawback and to simultaneously separate BuOH from the fermentation broth, *in situ* gas stripping was implemented into the fermentation process. Gas stripping with external nitrogen increased the redox potential of the culture and significantly enhanced the production of acids. On the contrary, the circulation of the fermentation gases (H_2 and CO_2) maintained a lower redox potential, what had positive influence on the formation of more reduced products like 1,3-PDO. A relatively high flow rate of FG is required to maintain a low BuOH level in the culture and ensure a high BuOH stripping rate. Applying gas stripping in co-substrate fermentation with glycerol and glucose is not recommendable, due to a strongly increased acid formation. A further optimization of process economics could be achieved by lowering the power input for stirring. Experiments with synthetic medium revealed that the highest recorded mass transfer rates of BuOH (K_Sa) were achieved at 300 rpm or even in non-stirred synthetic media. Additionally it was shown, that FG with 60 % H_2 content exhibited a higher selectivity in BuOH, a reduced water fraction in the condensates and a

positive influence on the redox conditions for the formation of both reduced target products on the expense of acid formation, compared to N_2. In Fig. 5-1 A and B it can be seen that the most effective increase in the simultaneous production of BuOH and 1,3-PDO can be achieved by the implementation of gas stripping with FG at high flow rates. In summary, under the best conditions tested 39 g/L BuOH and 53 g/L 1,3-PDO with a high productivity and a high yield were simultaneously produced from pure glycerol as a substrate and with a flow rate of 7 vvm FG.

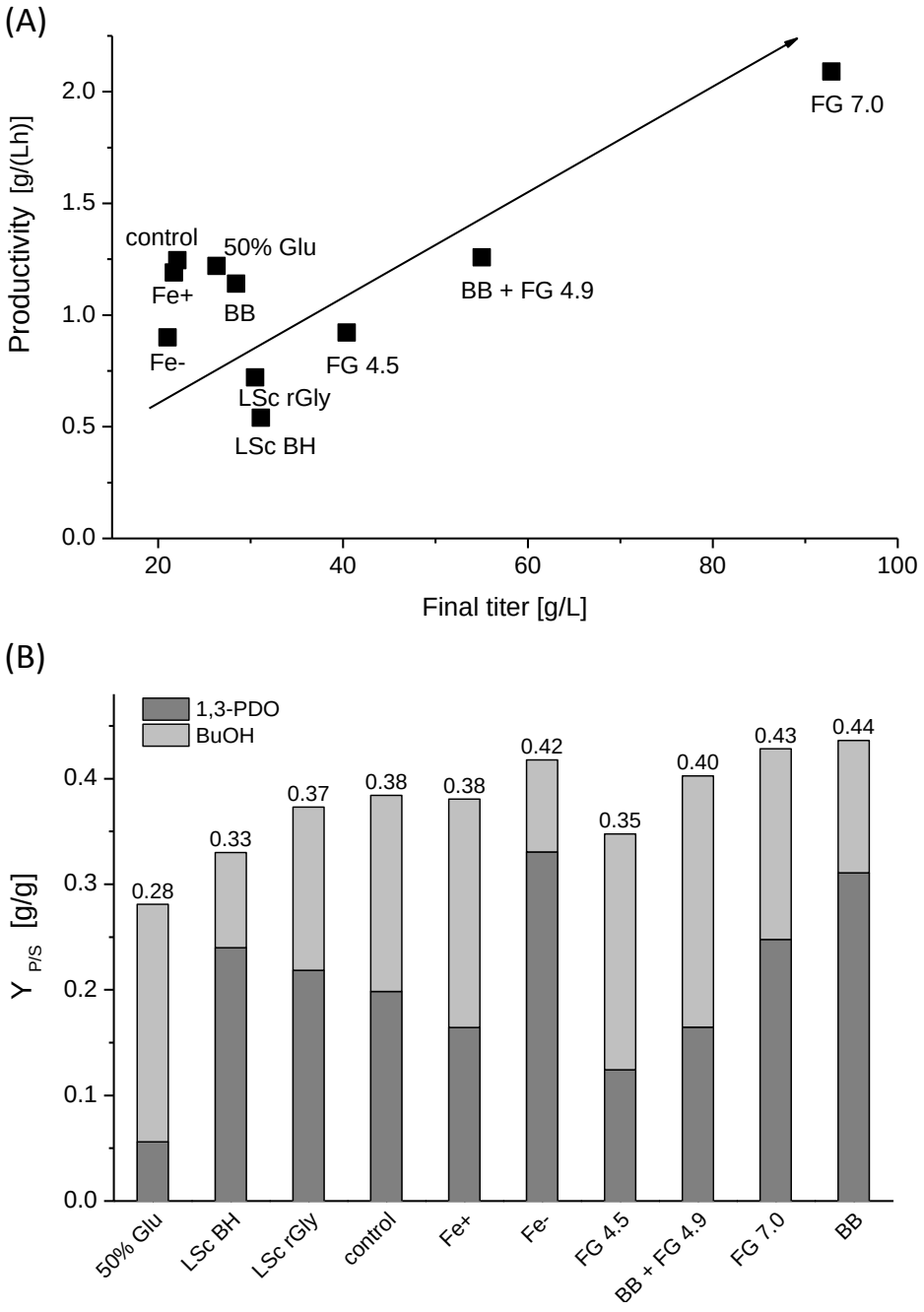

Fig. 5-1: (A) Final titer and productivity as well as (B) substrate yield of both products, BuOH and 1,3-PDO, either per glycerol or per glycerol+glucose, produced by *C. pasteurianum* DSMZ 525 during fermentation under different conditions: 50 % Glu = co-fermentation with 50 % glucose + 50 % glycerol, LSc BH = large scale with biomass hydrolysates, LSc rGly = large scale with raw glycerol, control = standard conditions, Fe+ = iron excess, Fe- = iron limitation, FG 4.5 = gas stripping with 4.5 vvm fermentation gases, BB+FG 4.9 = addition of Brilliant Blue

R250 and gas stripping with 4.9 vvm fermentation gases, FG 7.0 = gas stripping with 7.0 vvm fermentation gases, BB = batch fermentation with addition of Brilliant Blue R250.

For further process optimization, combinations of some of the studied parameters are recommended. Taking also into account a high substrate yield, the connection of gas stripping and addition of BB has a great potential to enhance the process performance. As Fig. 5-1 A shows, the small increase in flow rate from 4.5 vvm to 4.9 vvm, in combination with BB addition increased the product titer of both, BuOH and 1,3-PDO, by 36 % and the productivity by 37 %. The effect of BB in co-substrate fermentation has to be evaluated, due to the fact that glucose increases growth and BuOH titer, but also acid production, whereas Brilliant Blue R250 significantly decreases the formation of acids and thus limits the waste of the carbon source. In general the suitability of other cheap and non-toxic mediators might lead to new results, like recently reported for a new isolate of *C. acetobutylicum*, which exhibited an increased BuOH formation, when Neutral Red was added (Jiang et al., 2016). Still, the conversion of artificially added electrons by *C. pasteurianum* in electro-bioreactors needs to be clarified and demands further experiments with lower potentials, preferable around –1 V as suggested by Khosravanipour Mostafazadeh et al. (2016).

Besides media optimization or technical applications, genetic and metabolic engineering is one possibility to further increase the BuOH and 1,3-PDO formation (Sarchami et al., 2016b), (Branduardi et al., 2014), (Wischral et al., 2016). Though, it should be kept in mind that enhanced BuOH titers require either (I) a higher tolerance by the *clostridium* strain or (II) *in situ* removal of the inhibitory solvent. The intolerance is mostly caused by increased membrane fluidity at higher solvent concentrations (Venkataramanan et al., 2014). First proceedings have been made by systematic strain adaption (Liu et al., 2013b) or microbial engineering (Jones et al., 2016). Also the development of tolerant strains against raw substrates with impurities and toxic compounds is advantageous for sustainable biorefinery processes and are clearly less cost intensive than pre-treatment of the substrate (Jensen et al., 2012b).

However, as shown in this work, the highest effect on process performance can be achieved by including BuOH removal into the fermentation process. Among other downstream processing methods, gas stripping is one of the techniques with a relatively high energy demand, yet it still offers potential for process optimization. Considering this, the cooling conditions, i.e. compression of the effluent gas loaded with high amounts of water, will have the strongest impact on operational costs. The implementation of a two-stage condenser has the advantage that at first a large amount of water is separated and in the second stage more and higher concentrated BuOH is received. Also the combination of gas stripping and subsequent pervaporative treatment of the condensates could further reduce the energy demands (Xue et al., 2016). Alternatively Friedl et al. (Friedl and Sauer, 2016) suggests an *in line* separation instead of *in situ* applications. *In line* set-ups consist of an external by-pass loop next to the reactor, which allows an individual optimization of downstream processes like extraction, pervaporation, flash vaporization or reverse osmosis, without affecting the cultivation conditions. Even though some of these processes themselves exhibit a lower energy demand for BuOH separation compared to gas stripping, their positive effect on culture conditions and thus enhanced product formation is limited, especially with an *in line* set up. Recently, a study was performed to determine a sustainable ABE biorefinery process by comparing several downstream methods like gas stripping, liquid-liquid extraction and pervaporation. Altogether it was shown that gas stripping gave the most positive influence on product formation – as also shown in this study - and irrespective of the

slightly higher operationally costs, the application of gas stripping resulted in the lowest final prices for BuOH and thus represents the optimal choice for a biorefinery process (Belletante et al., 2016).

6 References

Abbad-Andaloussi S, Durr C, Raval G, Petitdemange H (1996): Carbon and electron flow in *Clostridium butyricum* grown in chemostat culture on glycerol and on glucose. Microbiology 142: 1149–1158.

Abdelradi F, Serra T (2015): Food–energy nexus in Europe: Price volatility approach. Energy Economics 48: 157–167.

Adams MW, Eccleston E, Howard JB (1989): Iron-sulfur clusters of hydrogenase I and hydrogenase II of *Clostridium pasteurianum*. Proceedings of the National Academy of Sciences 86: 4932–4936.

Andrade JC, Vasconcelos I (2003): Continuous cultures of *Clostridium acetobutylicum*: culture stability and low-grade glycerol utilisation. Biotechnology Letters 25: 121–125.

Asad-ur-Rehman, Wijesekara R. G S, Nomura N, Sato S, Matsumura M (2008): Pre-treatment and utilization of raw glycerol from sunflower oil biodiesel for growth and 1,3-propanediol production by *Clostridium butyricum*. Journal of Chemical Technology & Biotechnology 83: 1072–1080.

Ávila M, Gómez-Torres N, Hernández M, Garde S (2014): Inhibitory activity of reuterin, nisin, lysozyme and nitrite against vegetative cells and spores of dairy-related *Clostridium* species. International Journal of Food Microbiology 172: 70–75.

Barski P, Kowalczyk J, Lindstaedt A, Puzewicz-Barska J, Witt D (2012): Evaluation of solid phase extraction for downstream separation of propane-1,3-diol and butan-1-ol from fermentation broth. Process Biochemistry 47: 1005–1010.

Becerra M, Cerdán ME, González-Siso MI (2015): Biobutanol from cheese whey. Microbial Cell Factories 14: 1525.

Belletante S, Montastruc L, Negny S, Domenech S (2016): Optimal design of an efficient, profitable and sustainable biorefinery producing acetone, butanol and ethanol: Influence of the *in-situ* separation on the purification structure. Biochemical Engineering Journal 116: 195–209.

Bennett BD, Kimball EH, Gao M, Osterhout R, Van Dien, Stephen J, Rabinowitz JD (2009): Absolute metabolite concentrations and implied enzyme active site occupancy in *Escherichia coli*. Nature Chemical Biology 5: 593–599.

Biebl H (2001): Fermentation of glycerol by *Clostridium pasteurianum* — batch and continuous culture studies. Journal of Industrial Microbiology & Biotechnology 27: 18–26.

Biebl H, Marten S (1995): Fermentation of glycerol to 1,3-propanediol: use of cosubstrates. Applied Microbioly & Biotechnology 44: 15–19.

Biebl H, Zeng AP, Deckwer W (1999): Microbial production of 1,3-propanediol. Applied Microbiology & Biotechnology: 289–297.

Borisov IL, Malakhov AO, Khotimsky VS, Litvinova EG, Finkelshtein ES, Ushakov NV, Volkov VV (2014): Novel PTMSP-based membranes containing elastomeric fillers: Enhanced 1-butanol/water pervaporation selectivity and permeability. Journal of Membrane Science 466: 322–330.

Branduardi P, Ferra F de, **Longo V, Porro D (2014):** Microbial *n*-butanol production from *Clostridia* to non-*Clostridial* hosts. Engineering in Life Sciences 14: 16–26.

Buckel W, Thauer RK (2013): Energy conservation via electron bifurcating ferredoxin reduction and proton/Na+ translocating ferredoxin oxidation. Biochimica et Biophysica Acta (BBA)-Bioenergetics 1827: 94–113.

Calusinska M, Happe T, Joris B, Wilmotte A (2010): The surprising diversity of *clostridial* hydrogenases: a comparative genomic perspective. Microbiology 156: 1575–1588.

Charon M, Volbeda A, Chabriere E, Pieulle L, Fontecilla-Camps JC (1999): Structure and electron transfer mechanism of pyruvate: ferredoxin oxidoreductase. Current opinion in structural biology 9: 663–669.

Chatzifragkou A, Papanikolaou S (2012): Effect of impurities in biodiesel-derived waste glycerol on the performance and feasibility of biotechnological processes. Applied Microbiology & Biotechnology 95: 13–27.

Chatzifragkou A, Papanikolaou S, Dietz D, Doulgeraki AI, Nychas GE, Zeng A (2011): Production of 1,3-propanediol by *Clostridium butyricum* growing on biodiesel-derived crude glycerol through a non-sterilized fermentation process. Applied Microbiology & Biotechnology 91: 101–112.

Chauvel A, Marshall N, Lefebvre G (1989): Petrochemical processes. Technical and economic characteristics. Editions Technip, 2nd ed, Paris, France.

Chen C, Xiao Z, Tang X, Cui H, Zhang J, Li W, Ying C (2013): Acetone–butanol–ethanol fermentation in a continuous and closed-circulating fermentation system with PDMS membrane bioreactor. Bioresource Technology 128: 246–251.

Chen X, Jiang S, Zheng Z, Pan L, Luo S (2012): Effects of culture redox potential on succinic acid production by *Corynebacterium crenatum* under anaerobic conditions. Process Biochemistry 47: 1250–1255.

Choi O, Kim T, Woo HM, Um Y (2014): Electricity-driven metabolic shift through direct electron uptake by electroactive heterotroph *Clostridium pasteurianum*. Scientific reports 4: 6961.

Choi Y, Kim N, Kim S, Jung S (2003): Dynamic Behaviors of Redox Mediators within the Hydrophobic Layers as an Important Factor for Effective Microbial Fuel Cell Operation. Bulletin of the Korean Chemical Society 24: 437–440.

Ciriminna R, Della Pina C, Rossi M, Pagliaro M (2014): Understanding the glycerol market. European Journal of Lipid Science Technology 116: 1432–1439.

Clomburg JM, Gonzalez R (2013): Anaerobic fermentation of glycerol: a platform for renewable fuels and chemicals. Trends in Biotechnology 31: 20–28.

Dabrock B, Bahl H, Gottschalk G (1992): Parameters Affecting Solvent Production by *Clostridium pasteurianum*. Applied and Environmental Microbiology 58: 1233–1239.

Dhamole PB, Wang Z, Liu Y, Wang B, Feng H (2012): Extractive fermentation with non-ionic surfactants to enhance butanol production. Biomass and Bioenergy 40: 112–119.

Dietz D, Zeng A (2014): Efficient production of 1, 3-propanediol from fermentation of crude glycerol with mixed cultures in a simple medium. Bioprocess and Biosystems Engineering 37: 225–233.

Dooley KM, Cain AW, Knopf FC (1997): Supercritical fluid extraction of acetic acid, alcohols and other amphiphiles from acid-water mixtures. The Journal of Supercritical Fluids 11: 81–89.

Drożdżyńska A, Leja K, Czaczyk K (2011): Biotechnological Production of 1,3-Propanediol from Crude Glycerol. Journal of Biotechnology, Computational Biology and Bionanotechnology 92: 92–100.

Dubey V, Saxena C, Singh L, Ramana KV, Chauhan RS (2002): Pervaporation of binary water–ethanol mixtures through bacterial cellulose membrane. Separation and Purification Technology 27: 163–171.

Dürre P (2007): Biobutanol: An attractive biofuel. Biotechnology Journal 2: 1525–1534.

Elvers B, Wagemann K (2014): Herstellung von Grundchemikalien auf Basis nachwachsender Rohstoffe als Alternative zur Petrochemie? Chemie Ingenieur Technik 86: 2115–2134.

Evans PJ, Wang HY (1988): Enhancement of Butanol Formation by *Clostridium acetobutylicum* in the Presence of Decanol-Oleyl Alcohol Mixed Extractants. Applied and Environmental Microbiology 54: 1662–1667.

Ezeji TC, Karcher PM, Qureshi N, Blaschek HP (2005): Improving performance of a gas stripping-based recovery system to remove butanol from *Clostridium beijerinckii* fermentation. Bioprocess and Biosystems Engineering 27: 207–214.

Ezeji TC, Qureshi N, Blaschek HP (2003): Production of acetone, butanol and ethanol by *Clostridium beijerinckii* BA101 and *in situ* recovery by gas stripping. World Journal of Microbiology and Biotechnology 19: 595–603.

Ezeji TC, Qureshi N, Blaschek HP (2004): Acetone butanol ethanol (ABE) production from concentrated substrate: reduction in substrate inhibition by fed-batch technique and product inhibition by gas stripping. Applied Microbiology and Biotechnology 63: 653–658.

Fischer K, Gmehling J (1994): P-x and γ^{∞} Data for the Different Binary Butanol-Water Systems at 50°C. Journal of Chemical & Engineering Data 39: 309–315.

Friedl A, Sauer M (2016): Downstream process options for the ABE fermentation. FEMS Microbiology Letters 363: fnw073: 1-5.

Gallardo R, Alves M, Rodrigues LR (2017): Influence of nutritional and operational parameters on the production of butanol or 1,3-propanediol from glycerol by a mutant *Clostridium pasteurianum*. New Biotechnology 34: 59–67.

García V, Päkkilä J, Ojamo H, Muurinen E, Keiski RL (2011): Challenges in biobutanol production: How to improve the efficiency? Renewable and Sustainable Energy Reviews 15: 964–980.

Georgiou CD, Grintzalis K, Zervoudakis G, Papapostolou I (2008): Mechanism of Coomassie brilliant blue G-250 binding to proteins: a hydrophobic assay for nanogram quantities. Analytical and Bioanalytical Chemistry 391:391-403.

Girbal L, Vasconcelos I, Saint-Amans S, Soucaille P (1995): How neutral red modified carbon and electron flow in *Clostridium acetobutylicum* grown in chemostat culture at neutral pH. FEMS Microbiology Reviews 16: 151–162.

Gottumukkala LD, Parameswaran B, Valappil SK, Mathiyazhakan K, Pandey A, Sukumaran RK (2013): Biobutanol production from rice straw by a non-acetone producing *Clostridium sporogenes* BE01. Bioresource Technology 145: 182–187.

Green EM (2011): Fermentative production of butanol — the industrial perspective. Energy biotechnology – Environmental biotechnology. Current Opinion in Biotechnology 22: 337–343.

Grobben NG, Eggink G, Cuperus FP, Huizing HJ (1993): Production of acetone, butanol and ethanol (ABE) from potato wastes: fermentation with integrated membrane extraction. Applied Microbiology and Biotechnology 39: 494–498.

Groeger C, Sabra W, Zeng AP (2015): 4. Introduction to bioconversion and downstream processing: principles and process examples. In: Aresta M, Dibenedetto A, Dumeignil F (Ed.), Biorefineries. DE GRUYTER, Berlin, München, Boston, 81–108.

Groeger C, Sabra W, Zeng AP (2016): Study of *in situ* gas stripping and cellular metabolism for simultaneous production of 1,3-propanediol and *n*-butanol by *Clostridium pasteurianum*. Engineering in Life Sciences 16: 664–674.

Groeger C, Wang W, Sabra W, Utesch T, Zeng AP (2017): Metabolic and proteomic analyses of product selectivity and redox regulation in *Clostridium pasteurianum* grown on glycerol under varied iron availability. Microbial Cell Factories 16: 64.

Groot WJ, Soedjak HS, Donck PB, Lans RGJM, Luyben KCAM, Timmer JMK (1990): Butanol recovery from fermentations by liquid-liquid extraction and membrane solvent extraction. Bioprocess and Biosystems Engineering 5: 203–216.

Groot WJ, van der Lans RGJM, Luyben KCAM (1989): Batch and continuous butanol fermentations with free cells: integration with product recovery by gas-stripping. Applied Microbiology and Biotechnology 32: 305–308.

Grote K, Feldhusen J (Ed.) (2011): Dubbel. Springer Berlin Heidelberg, Berlin, Heidelberg.

Hahn HD, Dämbkes G, Rupprich N, Bahl H, Frey GD. (Ed.) (2013): Butanols. Ullmann's Encyclopedia of Industrial Chemistry. Wiley-VCH Verlag GmbH & Co. KGaA, Weinheim, Germany.

Hallenbeck PC, Benemann JR (2002): Biological hydrogen production; fundamentals and limiting processes. BIOHYDROGEN 2002 27: 1185–1193.

Hartlep M, Zeng AP (2002): Fedbatch-Verfahren für die mikrobielle Herstellung von 1, 3-Propandiol in *Klebsiella pneumoniae* und *Clostridium butyricum*. Chemie Ingenieur Technik 74: 663–664.

Harvey BG, Meylemans HA (2011): The role of butanol in the development of sustainable fuel technologies. Journal of Chemical Technology and Biotechnology 86: 2–9.

Hazelwood LA, Daran J, van Maris, A. J. A., Pronk JT, Dickinson JR (2008): The Ehrlich Pathway for Fusel Alcohol Production: a Century of Research on *Saccharomyces cerevisiae* Metabolism. Applied and Environmental Microbiology 74: 2259–2266.

Heitmann S, Krings J, Kreis P, Lennert A, Pitner W, Górak A, Schulte M (2012): Recovery of *n*-butanol using ionic liquid-based pervaporation membranes. Separation and Purification Technology 97: 108–114.

Herrmann G, Jayamani E, Mai G, Buckel W (2008): Energy Conservation via Electron-Transferring Flavoprotein in Anaerobic Bacteria. Journal of Bacteriology 190: 784–791.

Hongo M (1958): Change of solvent ratio by the addition of neutral red in the fermentation of pentose. Nippon Nogeikagaku Kaischi: 219–223.

Huang H, Ramaswamy S, Tschirner U, Ramarao B (2008): A review of separation technologies in current and future biorefineries. Separation and Purification Technology 62: 1–21.

Huber GW, Corma A (2007): Synergies between Bio- and Oil Refineries for the Production of Fuels from Biomass. Angewandte Chemie International Edition 46: 7184–7201.

Isar J, Rangaswamy V (2012): Improved *n*-butanol production by solvent tolerant *Clostridium beijerinckii*. Biomass and Bioenergy 37: 9–15.

Ishizaki A, Michiwaki S, Crabbe E, Kobayashi G, Sonomoto K, Yoshino S (1999): Extractive acetone-butanol-ethanol fermentation using methylated crude palm oil as extractant in batch culture of *Clostridium saccharoperbutylacetonicum* N1-4 (ATCC 13564). Journal of Bioscience and Bioengineering 87: 352–356.

Jang Y, Lee J, Malaviya A, Seung DY, Cho JH, Lee SY (2012): Butanol production from renewable biomass: Rediscovery of metabolic pathways and metabolic engineering. Biotechnology Journal 7: 186–198.

Jensen T, Kvist T, Mikkelsen M, Christensen P, Westermann P (2012a): Fermentation of crude glycerol from biodiesel production by *Clostridium pasteurianum*. Journal of Industrial Microbiology & Biotechnology 39: 709–717.

Jensen T, Kvist T, Mikkelsen M, Westermann P (2012b): Production of 1,3-PDO and butanol by a mutant strain of *Clostridium pasteurianum* with increased tolerance towards crude glycerol. AMB Express 2: 44.

Jiang C, Cao G, Wang Z, Li Y, Song J, Cong H, Zhang J, Yang Q (2016): Enhanced Butanol Production Through Adding Organic Acids and Neutral Red by Newly Isolated Butanol-Tolerant Bacteria. Applied Biochemistry and Biotechnology 180: 1416–1427.

Jones AJ, Venkataramanan KP, Papoutsakis T (2016): Overexpression of two stress-responsive, small, non-coding RNAs, 6S and tmRNA, imparts butanol tolerance in *Clostridium acetobutylicum*. FEMS Microbiology Letters 363.

Jones DT, Woods DR (1986): Acetone-butanol fermentation revisited. Microbiological Reviews 50: 484–524.

Kaeding T, DaLuz J, Kube J, Zeng AP (2015): Integrated study of fermentation and downstream processing in a miniplant significantly improved the microbial 1,3-propanediol production from raw glycerol. Bioprocess and Biosystems Engineering 38: 575–586.

Kamm B, Kamm M (2004): Biorefinery-systems. Chemical and biochemical engineering quarterly 18: 1–7.

Kanti P, Srigowri K, Madhuri J, Smitha B, Sridhar S (2004): Dehydration of ethanol through blend membranes of chitosan and sodium alginate by pervaporation. Separation and Purification Technology 40: 259–266.

Kao W, Lin D, Cheng C, Chen B, Lin C, Chang J (2013): Enhancing butanol production with *Clostridium pasteurianum* CH4 using sequential glucose–glycerol addition and simultaneous dual-substrate cultivation strategies. Bioresource Technology 135: 324–330.

Katayama T, Nitta T (1976): Solubilities of hydrogen and nitrogen in alcohols and n-hexane. Journal of Chemical and Engineering Data 21: 194–196.

Khosravanipour Mostafazadeh A, Drogui P, Brar SK, Tyagi RD, Le Bihan Y, Buelna G, Rasolomanana S (2016): Enhancement of biobutanol production by electromicrobial glucose conversion in a dual chamber fermentation cell using *C. pasteurianum*. Energy Conversion and Management 130: 165–175.

Kim D, Han S, Kim S, Shin H (2006): Effect of gas sparging on continuous fermentative hydrogen production. International Journal of Hydrogen Energy 31: 2158–2169.

Kim TS, Kim BH (1988): Electron flow shift in *Clostridium acetobutylicum* fermentation by electrochemically introduced reducing equivalent. Biotechnology Letters 10: 123–128.

Kraemer K, Harwardt A, Bronneberg R, Marquardt W (2011): Separation of butanol from acetone–butanol–ethanol fermentation by a hybrid extraction–distillation process. Computers & Chemical Engineering 35: 949–963.

Kraus GA (2008): Synthetic Methods for the Preparation of 1,3-Propanediol. Clean Soil Air Water 36:8, 648–651.

Kumar P, Barrett DM, Delwiche MJ, Stroeve P (2009): Methods for pretreatment of lignocellulosic biomass for efficient hydrolysis and biofuel production. Industrial & Engineering Chemistry Research 48: 3713–3729.

Kumar R, Singh S, Singh OV (2008): Bioconversion of lignocellulosic biomass: biochemical and molecular perspectives. Journal of Industrial Microbiology & Biotechnology 35: 377–391.

Laitinen A, Kaunisto J (1999): Supercritical fluid extraction of 1-butanol from aqueous solutions. The Journal of Supercritical Fluids 15: 245–252.

Lan EI, Liao JC (2011): Metabolic engineering of cyanobacteria for 1-butanol production from carbon dioxide. Metabolic Engineering 13: 353–363.

Lee CS, Aroua MK, Daud W, Cognet P, Pérès-Lucchese Y, Fabre P, Reynes O, Latapie L (2015): A review: Conversion of bioglycerol into 1,3-propanediol via biological and chemical method. Renewable and Sustainable Energy Reviews 42: 963–972.

Lee SY, Park JH, Jang SH, Nielsen LK, Kim J, Jung KS (2008): Fermentative butanol production by clostridia. Biotechnology and Bioengineering 101: 209–228.

Liao JC, Mi L, Pontrelli S, Luo S (2016): Fuelling the future: microbial engineering for the production of sustainable biofuels. Nature Reviews Microbiology 14: 288–304.

Liao Y, Lu K, Li S (2014): Process parameters for operating 1-butanol gas stripping in a fermentor. Journal of Bioscience and Bioengineering 118: 558–564.

Liu C, Xue C, Lin Y, Bai F (2013a): Redox potential control and applications in microaerobic and anaerobic fermentations. Biotechnology Advances 31: 257–265.

Liu X, Gu Q, Yu X (2013b): Repetitive domestication to enhance butanol tolerance and production in *Clostridium acetobutylicum* through artificial simulation of bio-evolution. Bioresource Technology 130: 638–643.

Lovley DR (2012): Electromicrobiology. Annual Review of Microbiology 66: 391–409.

Lu C, Dong J, Yang S (2013): Butanol production from wood pulping hydrolysate in an integrated fermentation–gas stripping process. Bioresource Technology 143: 467–475.

Lu C, Zhao J, Yang S, Wei D (2012): Fed-batch fermentation for *n*-butanol production from cassava bagasse hydrolysate in a fibrous bed bioreactor with continuous gas stripping. Bioresource Technology 104: 380–387.

Luehring P, Schumpe A (1989): Gas solubilities (hydrogen, helium, nitrogen, carbon monoxide, oxygen, argon, carbon dioxide) in organic liquids at 293.2 K. Journal of Chemical & Engineering Data 34: 250–252.

Madihah MS, Ariff AB, Sahaid KM, Suraini AA, Karim MI (2001): Direct fermentation of gelatinized sago starch to acetone–butanol–ethanol by *Clostridium acetobutylicum*. World Journal of Microbiology and Biotechnology 17: 567–576.

Malaviya A, Jang Y, Lee S (2012): Continuous butanol production with reduced byproducts formation from glycerol by a hyper producing mutant of *Clostridium pasteurianum*. Applied Microbiology and Biotechnology 93: 1485–1494.

Mariano AP, Keshtkar MJ, Atala DIP, Maugeri Filho F, Wolf Maciel MR, Maciel Filho R, Stuart P (2011): Energy Requirements for Butanol Recovery Using the Flash Fermentation Technology. Energy & Fuels. Energy Fuels 25: 2347–2355.

Marsili E., Zhang X. (2010): Shuttling via soluble compounds. In: Bioelectrochemical systems: from extracellular electron transfer to biotechnological application. Editors: Rabaey K., Angenent L., Schröder U., Keller J. IWA Publishing, London- New York: 59–79.

Massoudi R, King Jr AD (1973): Solubility of alcohols in compressed gases. Comparison of vapor-phase interactions of alcohols and homomorphic compounds with various gases. II. 1-Butanol, diethyl ether, and n-pentane in compressed nitrogen, argon, methane, ethane, and carbon dioxide at 25. deg. The Journal of Physical Chemistry 77: 2016–2018.

Matsuda F, Ishii J, Kondo T, Ida K, Tezuka H, Kondo A (2013): Increased isobutanol production in *Saccharomyces cerevisiae* by eliminating competing pathways and resolving cofactor imbalance. Microbial Cell Factories 12: 1.

Matsumura M, Kataoka H, Sueki M, Araki K (1988): Energy saving effect of pervaporation using oleyl alcohol liquid membrane in butanol purification. Bioprocess and Biosystems Engineering 3: 93–100.

Melero JA, Iglesias J, Garcia A (2012): Biomass as renewable feedstock in standard refinery units. Feasibility, opportunities and challenges. Energy & Environmental Science 5: 7393.

Menon S, Ragsdale SW (1996): Unleashing hydrogenase activity in carbon monoxide dehydrogenase/acetyl-CoA synthase and pyruvate: ferredoxin oxidoreductase. Biochemistry 35: 15814–15821.

Moon C, Hwan Lee C, Sang B, Um Y (2011): Optimization of medium compositions favoring butanol and 1,3-propanediol production from glycerol by *Clostridium pasteurianum*. Bioresource Technology 102: 10561–10568.

Moulis J, Davasse V, Meyer J, Gaillard J (1996): Molecular mechanism of pyruvate-ferredoxin oxidoreductases based on data obtained with the *Clostridium pasteurianum* enzyme. FEBS letters 380: 287–290.

Nakas JP, Schaedle M, Parkinson CM, Coonley CE, Tanenbaum SW (1983): System development for linked-fermentation production of solvents from algal biomass. Applied and Environmental Microbiology 46: 1017–1023.

Nielsen DR, Prather KJ (2009): *In situ* product recovery of *n*-butanol using polymeric resins. Biotechnology and Bioengineering 102: 811–821.

Nørskov AM, Mellor RB (1996): Electron transferring dyes in the nitrate reductase reaction: non-toxic alternatives to methyl viologen. World Journal of Microbiology & Biotechnology 12: 293–294.

Oudshoorn A, van der Wielen LAM, Straathof AJJ (2009): Assessment of Options for Selective 1-Butanol Recovery from Aqueous Solution. Industrial and Engineering Chemical Research 48: 7325–7336.

Park DH, Zeikus JG (1999): Utilization of Electrically Reduced Neutral Red by *Actinobacillus succinogenes*: Physiological Function of Neutral Red in Membrane-Driven Fumarate Reduction and Energy Conservation. Journal of Bacteriology 181: 2403–2410.

Peguin S, Goma G, Delorme P, Soucaille P (1994): Metabolic flexibility of *Clostridium acetobutylicum* in response to methyl viologen addition. Applied Microbiology and Biotechnology 42: 611–616.

Peters JW (1999): Structure and mechanism of iron-only hydrogenases. Current opinion in structural biology 9: 670–676.

Petitdemange H, Cherrier C, Raval G, Gay R (1976): Regulation of the NADH and NADPH-ferredoxin oxidoreductases in *Clostridia* of the butyric group. Biochimica et Biophysica Acta (BBA) - General Subjects 421: 334–347.

Pflügl S, Marx H, Mattanovich D, Sauer M (2012): 1, 3-Propanediol production from glycerol with *Lactobacillus diolivorans*. Bioresource Technology 119: 133–140.

Pham T, Mauvais G, Vergoignan C, Coninck J de, **Dumont F, Lherminier J, Cachon R, Feron G (2008):** Gaseous environments modify physiology in the brewing yeast *Saccharomyces cerevisiae* during batch alcoholic fermentation. Journal of applied microbiology 105: 858–874.

Preisig HA, Wittgens B (2012): Thinking Towards Synergistic Green Refineries. Energy Procedia 20: 59–67.

Qureshi N, Hughes S, Maddox I, Cotta M (2005): Energy-efficient recovery of butanol from model solutions and fermentation broth by adsorption. Bioprocess and Biosystems Engineering 27: 215–222.

Qureshi N, Saha B, Cotta M (2007): Butanol production from wheat straw hydrolysate using *Clostridium beijerinckii*. Bioprocess and Biosystems Engineering 30: 419–427.

Rabaey K, Rozendal RA (2010): Microbial electrosynthesis — revisiting the electrical route for microbial production. Nature Reviews Microbiology 8: 706–716.

Regestein L, Doerr EW, Staaden A, Rehmann L (2015): Impact of butyric acid on butanol formation by *Clostridium pasteurianum*. Bioresource Technology 196: 153–159.

Roffler SR, Blanch HW, Wilke CR (1987): *In-situ* recovery of butanol during fermentation: 1 + 2. Bioprocess and Biosystems Engineering 2: 1–12.

Rosenbaum M, Aulenta F, Villano M, Angenent LT (2011): Cathodes as electron donors for microbial metabolism: Which extracellular electron transfer mechanisms are involved? Bioresource Technology 102: 324–333.

Sabra W, Groeger C, Sharma PN, Zeng AP (2014): Improved *n*-butanol production by a non-acetone producing *Clostridium pasteurianum* DSMZ 525 in mixed substrate fermentation. Applied Microbiology and Biotechnology: 4267–4276.

Sabra W, Groeger C, Zeng AP (2015): Microbial Cell Factories for Diol Production. In: Advances in Biochemical Engineering/Biotechnology. Springer Berlin Heidelberg, Berlin, Heidelberg.

Sabra W, Wang W, Surandram S, Groeger C, Zeng AP (2016): Fermentation of mixed substrates by *Clostridium pasteurianum* and its physiological, metabolic and proteomic characterizations. Microbial Cell Factories 15:114: 1–14.

Saha BC (2003): Hemicellulose bioconversion. Journal of Industrial Microbiology and Biotechnology 30: 279–291.

Saint-Amans S, Perlot P, Goma G, Soucaille P (1994): High production of 1, 3-propanediol from glycerol by *Clostridium butyricum* VPI 3266 in a simply controlled fed-batch system. Biotechnology Letters 16: 831–836.

Sander R (2015): Compilation of Henry's law constants (version 4.0) for water as solvent. Atmospheric Chemistry and Physics 15: 4399–4981.

Santangelo F, Stoffers M and Górak A: Extraction of butanol from aqueous solutions and fermentation broth using ionic liquids, Proceedings of the 19th international Solvent extraction conference.

Sarchami T, Johnson E, Rehmann L (2016a): Optimization of fermentation condition favoring butanol production from glycerol by *Clostridium pasteurianum* DSM 525. Bioresource Technology 208: 73–80.

Sarchami T, Munch G, Johnson E, Kießlich S, Rehmann L (2016b): A Review of Process-Design Challenges for Industrial Fermentation of Butanol from Crude Glycerol by Non-Biphasic *Clostridium pasteurianum*. Fermentation 2: 13.

Sattler K (2012): Thermische Trennverfahren: Grundlagen, Auslegung, Apparate. John Wiley & Sons.

Saxena R, Anand P, Saran S, Isar J (2009): Microbial production of 1,3-propanediol: Recent developments and emerging opportunities. Biotechnology Advances 27: 895–913.

Scherer PA, Thauer , R. K. (1978): Purification and Properties of Reduced Ferredoxin: CO2 Oxidoreductase from *Clostridium pasteurianum*, a Molybdenum Iron-Sulfur-Protein. European Journal of Biochemitsry 85: 125–135.

Schneider DA, Gourse RL (2004): Relationship between Growth Rate and ATP Concentration in *Escherichia coli*. A Bioassay for available cellular ATP. Journal of Biological Chemistry 279: 8262–8268.

Serrano-Ruiz JC, Ramos-Fernández EV, Sepúlveda-Escribano A (2012): From biodiesel and bioethanol to liquid hydrocarbon fuels: new hydrotreating and advanced microbial technologies. Energy & Environmental Science 5: 5638.

Steinigeweg S, Gmehling J (2002): *n*-Butyl acetate synthesis via reactive distillation: thermodynamic aspects, reaction kinetics, pilot-plant experiments, and simulation studies. Industrial & Engineering Chemistry Research 41: 5483–5490.

Sun Y, Yan L, Fu H, Xiu Z (2013): Selection and optimization of a salting-out extraction system for recovery of biobutanol from fermentation broth. Engineering in Life Sciences 13: 464–471.

Tal M, Silberstein A, Nusser E (1985): Why does Coomassie Brilliant Blue R interact differently with different proteins? A partial answer. Journal of Biological Chemistry 260: 9976–9980.

Thauer RK, Jungermann K, Decker K (1977): Energy conservation in chemotrophic anaerobic bacteria. Bacteriological reviews 41: 100–180.

Truong K , Blackburn JW (1984): The stripping of organic chemicals in biological treatment processes. A new approach to prediction of the fates of organic chemicals in biological processes. Environmental Progress and Sustainable Energy 3: 143–152.

Uragami T, Takigawa K (1990): Permeation and separation characteristics of ethanol-water mixtures through chitosan derivative membranes by pervaporation and evapomeation. Polymer 31: 668–672.

Valdez-Vazquez I, Pérez-Rangel M, Tapia A, Buitrón G, Molina C, Hernández G, Amaya-Delgado L (2015): Hydrogen and butanol production from native wheat straw by synthetic microbial consortia integrated by species of *Enterococcus* and *Clostridium*. Fuel 159: 214–222.

Vane LM (2005): A review of pervaporation for product recovery from biomass fermentation processes. Journal of Chemical Technology and Biotechnology 80: 603–629.

Vane LM (2008): Separation technologies for the recovery and dehydration of alcohols from fermentation broths. Biofuels, Bioproducts and Biorefining 2: 553–588.

Venkataramanan KP, Kurniawan Y, Boatman JJ, Haynes CH, Taconi KA, Martin L, Bothun GD, Scholz C (2014): Homeoviscous response of *Clostridium pasteurianum* to butanol toxicity during glycerol fermentation. Journal of Biotechnology 179: 8–14.

Voget CE, Mignone CF, Ertola RJ (1985): Butanol production from apple pomace. Biotechnology Letters 7: 43–46.

Vollenweider S, Lacroix C (2004): 3-Hydroxypropionaldehyde: applications and perspectives of biotechnological production. Applied Microbiology and Biotechnology 64: 16–27.

Vrije T de, **Budde M, van der Wal H, Claassen PAM, López-Contreras AM (2013):** "*In situ*" removal of isopropanol, butanol and ethanol from fermentation broth by gas stripping. Bioresource Technology 137: 153–159.

Waldron KW (Ed.) (2014): Advances in Biorefineries: Biomass and Waste Supply Chain Exploitation. Elsevier. Cambridge, UK.

Wang Y, Tao F, Ni J, Li C, Xu P (2015): Production of C3 platform chemicals from CO2 by genetically engineered cyanobacteria. Green Chemistry 17: 3100–3110.

Weast RC (Ed.) (1980): CRC Handbook of Chemistry and Physics. CRC Press, Boca Raton, Florida.

Westermeier R (2016): Electrophoresis in practice: A guide to methods and applications of DNA and protein separations. John Wiley & Sons, 5. Edition, Weinheim, Germany.

Winogradsky S (1894): Sur l'assimilation de l'azote gazeux de l'atmosphere par les microbes. Gauthier-Villars et Fils, Imprimeurs des CR des séances de l'Acad. des Sciences.

Wischral D, Zhang J, Cheng C, Lin M, De Souza, Lucas Monteiro Galotti, Pessoa, Fernando L Pellegrini, Pereira N, Yang S (2016): Production of 1, 3-propanediol by *Clostridium beijerinckii* DSM 791 from crude glycerol and corn steep liquor: Process optimization and metabolic engineering. Bioresource Technology 212: 100–110.

Xin B, Wang Y, Tao F, Li L, Ma C, Xu P (2016): Co-utilization of glycerol and lignocellulosic hydrolysates enhances anaerobic 1,3-propanediol production by *Clostridium diolis*. Scientific Reports 6: 19044.

Xiu Z, Zeng AP (2008): Present state and perspective of downstream processing of biologically produced 1,3-propanediol and 2,3-butanediol. Applied Microbiology and Biotechnology 78: 917–926.

Xue C, Du G, Sun J, Chen L, Gao S, Yu M, Yang S, Bai F (2014): Characterization of gas stripping and its integration with acetone–butanol–ethanol fermentation for high-efficient butanol production and recovery. Biochemical Engineering Journal 83: 55–61.

Xue C, Liu F, Xu M, Zhao J, Chen L, Ren J, Bai F, Yang S (2016): A novel *in situ* gas stripping-pervaporation process integrated with acetone-butanol-ethanol fermentation for hyper *n*-butanol production. Biotechnol. Bioeng. 113: 120–129.

Xue C, Zhao J, Liu F, Lu C, Yang S, Bai F (2013): Two-stage *in situ* gas stripping for enhanced butanol fermentation and energy-saving product recovery. Bioresource Technology 135: 396–402.

Xue C, Zhao J, Lu C, Yang S, Bai F, Tang I (2012): High-titer *n*-butanol production by C*lostridium acetobutylicum* JB200 in fed-batch fermentation with intermittent gas stripping. Biotechnology and Bioengineering 109: 2746–2756.

Yang GQ, Du B, Fan LS (2007): Bubble formation and dynamics in gas–liquid–solid fluidization—A review. Chemical Engineering Science 62: 2–27.

Yerushalmi L, Volesky B, Szczesny T (1985): Effect of increased hydrogen partial pressure on the acetone-butanol fermentation by *Clostridium acetobutylicum*. Applied Microbiology and Biotechnology 22: 103–107.

Zeng AP (1995): A new balance equation of reducing equivalents for data consistency check and bioprocess calculation. Journal of Biotechnology 43: 111–124.

Zeng AP (1996): Pathway and kinetic analysis of 1,3-propanediol production from glycerol fermentation by *Clostridium butyricum*. Bioprocess Engineering 14: 169–175.

Zeng AP, Biebl H, Schlieker H, Deckwer W (1993): Pathway analysis of glycerol fermentation by *Klebsiella pneumoniae*: Regulation of reducing equivalent balance and product formation. Enzyme and Microbial Technology 15: 770–779.

Zhou M, Chen J, Freguia S, Rabaey K, Keller J (2013): Carbon and Electron Fluxes during the Electricity Driven 1,3-Propanediol Biosynthesis from Glycerol. Environmental Science and Technology 47: 11199–11205.

7 Appendix

7.1 Physical and chemical properties of substrates and products by *C. pasteurianum* DSMZ 525

Table 7-1: Physical and chemical properties of the substrates and main products produced by *C. pasteurianum* DSMZ 525.

Compound		Density [g/cm³]	Molar Mass [g/mol]	Melting point [°C]	Boiling point [°C]	Vapor pressure [mbar] 20°C / 40°C	Solubility in water 20°C
CO_2		$1.98*10^{-3}$	44.01	-	-	-	-
H_2		$8.9*10^{-3}$	2.02	-	-	-	-
Glycerol	$C_3H_8O_3$	1.26	92.09	18	290	<0.001/<0.001	completely
Glucose	$C_6H_{12}O_6$	1.56	180.16	146	-	-	~470 g/L
***n*-Butanol**	$C_4H_{10}O$	0.81	74.12	-89	118	6.67 / 25.1	7.7 w- %
1,3-Propane-diol	$C_3H_8O_2$	1.05	76.10	-26	213	1.07	100 g/L
Ethanol	C_2H_6O	0.79	46.07	-114	78	58 / 178	completely
Acetic acid	$C_2H_4O_2$	1.05	60.05	17	118	16	completely
Butyric acid	$C_4H_8O_2$	0.96	88.11	-5	163	0.9	completely
Lactic acid	$C_3H_6O_3$	1.21	90.08	53	122	0.1 (25°C)	completely
Formic acid	$C_1H_2O_2$	1.22	46.03	8	101	44.6 / 114	completely

Data from: http://www.dguv.de/ifa/gestis/gestis-stoffdatenbank/index.jsp (08.09.2017)

7.2 Reactor geometry semi-pilot scale reactors

Table 7-2: Geometrical dimensions of the semi-pilot scale reactors.

30 L Reactor (Type NLF)

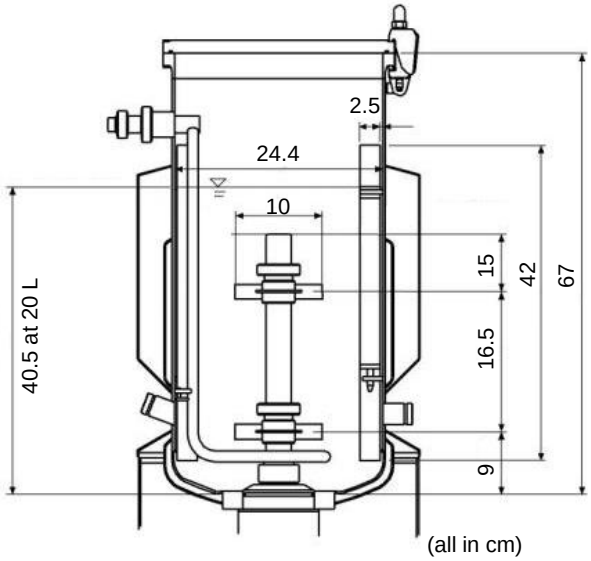

300 L Reactor (Type P)

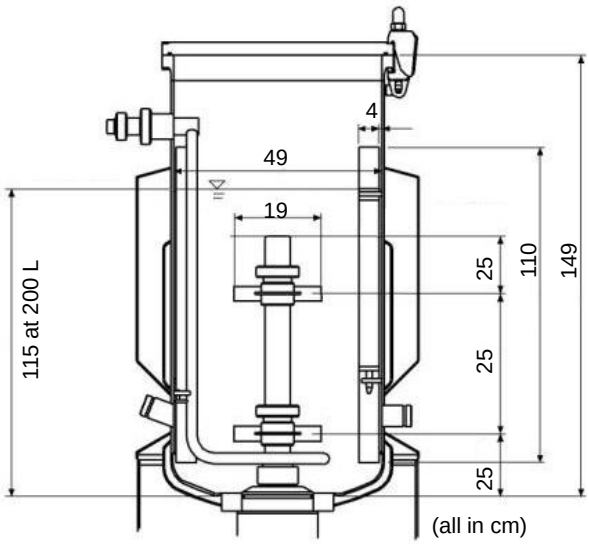

	30 L	**300 L**
Baffles	4 baffles, 90°orientation	4 baffles, 90°orientation
	width 2.5 cm	width 4 cm
	length 42 cm	length 110 cm
	6 cm from ground	10 cm from ground
Impeller	2 six-blade impeller	2 six-blade impeller
	Blades: 2 x 3.3 cm	Blades: 4 x 5 cm
Gassing ring	diameter 10 cm	diameter 20 cm

7.3 Utilized Chemicals

Table 7-3: Utilized chemicals.

Chemical	Grade	Company
Cultivation		
Acrolein	≥ 95 % GC as anhydrous	Fluka (Sigma-Aldrich Chemie GmbH)
Ammoniumsulphate $(NH_4)_2SO_4$	99,5 %	Carl Roth GmbH + Co. KG
Ammonium chloride NH_4Cl	≥ 99,5 %	Carl Roth GmbH + Co. KG
Antifoam	Silicon-Antischaumemulsion	Carl Roth GmbH + Co. KG
Antifoam (Dechema)	Antifoam 204	Sigma-Aldrich Chemie GmbH
Biotin	Pure	Amresco
Boric acid H_3BO_3	Extra pure	Merck KGaA
Brilliant Blue R 250 $C_{45}H_{44}N_3NaO_7S_2$	-	Carl Roth GmbH + Co. KG
Calcium carbonate $CaCO_3$	≥ 98,5 %	Carl Roth GmbH + Co. KG
Calcium chloride dihydrate $CaCl_2*2H_2O$	≥ 99,0 %	Carl Roth GmbH + Co. KG
Citric acid	p.a.	Merck KGaA
Cobalt (II) chloride hexahydrate $CoCl_2*6H_2O$	Pro analysis	Merck KGaA
Cupper (II) chloride dihydrate $CuCl_2*2H_2O$	Pro analysis	Merck KGaA
Curcumin $C_{21}H_{20}O_6$	Zur Synthese	Merck KGaA
di-Potassium hydrogen phosphate K_2HPO_4	≥ 99 %	Carl Roth GmbH + Co. KG
di-Sodium hydrogen phosphate Na_2HPO_4	≥ 99 %	Carl Roth GmbH + Co. KG
di-Sodium sulphide trihdyrate Na_2S*3H_2O	AnalaR NORMAPUR	VWR International Ltd.
Glucose $C_6H_{12}O_6$	Pa. ACS	Carl Roth GmbH + Co. KG
Glycerol $C_3H_8O_3$	98 %	Carl Roth GmbH + Co. KG
Hydrochloric acid HCl	ROTIPURAN 25 %,	Carl Roth GmbH + Co. KG
Hydrochloric acid HCl	37%, rauchend	Carl Roth GmbH + Co. KG
Iron (III) chloride $FeCl_3$	≥ 98 %	Carl Roth GmbH + Co. KG
Iron(II) sulfate heptahydrate $FeSO_4*7H_2O$	≥ 99,0 %	Carl Roth GmbH + Co. KG
L(+)-Cysteine hydrochloride-monohydrate	≥ 99,0 %	Carl Roth GmbH + Co. KG
Magnesium chloride hexahydrate $MgSO_4*6H_2O$	Pro analysis	Merck KGaA
Magnesium sulphate heptahydrate $MgSO_4*7H_2O$	≥ 99 %	Carl Roth GmbH + Co. KG
Manganese (II) chloride dihydrate $MnCl_2*4H_2O$	98 %	Carl Roth GmbH + Co. KG

Chemical	Grade	Company
Meat extract	For nutrient media	Carl Roth GmbH + Co. KG
Nickel (II) chloride hexahydrate $NiCl_2$ *$6H_20$	Pro analysis	Merck KGaA
Panthothenate	For Biochemistry	Merck KGaA
Peptone ex casein	Tryptic digest, for microbiology	Carl Roth GmbH + Co. KG
Potassium chloride KCl	≥ 99,5 %	Carl Roth GmbH + Co. KG
Potassium dihydrogen phosphate KH_2PO_4	≥ 99 %	Carl Roth GmbH + Co. KG
Potassium ferricyanide (III) trihydrate $K_3Fe(CN)_6$ *$3H_2O$	1000100 mg/dl in water	Dr. Schlag GmbH
Protease Inhibitor	Complete mini, EDTA free	Roche Diagnostics Deutschland GmbH
Resazurin sodium salt $C_{12}H_6NNaO_4$	For cell culture	Sigma-Aldrich Chemie GmbH
Silicon oil	-	Carl Roth GmbH + Co. KG
Sodium Acetate $NaC_2H_3O_2$	≥ 99 %	Carl Roth GmbH + Co. KG
Sodium chloride NaCl	99,5 %, p.a.	Carl Roth GmbH + Co. KG
Sodium dihydrogen phosphate NaH_2PO_4	≥ 98 %	Carl Roth GmbH + Co. KG
Sodium hydroxide NaOH	99 %, p.a.	Carl Roth GmbH + Co. KG
Sodium molybdate dihydrate Na_2MoO_4*$2H_2O$	p.a.	Merck KGaA
Sodium sulfate Na_2SO_4	≥ 99 %	Merck KGaA
Soluble starch	ACS reagent	Sigma-Aldrich Chemie GmbH
Sulphuric acid H_2SO_4	ROTIPURAN 98 %	Carl Roth GmbH + Co. KG
Toluol	≥ 99 %	Fluka (Sigma-Aldrich Chemie GmbH)
DL-Tryptophan	≥ 99 %	Fluka (Sigma-Aldrich Chemie GmbH)
Yeast extract	For bacteriology	Carl Roth GmbH + Co. KG
Zinc chloride ZnCl2	ACS, ISO, Reag., Ph Eur	Merck KGaA
Proteomics		
2-D Quant Kit	-	GE Healthcare Life Sciences
Acetone	≥99.9 % HPLC-Grade	Sigma-Aldrich Chemie GmbH
Acetonitril	≥99,98 %, Ultra LC-MS	Carl Roth GmbH + Co. KG
CHAPS	PUFFERAN® ≥98 %, für die Biochemie	Carl Roth GmbH + Co. KG
DTT 1,4-Dithiothreitol	≥99 %, p.a. für die Biochemie	Carl Roth GmbH + Co. KG

Chemical	Grade	Company
Formic acid	LC-MS Ultra 98 %	Sigma-Aldrich Chemie GmbH/Fluka
IPG buffer 3–10	-	GE Healthcare Life Sciences
Phenol	zur Extraktion von Nukleinsäuren	Carl Roth GmbH + Co. KG
Rotiphorese® Gel 40 (37.5:1)	aqueous 40 % acrylamide and bisacrylamide stock solution (37.5:1)	Carl Roth GmbH + Co. KG
TFA	LC-MS Ultra ≥99.0 %	Sigma-Aldrich Chemie GmbH/Fluka
Thiourea	≥99 % p.a.	Carl Roth GmbH + Co. KG
Tris-buffer	≥99,9 %, p.a.	Carl Roth GmbH + Co. KG
Trypsin	-	Promega
α-Iodoacetamide	≥99 %	Calbiochem
Gases		
Carbon dioxide CO_2	10 mol%	Messer Industriegase GmbH
Hydrogen H_2	10 mol%	Messer Industriegase GmbH
Mixture H_2 /CO_2	60 mol% H_2	Messer Industriegase GmbH
	40 mol% CO_2	
Nitrogen N_2	Pure, compressed	Linde AG

7.4 Utilized Devices

Table 7-4: Utilized devices.

Devices		Type	Company
Bioreactors	Bioreactor 2 L	VSF - 2000	Bioengineering Ag, Wald, CH
	Bioreactor 30 L	NLF	Bioengineering Ag, Wald, CH
	Bioreactor 300 L	P	Bioengineering Ag, Wald, CH
Periphery	Controler	pH controler SPC; Temperature controler SPC;	Bioengineering AG, Wald, CH
		Agitation controler SPC	
	Redox amplifier	pH 531	WTW Wissenschaftlich-Technische Werkstätten GmbH, Weilheim, D

Devices		Type	Company
	Redox probe	Orbisint S CPS72-0PB4GS	Endress+Hauser Messtechnik GmbH+Co.KG, Weil am Rhein, D
	pH probe	405-DPAS-SC-K8S/225	Mettler Toledo, Gießen, D
	pH probe (NLF/ P)	50453 / 50212	Bioengennering AG, Wald, CH
	Peristaltic pumps	101 U/R	Watson Marlow Limited, Falmouth, UK
	Separate vessels	Media Storage vessel 300L	Bioengineering Ag, Wald, CH
DASGIP Reactors	Bioreactors 300 mL	SR0700	Eppendorf AG, Hamburg, D
	Periphery system	DASGIP Bioblock Advanced Stirrer Line SR	Eppendorf AG, Hamburg, D
	pH probe	405-DPAS-SC-K8S/224	Mettler Toledo, Gießen, D
	Redox probe	Pt4805-SC-DPASK8S/225	Mettler Toledo, Gießen, D
Gas stripping	Mini Laboratory pump	VP86	VWR, Leuven, B
	Miniport (10 L/min)	N79 KN.18	KNF Neuberger GmbH, Freiburg, D
	Mini Vacuum pump	Z1303-6007-8500	Optim-Import B.V., AaLten, NL
	Gossenstabil DC power supply	14 K 24 R 1.8	GMC-I Messtechnik GmbH, Nürnberg, D
	Condenser	Ewt-B3-12 x 50	Edelstahlwärmetauscher, Hannover, D
	Circulation Thermostat	ministat 230	Peter Huber Kältemaschinenbau GmbH, Offenburg, D
	Flow regulator	EL-Flow	Bronkhorst High-Tech B.V. AK Ruurlo, NL
At Dechema	Potentiostat PCI4	Series G Family	Gamry Instruments, Warminster, USA
	Heat box	Certomat HK	B. Braun International GmbH, Melsungen, D
Analytics			
HPLC	Kontron HPLC	Autosampler 360	Kontron, Rossdorf, D
		Pump 322	Kontron, Rossdorf, D
		HPLC 332 detector	Kontron, Rossdorf, D
		Aminex HPX-87H column (300 x 7.8mm)	Bio-Rad Laboratories GmbH, München, D
		Refractive Index detector RID-6A	Shimadzu, Kyoto, J

Devices		Type	Company
Spectrophotometer		Spectrophotometer V-1200	VWR, Leuven, BE
		Multiskan® Spectrum	Thermo Fischer Scientific, Waltham, USA
Proteomics	Homogenizer	FastPrep® -24 high-speed homogenizer	MP Biomedicals, produced by: Johari Digital Healthcare Ltd. , Jodhpur, IN
	Vacuum centrifuge	RVC 2-25 CD plus	Martin Christ Gefriertrocknungsanlagen GmbH, Osterode, D
	1D	Ettan IPGPhor 3 Isoelectric focusing unit	GE Healthcare, Freiburg, D
	2D	Ettan DALT twelve vertical system	Amersham Biosciences (GE Healthcare), Freiburg, D
	Molecular Imager® VersaDoc™	MP4000	Bio-Rad Laboratories GmbH, München, D
	Pre-separation	UltiMate® 3000, RSLCnano system	Thermo Fisher Scientific, Waltham, USA
	Mass spectrometer	nanoLC-ESI-MS/MS amaZon ETD ion-trap mass spectrometer	Bruker Daltonik, Billerica, USA.
		amaZon ETD ion-trap mass spectrometer	Bruker Daltonik, Billerica, USA.
		CaptiveSpray nano-ESI source	Bruker Daltonik, Billerica, USA.
	Columns	Acclaim® PepMap100 C18 column (100 µm x 2 cm, 5 µm)	Thermo Fisher Scientific, Waltham, USA
		Acclaim® PepMap RSLC C18 (75 µm x 15 cm, 2 µm)	Thermo Fisher Scientific, Waltham, USA
MilliGascounter		Typ MGC-1PMMA	Dr.-Ing. Ritter Apparatebau GmbH & Co. KG, Bochum, D
Mass spectrometer (gas measurement)		OmniStar	Balzer Instruments/ Pfeiffer Vacuum GmbH, Asslar , D

7.5 Utilized Software

Table 7-5: Utilized softwares.

Devices	Software
Gas measurement	Lab view V. 15
Bioreactors 30 L / 300 L	PCS Inc. X- Controle: License 94092811, PCS controle system AG, Freiburg, D.
Potentiostat Dechema	Gamry Framework 6.1 Build 2107 © 2013 and Gamry Echem Analyst 6.1 © 2012, Warminster, USA
Multiskan® Spectrum	SkanIt Software 2.4.4.5 Research Edition, © 2004-2007, Thermo Fischer Scientific, Waltham, USA.
HPLC	Chromleon Client 6.80 SR15 Build 4656 (243203), Thermo Fisher Scientific, Waltham, USA.
Origin	Origin 8.5.1 G SR1, OriginLab Corporation, Northampton, USA.
Proteomics	Compass DataAnalysis (version 4.1), Bruker Corporation, Billerica, USA.
	Progenesis SameSpots (v 3.3) Nonlinear dynamic, UK.
	ProteinScape™ software, Bruker Corporation, Billerica, USA.

7.6 Conversion reactions for carbon and NADH balance

Table 7-6: Main metabolic conversion steps of glycerol and glucose into main products by *C. pasteurianum* DSMZ 525.

Glycerol Conversion	
Glycerol + NADH → **1,3-Propanediol**	(7-1)
Glycerol → **Ethanol** + CO_2 + ATP + FdH_2	(7-2)
Glycerol → **Acetate** + CO_2 + 2 ATP + 2 NADH + FdH_2	(7-3)
Glycerol → **Lactate** + ATP + NADH + H_2O	(7-4)
2 Glycerol → **Butyrate** + 2 CO_2 + 3 ATP + 2 FdH_2 + 2 NADH	(7-5)
2 Glycerol → **Butanol** + 2 CO_2 + 2 ATP + 2 FdH_2	(7-6)
NADH + H^+ → NAD^+ + H_2	(7-7)
Glucose Conversion	
Glucose + 2 NADH → 2 **Ethanol** + 2 CO_2 + 2 ATP + 2 FdH_2	(7-8)
Glucose → 2 **Acetate** + 2 CO_2 + 4 ATP + 2 NADH + 2 FdH_2	(7-9)
Glucose → **Butyrate** + 2 CO_2 + 3 ATP + 2 FdH_2	(7-10)
Glucose + 2 NADH → **Butanol** + 2 CO_2 + 2 ATP + 2 FdH_2	(7-11)
Butyrate + ATP + 2 NADH → **Butanol**	(7-12)
1 g/L **Biomass** = 13.2 mmol NADH	(Zeng, 1995)

7.7 Supplements for the result section

Table 7-7: Proteins showing significant change in expression levels, compared between iron excess (Fe+) and iron limitation (Fe-) conditions, as well as between the exponential growth phase (early) and the stationary phase (late). (Table from Groeger et al., 2017).

Accession No.	Protein Name	Cluster of Orthologous Groups (COG)	Conserved Protein Domain	Spot No.	Fold change iron-related				Fold change growth-related			
					Early phase higher at		Late phase higher at		Fe+ higher at		Fe- higher at	
					Fe-	Fe+	Fe-	Fe+	early	late	early	late
Amino acid transport and metabolism												
F502_05097	amino peptidase 1	COG1362	Lap4	298	1.9		1.7					
F502_05412	carbamoyl phosphate synthase large subunit	COG0458	CarB	89		1.8			1.9			
F502_07028	cysteine synthase a	COG0031	CysK	449	1.8					2.1		
F502_17572	glutamine synthetase type III	COG3968	GlnA3	187	1.6					1.9		
				190	1.6					1.6		
F502_18676	threonine synthase	COG0498	ThrC	312		1.6			2.2			
Carbohydrate transport and metabolism												
F502_03412	propanediol dehydratase small subunit	COG4910	PduE	594	1.9		1.9					
F502_07638	flavodoxin	COG0716	FldA	594								
F502_03417	glycerol dehydratase reactivation factor large subunit	No COG		220					2.1			
F502_03937	glycogen synthase	COG0297	GlgA	329	2.7					2.3		
F502_06067	enolase	COG0148	Eno	695	4.1		4.0			2.0		2.0
				696	4.8		1.8			2.5		
F502_06077	triosephosphate isomerase	COG0149	TpiA	491				1.5		2.6		
F502_06087	glyceraldehyde 3-phosphate dehydrogenase	COG0057	GapA	409		1.6			2.4			
F502_07098	glycoside hydrolase	COG1543		277	2.0					1.8		
F502_12758	dihydroxyacetone kinase	COG2376	DAK1	158		1.7		2.0	1.7		2.1	
				179		1.7		1.7	2.2		2.3	
Cell cycle control / Cell division												
F502_08238	cell division protein	COG3599	DivIVA	503					2.7		2.0	

Accession No.	Protein Name	Cluster of Orthologous Groups (COG)	Conserved Protein Domain	Spot No.	Fold change iron-related				Fold change growth-related			
					Early phase higher at		Late phase higher at		Fe+ higher at		Fe- higher at	
					Fe-	Fe+	Fe-	Fe+	early	late	early	late
Cell wall / Membrane / Envelope biogenesis												
F502_00655	peptidoglycan-binding protein	COG1388	LysM	233	7.9					6.1	1.6	
F502_01965	spore coat protein F-related protein	COG5577	CotF	549	1.5		2.1					1.6
Coenzyme transport and metabolism												
F502_07578	pyridoxal biosynthesis lyase	COG0214	PdxS	460		2.5			2.2			
Energy production and conversion												
F502_05017	NifU-related domain containing protein	COG0822	IscU	519	0.4	2.4	0.6	1.6	1.3	0.8	0.9	1.1
				520		3.7		2.9	1.9		1.5	
F502_06282	electron transfer flavoprotein subunit alpha	COG2025	FixB	440				1.5				
F502_06287	electron transfer flavoprotein subunit alpha/beta-like protein	COG2086	FixA	487				1.7				
F502_06447	bifunctional acetaldehyde-CoA/alcohol dehydrogenase	COG1012	AdhE	119				2.1		3.7		1.6
				715	1.5			2.9		5.3		
				717	1.6			3.0		4.7		
F502_07493	nitroreductase	COG0778	NfnB	537	2.3		2.9					1.8
F502_07643	pyruvate:ferredoxin (flavodoxin) oxidoreductase. homodimeric	COG0674	PorA	70		2.4		2.4	1.5			
				75				2.4	0.6	1.8		
				76				2.7		1.9		
				77		1.5		2.3				
				87		2.0		2.8			1.5	
				90		2.2		2.8	1.6		2.0	
F502_07648	Pyruvate:ferredoxin oxidoreductase	COG0674	PorA	40				2.3		1.6		
				57				2.3		2.1		
				58		1.5		2.4		2.1		
				59		2.1		2.8				
F502_09238	rubredoxin / flavodoxin /	COG0426	NorV	131	1.7					2.0		
	oxidoreductase			730						2.0		1.6
F502_09488	hydratase (aconitase A)	COG1048	AcnA	156		2.4		2.5	1.9		2.0	
F502_11871	butyrate kinase	COG3426	Buk	383	1.6					1.7		

Accession No.	Protein Name	Cluster of Orthologous Groups (COG)	Conserved Protein Domain	Spot No.	Fold change iron-related				Fold change growth-related			
					Early phase higher at		Late phase higher at		Fe+ higher at		Fe- higher at	
					Fe-	Fe+	Fe-	Fe+	early	late	early	late
F502_11976	pyruvate carboxylase	COG1038	PycA	71		1.5		2.7		1.7		
F502_12091	F0F1 ATP synthase subunit beta	COG0055	AtpD	645	2.1		1.9					
				646	2.2		2.4					
F502_12878	desulfo ferrodoxin	COG2033	SorL	611		2.2		2.8				
F502_13493	flavodoxin	COG0716	FldA	575	14.3		8.0			1.6		
F502_14390	[FeFe]- hydrogenase	COG4624	Nar1 PurB	303		2.1			2.5			
F502_04707	adenylosuccinate lyase	COG0015		303								
F502_15080	rubrerythrin	COG1592	YotD	558		2.2		4.5		2.0		
F502_16610	glycolate oxidase	COG0277	GlcD	315				1.8		2.3		1.9
F502_18287	hydrogenase-1	COG1034	NuoG	223		4.5		1.6	2.3			
				224		5.1		1.9	3.6			
F502_18651	NADP-dependent glyceraldehyde-3-phosphate dehydrogenase	COG1012	AdhE	736	2.7		1.5			2.1		
F502_19556	formate acetyltransferase	COG1882	PflD	174	4.5		5.7					
				175	8.0		6.5					
				178	2.5						3.4	
				181	3.7				1.7		7.4	
Function unknown / General function prediction only												
F502_02435	aldo / keto reductase	COG1453		362		2.6			2.9			
F502_05012	hypothetical protein (GGGtGRT protein)	No COG		400		7.1		2.2	3.0			
F502_05962	hypothetical protein	No COG		635	2.0					1.5		
F502_06682	hypothetical protein	COG2607		318		3.4		3.8	1.7		2.0	
F502_15420	hypothetical protein	No COG		597	1.7		2.8		1.5			
F502_16320	hypothetical protein	COG0393	YbjQ	637	2.3		2.0					
Lipid transport and metabolism												
F502_06297	3-hydroxybutyryl-CoA dehydratase	COG1024	CaiD	472		2.1			2.2			
F502_10483	biotin carboxylase	COG0439	AccC	302	2.5			1.6		2.1	1.9	
Nucleotide transport and metabolism												
F502_17300	bifunctional phospho-ribosylaminoimidazole-carboxamide formyltransferase / IMP cyclohydrolase	COG0138	PurH	281					1.7		1.6	

Accession No.	Protein Name	Cluster of Orthologous Groups (COG)	Conserved Protein Domain	Spot No.	Fold change iron-related				Fold change growth-related			
					Early phase higher at		Late phase higher at		Fe+ higher at		Fe- higher at	
					Fe-	Fe+	Fe-	Fe+	early	late	early	late
Posttranslational modification / Protein turnover / Chaperones												
F502_03242	heat shock protein (molecular chaperone GrpE)	COG0576	GrpE	481				2.1		2.2		
F502_03247	molecular chaperone DnaK	COG0443	Dank	217	1.6					1.8		
F502_03987	peptidase	COG1026	Cym1	106	2.3					2.1		
				107	3.6		1.6			2.4		
F502_05557	ATP-dependent Clp protease ATP-binding subunit	COG0542	ClpA	165	1.8		2.1					
				168			1.9		1.7			
F502_06242	chaperonin	COG0459	GroEL	258	1.6					2.0		
F502_06247	co-chaperonin	COG0234	GroES	613				1.5		2.6		
F502_07608	Thij / PfpI family protein	COG0693	ThiJ	553	1.8		1.6					
F502_10228	heat shock protein (molecular chaperone IbpA)	COG0071	IbpA	600			2.5			3.0		6.9
F502_15425	heat shock protein 90	COG0326	HtpG	196	2.2					2.4		
				206	1.6					1.5		
F502_18446	clpb protein	COG0542	ClpA	138	1.8			1.5		2.8		
				716	2.5			2.4		4.4		
F502_18743	ATPase with chaperone activity clpC. two ATP-binding domain protein	COG0542	ClpA	147	2.1		2.1			2.0		2.0
			ClpA	149	2.5		1.7			2.4		1.6
Signal transduction / Stress response / Defense mechanism												
F502_04082	GTP-binding protein	COG1217	TypA	47					1.7		1.8	
				148		1.7			2.4		2.1	
F502_07703	chemotaxis histidine kinase. CheA (contains CheW-like adaptor domain)	COG0643	CheA	155	3.6		2.2				1.6	
F502_10768	lipid hydroperoxide peroxidase	COG2077	Tpx	572	3.9		2.2			2.5		
F502_13258	CBS domain-containing protein	COG0517	CBS	606	4.5		4.8			1.7		1.9
F502_14770	serine protein kinase	COG2766	PrkA	193	4.7		1.5			3.4		
				197	3.7		2.6			2.1		
				200	6.2		1.9			3.6		
				201	3.8					2.6		

Accession No.	Protein Name	Cluster of Orthologous Groups (COG)	Conserved Protein Domain	Spot No.	Fold change iron-related				Fold change growth-related			
					Early phase higher at		Late phase higher at		Fe+ higher at		Fe- higher at	
					Fe-	Fe+	Fe-	Fe+	early	late	early	late
F502_16565	nitrogen regulatory protein P-II	COG0347	GlnK	638	3.1		1.8					
F502_17612	alkyl hydroperoxide reductase	COG0450	AhpC	567	5.3		2.9			2.4		
F502_17637	spore coat protein	COG3546	CotJC	548	2.3		3.9					2.1
F502_18092	stage V sporulation protein T	COG2002	AbrB	544	6.1		4.5			1.7		
Transcription / Defense mechanisms												
F502_12326	transcription accessory protein	COG2183	Tex	160		1.7	1.8		4.7		1.5	
Translation / Ribosomal structure and biogenesis												
F502_04537	30S ribosomal protein S2	COG0052	RpsB	497		2.1		2.1	2.7		2.7	
				500		2.4		1.9				
F502_06817	ribosomal 5S rRNA E-loop binding protein Ctc/L25/TL5	COG1825	RplY	504	3.5					3.9		
F502_12196	Ribosome-associated protein Y (PSrp-1)	COG1544	RaiA	565	2.4					2.4		
F502_18808	elongation factor Tu	COG0050	TufB	327		1.7		1.5	1.5		1.4	
F502_18833	50S ribosomal protein L1	COG0081	RplA	681		2.4		1.5	2.0			
F502_18948	50S ribosomal protein L5	COG0094	RplE	752		2.1			1.8			
F502_18963	50S ribosomal protein L6	COG0097	RplF	753		2.4			2.3			

Notes

The existence of more than one value of fold change for a single protein indicates that this protein appeared as multiple spots on the 2-D gels.

*1 COG: according to the annotation for *C. pasteurianum* DSM 525 by BioCyc database collection (http://www.biocyc.org/organism-summary?object=CPAS1262449, 08.09.2017)

*2 Conserved Protein Domain Family: according to the definition by NCBI Conserved Domains and Protein Classification (https://www.ncbi.nlm.nih.gov/cdd, 08.09.2017)

7.7.1 Gas stripping with *C. pasteurianum* isolate K1

In the prior section it could be shown, that *in situ* gas stripping with fermentation gases reduced the RP of the cultivation broth and led to the formation or more reduced products. To evaluate this phenomenon the effect of FG gassing was analyzed with another strain, the *C. pasteurianum* isolate K1. The isolate was cultivated VSF reactors in Biebl medium according to Chapter 3.2.2 and with the pre-cultures as described by Kaeding et al. (Kaeding et al., 2015). The effluent gas composition of this strain equals the DSMZ 525 strain, with up to 60 mol% H_2 and 40 mol% CO_2.

Using gas stripping with own fermentation gases at 4.5 vvm the average biomass concentration in the stationary growth phase was enhanced to 8.4 g/L, compared to 7.4 g/L without GS. Indeed, without gas stripping and under the same cultivation conditions the bacteria produced up to 66.5 g/L 1,3-PDO and 3.3 g/L BuOH (see also Table 7-8). Fig. 7-1 shows the product formation with gas stripping, using own FG and 4.5 vvm. GS started at 18 h when the BuOH concentration in the reactor reached 0.5 g/L. Indeed, it can be seen that the BuOH formation was increased and a final amount of 9.6 g/L BuOH was produced with a maximum of 6 g/L in the fermenter at the end of the fermentation. Accordingly, a low stripping rate of 0.10 g/(Lh) was achieved. Nevertheless the stripping leads to a slightly increased final 1,3-PDO titer of 71 g/L, with a yield of 0.36 $g/g_{glycerol}$. The formation of organic acids were also enhanced to 24 g/L butyrate, 12 g/L acetate and 6 g/L formate, compared to 22 g/L butyrate, 8 g/L acetate and 4 g/L formate without GS. Altogether this data are quite in the same range and show no significant increase in product formation, due to sparging with fermentation gases.

On the one hand, the sparging was possibly started too late to affect the metabolism, on the other hand, the BuOH concentration prior this time point was too low to justify the energy demand of a gas stripping process. Hence, this strain is suitable for the single production of 1,3-PDO, but the simultaneous production of BuOH could not be improved by implementing gas stripping with FG. For this isolated *C. pasteurianum* K1 strain Kaeding et al. (Kaeding et al., 2015) reported high 1,3-PDO titers (up to 60 g/L) and yields (0.52 g/g glycerol) in optimized fed-batch fermentations. This was realized without gas stripping in a much shorter fermentation time of ~25 h. Thus, the economic aspects for including a GS-unit are not feasible for the simultaneous production of BuOH and 1,3-PDO with the isolate *C. pasteurianum* K1.

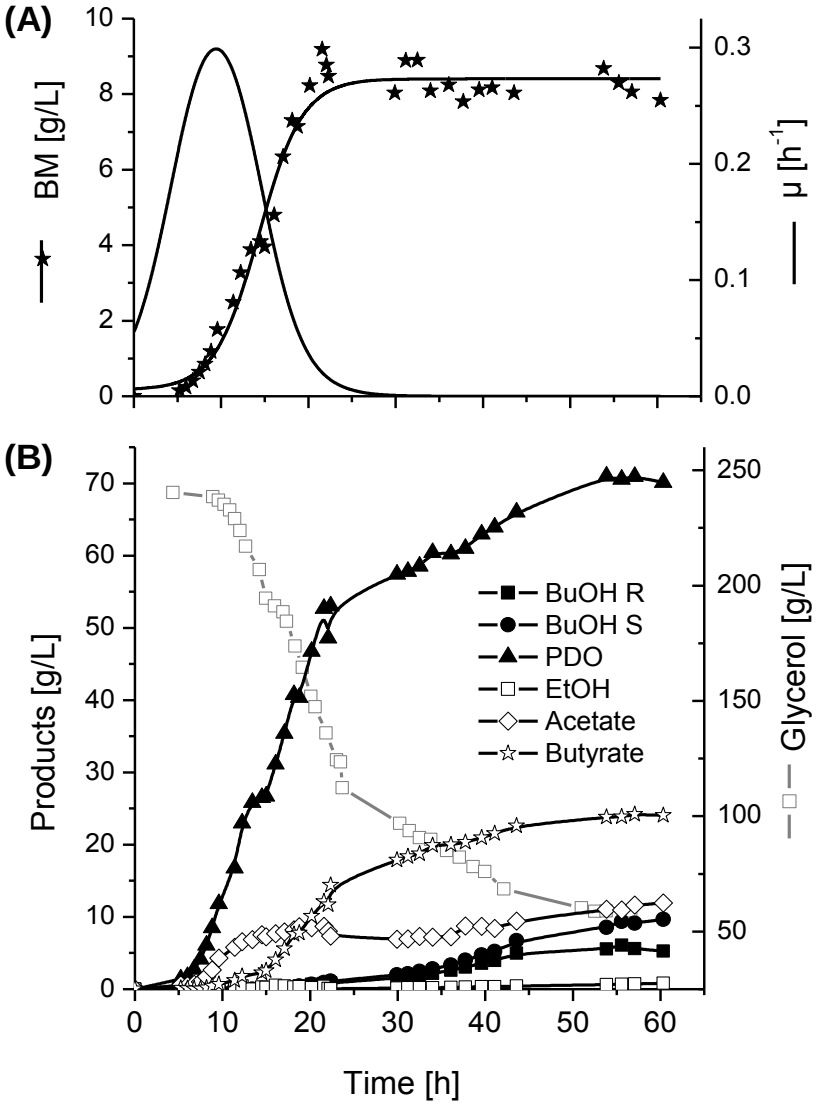

Fig. 7-1: Product formation by *C. pasteurianum* isolate K1 during growth on pure glycerol. Gas stripping with own fermentation gases at 4.5 vvm started at 18 h. (Butanol amounts are accumulated from reactor and condensates).

Table 7-8: Carbon recovery and final product concentrations in fermentations of pure glycerol using *C. pasteurianum* isolate K1 (*C. p.* K1) without and with gas stripping (with FG at 4.5 vvm).

Experiment	Carbon Recovery [%]	BuOH [g/L]	1,3-PDO [g/L]	EtOH [g/L]	Butyrate [g/L]	Acetate [g/L]	Formate [g/L]
C. p. K1, no GS	95	3.3	66.5	0.0	22.5	7.5	4.0
C. p. K1, FG 4.5 vvm	99	9.6	70.9	0.8	24.1	12.0	5.6

7.8 List of Figures

7.9 List of Tables